B E R I C H T E
aus dem
I N S T I T U T F Ü R M E E R E S K U N D E
an der
CHRISTIAN-ALBRECHTS-UNIVERSITÄT - Kiel

Nr. 132
1 9 8 4

I S O P Y C N I C A T L A S

O F T H E

N O R T H A T L A N T I C O C E A N

- monthly mean maps and sections -

by

J. Bauer and J.D. Woods

DOI 10.3289/IFM_BER_132

Copies are available from
Institut für Meereskunde an der Universität
Abt. Regionale Ozeanographie
Düsternbrooker Weg 20
D-2300 Kiel 1, FRG

ISSN 0341 - 8561

C o n t e n t s

1. INTRODUCTION

The distributions presented in this volume have been derived from the well-known Robinson-Bauer-Schroeder (1979) analysis of bathythermograph and hydrocast archive data to give monthly mean temperature and mean salinity values at standard depths in a 1°x 1° array. Their analyzed data have been interpolated onto density surfaces and are presented as isopycnic maps and sections. The analysis was undertaken as part of an investigation of water mass conversion and circulation in the warm water sphere of the North Atlantic Ocean.

Isopycnic analysis was introduced into oceanography fifty years ago by Montgomery (1938) and Parr (1938). Isopycnic maps and sections have since appeared in many atlases and papers, although the traditional isobaric presentation remains much more common. A selection of publications including isopycnic maps or sections is listed on page 3.

Presentation of hydrographic data as distributions on isopycnic surfaces offers a number of advantages over the more common isobaric presentation. Firstly, mixing occurs more freely along density surfaces than across them because the former involves no work against the Archimedes force. The power input to three dimensional turbulence in the stratified interior of the ocean is so weak that diapycnic mixing normally achieves very much less vertical transport of passive scalars than isopycnic mixing along inclined (baroclinic) density surfaces by quasi-geostrophic turbulence (Garrett, 1982).

$$\text{i.e.} \quad K_d \, \nabla_d S \ll b^2 \cdot K_i \, \nabla_i S$$

where the subscripts $_d$ and $_i$ refer to components of the diffusivities K and the gradients ∇ directed across and along the density surface respectively, and b is the slope of the density surface. For that reason, isopycnic analysis has proved particularly valuable in geochemistry (Broecker, 1981) and especially in studying the spreading of transient tracers (Sarmiento et al., 1982).

Isopycnic analysis is also the first step in mapping the distribution of potential vorticity, which is inversely proportional to the spacing between two isopycnic surfaces. Maps of thickness have been published by Tsuchiya (1968). Potential vorticity is mixed along density surfaces like Rhines, 1979. Maps of the large-scale isopycnic distribution of Sverdrupian potential vorticity (in which the relative vorticity is assumed to be negligible compared with the planetary vorticity because of the large scale) have been

published by Sarmiento (1982) and McDowell, Rhines & Keffer, 1982. Mesoscale isopycnic maps of thickness and potential vorticity have been published by Leach, Minnett & Woods (1984) and Fischer, Leach & Woods (1985).

The analysis of climatological data onto isopycnic (rather than isobaric) surfaces also facilitates comparison with expedition data, since it eliminates spurious differences arising from transient vertical displacement by internal waves and quasi-geostrophic eddies (see, for example, the comparison in Leach, Minnett & Woods, 1985).

Some publications that include isopycnic maps or sections

Date	Authors	Reference
1937	R.B. Montgomery	**Bull. American Met. Soc. 18, 210-212**
1938	E.A. Parr	**J. Mar. Res. 1, 269-290**
1942	R.B. Montgomery & M.J. Pollak	**J. Mar. Res. 5, 20-27**
1965	J.L. Reid	**Intermediate waters of the Pacific Ocean**
1968	M. Tsuchiya	**Upper waters of the intertropical Pacific Oc.**
1968	R.A. Barkley	**Oceanographic Atlas of the Pacific Ocean**
1970-73	C.M. Love (Ed.)	**Eastropac atlas (7 volumes)**
1971	K. Wyrtki	**Oceanographic atlas of the International Indian Ocean expedition**
1971	J.L. Reid & R.J. Lynn	**Deep-Sea Res. 18, 1063-1088**
1972	J.E. Callahan	**Deep-Sea Res. 19, 563-575**
1973	J.L. Reid	**Northwest Pacific ocean waters in winter**
1981	A.L. Gordon & E.J. Molinelli	**Southern Ocean Atlas**
1982	S. Levitus	**Climatological Atlas of the World Ocean**
1982	J.L. Sarmiento C.G.H. Rooth & W. Roether	**J. Geophys. Res. 87, 8047-8056.**

2. DATA PROCESSING

2.1 The Robinson-Bauer-Schroeder numerical atlas

The starting point for our work was the numerical version of the atlas produced by Robinson, Bauer & Schroeder (1979). Descriptions of the archive data used in the compilation of the atlas, and the processing method, are given in Robinson, Bauer & Schroeder (1979). Its special feature is that the concentration of bathythermograph data is sufficient to justify calculation of monthly mean temperature at intervals of 1° latitude and longitude in the top 150 m. The high spatial resolution has been retained for temperature at depths greater than 150 m and for salinity at all depths, although the data base is then too small to justify stratification by month of the year. The monthly mean temperatures at depths down to 150 m and the high spatial resolution provide information about the seasonal cycle that is missing missing from atlases (e.g. Levitus, 1982) which use hydrocast, but not bathythermograph data.

2.2 Seasonal variation

The Robinson-Bauer-Schroeder numerical atlas offers us the possibility of climatological isopycnic analysis of the seasonally varying component of the upper ocean. On the other hand the limitations of the atlas (no monthly mean temperatures below 150 m or salinities at any depth) forced us to base our analysis on a pseudo-monthly-mean density, which is only an approximation to the monthly mean density that would be calculated from an "ideal" atlas comprising monthly mean temperature and salinity at all depths. Our assumption is that the difference between the pseudo- and ideal- monthly mean density distributions are not so serious as to invalidate the isopycnic distributions presented herein. Differences can arise from a variety of sources. We shall briefly consider three of them, namely (1) seasonal variation below 150 m, (2) seasonal variation of salinity in the top 150 m and (3) secular change of temperature and salinity.

(1) Seasonal variation below 150 metres

The numerical atlas data exhibit significant variation of temperature at 150 m, the maximum depth for which monthly mean values are given. An estimate of the maximum depth of seasonal variation might be obtained by determining the depth at which the seasonal minimum surface temperature occurs in the annual mean temperature profile. Robinson et al. (1979) used a similar method, based on the monthly mean surface temperature minus 2 Fahrenheit degrees (approximately 1 K), to determine the depth of the mixed layer each month. Only in or near the tropics is the annual maximum depth of the mixed layer, so calculated, less than 150 m. Seasonal variation extends deeper at higher latitudes.

(2) Seasonal variation of salinity

Seasonal variation of salinity at North Atlantic Ocean Weather Stations has been described by Taylor & Stephens (1980). Table 1 shows the range of surface density variations due to the seasonal cycle of salinity. The changes are small and contribute little to the seasonal variation of density in the seasonal pycnocline. If there were no seasonal variation of salinity, isohalines would remain vertical in an isopycnally plotted section through the seasonal pycnocline. The isohalines in fig. 1 do indeed rise almost vertically through the seasonal pycnocline, showing that neglect of the seasonal variation of salinity will not normally lead to serious error in calculation of the depths of isopycnals in the seasonal pycnocline. The neglect of seasonal variation of salinity in our analysis and the data bias towards summer samples do not therefore seem to be serious.

Table 1: Annual range of surface density due to salinity changes observed at Ocean Weather Stations (after Taylor & Stephens, 1980)

$\beta\Delta S$/kg m^{-3}	OWS	Latitude	Longitude
0.048	A	62° N	33° W
0.143	B	56.5° N	51° W
0.080	C	52.7° N	35.5° W
0.177	D	44° N	41° W
0.070	E	35° N	48° W
0.040	I	59° N	19° W
0.028	J	52.5 N	20° W
0.021	K	45° N	16° W
0.068	M	66° N	2° E

(3) Longer term changes of temperature and salinity

Pu & Pollard (1984) have shown that the salinity in the North East Atlantic has changed significantly over recent decades. There is also evidence of interannual and decadal variation of temperature. The archive data set sampled this secular variation unevenly over the period 1900 to 1974, with different sampling profiles for temperature and salinity in the upper 150 m because the former is dominated by bathythermographs and the latter by hydrocasts. Below 150 m, both temperature and salinity were obtained from hydrocast data with the same sampling profile. Our knowledge concerning interannual and decadal variation is not sufficient to justify attempting to correct for these sampling biases.

2.3 Density profiles

The monthly mean density profiles were calculated for the whole water column, from the atlas temperature and salinity data. Density inversions were eliminated by monotonisation wherever they occurred, above 150 m in the winter months. Wherever density values at depths greater than 150 m made inversions, they were replaced with the value at 150 m (fig. 2). Temperature was corrected to the value consistent with salinity and density where this correction was made.

2.4 Isopycnals

Values of pressure, temperature and salinity were interpolated vertically onto selected density surfaces.

3. THE NUMERICAL ATLAS ON THE IFM COMPUTER

This chapter gives a brief introduction to using the numerical atlas installed on the computer of the Institut für Meereskunde (VAX 11/750). It describes the general structure of the data, and the programs used to extract the products illustrated in this atlas.

3.1 General data structure

The numerical atlas installed at the IfM computer contains hydrographical data of the Atlantic Ocean between 5° S and 60° N and 0° W and 90° W in a 1° x 1° geographical grid and at the following depth levels: 0, 30, 60, 90, 125, 150, 183, 200, 244, 250, 300, 305, 366, 400, 500, 600, 700, 800, 900, 1000, 1100, 1200, 1300, 1400, 1500, 1750, 2000, 2500, 3000, 4000, 5000, 6000, 7000 m. The basic data set contains 4266 profiles recorded in 112074 cycles of 17 variables.

It starts at the north-west corner of the North Atlantic. Along each latitude profiles are aligned from west to east. The mean value calculated by averaging the sample values lying in a 1° x 1° grid square is labeled to the centre of the grid square (fig. 3). Position values are positive north of the equator and east of the Greenwich meridian and negative south of the equator and west of Greenwich. The data is stored in the MK4-Format (Holtorff, 1980), a binary code for real numbers, used at the IFM for all kinds of data processing. It is therefore compatible with other data used at the IFM. The standard processing programmes of the MK4-System could be applied for further processing of the atlas data and various transfer programs allow an uncomplicated transfer to other computers (Holtorff, 1984).

3.2 Processing programs

The computer programs used to obtain the products presented in this volume from the numerical atlas are briefly described below.

Various kinds of subsets can be extracted from a data set by program **EXTRAC**. It was applied here to select monthly files in profile form from the atlas data set.

σ_θ was calculated from monthly mean temperatures and all-data mean salinities using program **EICH5**.

Program **MONINT** monotonized the density, reiterated temperature and interpolated temperature, salinity and depth on selected σ_θ values.

Again **EXTRAC** selected single surfaces of constant σ_θ out of the interpolated profiles.

Program **MEGRUM** a two-dimensional interpolation contour program for geographical data fields was used to produce the horizontal charts. The positions of the isolines are converted into geographical coordinates.

The plotting of the charts was done with **PLMEGR**, which plots a cartographic projection on a cylinder mantle (e.g. Mercator projection). The possibility to include data sets with geographical coordinates was used here to plot coastlines and isolines.

The objective analysis program **OBJANT** was applied to produce equally spaced profiles along the tracks of the SFB standard sections.

The contouring of the vertical sections was done with program **CONREC**.

4. REFERENCES

Barkley, R.A., 1968: Oceanographic Atlas of the Pacific Ocean, University of Hawaii Press, Honolulu.

Broecker, W.S., 1981: Geochemical tracers and ocean circulation. In "Evolution of physical oceanography", edited by B. Warren & C. Wunsch MIT Press, Cambridge, Mass., pp. 434-460.

Callahan, J.E., 1972: The structure and circulation of deep water in the Antarctic. Deep-Sea Res., 19, 563-575.

Fischer, J., H. Leach & J.D. Woods, 1985: Components of Upper Ocean Potential Vorticity at the North Atlantic Polar Front. (In preparation).

Garrett, C., 1982: On the parameterization of diapycnal fluxes due to double-diffusive intrusions. J. Phys. Oceanogr. 12(9), 953-959.

Gordon, A.L. & E.J. Molinelli, 1981: Southern Ocean Atlas. Pt. 1. Thermo- and Chemical Distributions. Columbia University Press, N.Y.

Holtorff, J., 1980: MK4-Documentation. Dept. of Theoretical Oceanography, Institut für Meereskunde, Kiel.

Holtorff, J., 1984: Program Library of the Inst. f. Meeresk. (unpublished) Dept. of Theoretical Oceanography, Institut für Meereskunde, Kiel.

Leach, H., P.J. Minnett & J.D. Woods, 1985: Deep-Sea Res. (in press)

Levitus, S., 1982: Climatological Atlas of the World Ocean. NOAA Professional Paper 13, U.S. Dept. of Commerce, National Oceanic and Atmospheric Administration, 173 pp.

Love, C.M. (Editor) 1970-1973: EASTROPAC Atlas (7 volumes). U.S. Dept. of Commerce.

McDowell, S., P. Rhines & T. Keffer, 1982: North Atlantic potential vorticity and its relation to the general circulation. J. Phys. Oceanogr. 12, 1417-1436.

Meincke, J. & A. Sy, 1983: Large-scale effects of the Mid-Atlantic Ridge on the North Atlantic Current. ICES Hydrography Committee, C.M. 1983/C:8, 10 pp.

Montgomery, R.B., 1937: A suggested method for representing gradient, flow in isentropic surfaces. Bull. Amer. Met. Soc. 18(6-7): 210-212.

Montgomery, R.B., 1938: Circulation in Upper Layers of Southern North Atlantic Deduced with Use of Isentropic Analysis.
Papers in Physical Oceanography and Meteorology, MIT and WHOI, 6(2), 55 pp.

Montgomery, R.B. & M.J. Pollack, 1942: Sigma-T surfaces in the Atlantic Ocean.
J. Mar. Res. 5, 20-27.

Parr, A.E., 1938: Analysis of current profiles by a study of pycnomeric distortion and identifying properties.
J. Mar. Res. 1, 269-290.

Pu, S. & R. Pollard, 1984: Structure and ventilation of the upper Atlantic Ocean northeast of the Azores.
Ms. 2nd draft 27.1.84.

Reid, J.L., 1965: Intermediate waters of the Pacific Ocean.
The Johns Hopkins Press, Baltimore.

Reid, J.L. & R.J. Lynn, 1971: On the influence of the Norwegian-Greenland and Weddell Seas upon the Bottom Waters of the Indian and Pacific Oceans.
Deep-Sea Res. 18, 1063-1088.

Reid, J.L., 1973: Northwest Pacific Ocean Waters in Winter.
The Johns Hopkins Press, Baltimore.

Rhines, P.B., 1979: Geostrophic Turbulence.
Ann. Rev. Fluid Mech. 11, 401-441.

Robinson, M., R. Bauer & E. Schroeder, 1979: Atlas of North Atlantic - Indian Ocean Monthy Mean Temperatures and Mean Salinities of the Surface Layer.
Dept. of the Navy, Washington, D.C.

Sarmiento, J.L., 1982: Time scales of thermocline exchange with surface waters.
Unpublished manuscript.

Sarmiento, J.L., C.G.H. Rooth & W. Roether, 1982: The North Atlantic Tritium Distribution in 1972.
J. Geophys. Res. 87(C10), 8047-8056.

Taylor, A.H. & J.A. Stephens, 1980: Seasonal and Year-to-year Variations in Surface Salinity at the nine North Atlantic Ocean Weather Stations.
Oceanologica Acta, 3(4), 421-430.

Tsuchiya, M., 1968: Upper waters of the intertropical Pacific Ocean.
The Johns Hopkins Press, Baltimore.

Wyrtki, K., 1971: Oceanographic Atlas of the International Indian Ocean Expedition.
National Science Foundation, Washington, U.S.A.

5. ACKNOWLEDGEMENTS

This work was supported by the Deutsche Forschungsgemeinschaft (German Research Society) under contract DFG-SFB-133 as part of the collaborative research program "Warm water sphere of the Atlantic" at the Institut für Meereskunde, Christian-Albrechts-Universität, Kiel.

The data set we used is the numerical atlas produced by M. Robinson, R. Bauer and E. Schroeder (1979), which we bought from Compass System Inc., 4640 Jewell St. #204, San Diego, CA. 92109, USA.

We thank Detlef Stammer for help with the computer plots and Alfred Eisele for the cartography.

6. FIGURES

6.1. List of figures

Page

Monthly mean sections

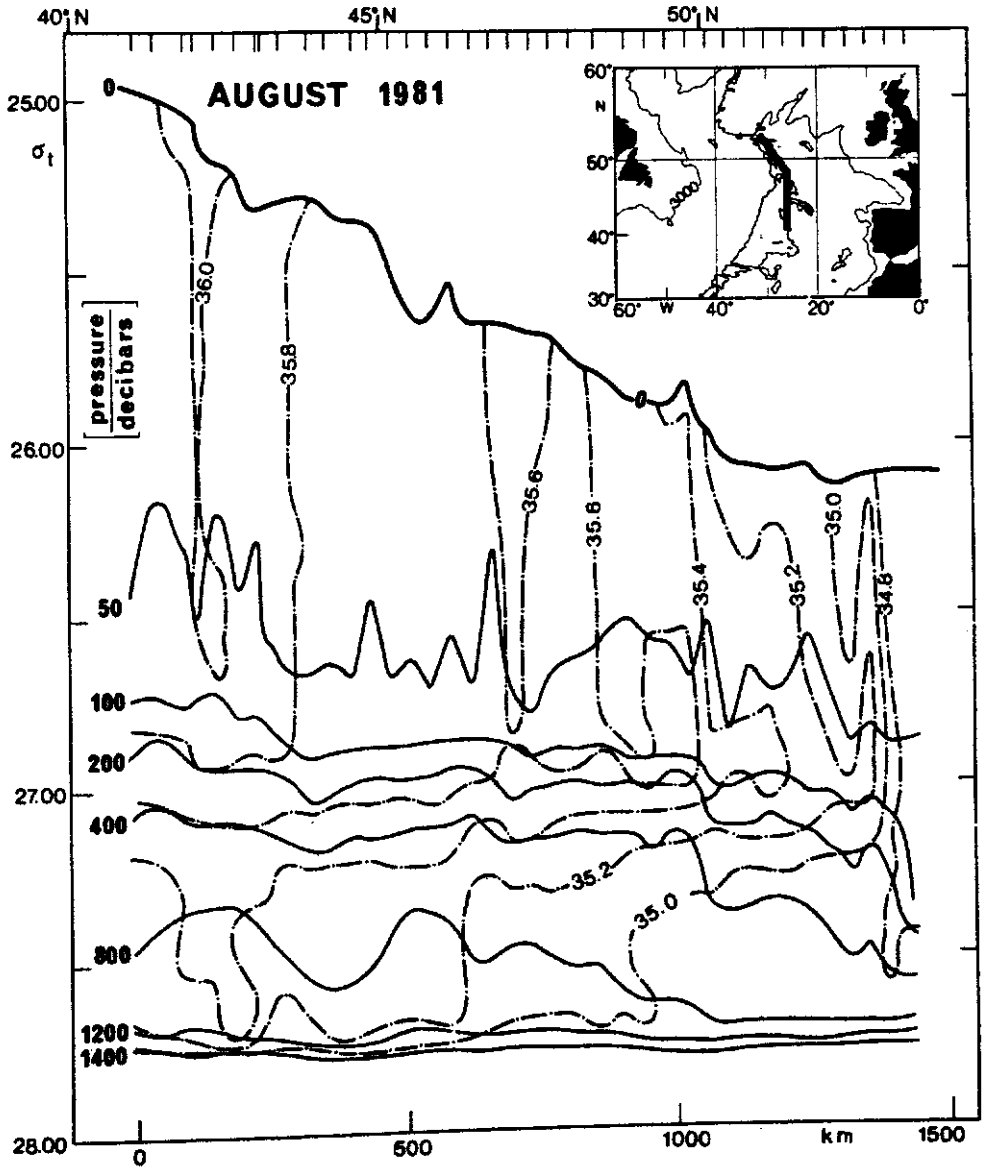

Fig. 1: Isopycnic presentation of the distribution of salinity and pressure in a hydrographic section going north from the Azores (data from Meincke & Sy, 1983).

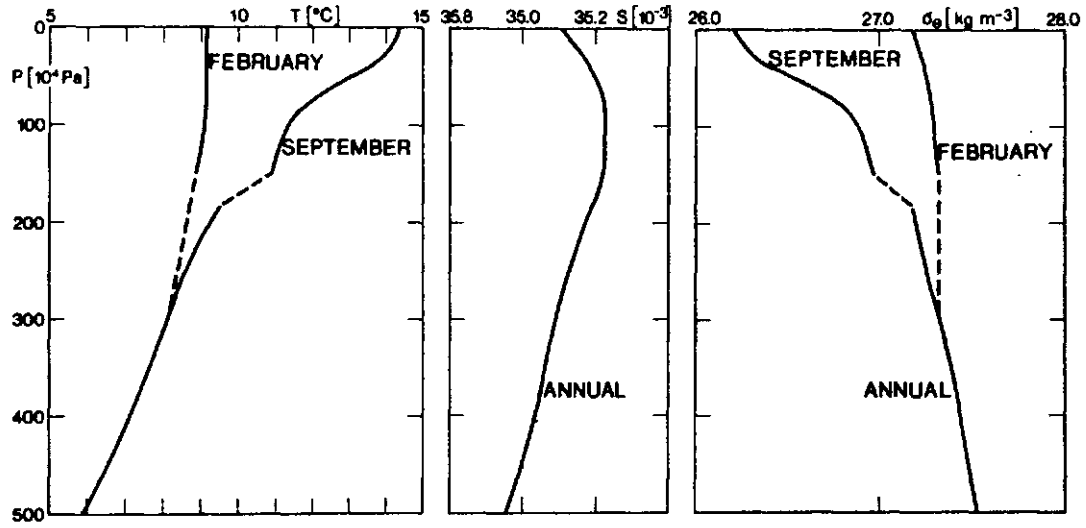

Fig. 2: Monthly mean profiles of temperature, salinity and density from the atlas for the 1° x 1° square at position 50°N 35°W in February and September. The broken lines indicate the procedure used to obtain monthly mean values in the seasonally-varying layer below 150 metres.

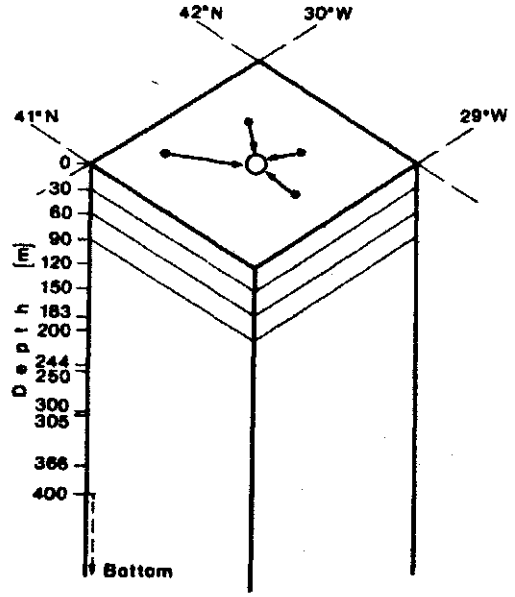

Fig. 3: Horizontal and vertical positioning of the atlas data. The data cycle containing the mean values calculated by averaging the samples lying between 41°N and 42°N and 29°W and 30°W are labeled at the position: ϕ = 41°30', λ = -29° -30'.

Fig. 4:
PRESSURE (10^4 Pa) on σ_θ = 25.0 kg m^{-3} JANUARY

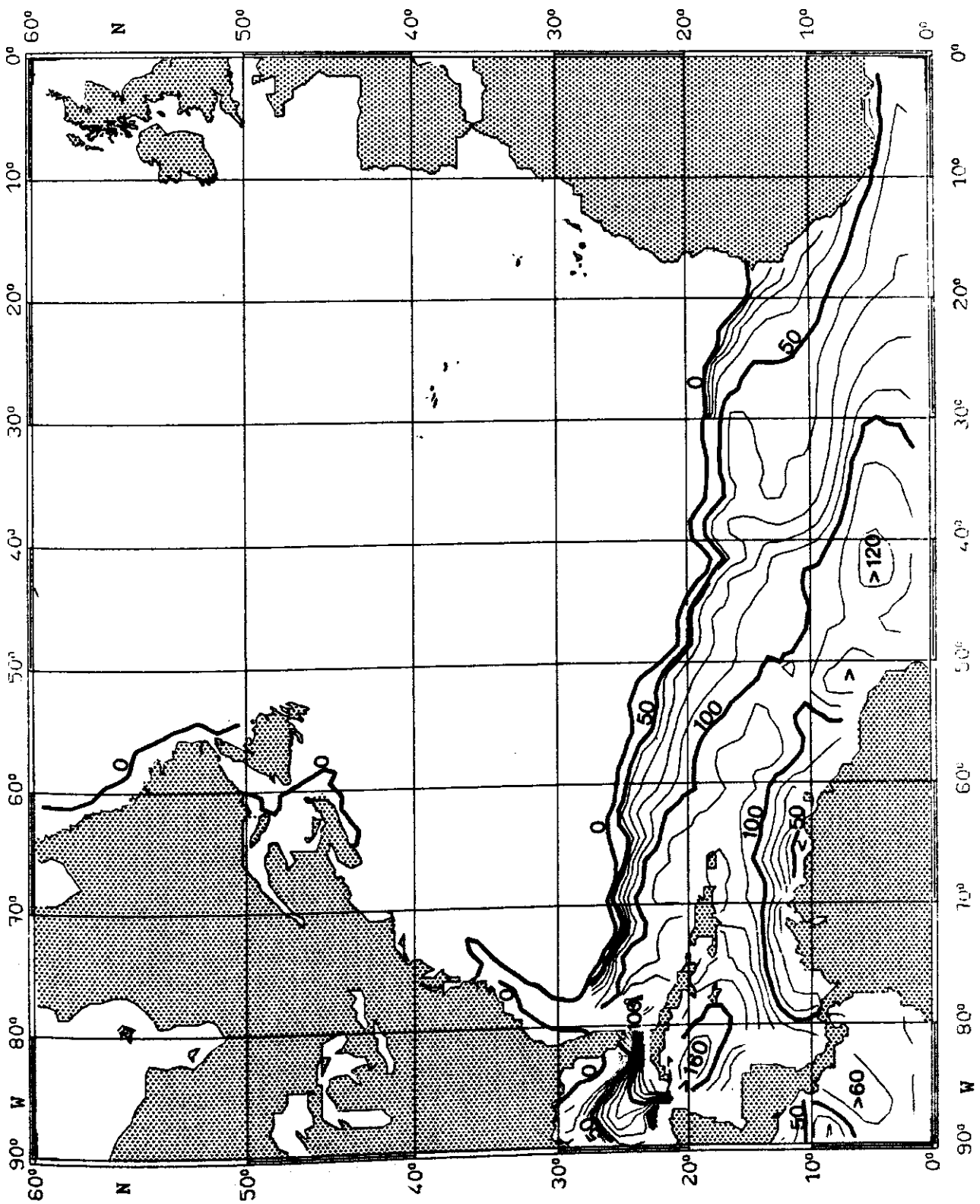

Fig. 5:
TEMPERATURE (°C) on σ_θ = 25.0 kg m^{-3} JANUARY

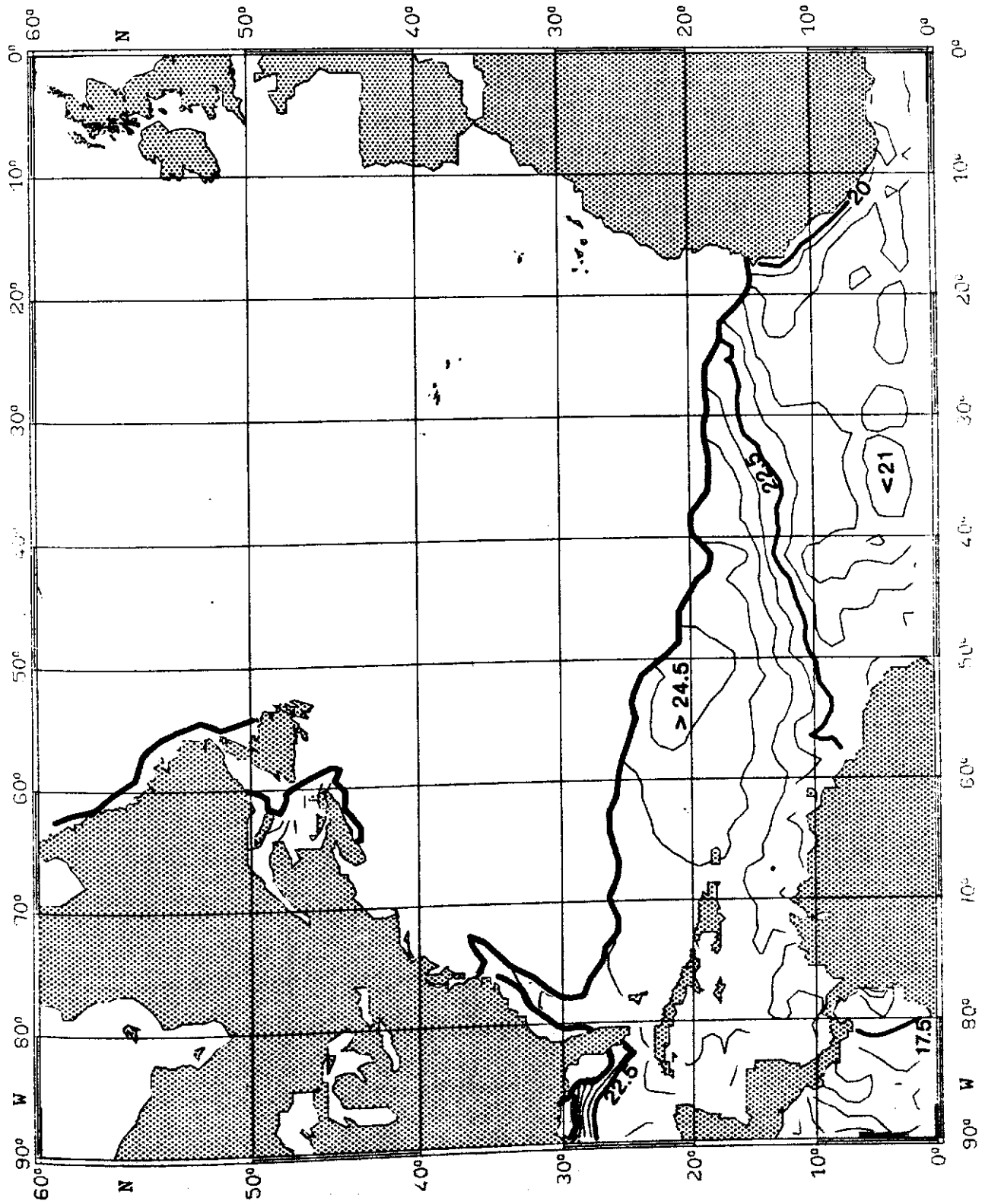

Fig. 6:
SALINITY (10^{-3}) on σ_θ = 25.0 kg m^{-3} JANUARY

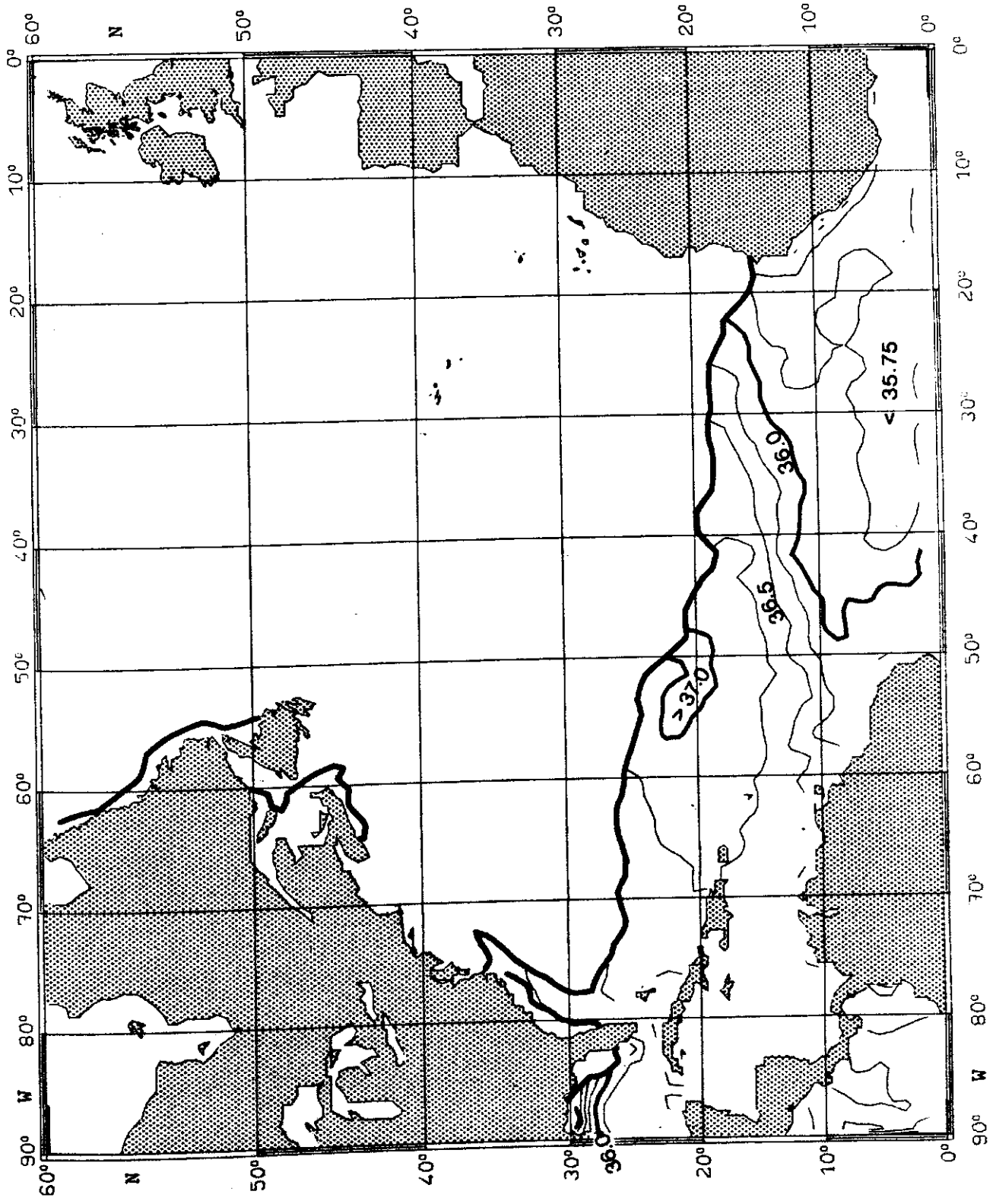

Fig. 7:

PRESSURE (10^4 Pa) on σ_θ = 26.0 kg m^{-3} JANUARY

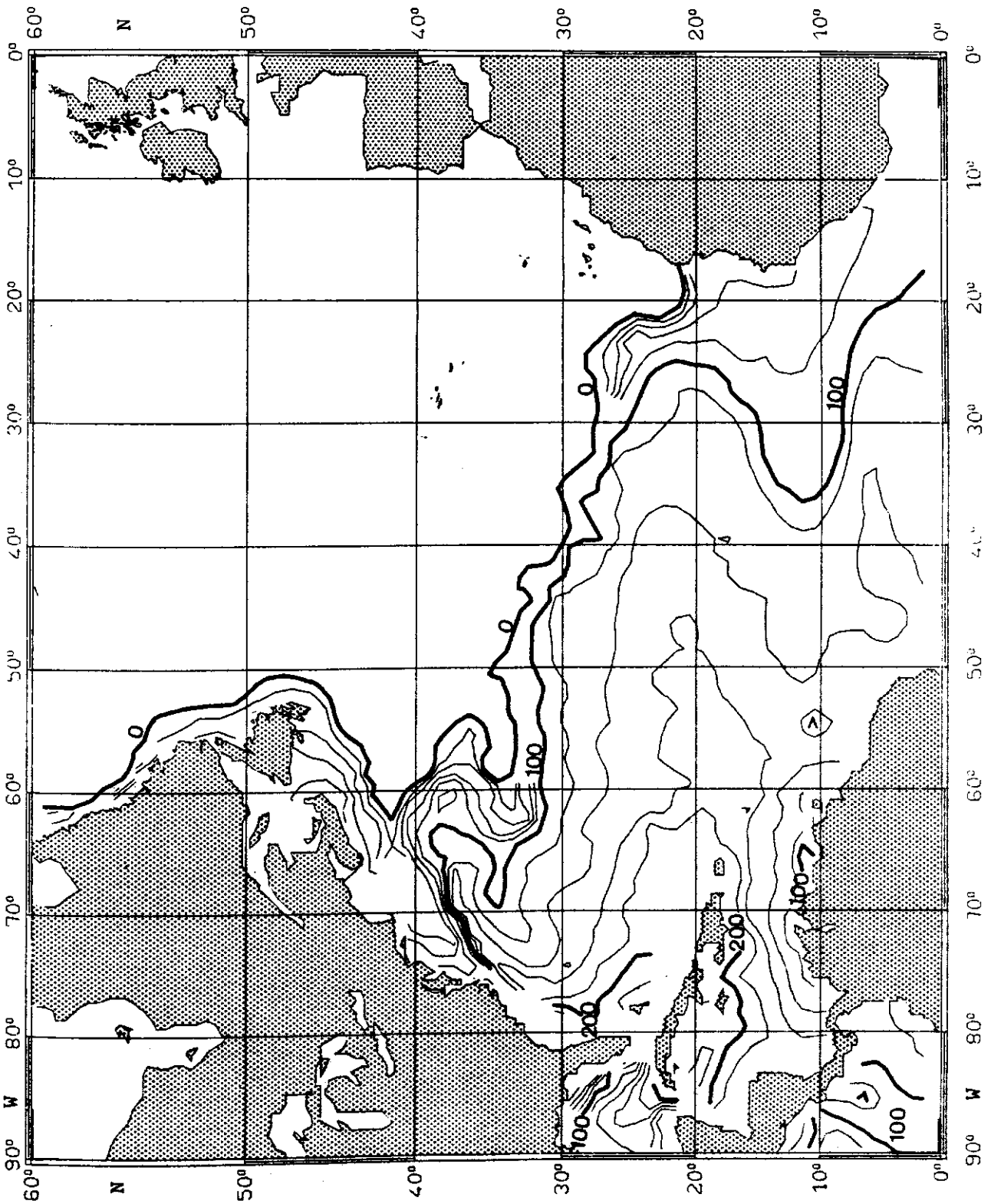

Fig. 8:

TEMPERATURE (°C) on σ_θ = 26.0 kg m^{-3} JANUARY

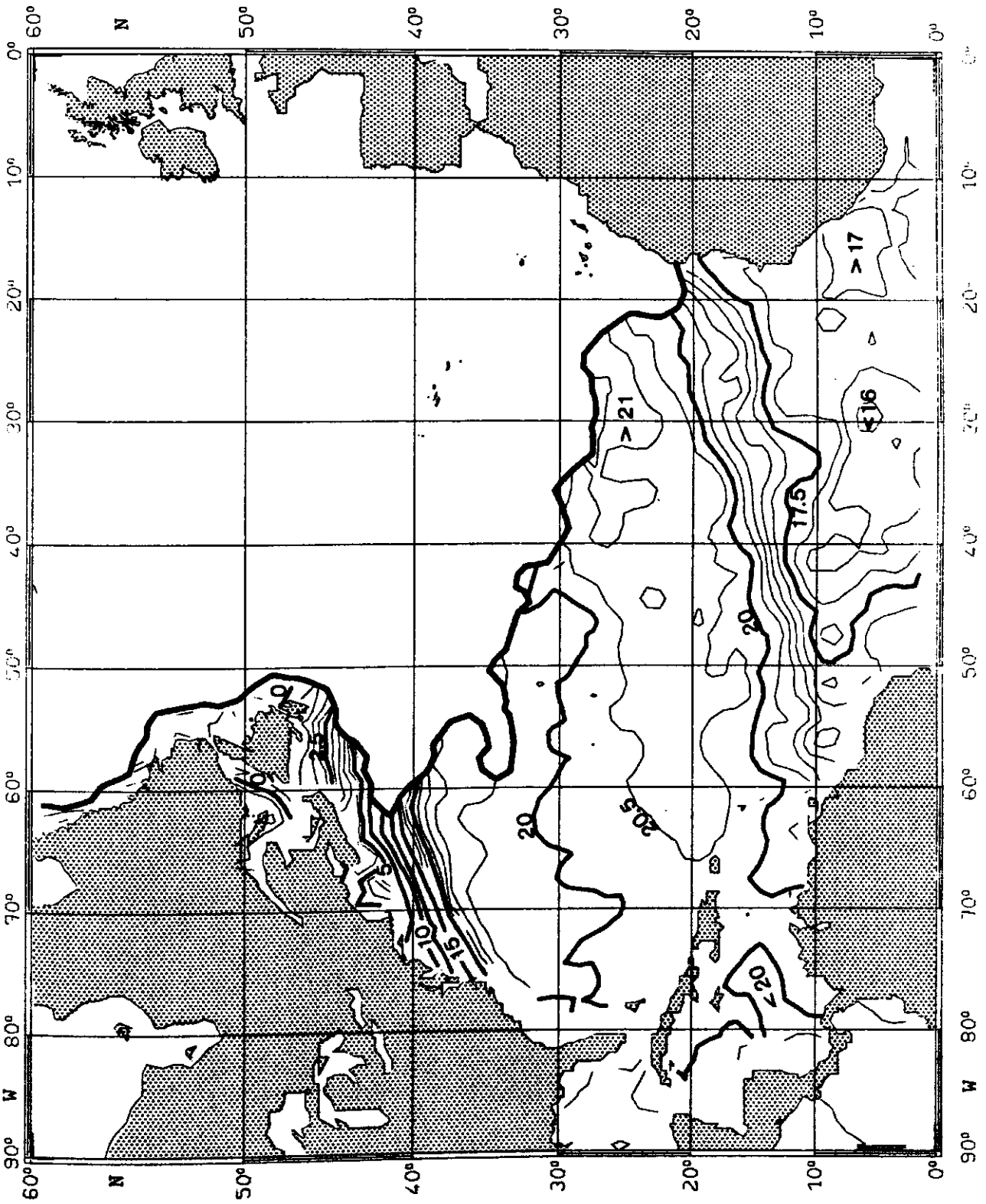

Fig. 9:

SALINITY (10^{-3}) on σ_θ = 26.0 kg m^{-3} JANUARY

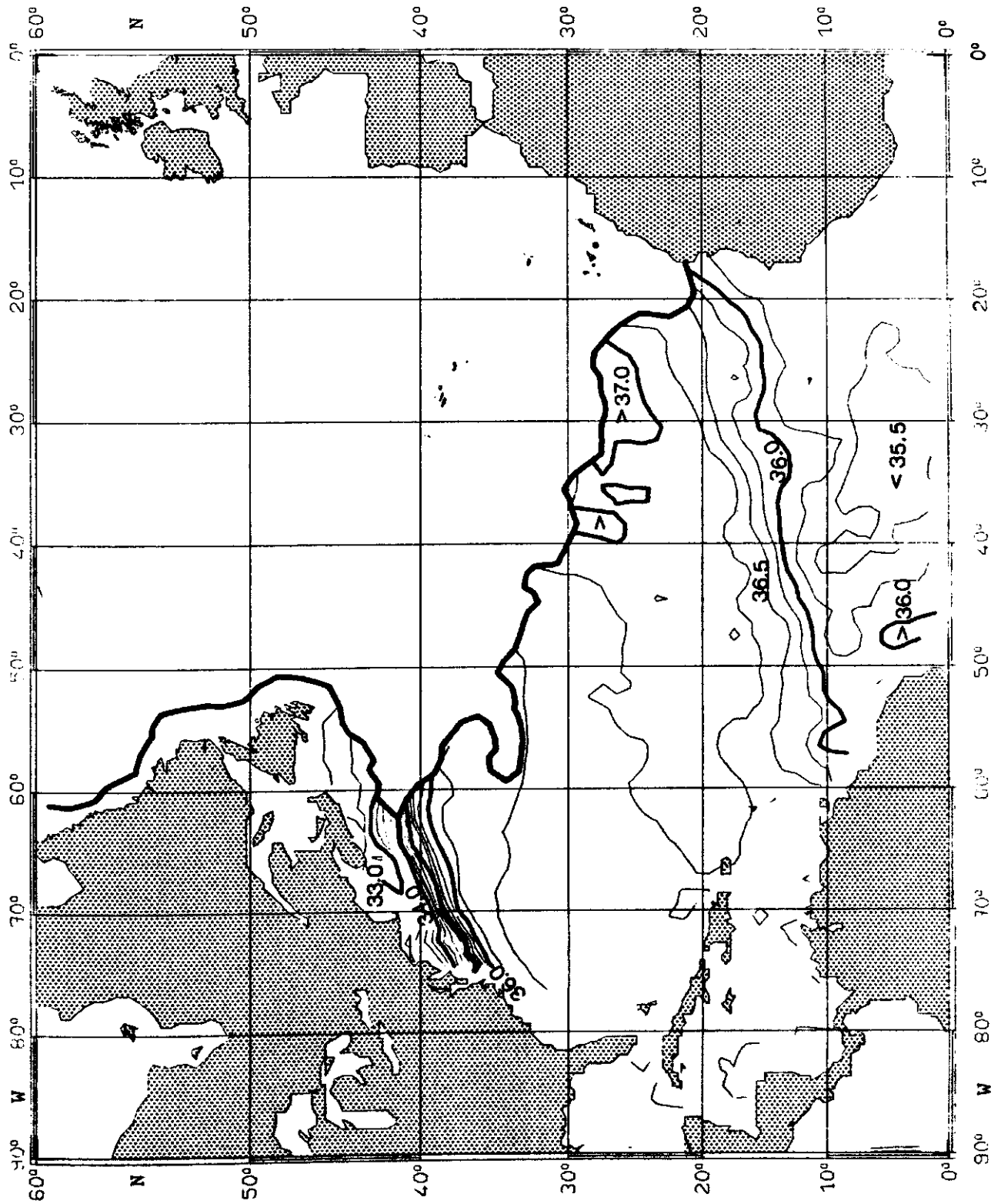

Fig. 10:

PRESSURE (10^4 Pa) on σ_θ = 27.0 kg m^{-3} JANUARY

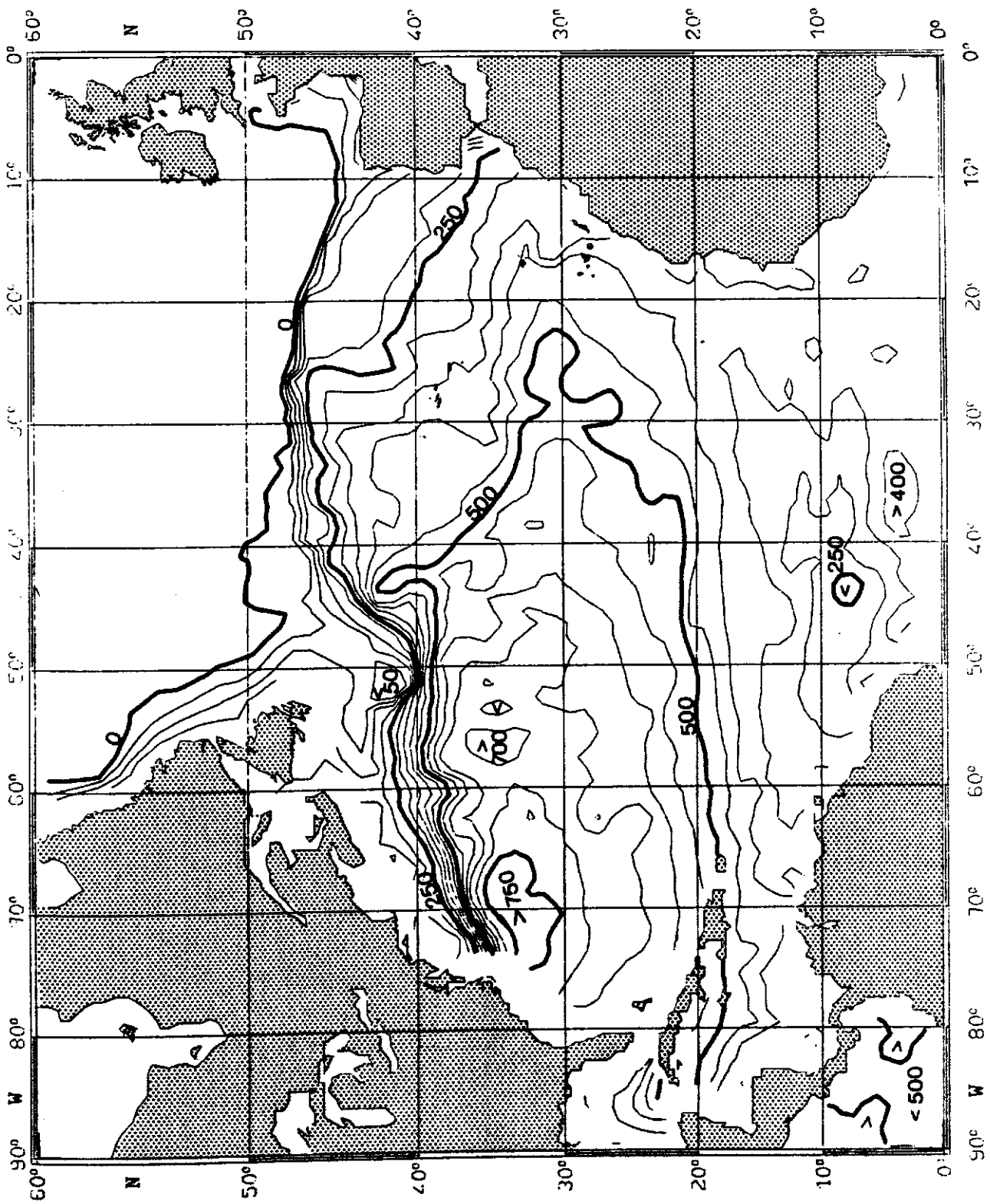

Fig. 11:

TEMPERATURE (°C) on σ_θ = 27.0 kg m^{-3} JANUARY

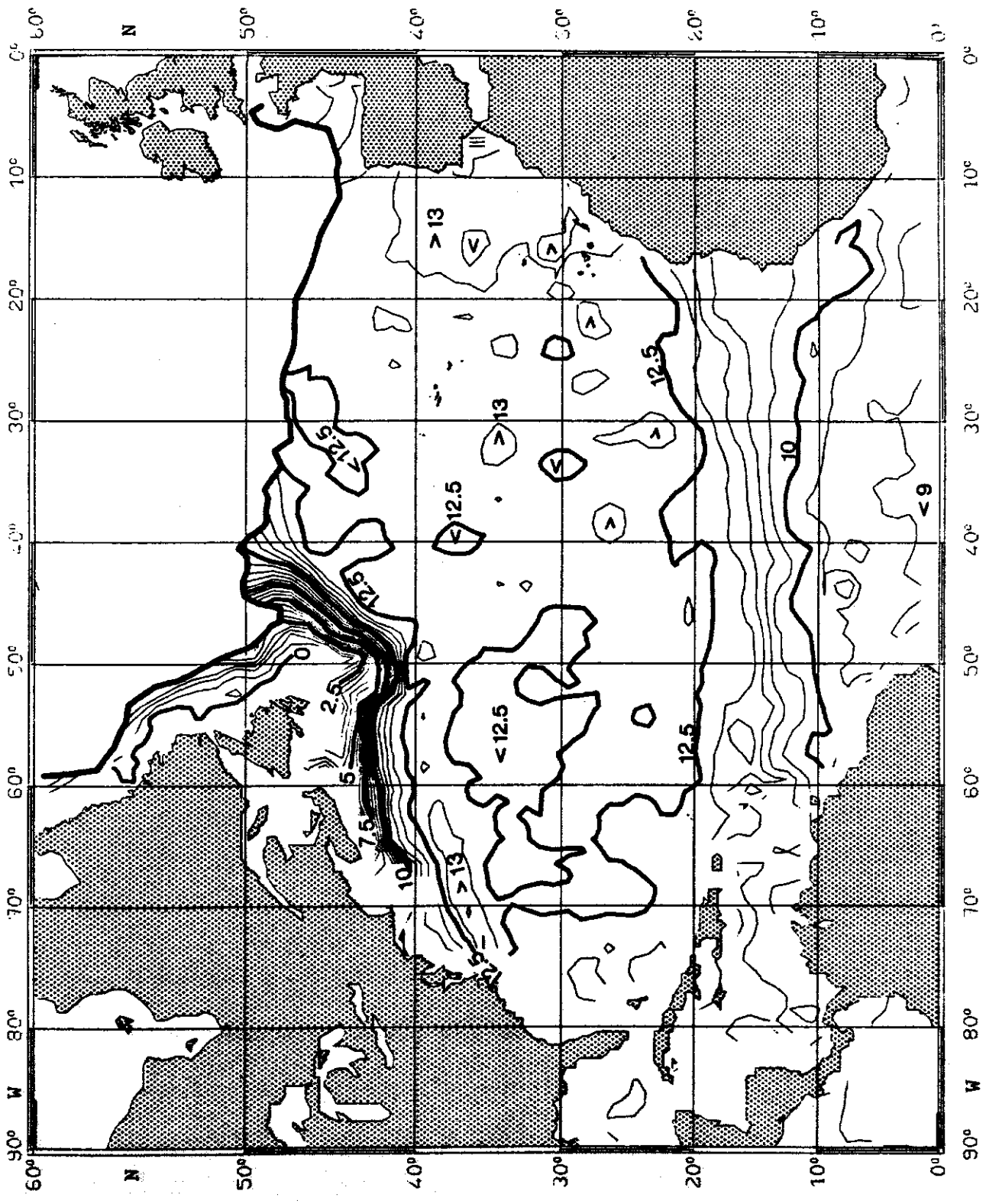

Fig. 12:

SALINITY (10^{-3}) on σ_θ = 27.0 kg m^{-3} JANUARY

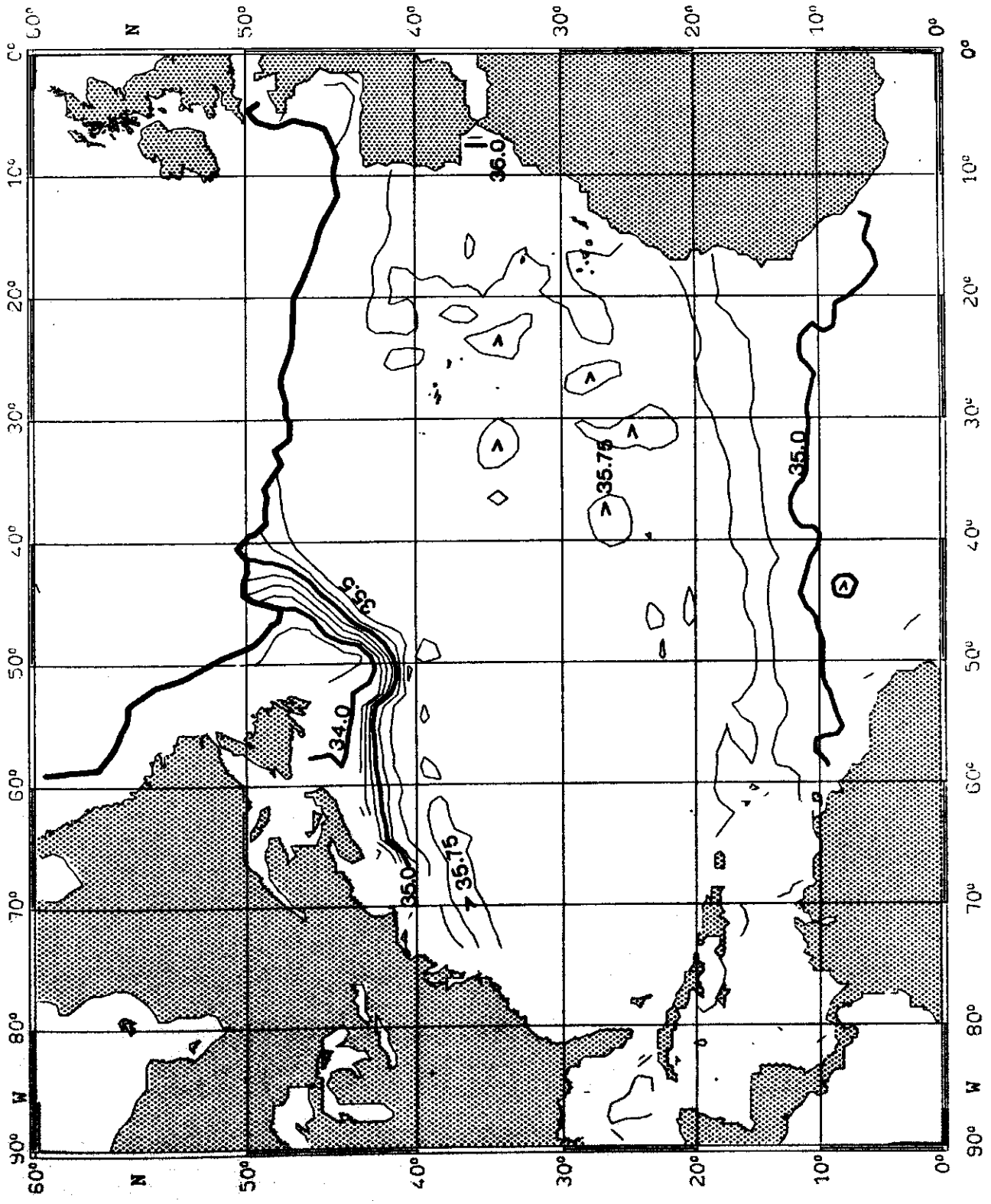

Fig. 13:

PRESSURE (10^4 Pa) on σ_θ = 25.0 kg^{-3} FEBRUARY

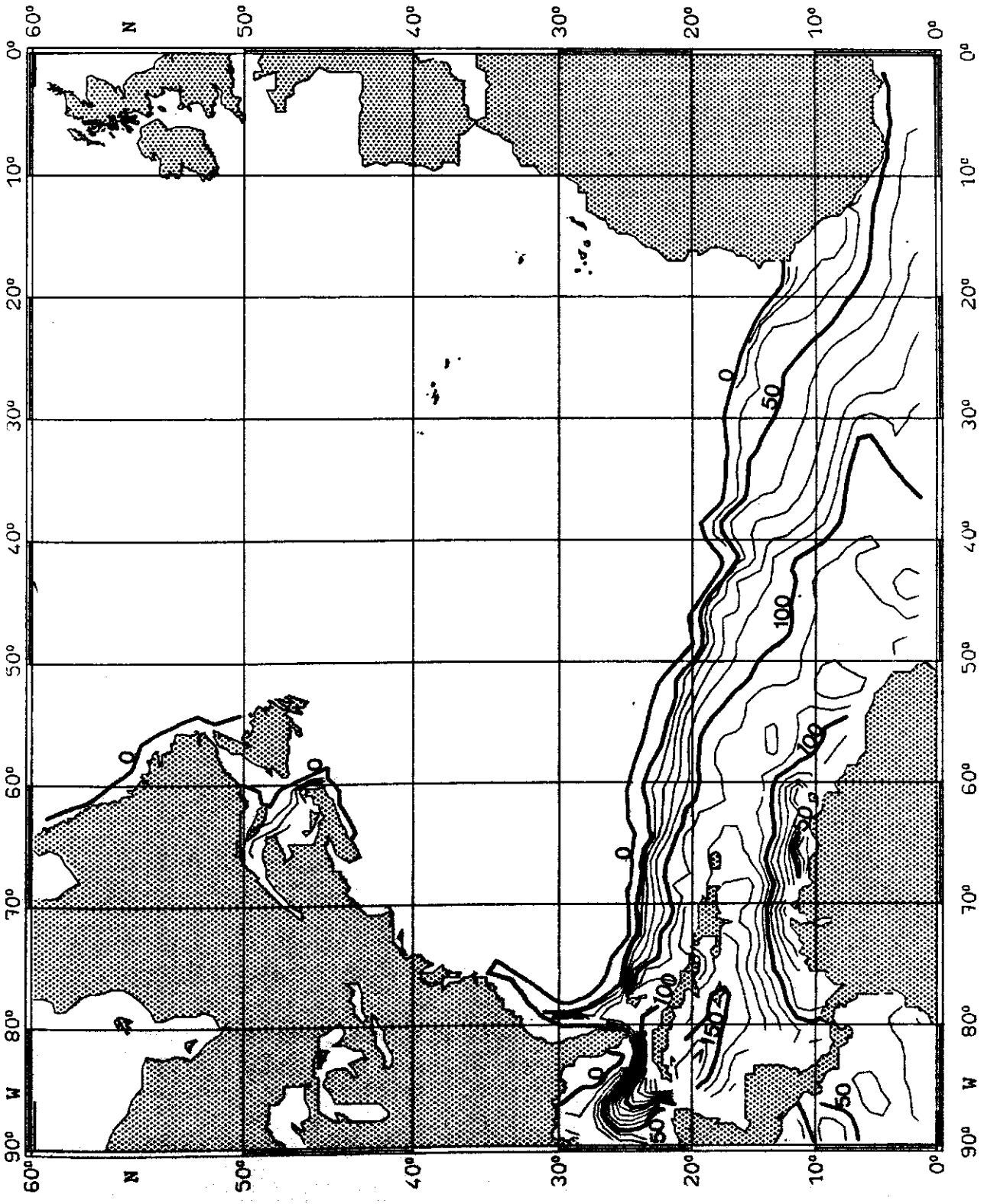

Fig. 14:

TEMPERATURE (°C) on σ_θ = 25.0 kg m^{-3} FEBRUARY

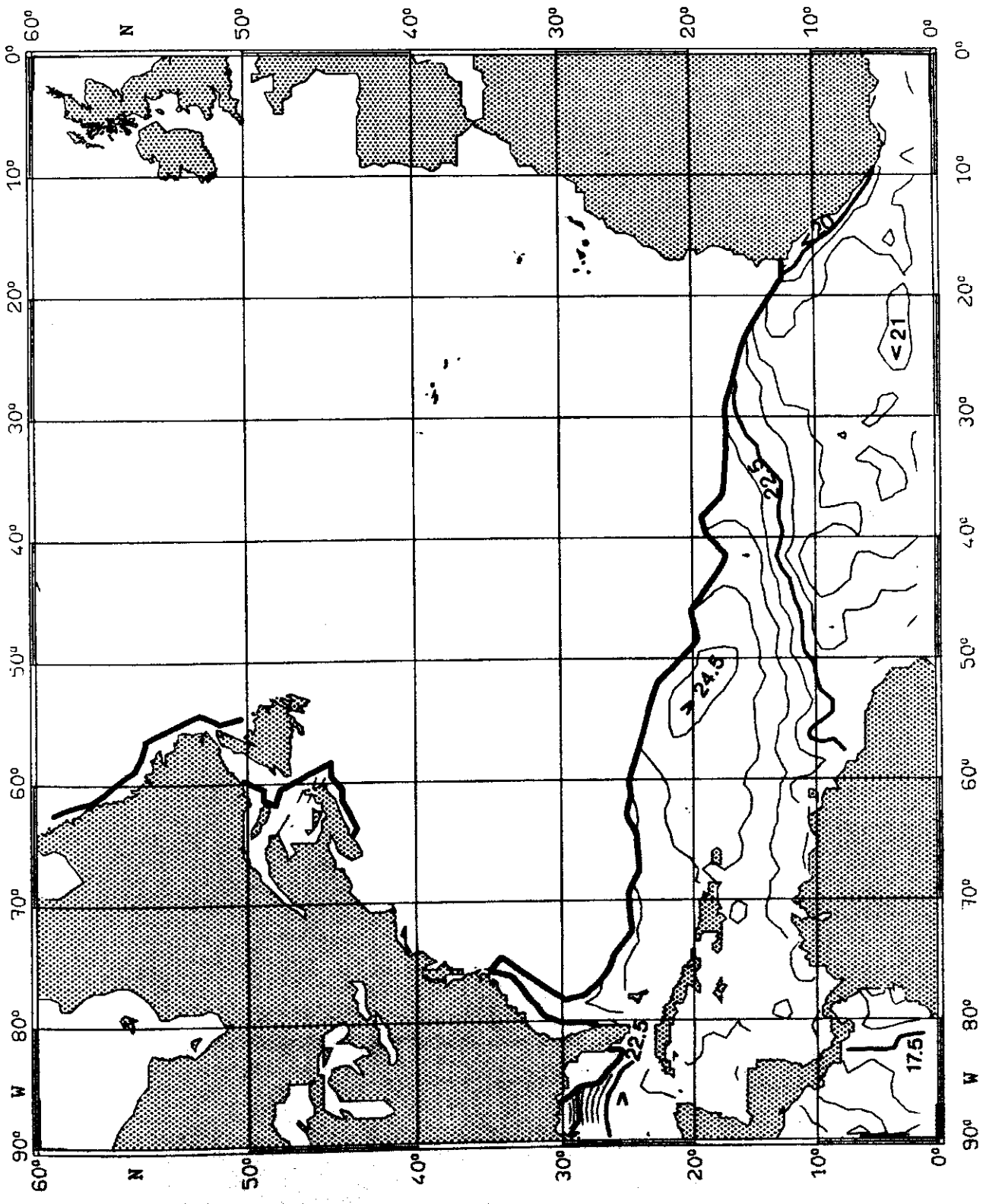

Fig. 15:

SALINITY (10^{-3}) on σ_θ = 25.0 kg m^{-3} FEBRUARY

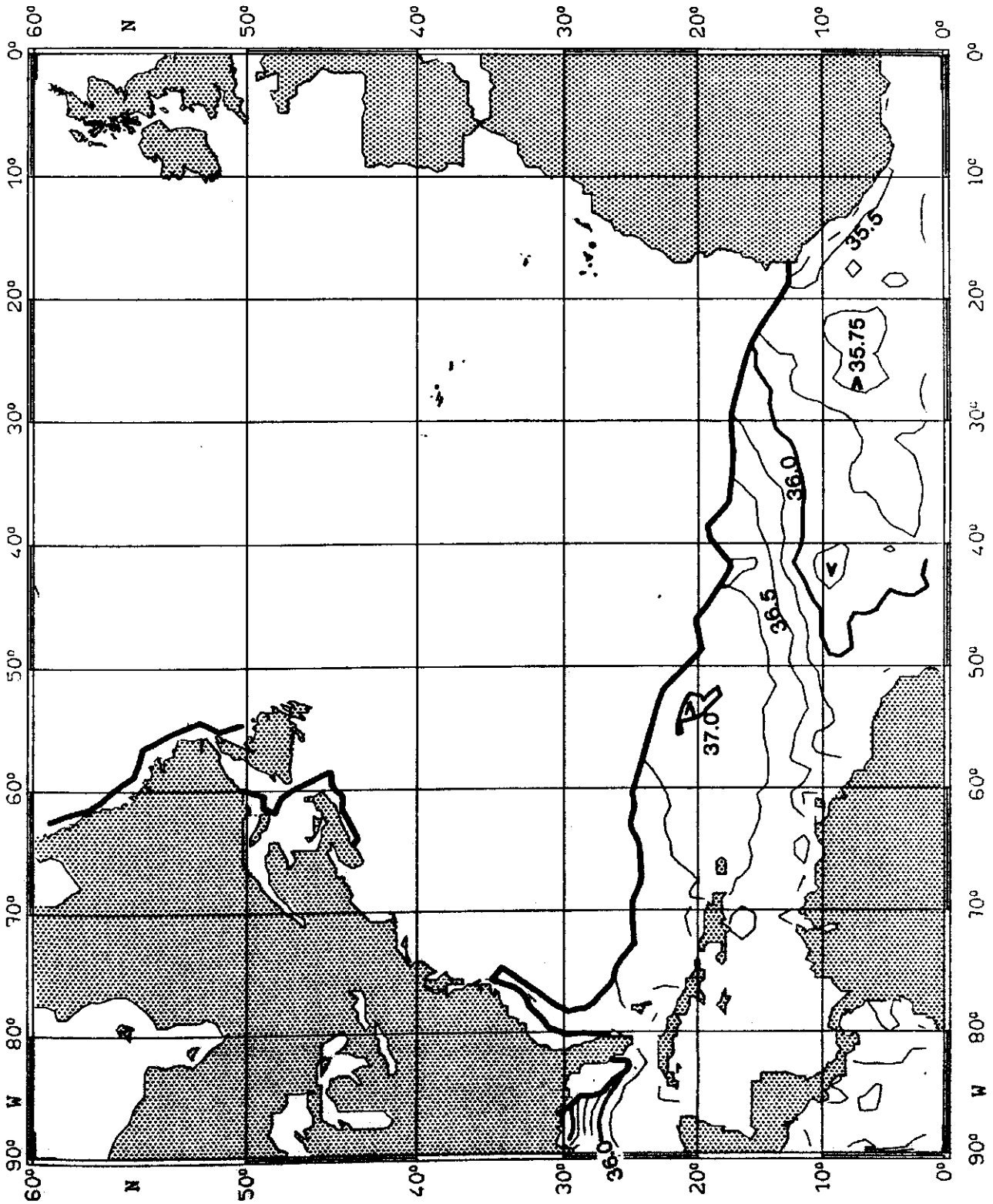

Fig. 16:

PRESSURE (10^4 Pa) on σ_θ = 26.0 kg m^{-3} FEBRUARY

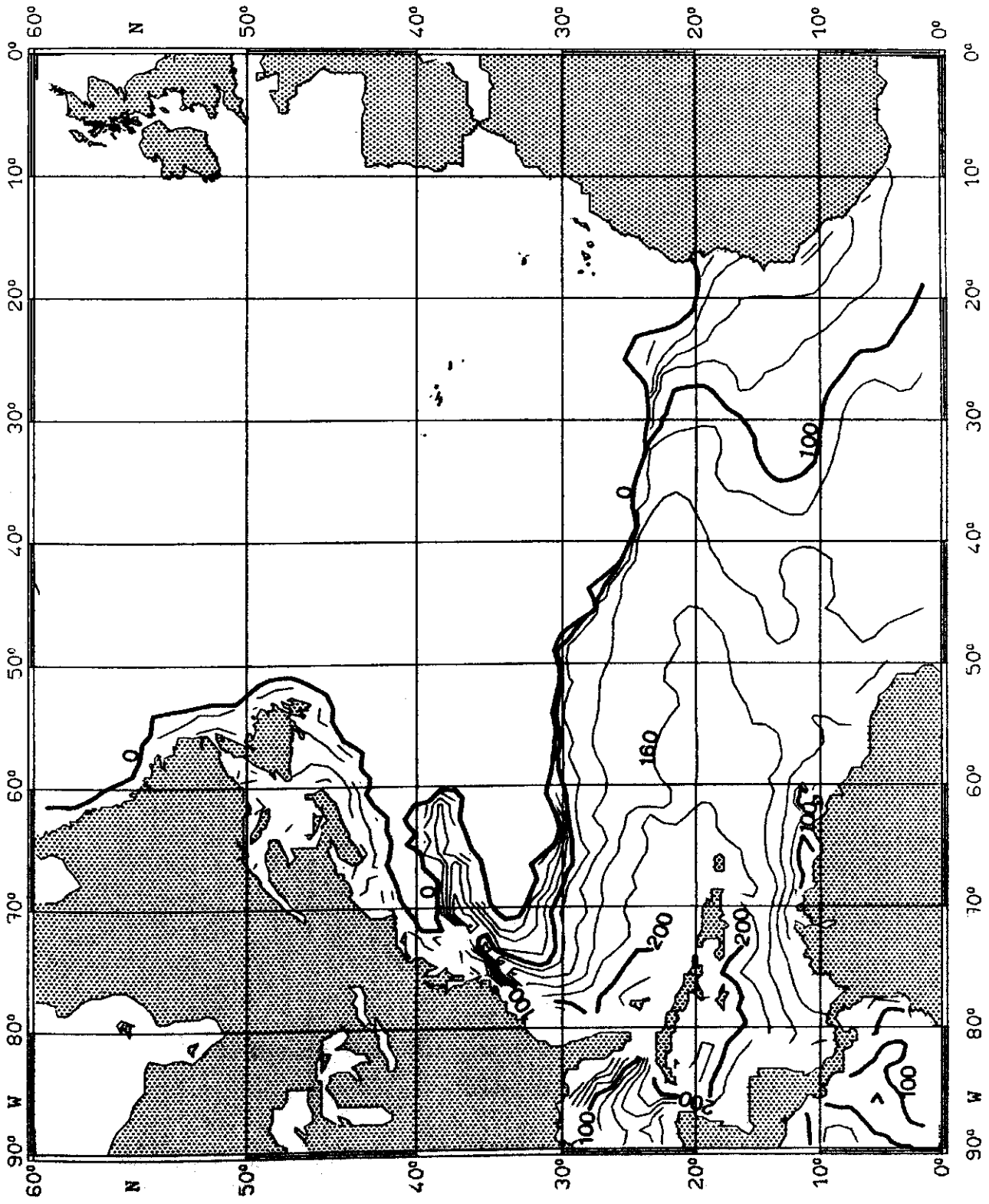

Fig. 17:

TEMPERATURE (°C) on σ_θ = 26.0 kg m FEBRUARY

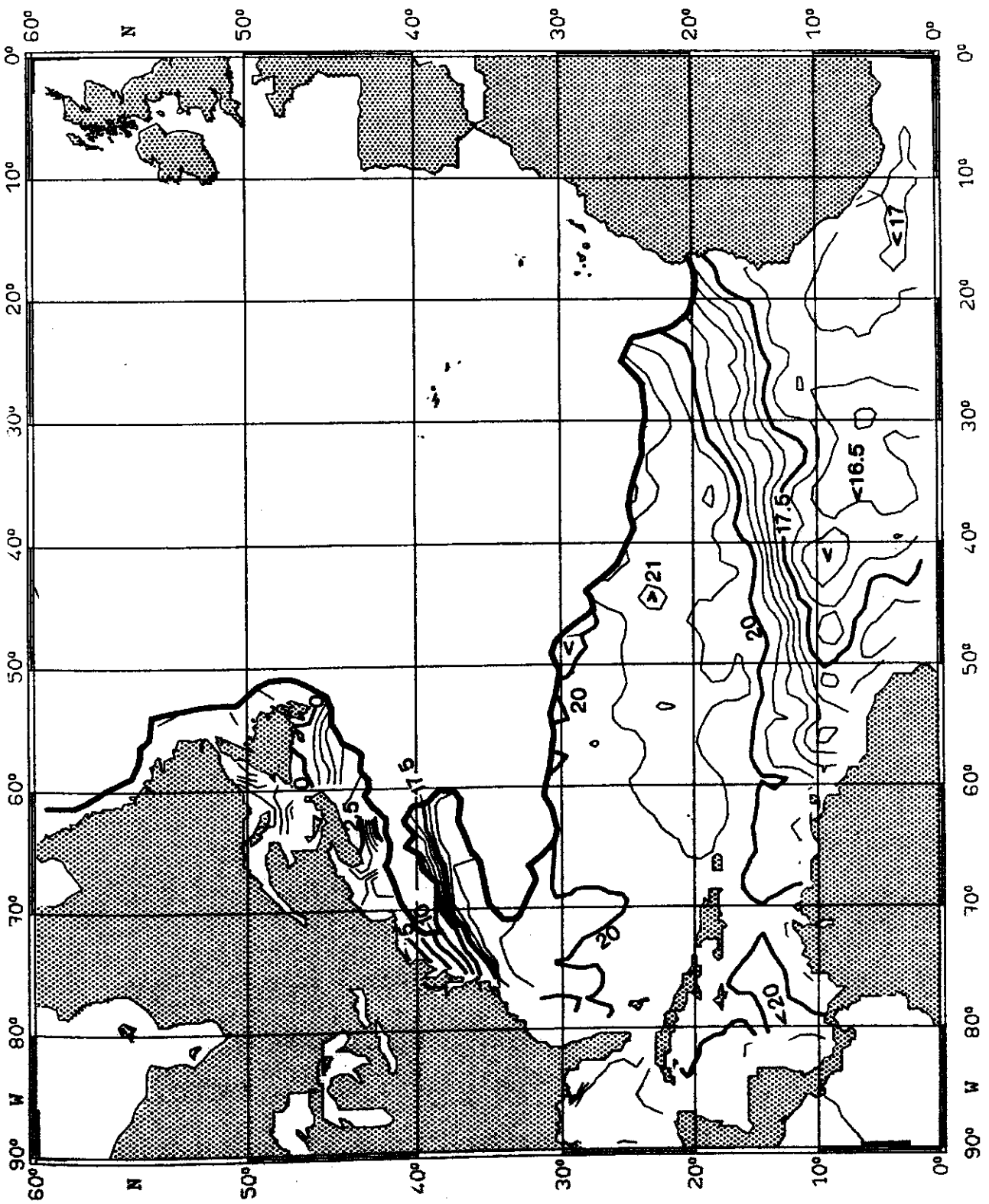

Fig. 18:

SALINITY (10^{-3}) on σ_θ = 26.0 kg m^{-3} FEBRUARY

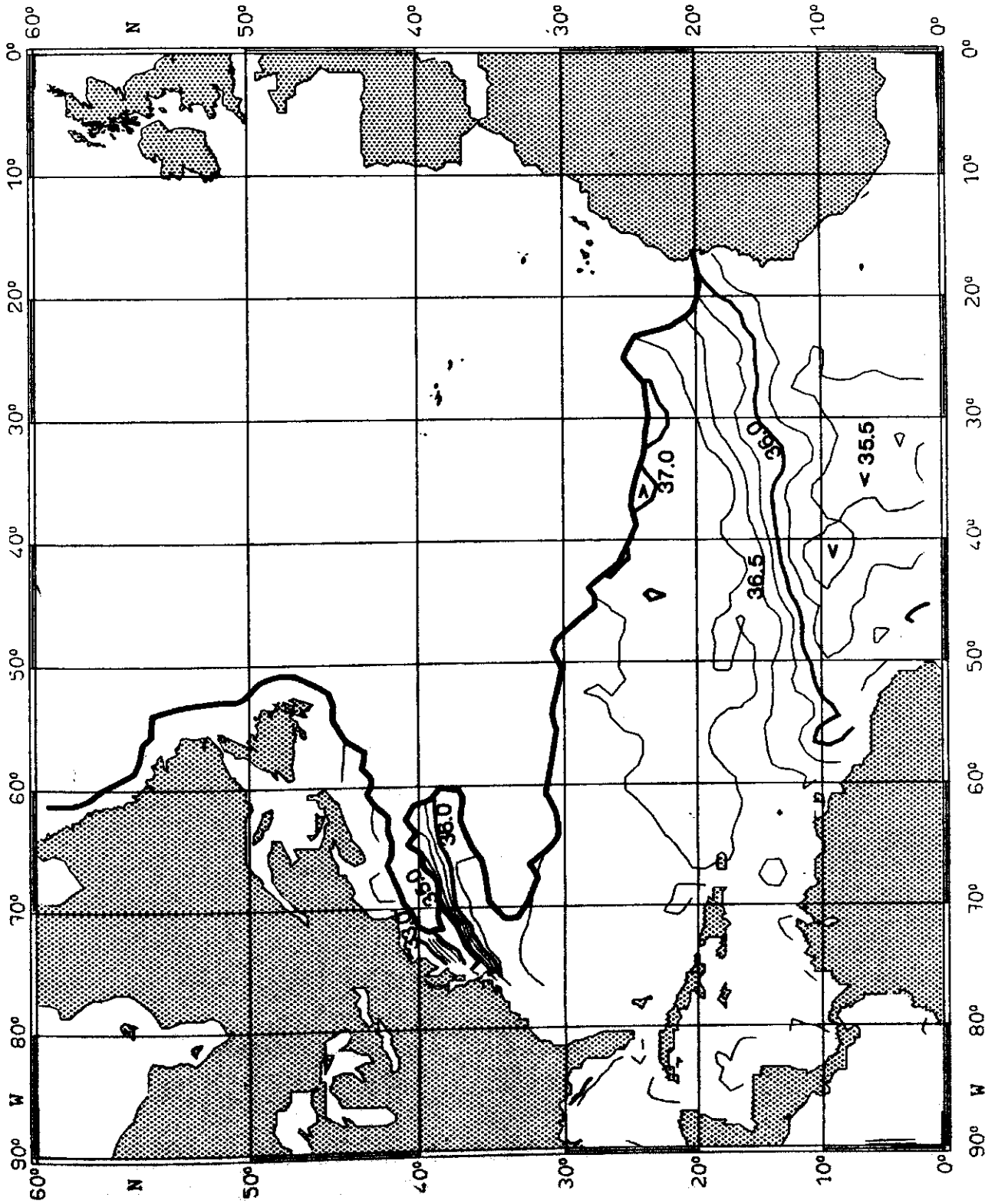

Fig. 19:

PRESSURE (10^4 Pa) on σ_θ = 27.0 kg m^{-3} FEBRUARY

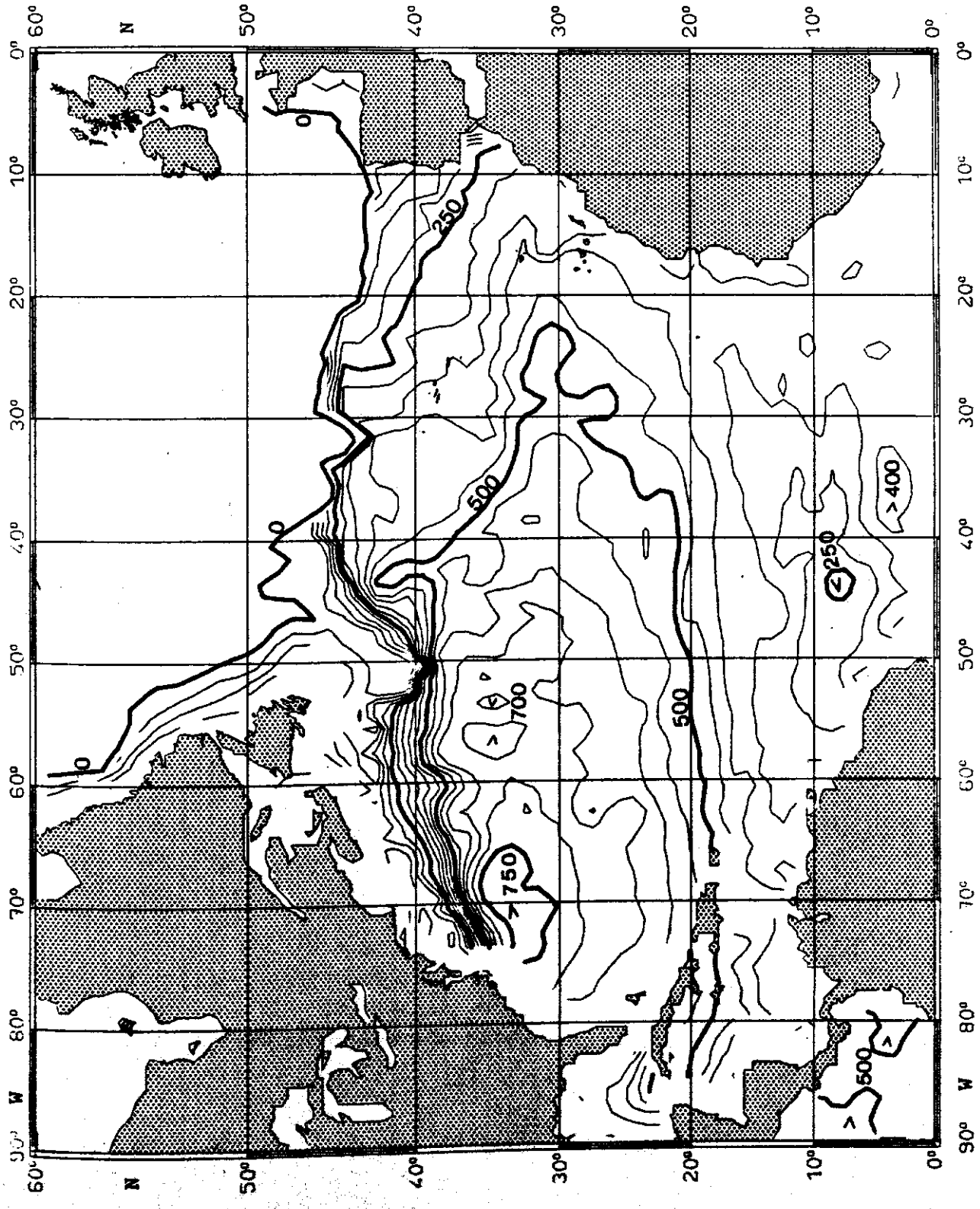

Fig. 20:

TEMPERATURE (°C) on σ_θ = 27.0 kg m^{-3} FEBRUARY

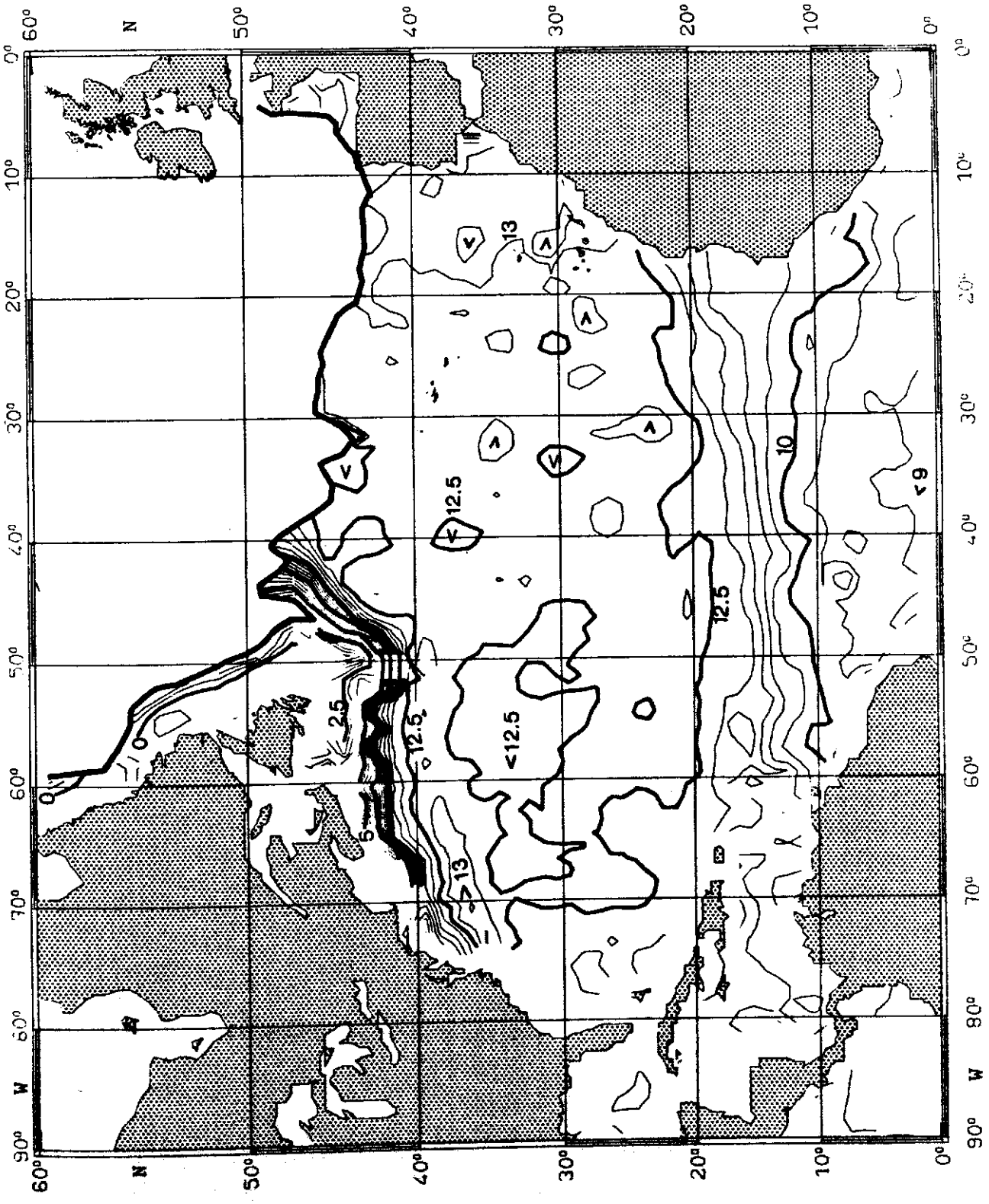

Fig. 21:

SALINITY (10^{-3}) on σ_θ = 27.0 kg m^{-3} FEBRUARY

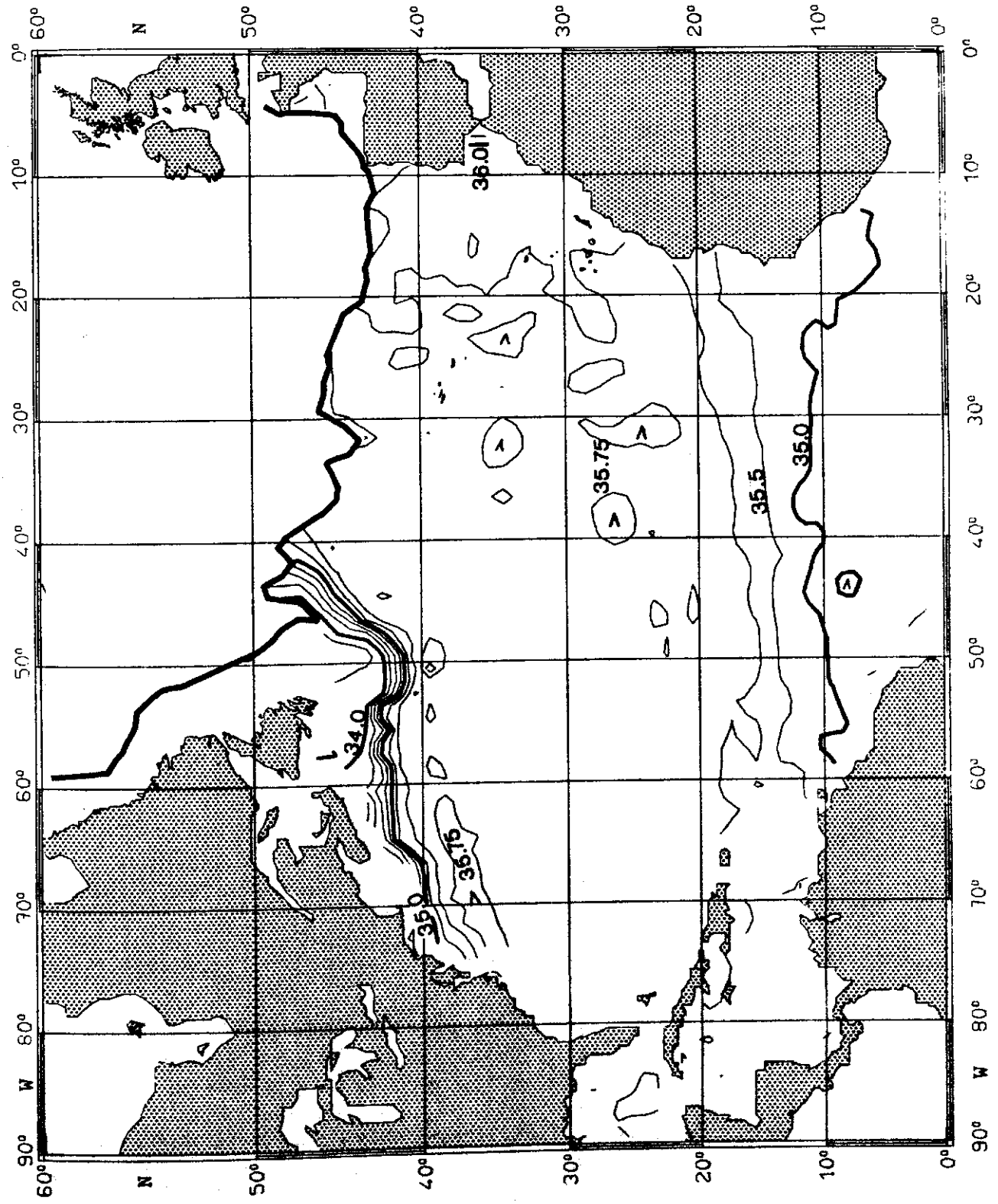

Fig. 22:

PRESSURE (10^4 Pa) on σ_θ = 27.5 kg m^{-3} FEBRUARY

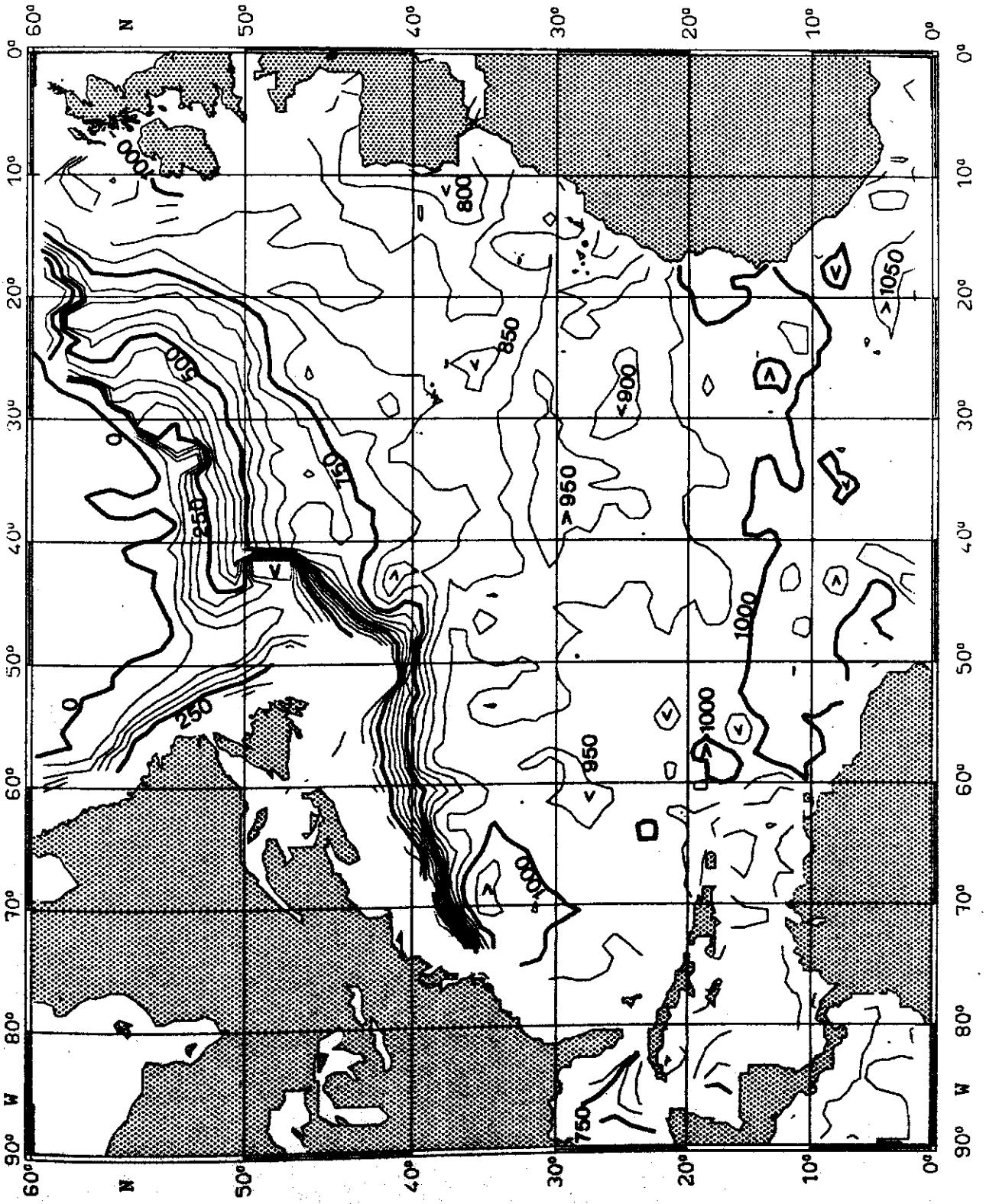

Fig. 23:

TEMPERATURE (°C) on σ_θ = 27.5 kg m^{-3} FEBRUARY

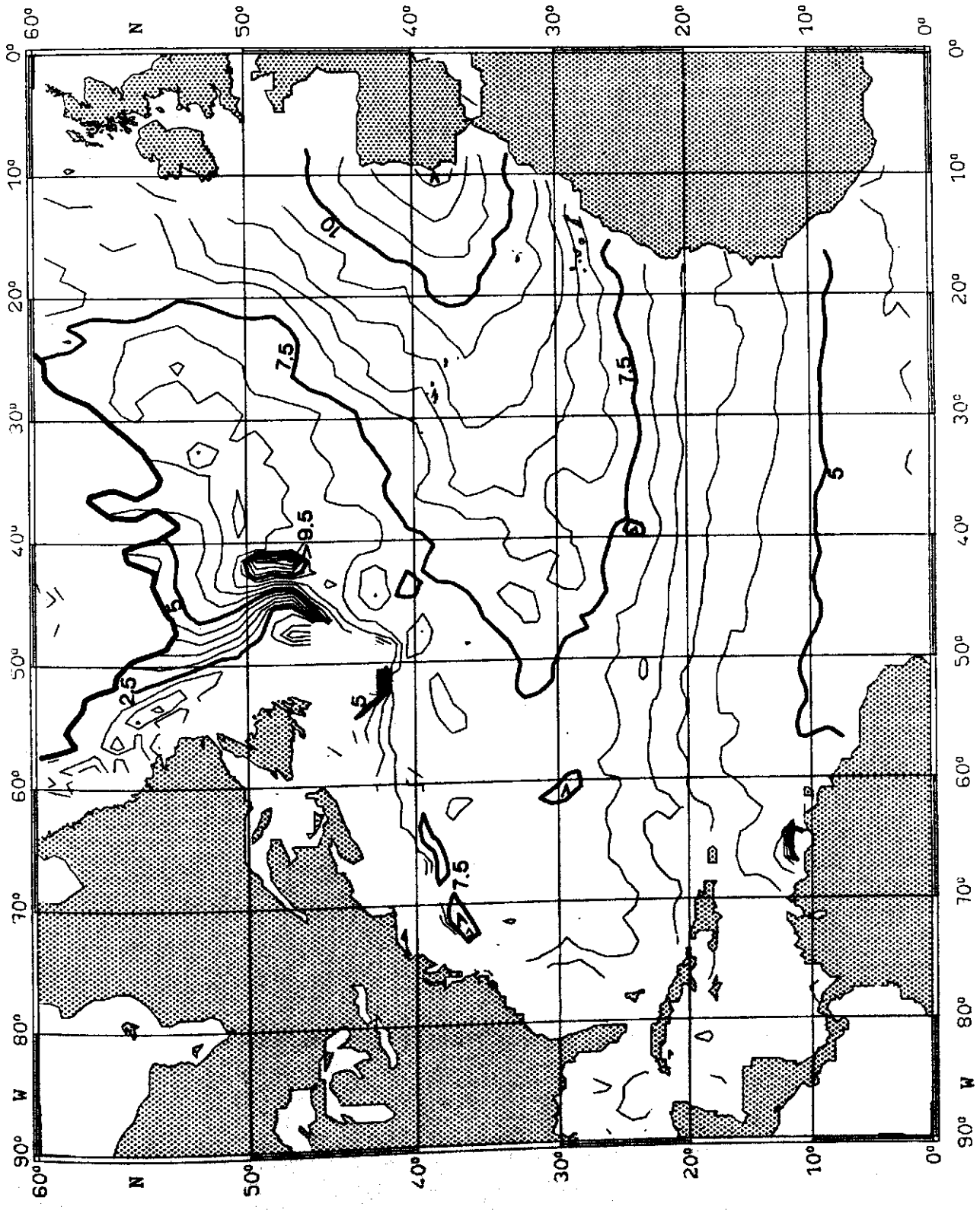

Fig. 24:

SALINITY (10^{-3}) on σ_θ = 27.5 kg m^{-3} FEBRUARY

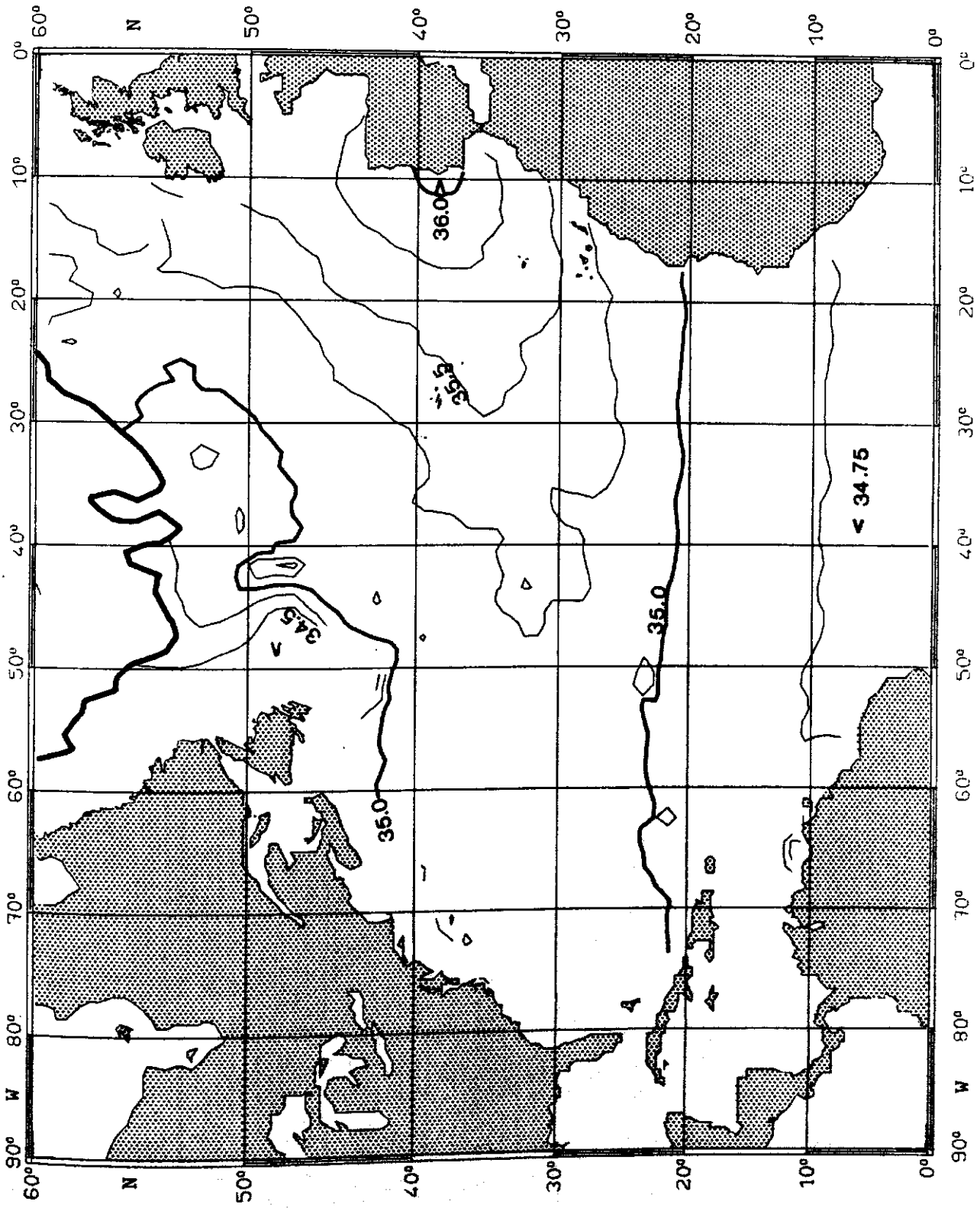

Fig. 25:

PRESSURE (10^4 Pa) on σ_θ = 25.0 kg m^{-3} MARCH

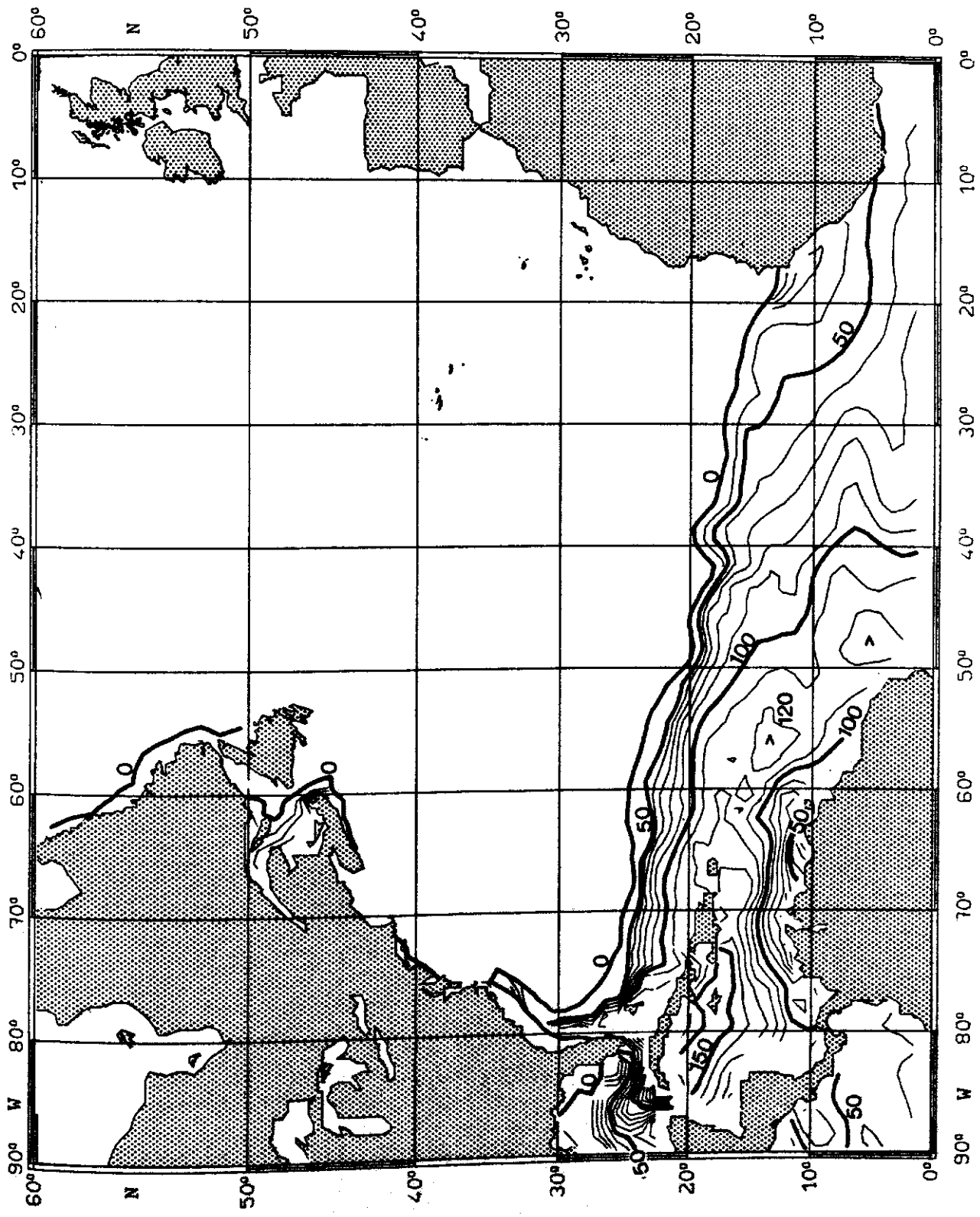

Fig. 26:

TEMPERATURE (°C) on σ_θ = 25.0 kg m^{-3} MARCH

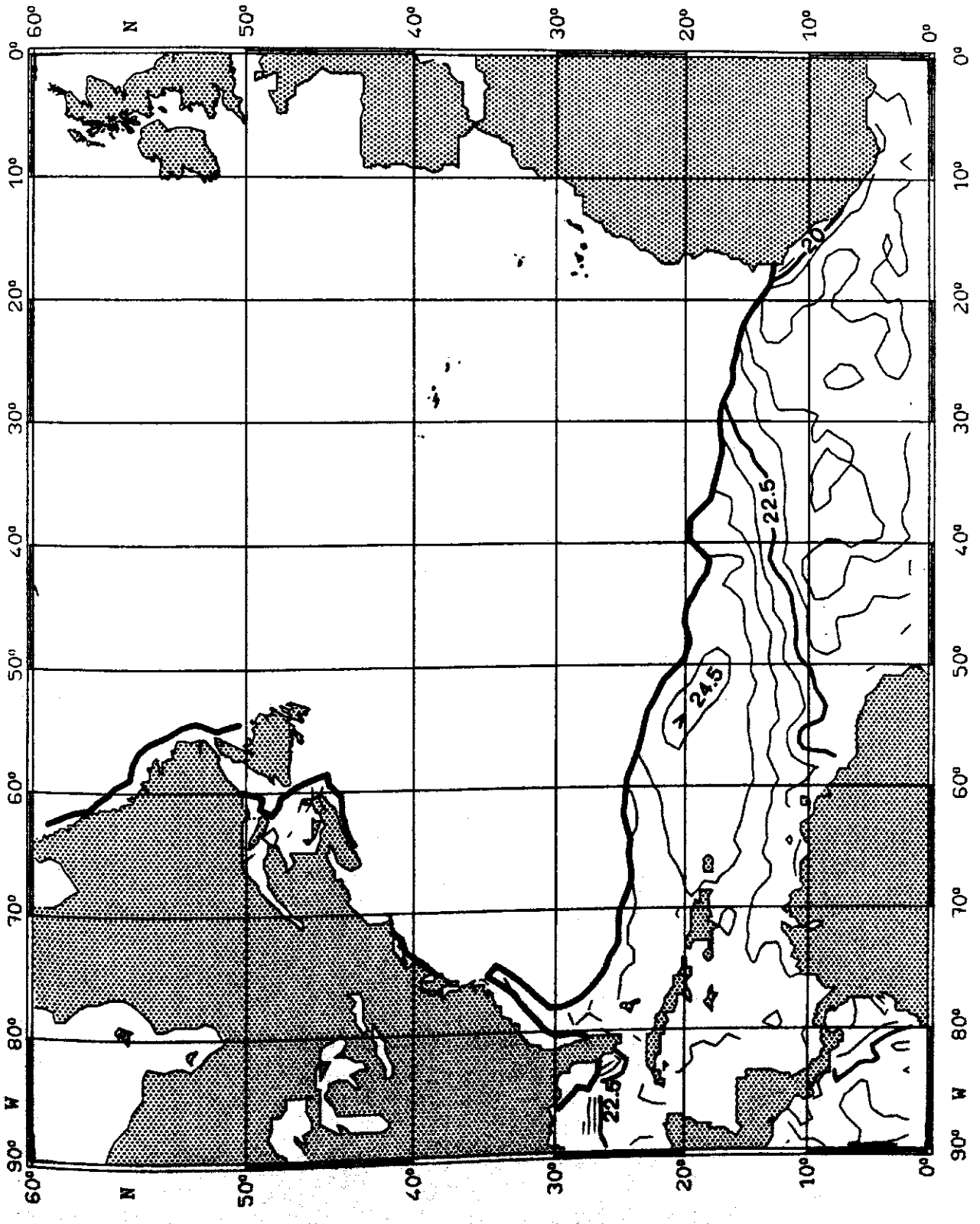

Fig. 27:

SALINITY (10^{-3}) on σ_θ = 25.0 kg m^{-3} MARCH

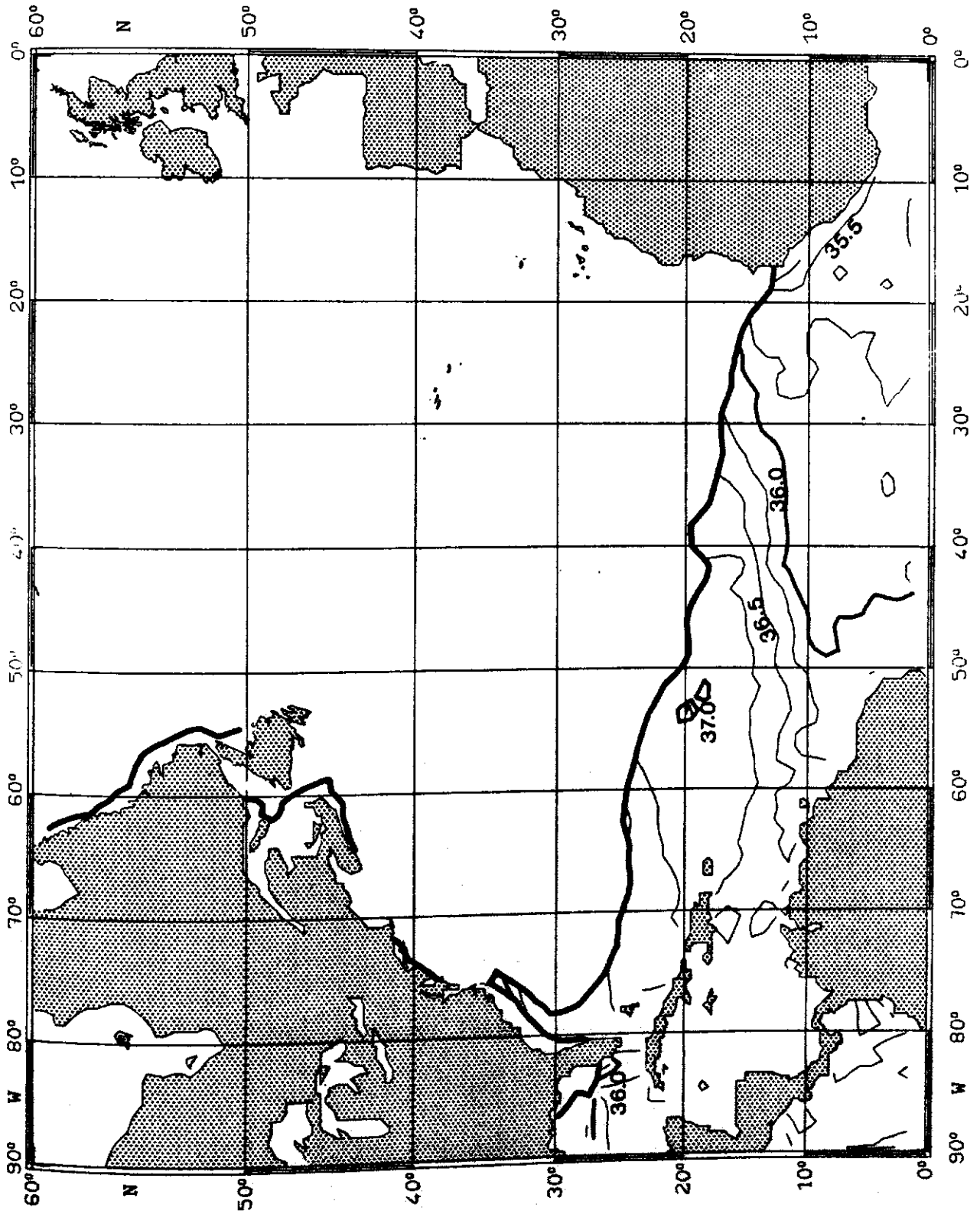

Fig. 28:

PRESSURE (10^4 Pa) on σ_θ = 26.0 kg m^{-3} MARCH

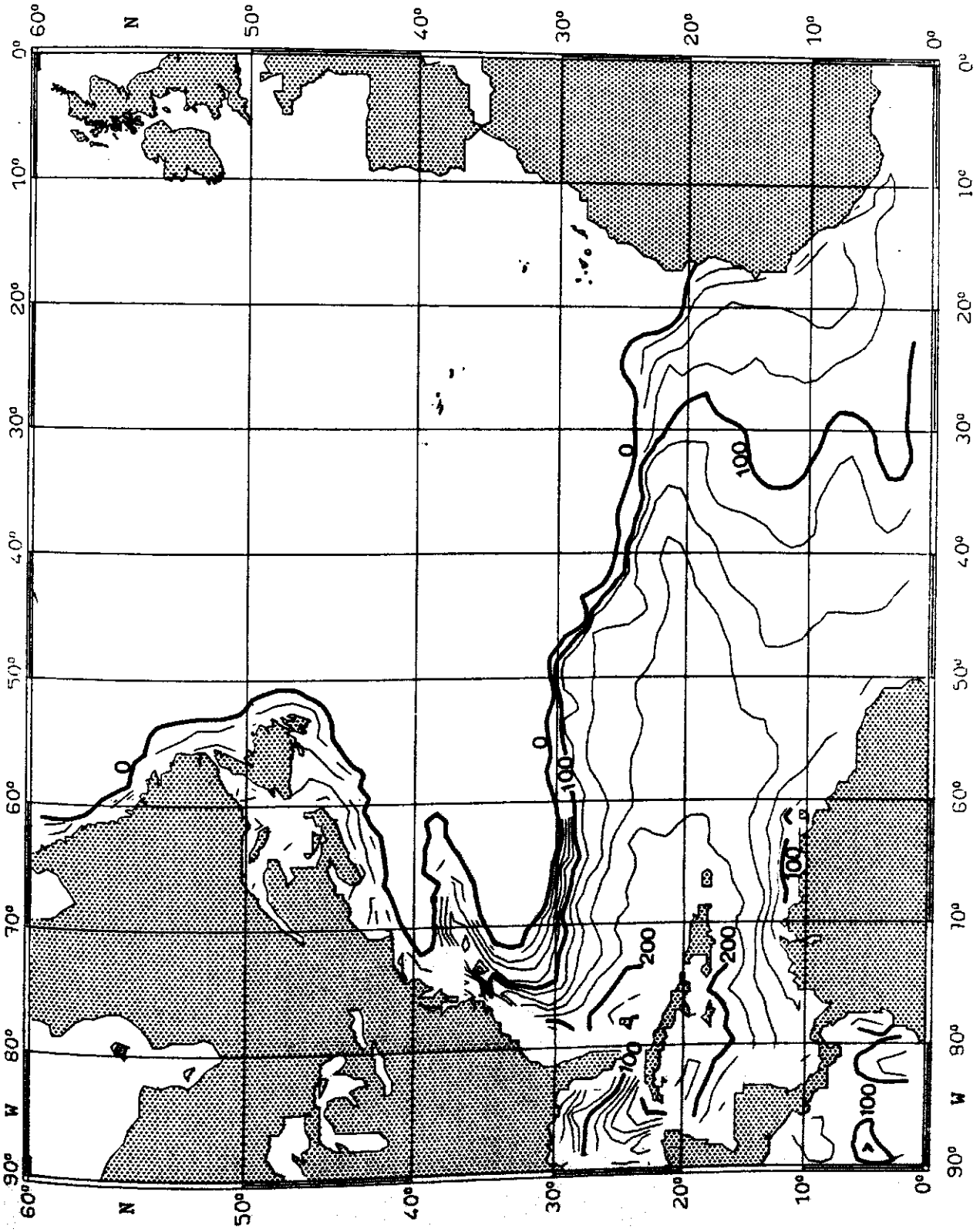

Fig. 29:

TEMPERATURE (°C) on σ_θ = 26.0 kg m^{-3} MARCH

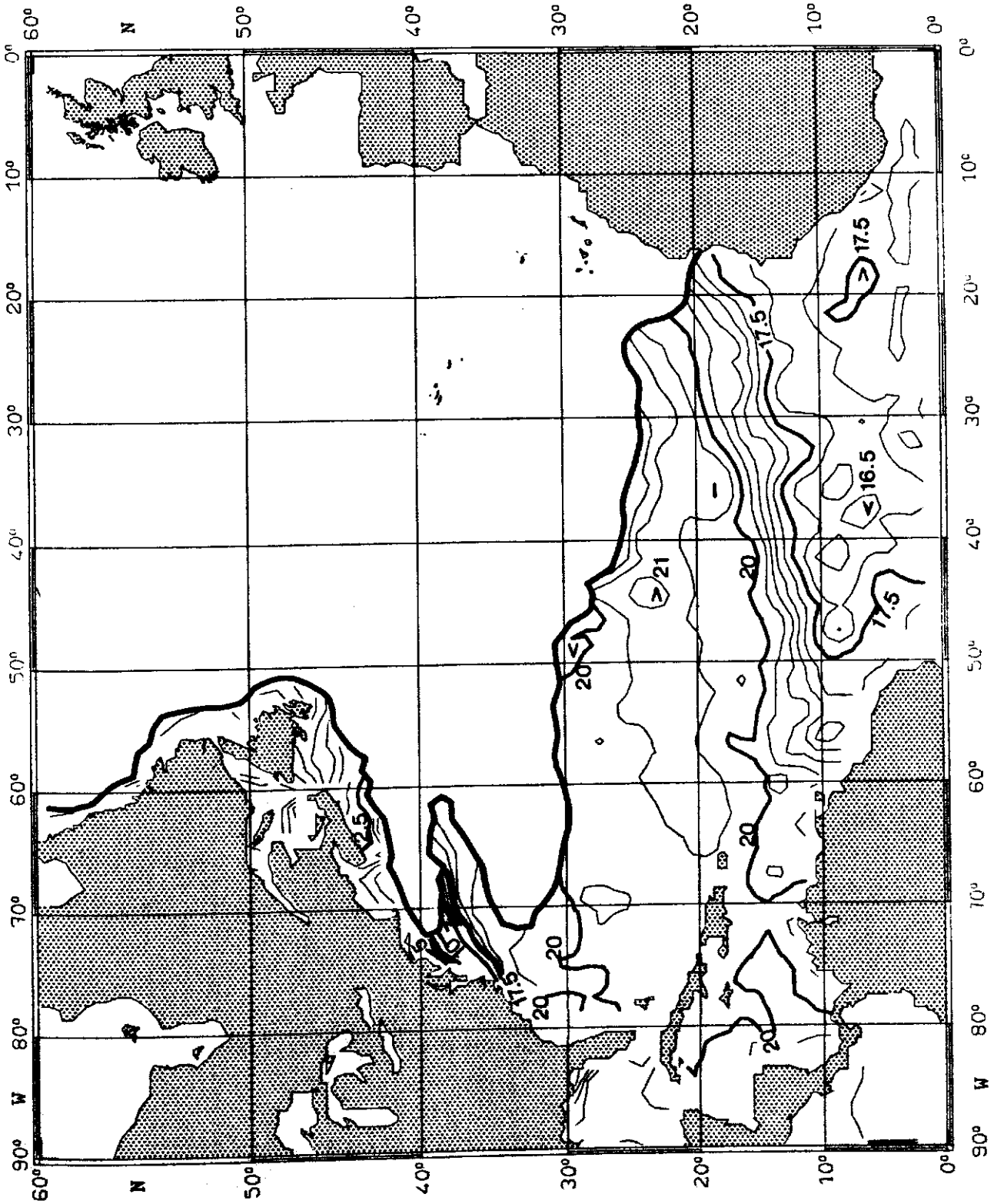

Fig. 30:

SALINITY (10^{-3}) on σ_θ = 26.0 kg m^{-3} MARCH

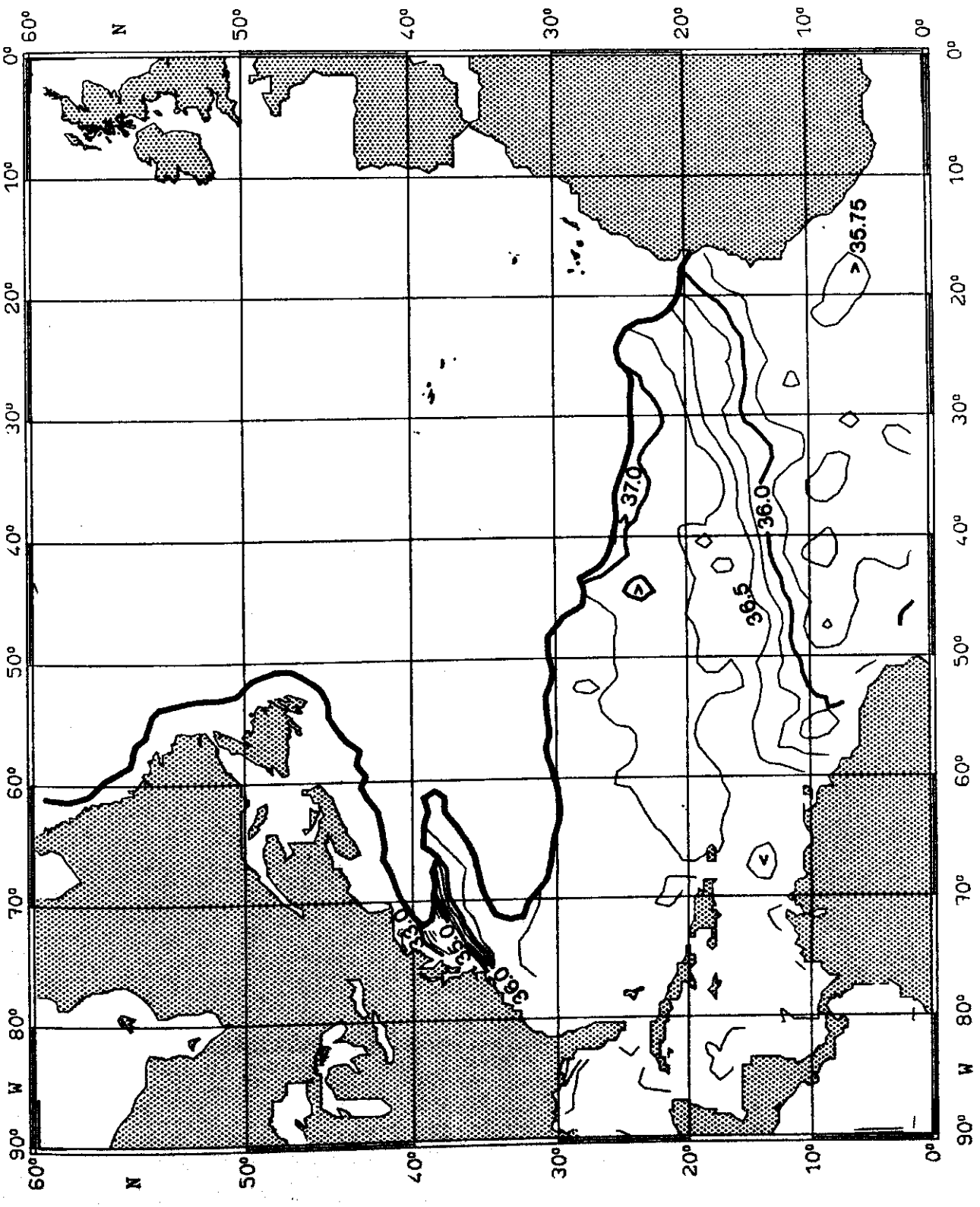

Fig. 31:

PRESSURE (10^4 Pa) on σ_θ = 27.0 kg m^{-3} MARCH

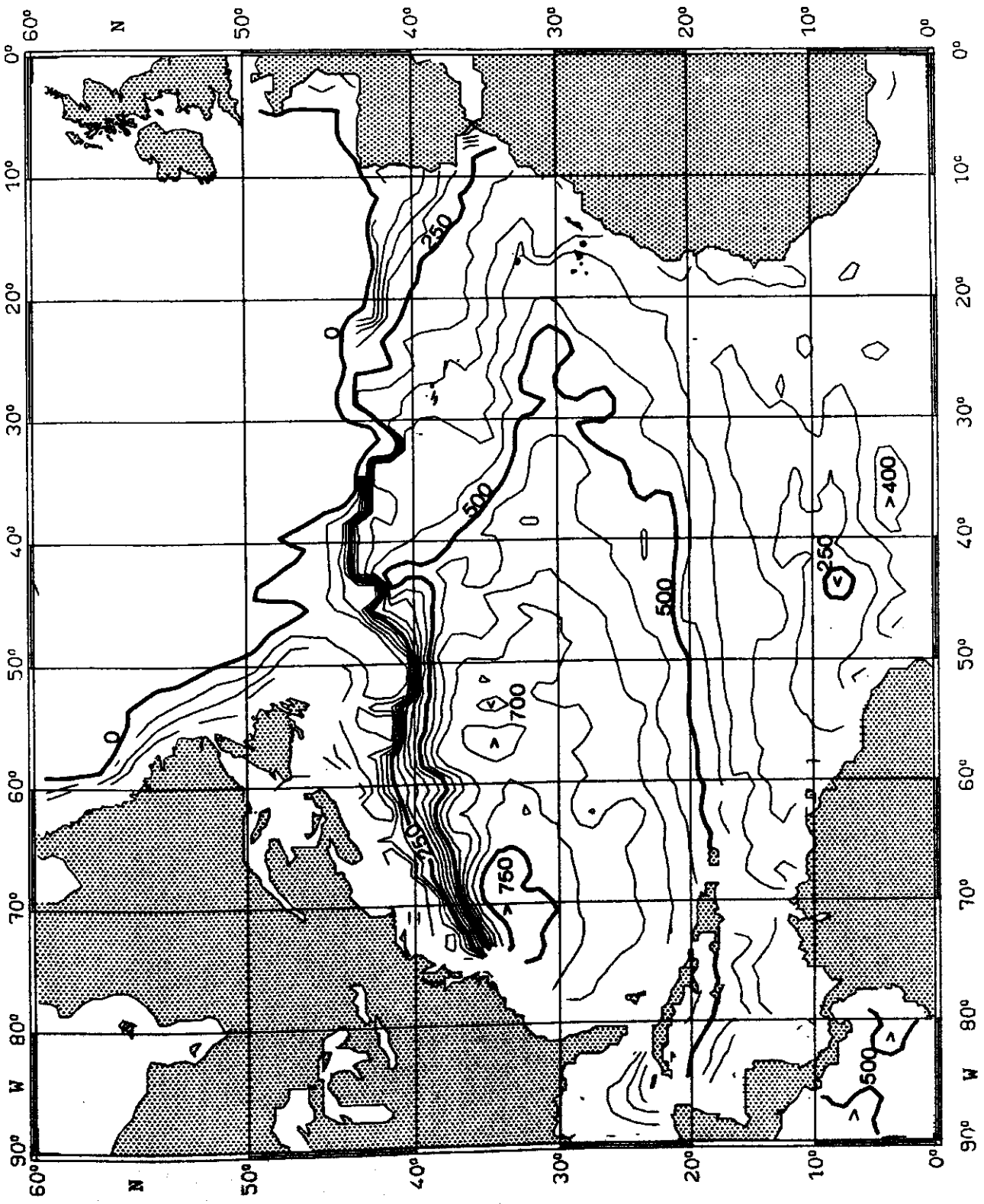

Fig. 32:

TEMPERATURE (°C) on σ_θ = 27.0 kg m^{-3} MARCH

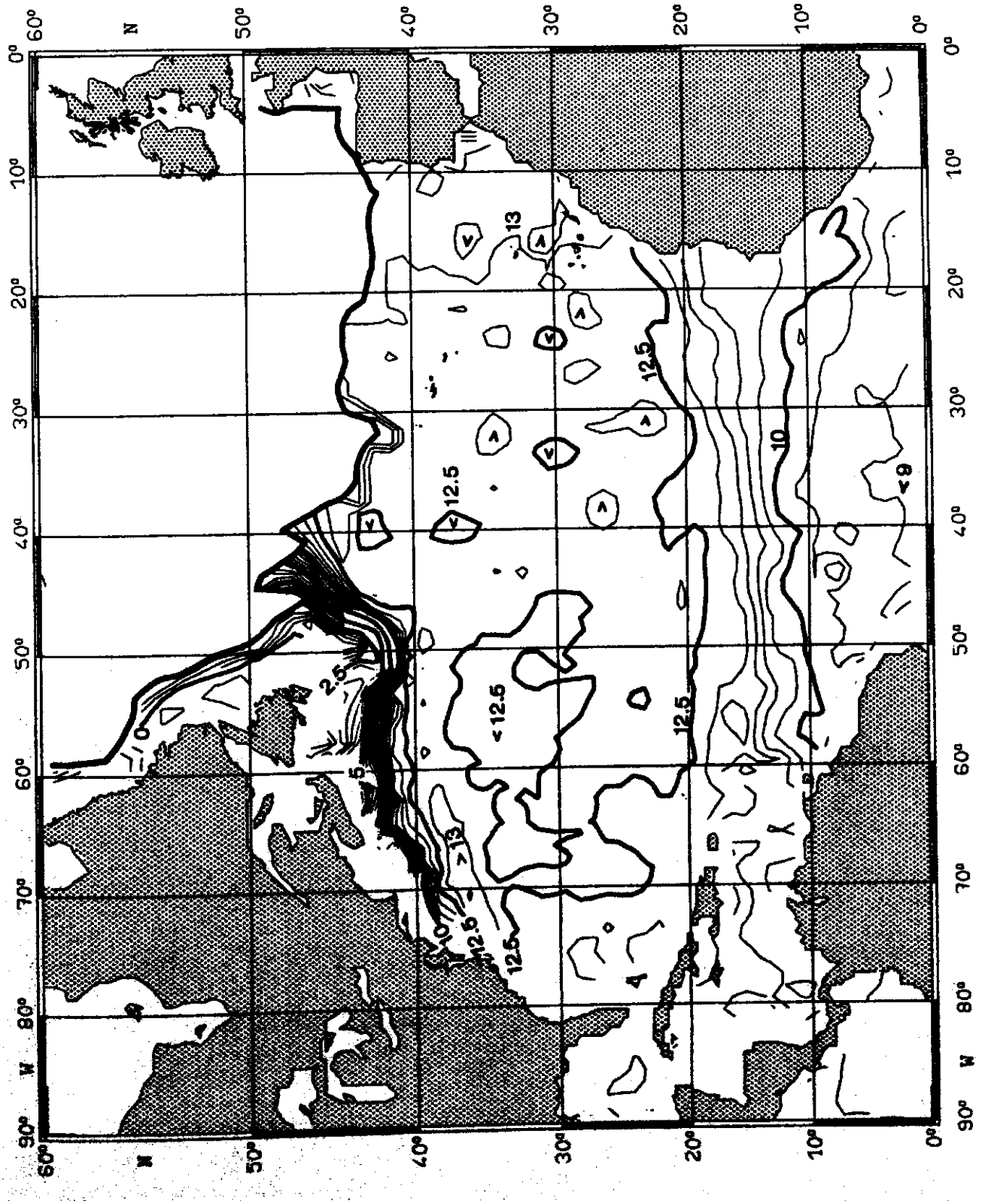

Fig. 33:

SALINITY (10^{-3}) on σ_θ = 27.0 kg m^{-3} MARCH

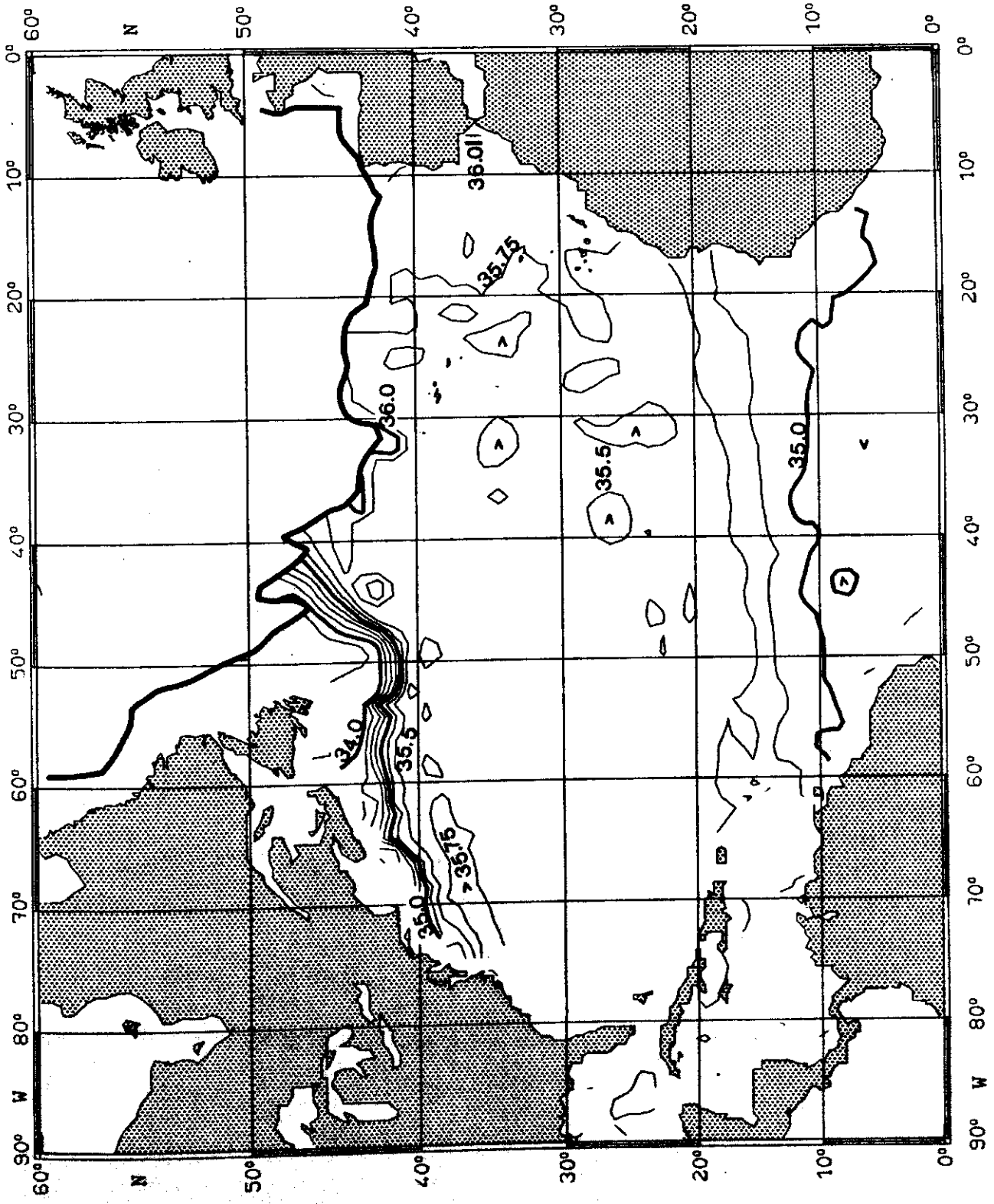

Fig. 34:

PRESSURE (10^4 Pa) on σ_θ = 27.5 kg m^{-3} MARCH

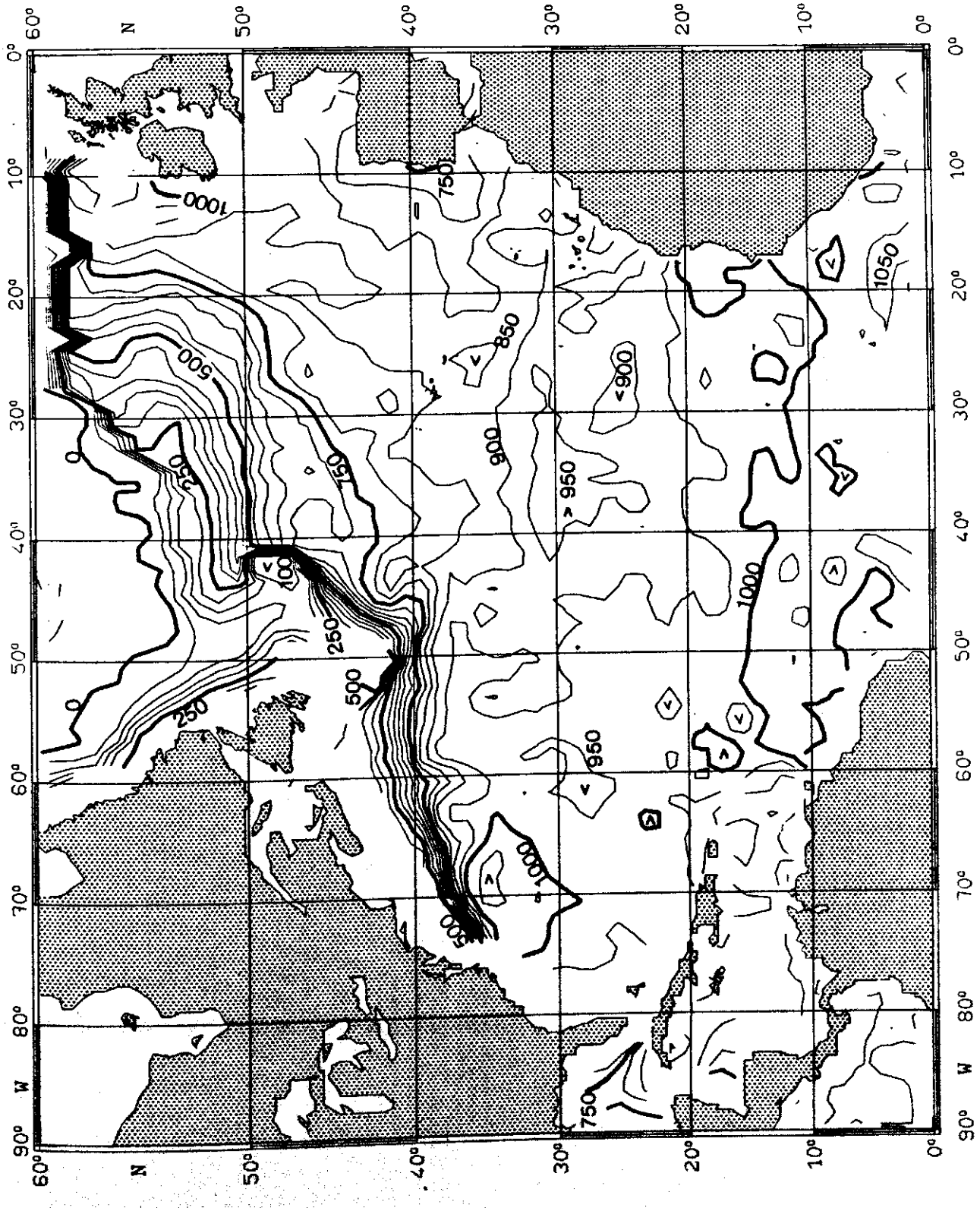

Fig. 35:

TEMPERATURE (°C) on σ_θ = 27.5 kg m^{-3} MARCH

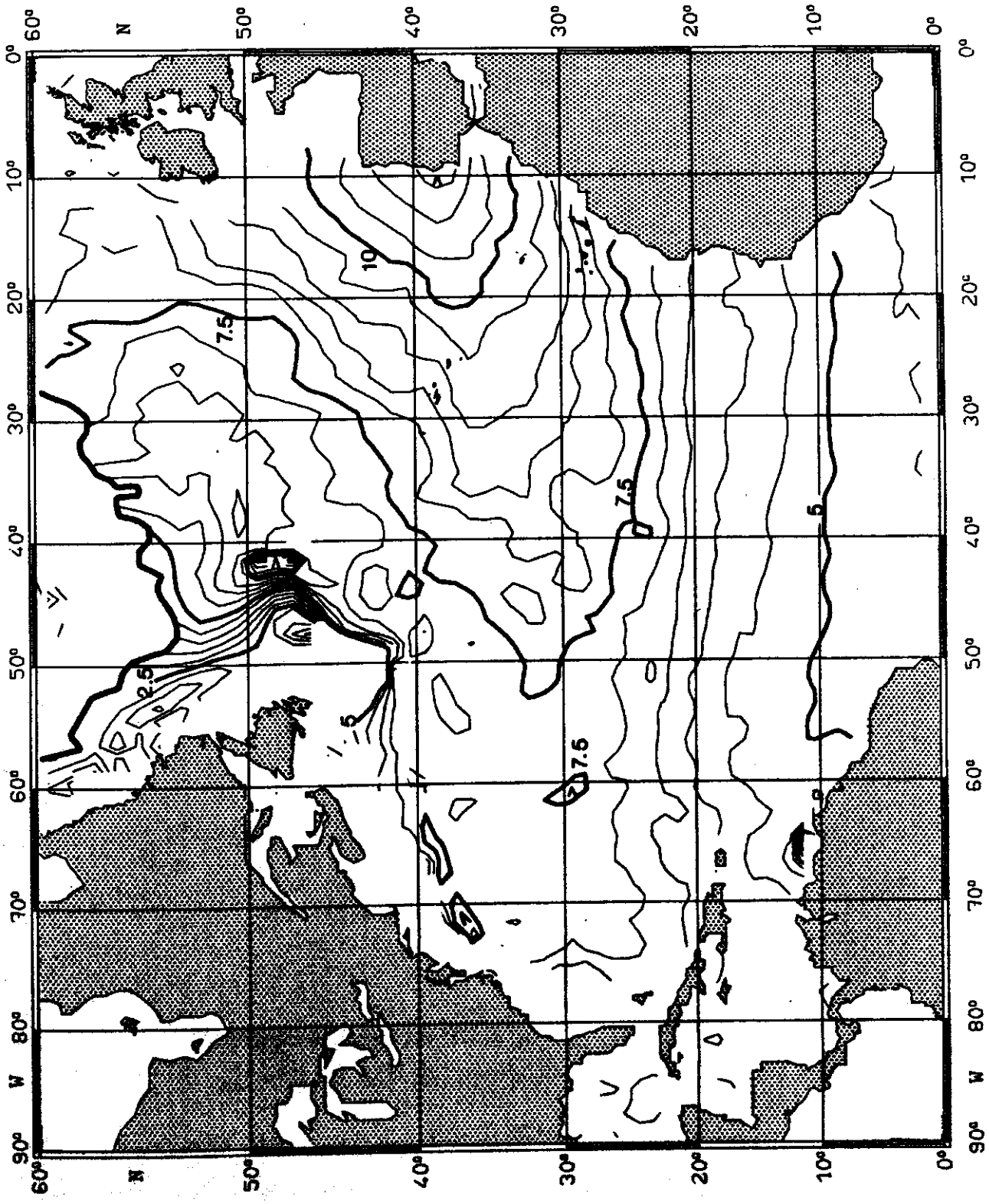

Fig. 36:

SALINITY (10^{-3}) on σ_θ = 27.5 kg m^{-3} MARCH

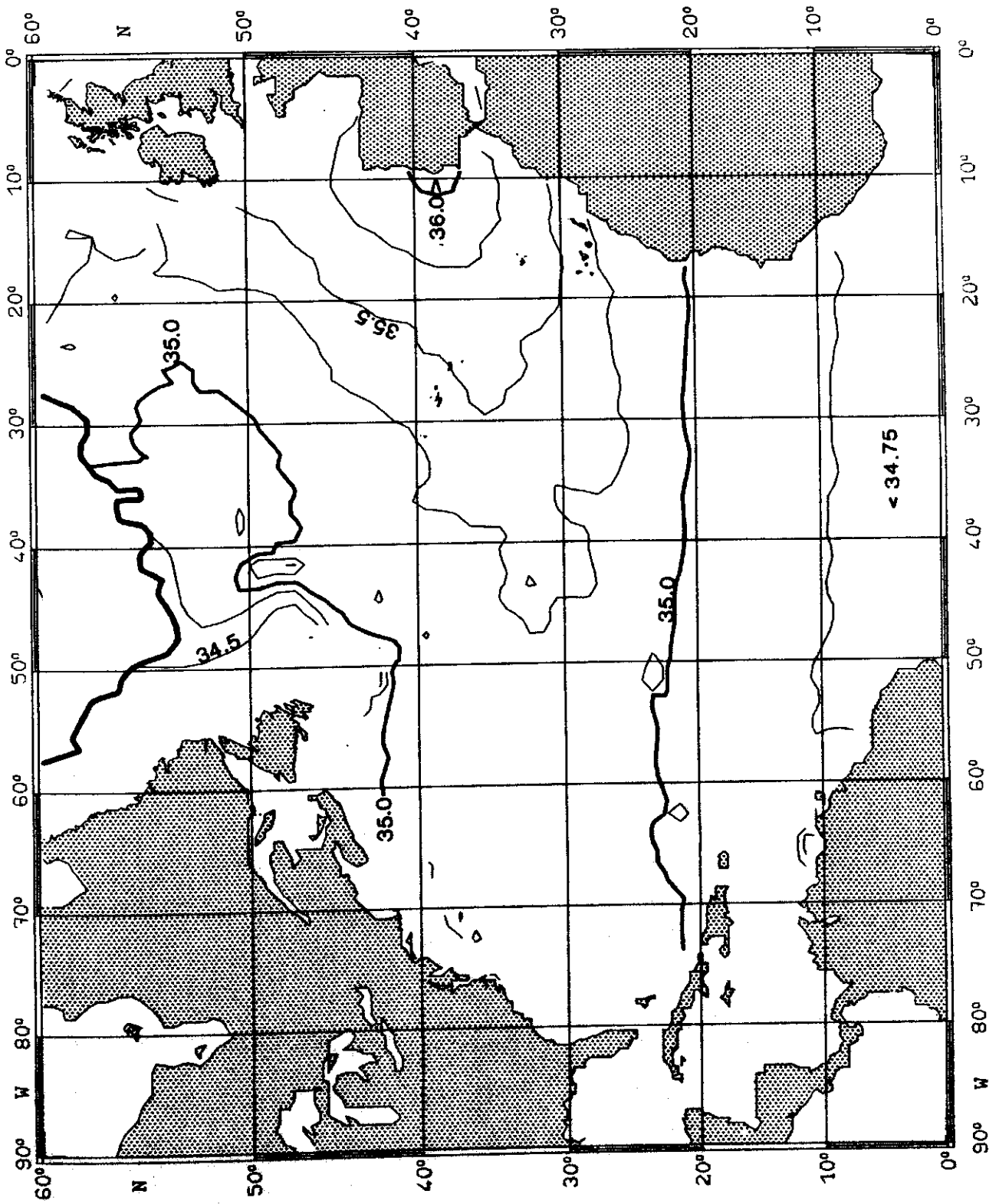

Fig. 37:

PRESSURE (10^4 Pa) on σ_θ = 25.0 kg m^{-3} APRIL

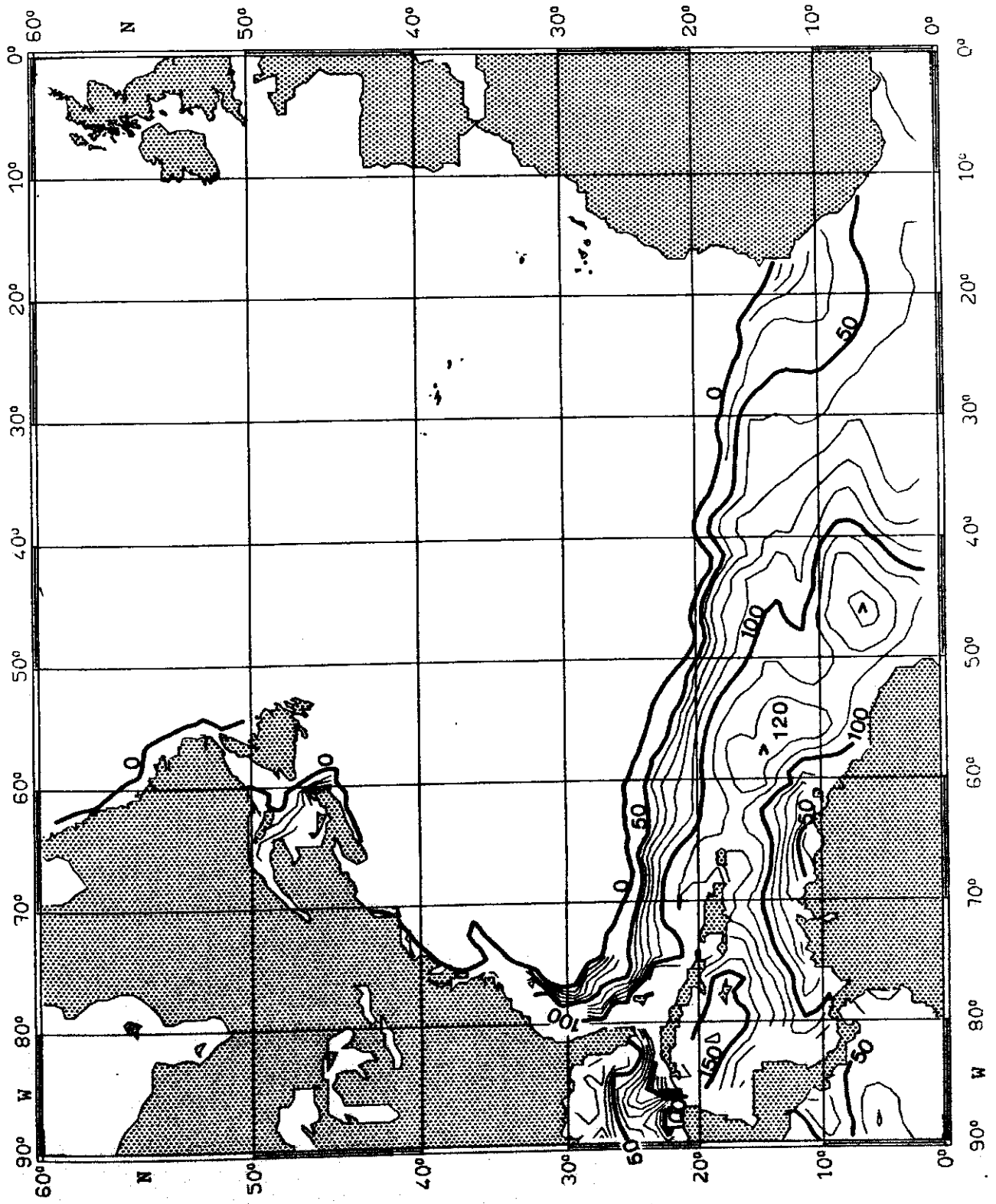

Fig. 38:

TEMPERATURE (°C) on σ_θ = 25.0 kg m APRIL

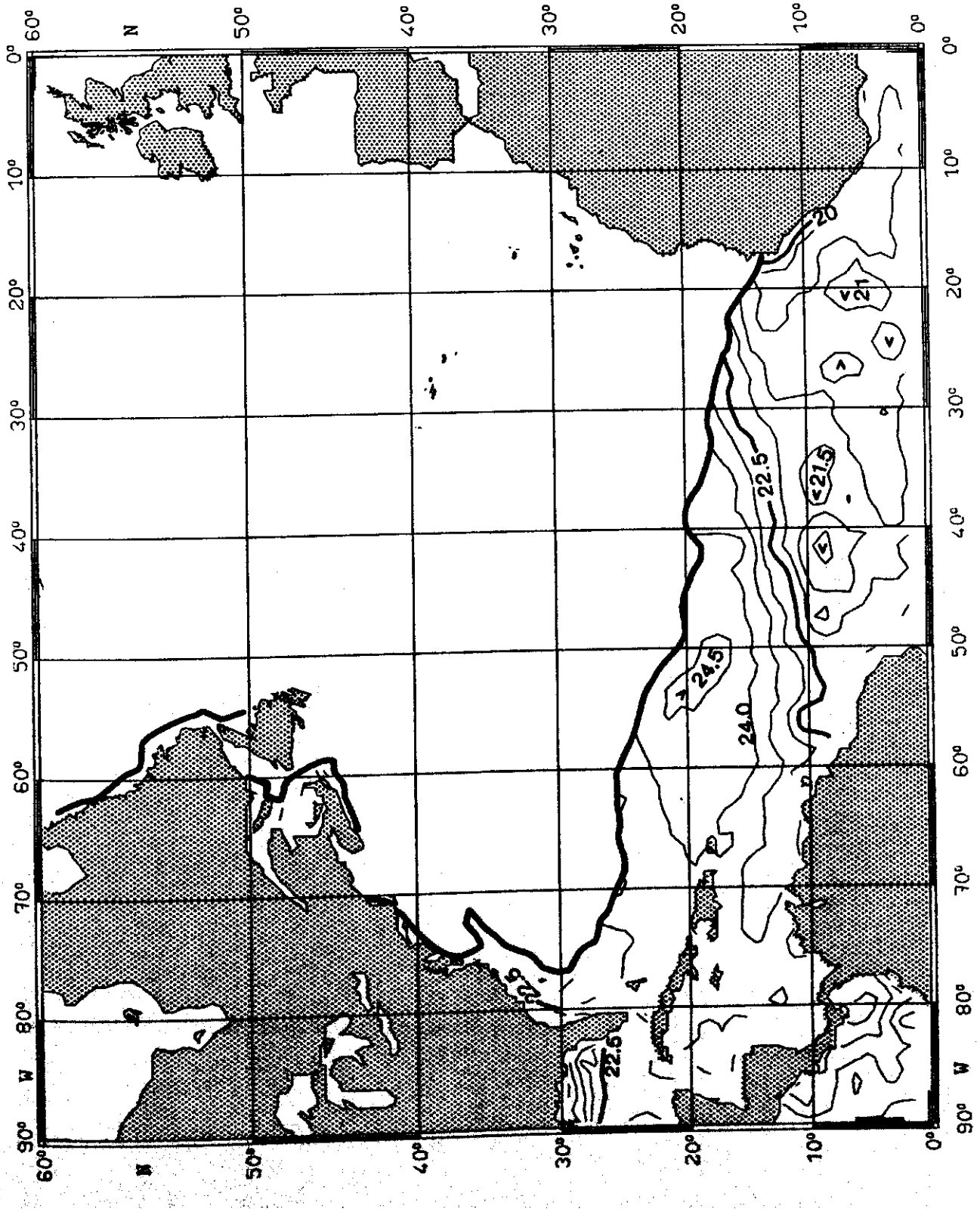

Fig. 39:

SALINITY (10^{-3}) on σ_θ = 25.0 kg m^{-3} APRIL

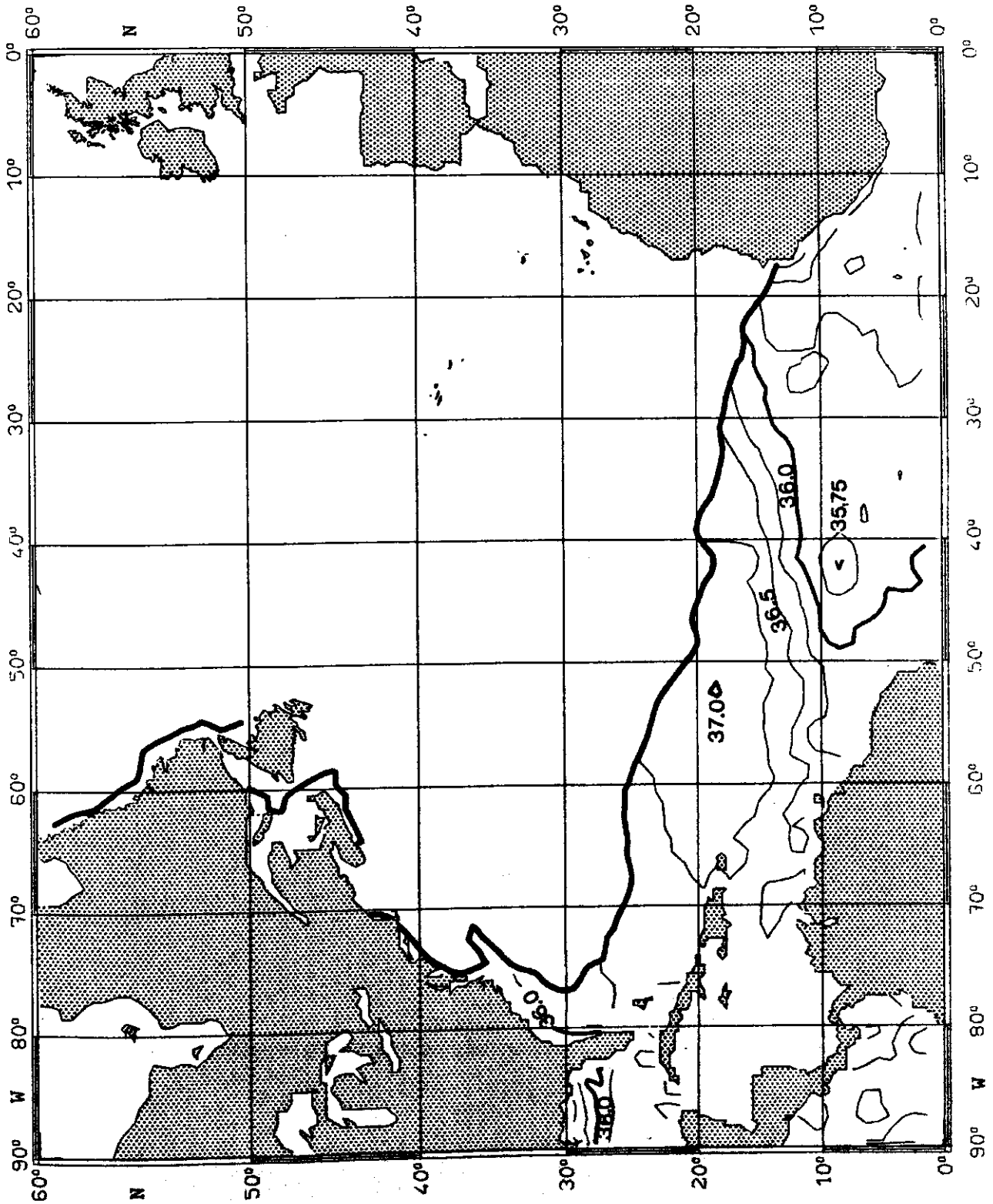

Fig. 40:

PRESSURE (10^4 Pa) on σ_θ = 26.0 kg m^{-3} APRIL

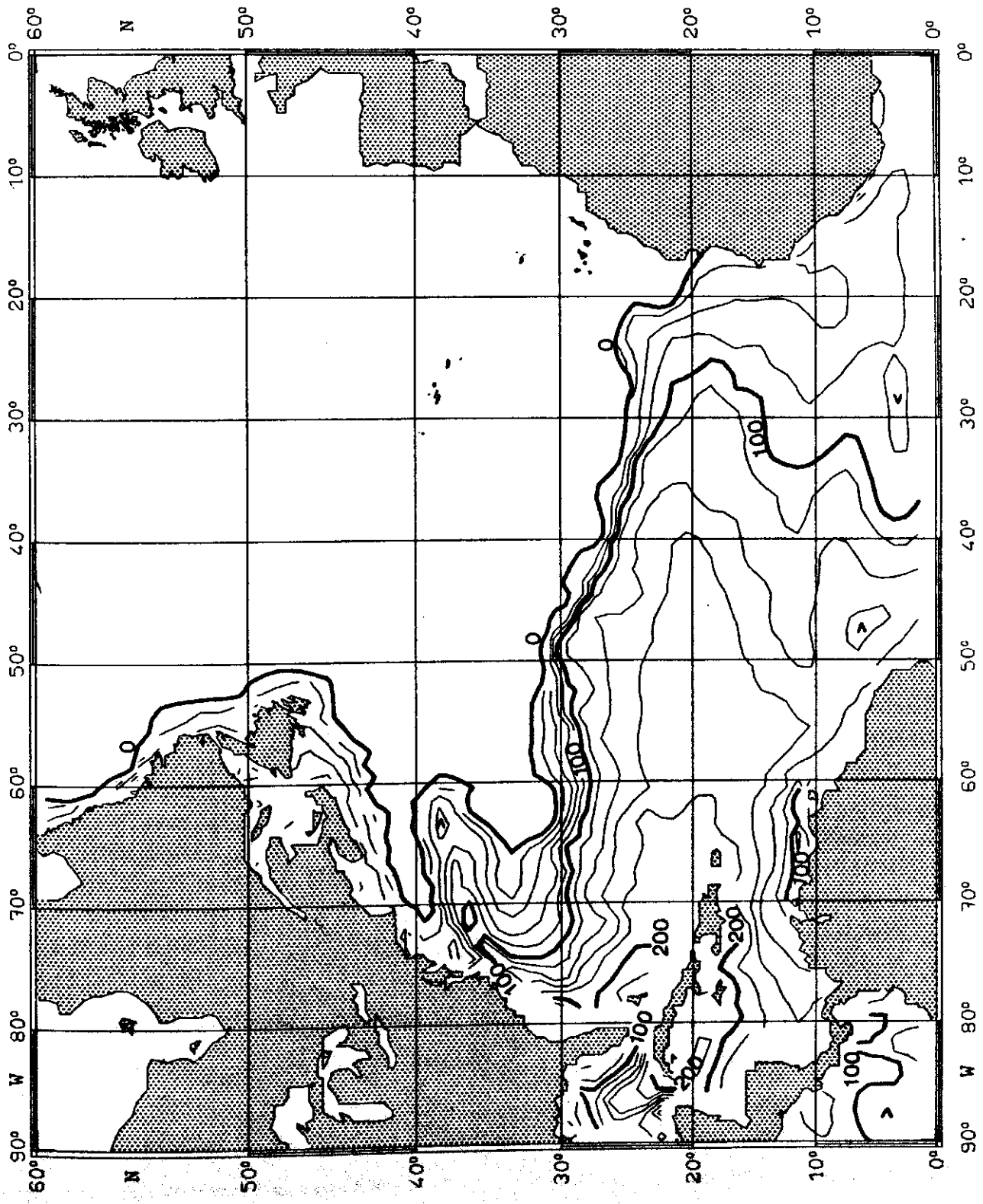

Fig. 41:

TEMPERATURE (°C) on σ_θ = 26.0 kg m^{-3} APRIL

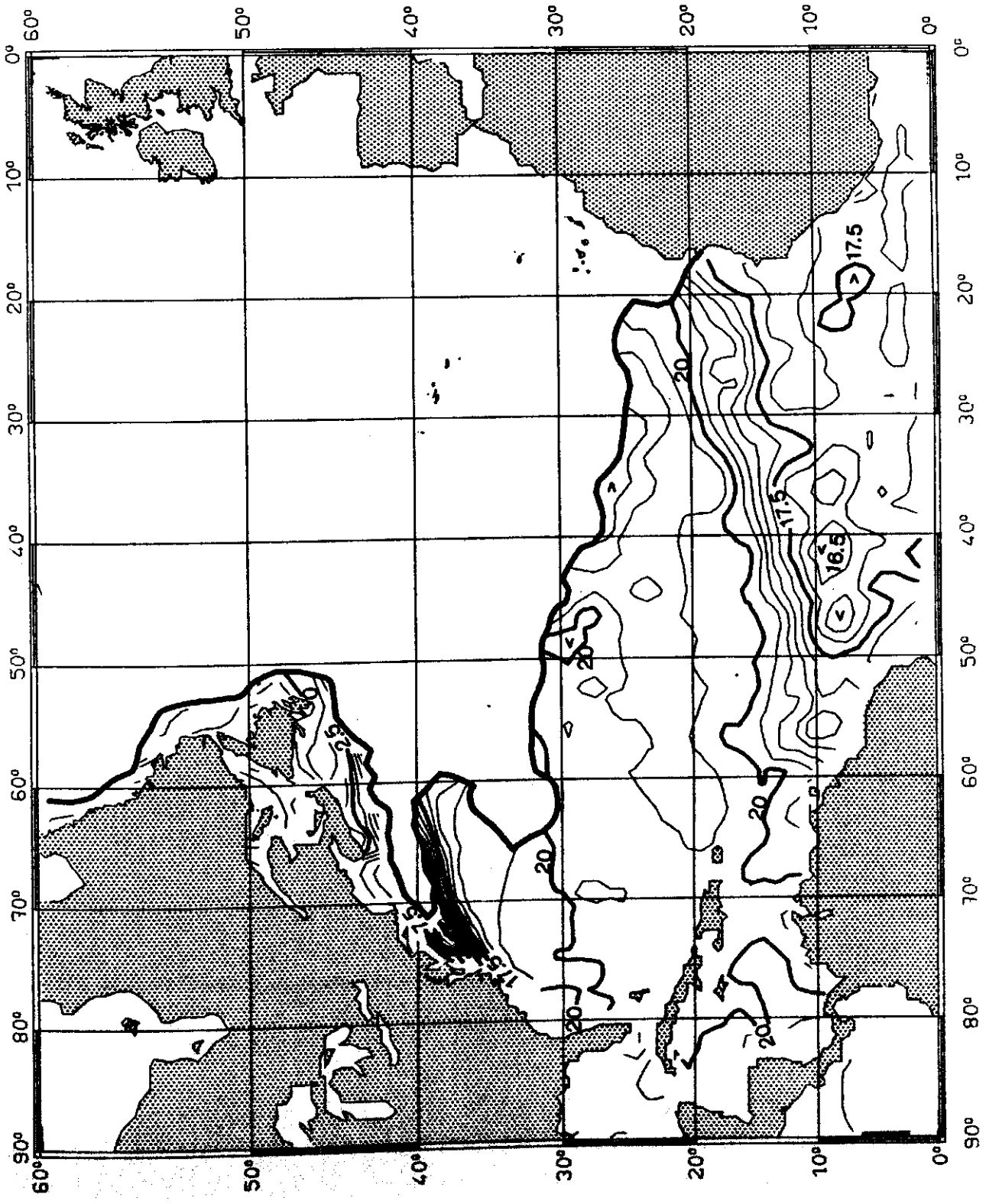

Fig. 42:

SALINITY (10^{-3}) on σ_θ = 26.0 kg m^{-3} APRIL

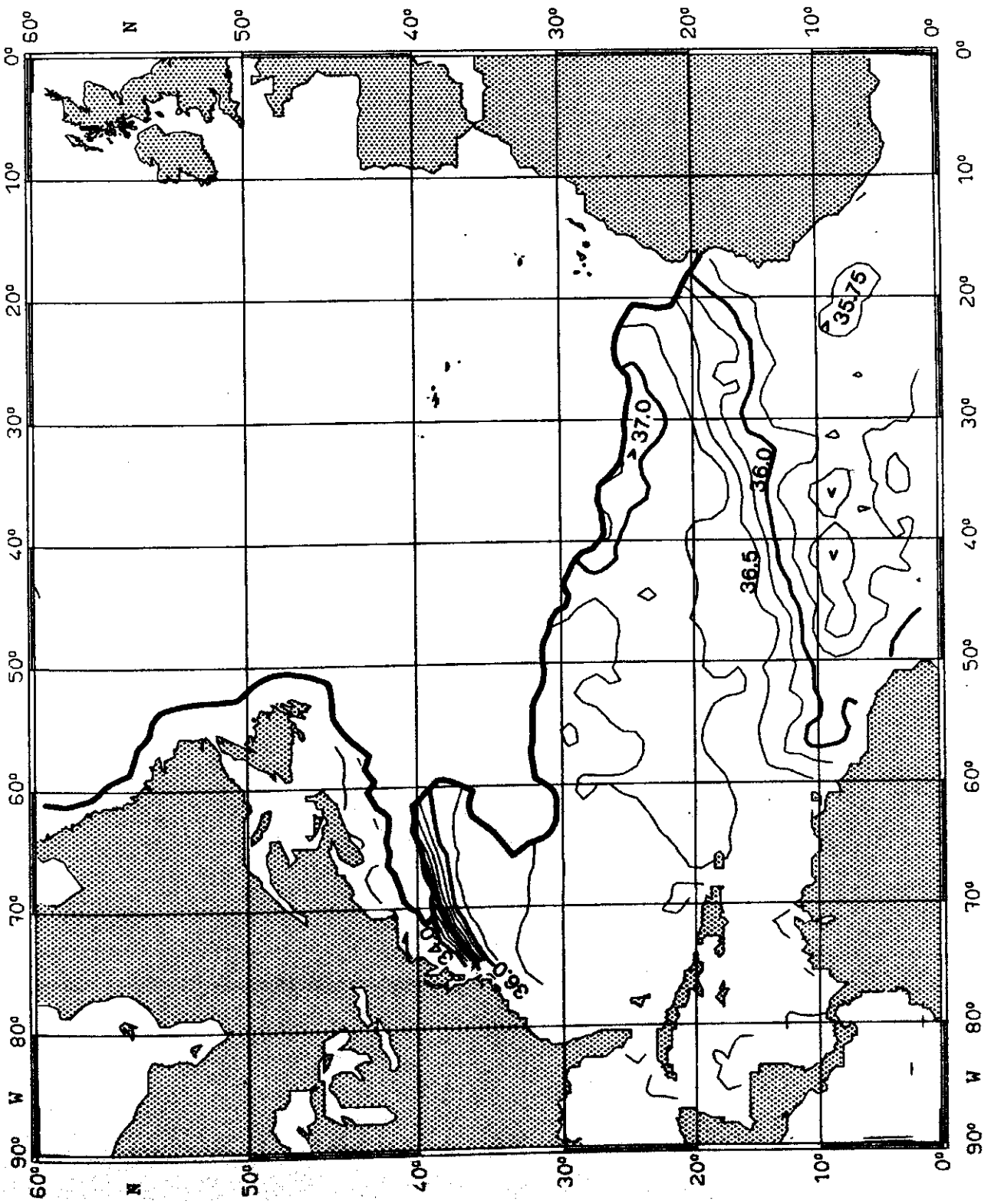

Fig. 43:

PRESSURE (10^4 Pa) on σ_θ = 27.0 kg m^{-3} APRIL

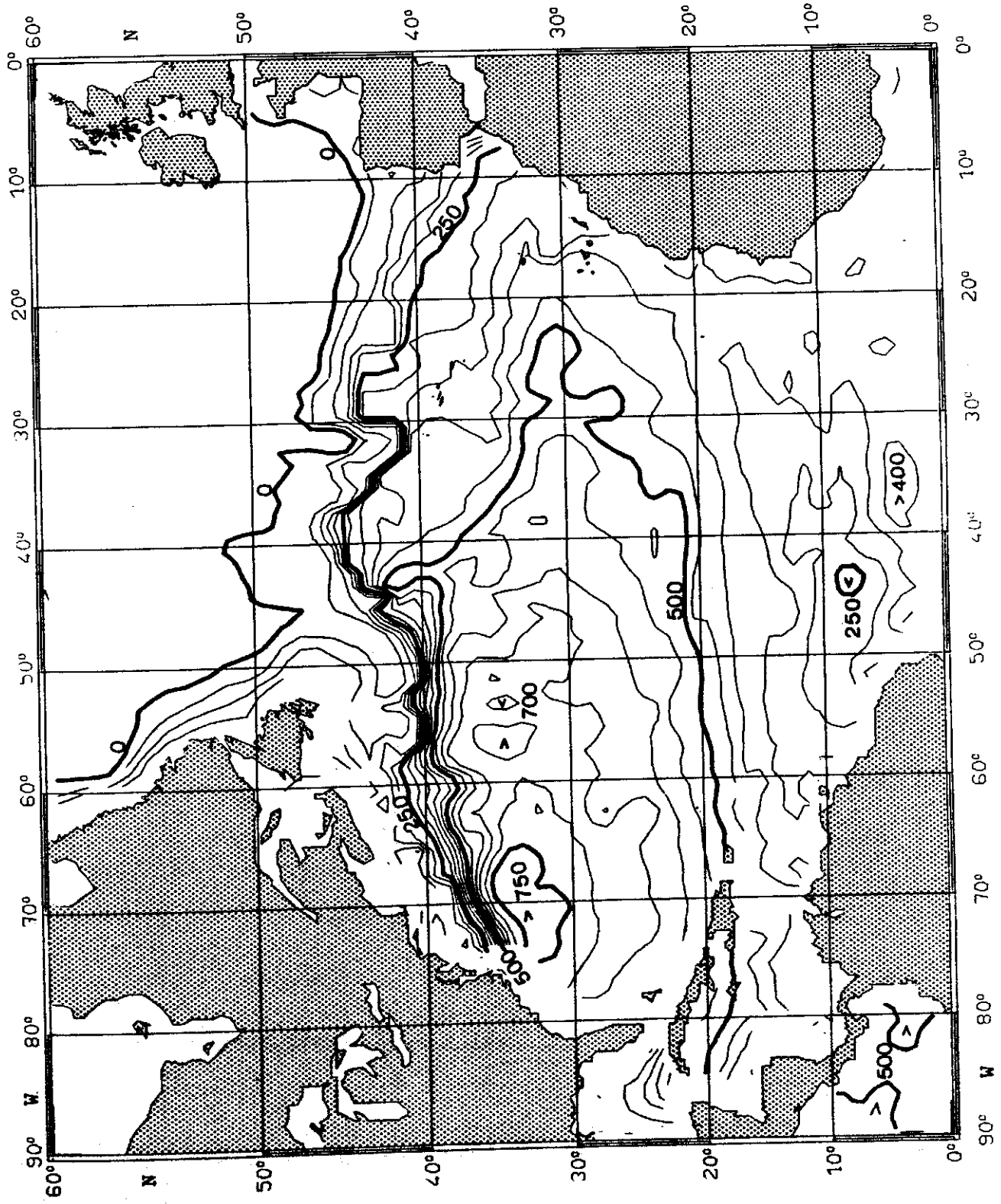

Fig. 44:

TEMPERATURE (°C) on σ_θ = 27.0 kg m^{-3} APRIL

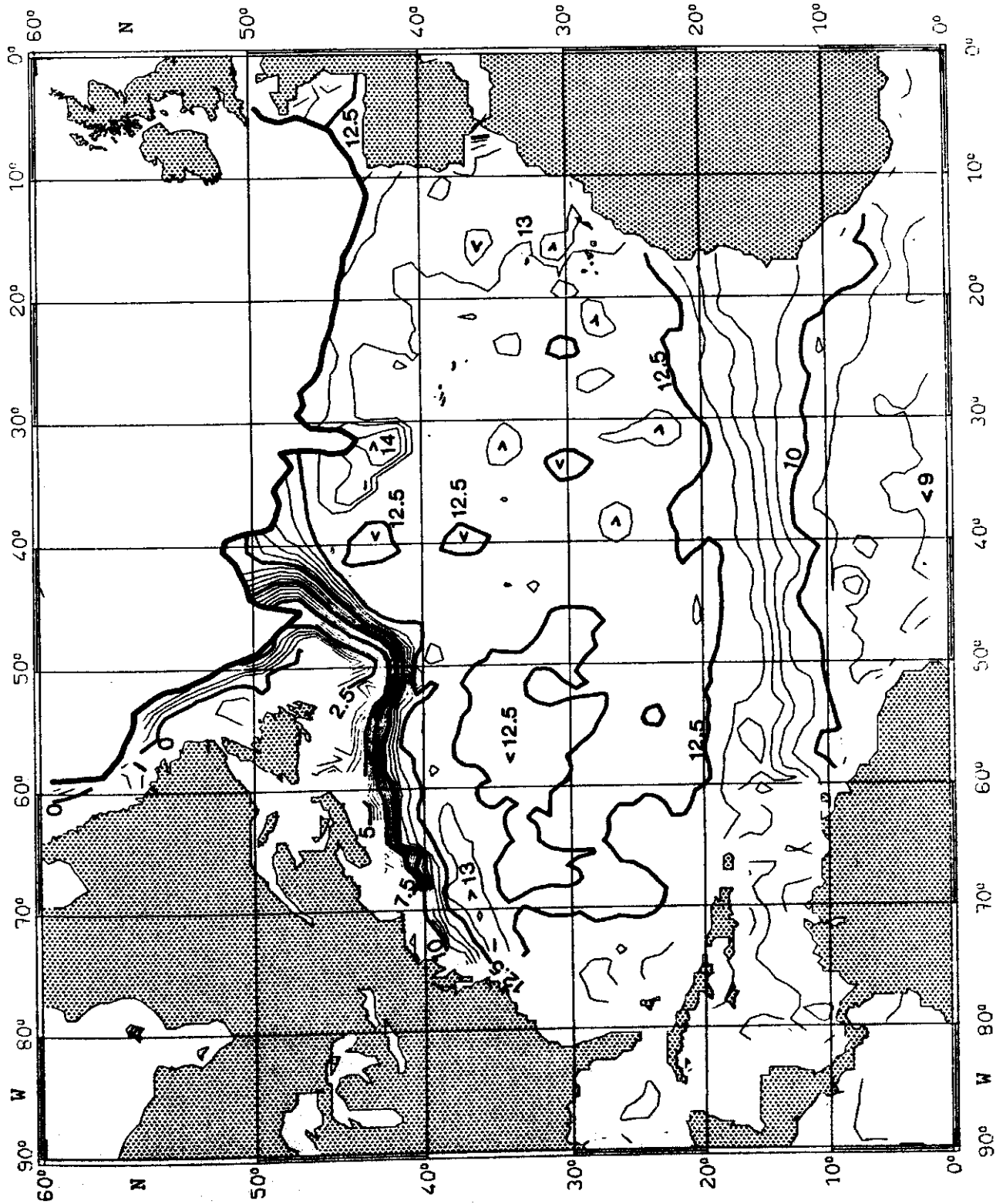

Fig. 45:

SALINITY (10^{-3}) on σ_θ = 27.0 kg m^{-3} APRIL

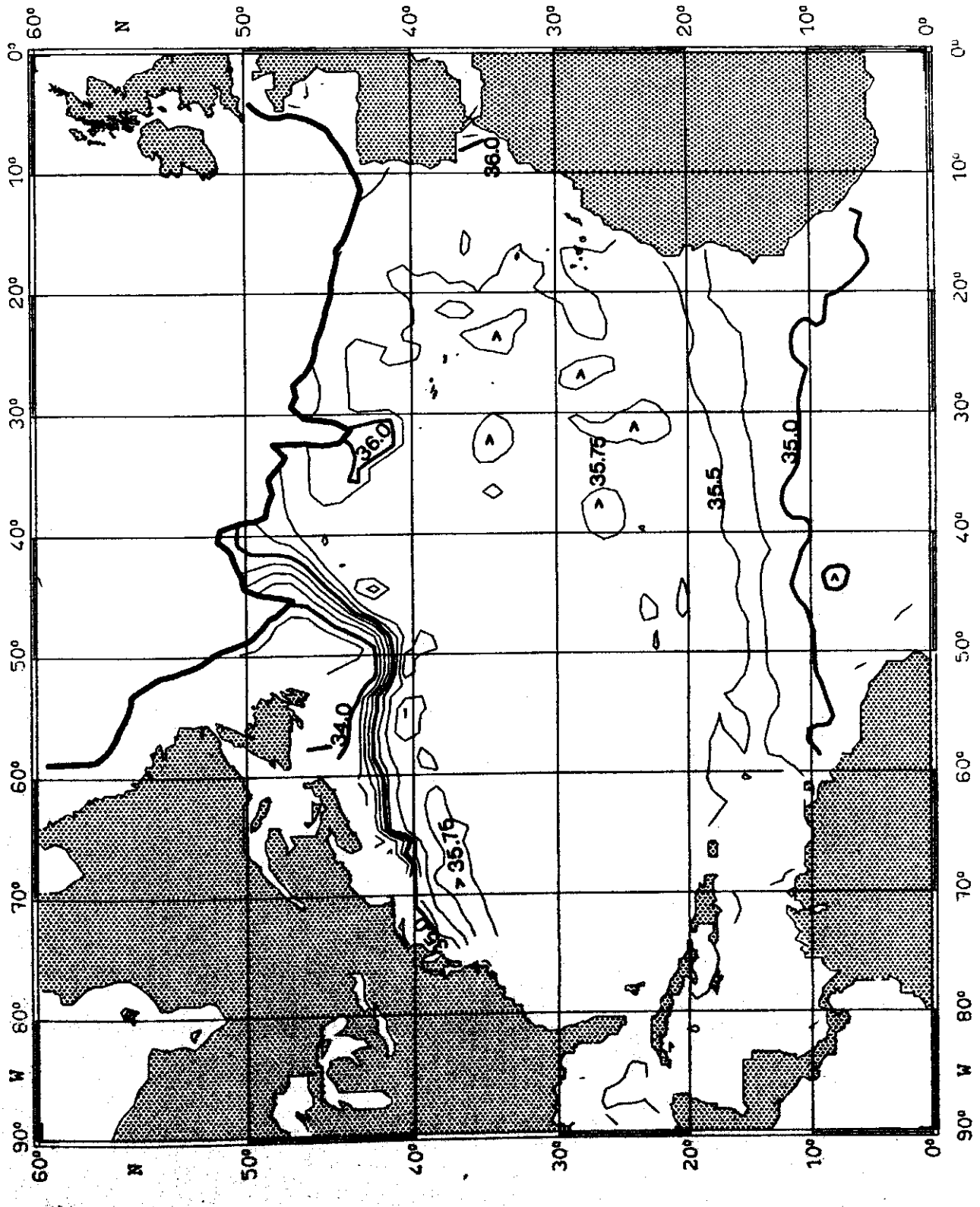

Fig. 46:

PRESSURE (10^4 Pa) on σ_θ = 25.0 kg m^{-3} MAY

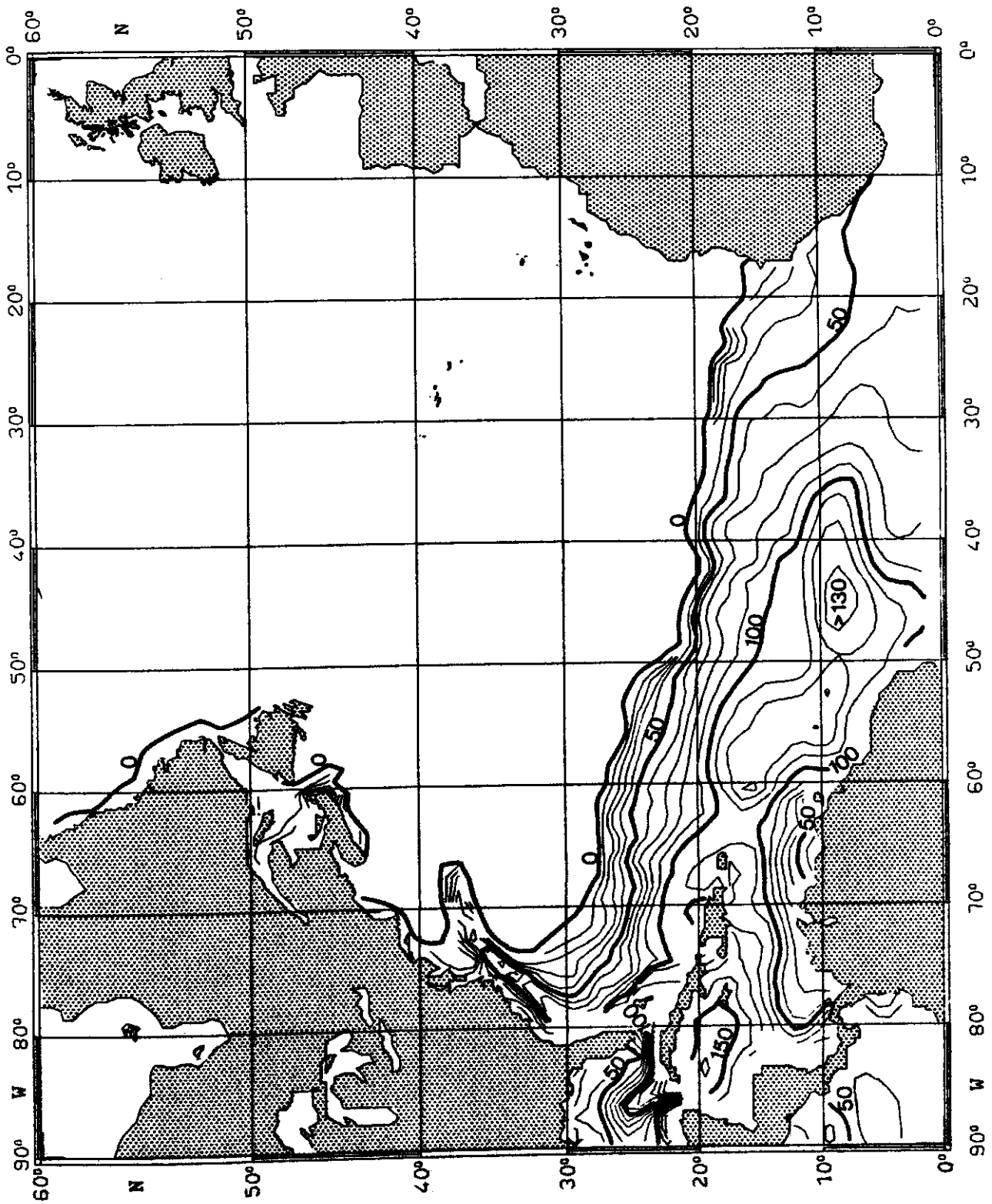

Fig. 47:

TEMPERATURE (°C) on σ_θ = 25.0 kg m^{-3} MAY

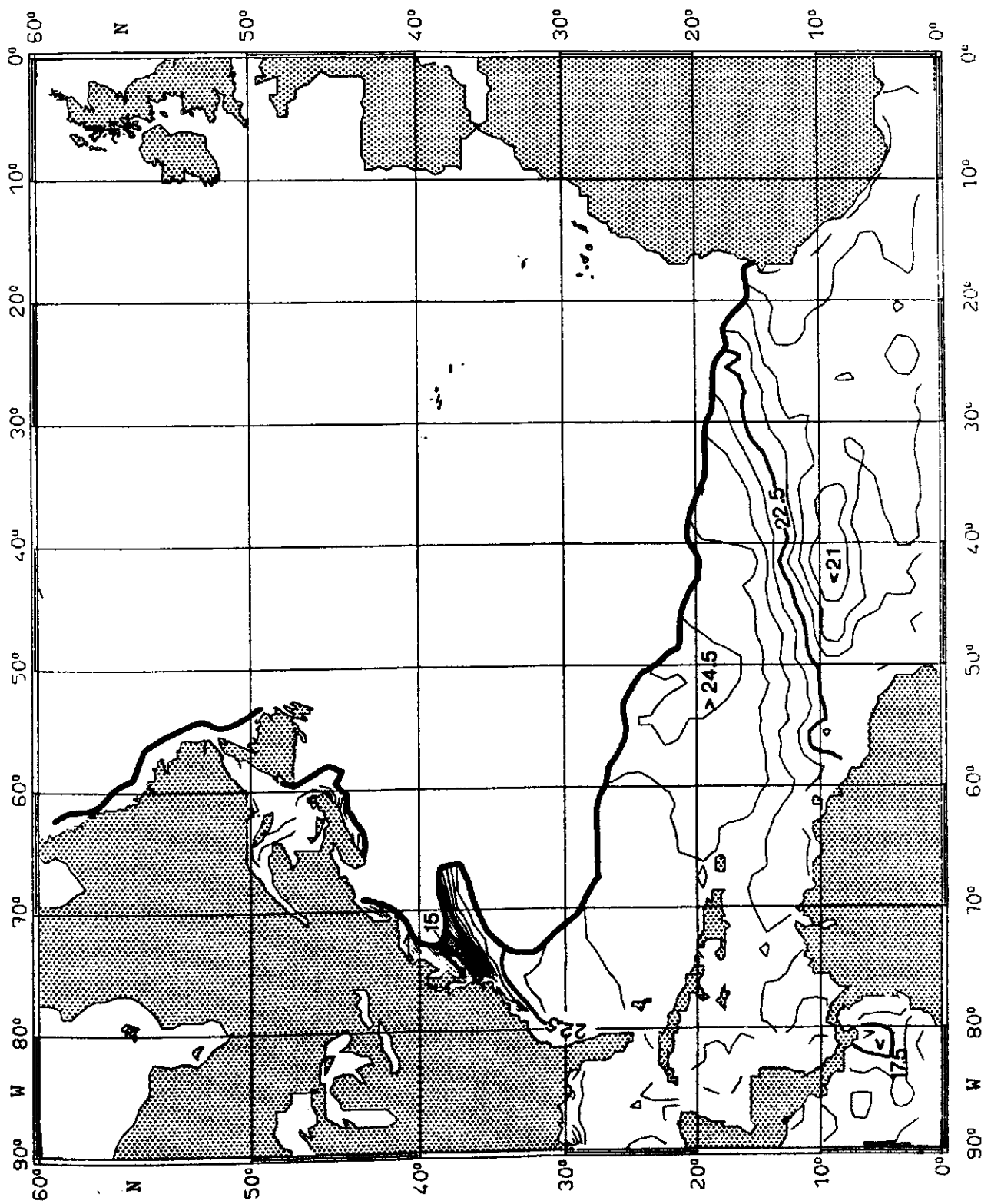

Fig. 48:

SALINITY (10^{-3}) on σ_θ = 25.0 kg m^{-3} MAY

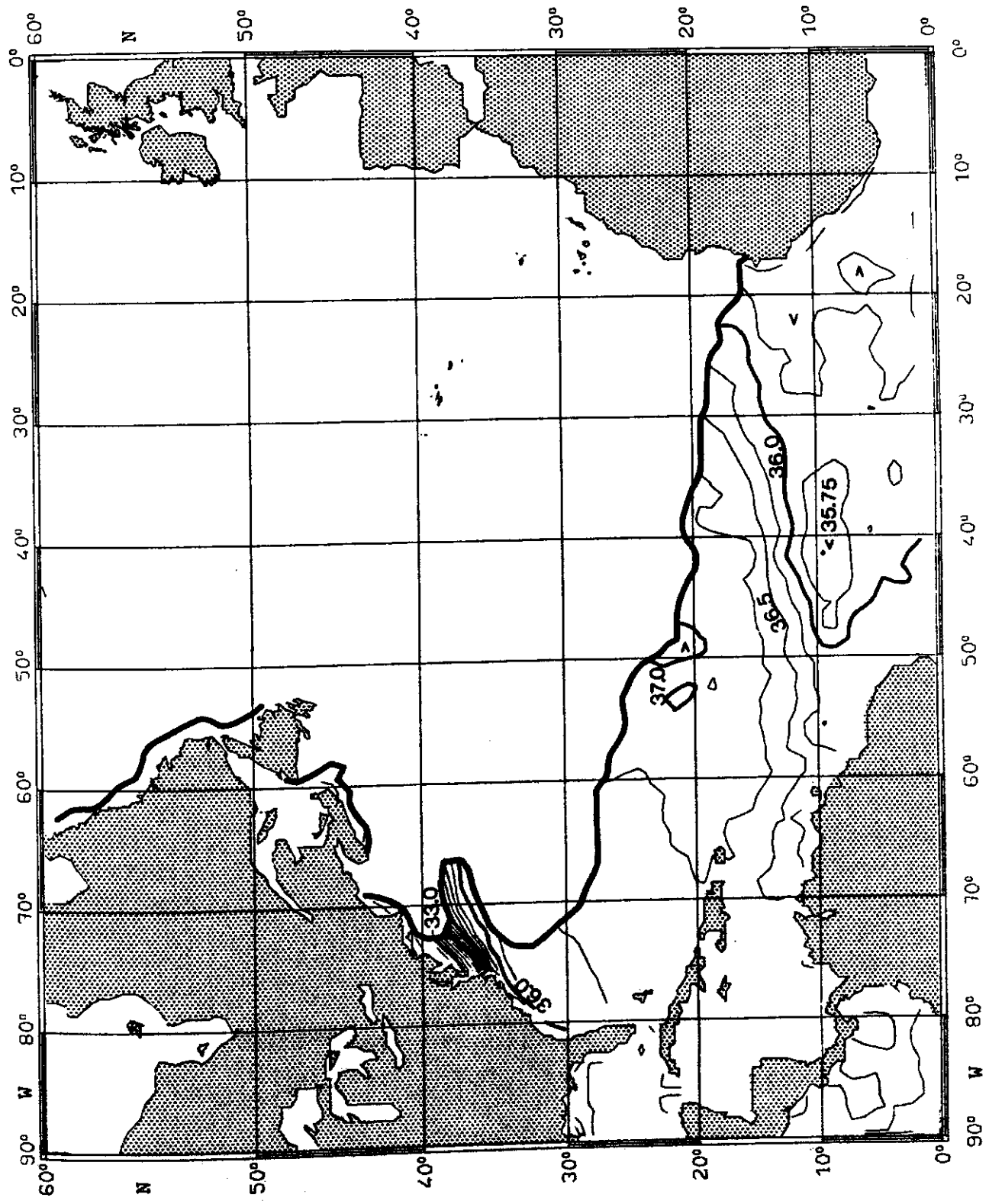

Fig. 49:

PRESSURE (10^4 Pa) on σ_θ = 26.0 kg m^{-3} MAY

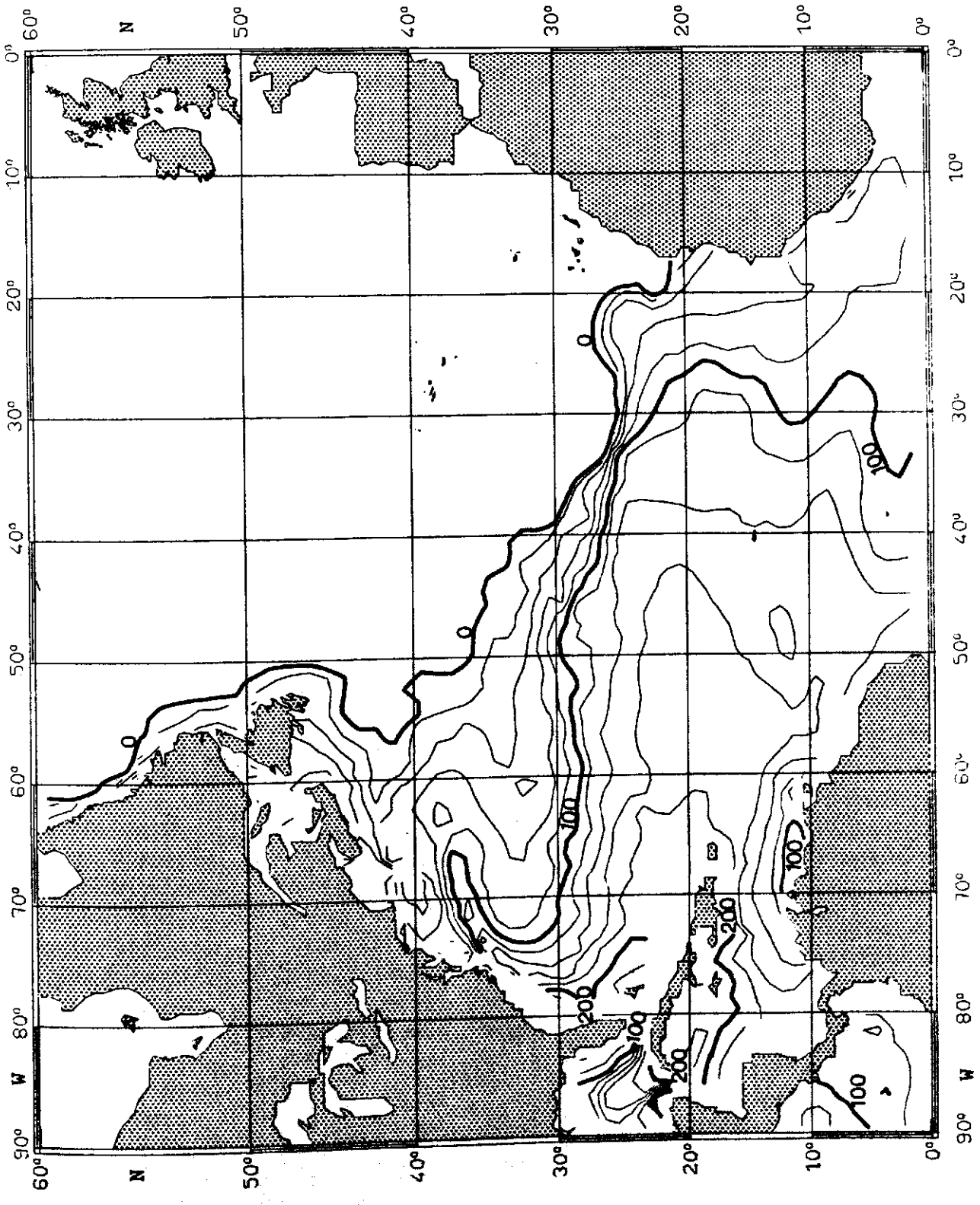

Fig. 50:

TEMPERATURE (°C) on σ_θ = 26.0 kg m^{-3} MAY

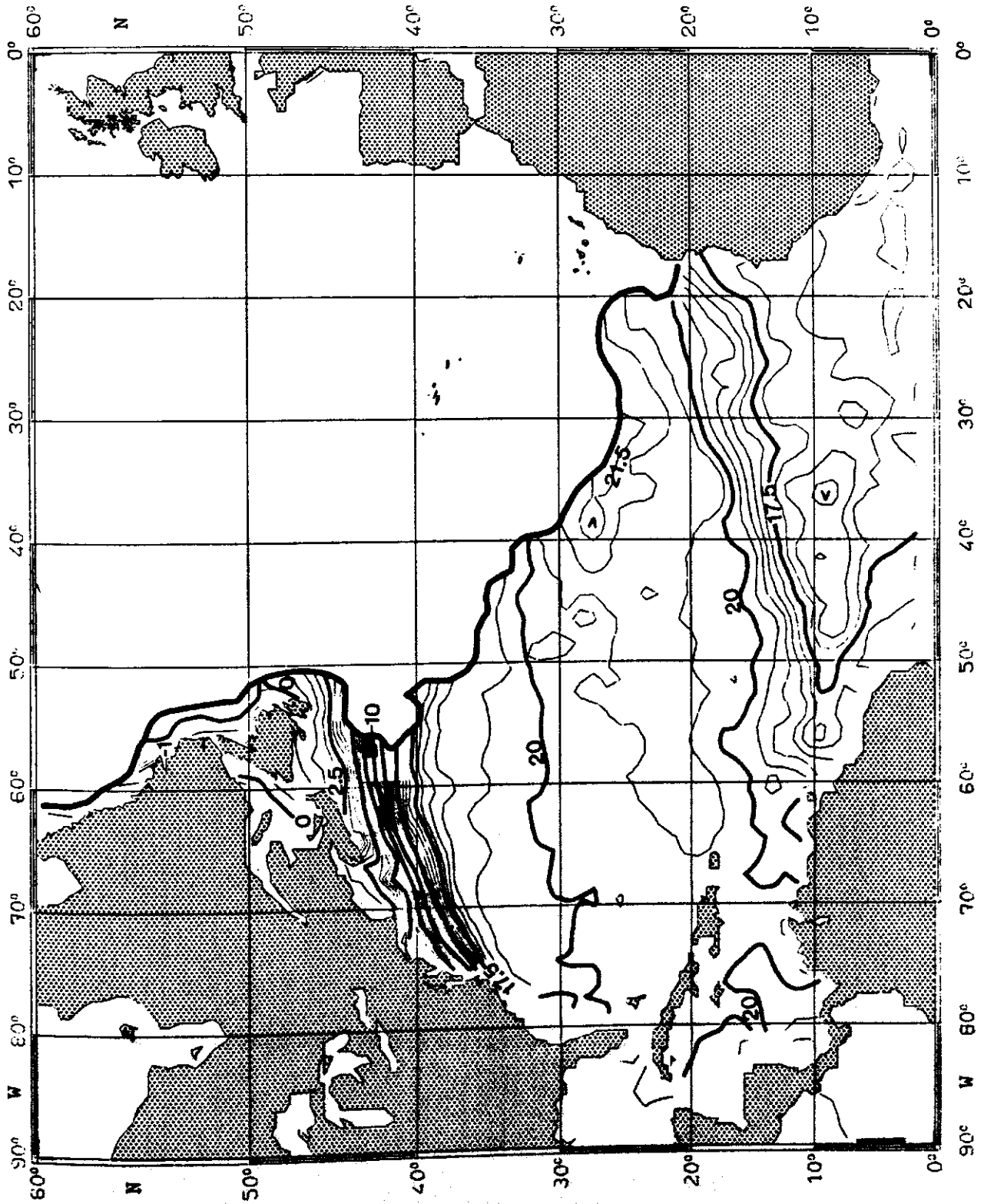

Fig. 51:

SALINITY (10^{-3}) on σ_θ = 26.0 kg m^{-3} MAY

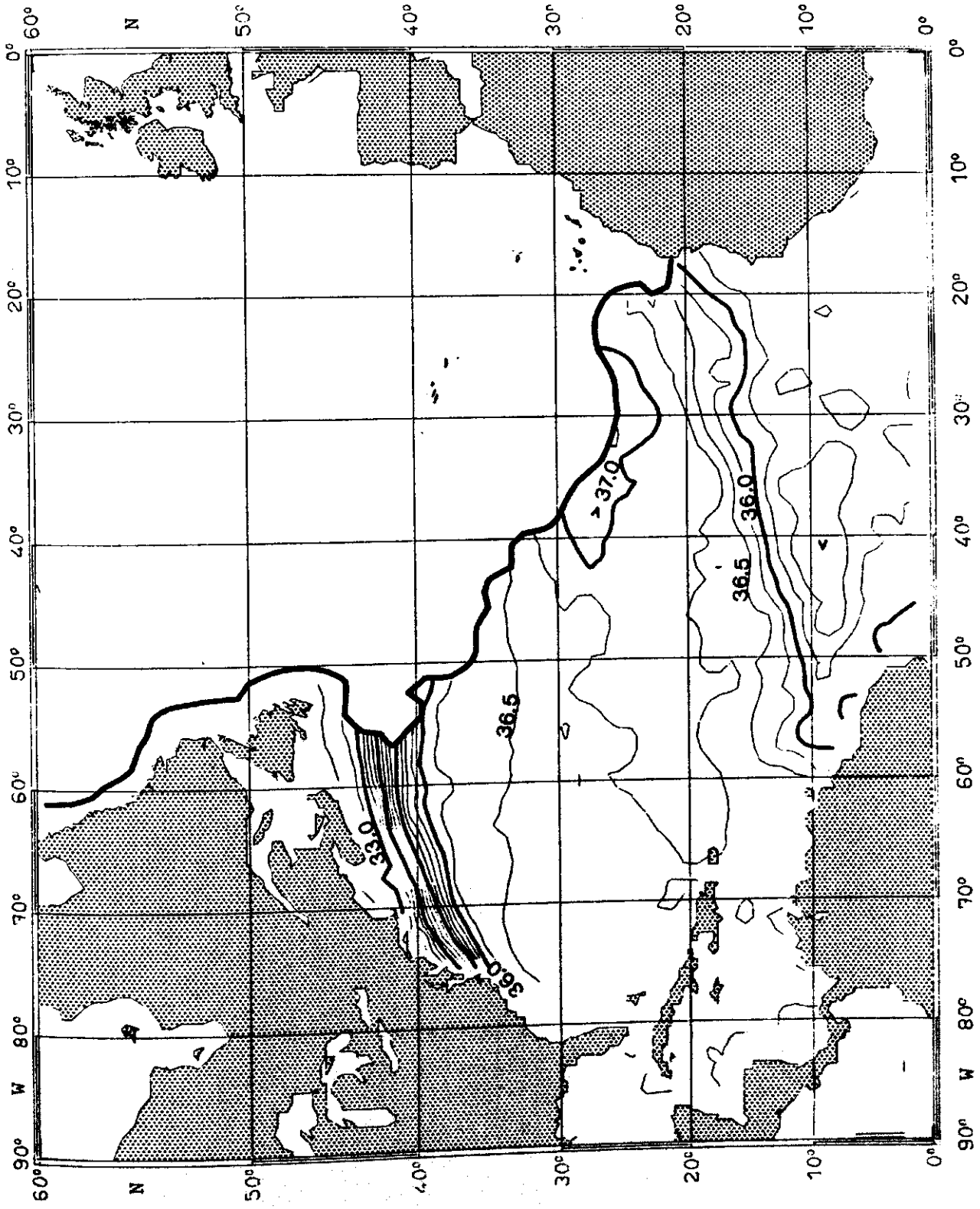

Fig. 52:

PRESSURE (10^4 Pa) on σ_θ = 27.0 kg m^{-3} MAY

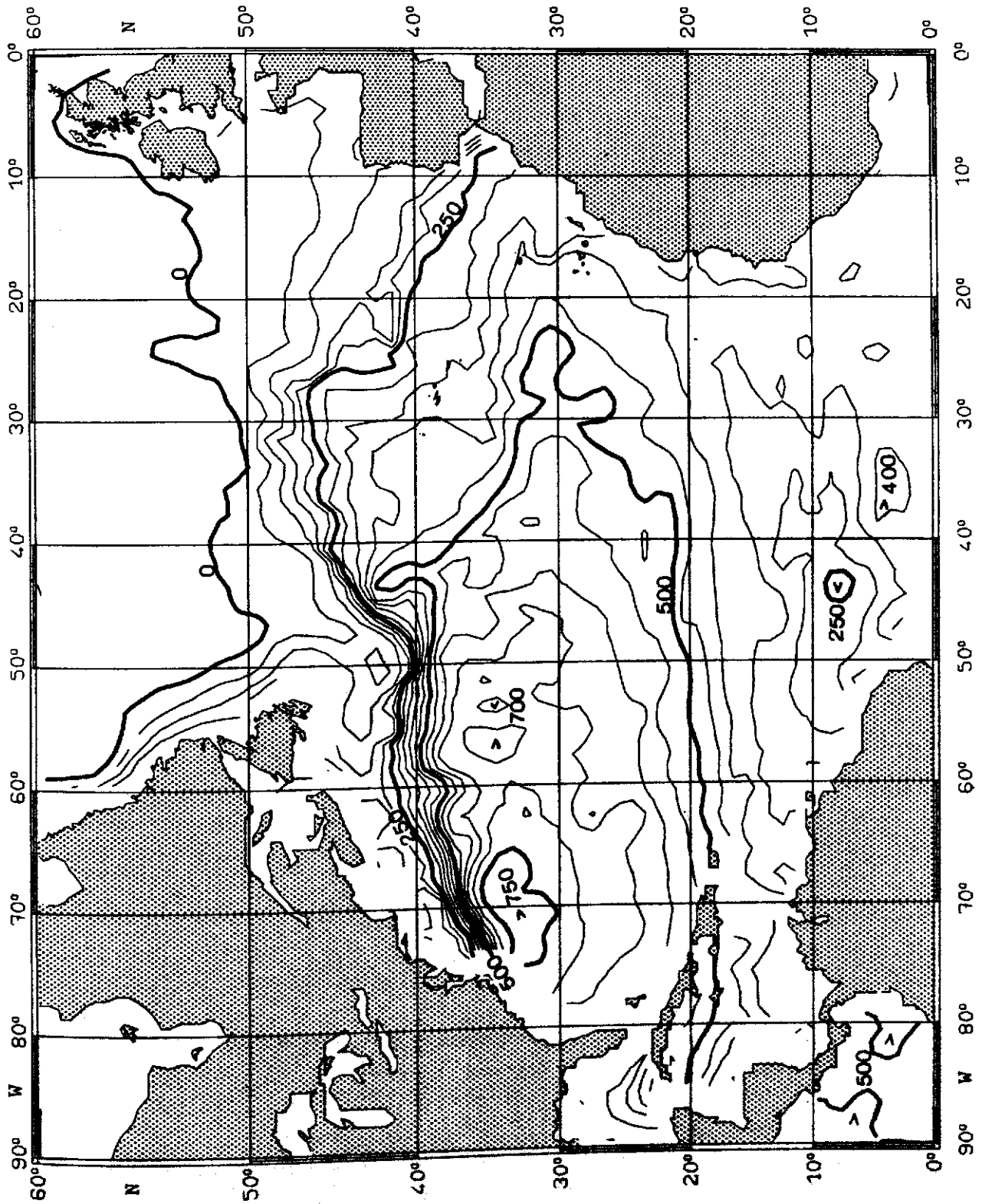

Fig. 53:

TEMPERATURE (°C) on σ_θ = 27.0 kg m^{-3} MAY

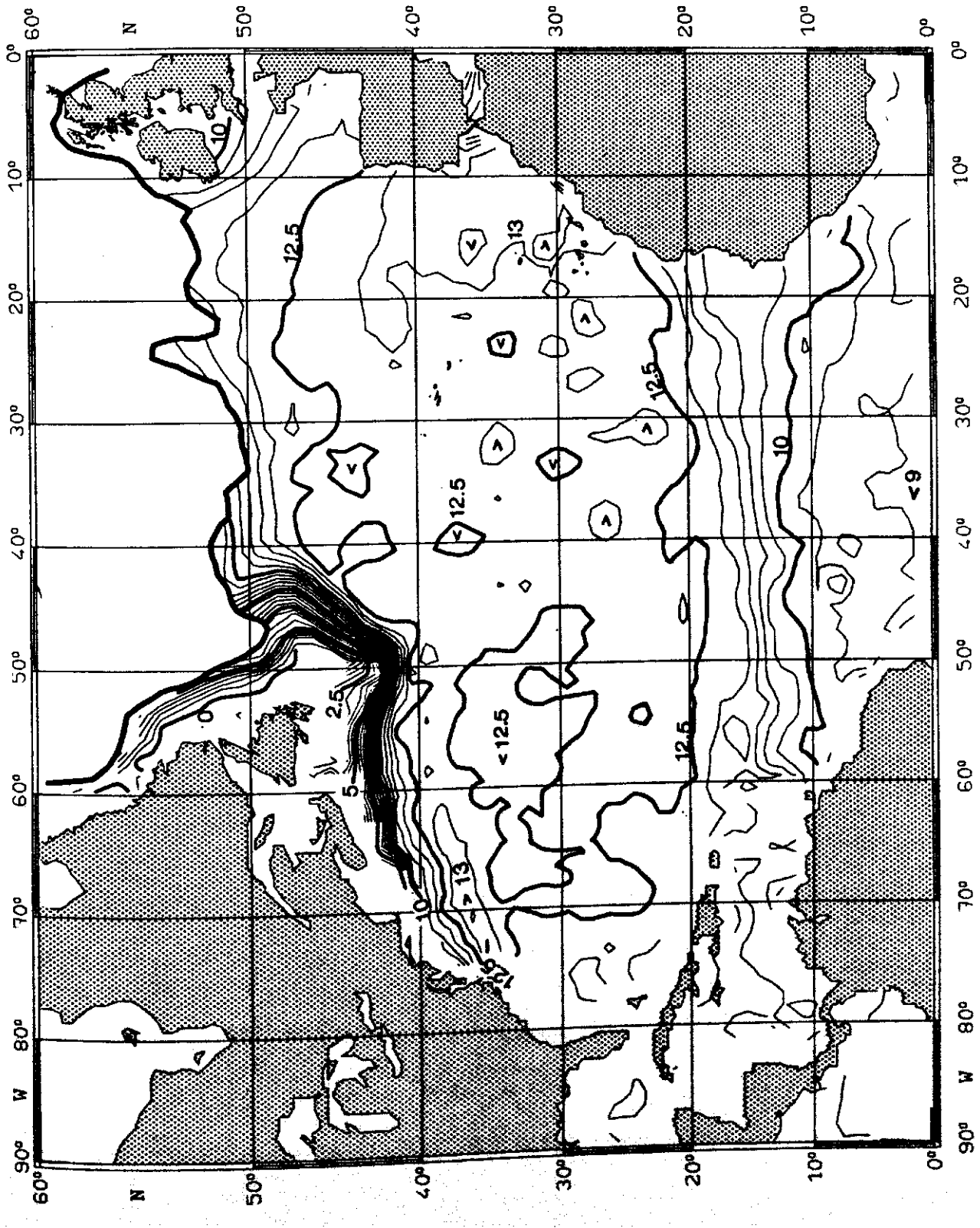

Fig. 54:

SALINITY (10^{-3}) on σ_θ = 27.0 kg m^{-3} MAY

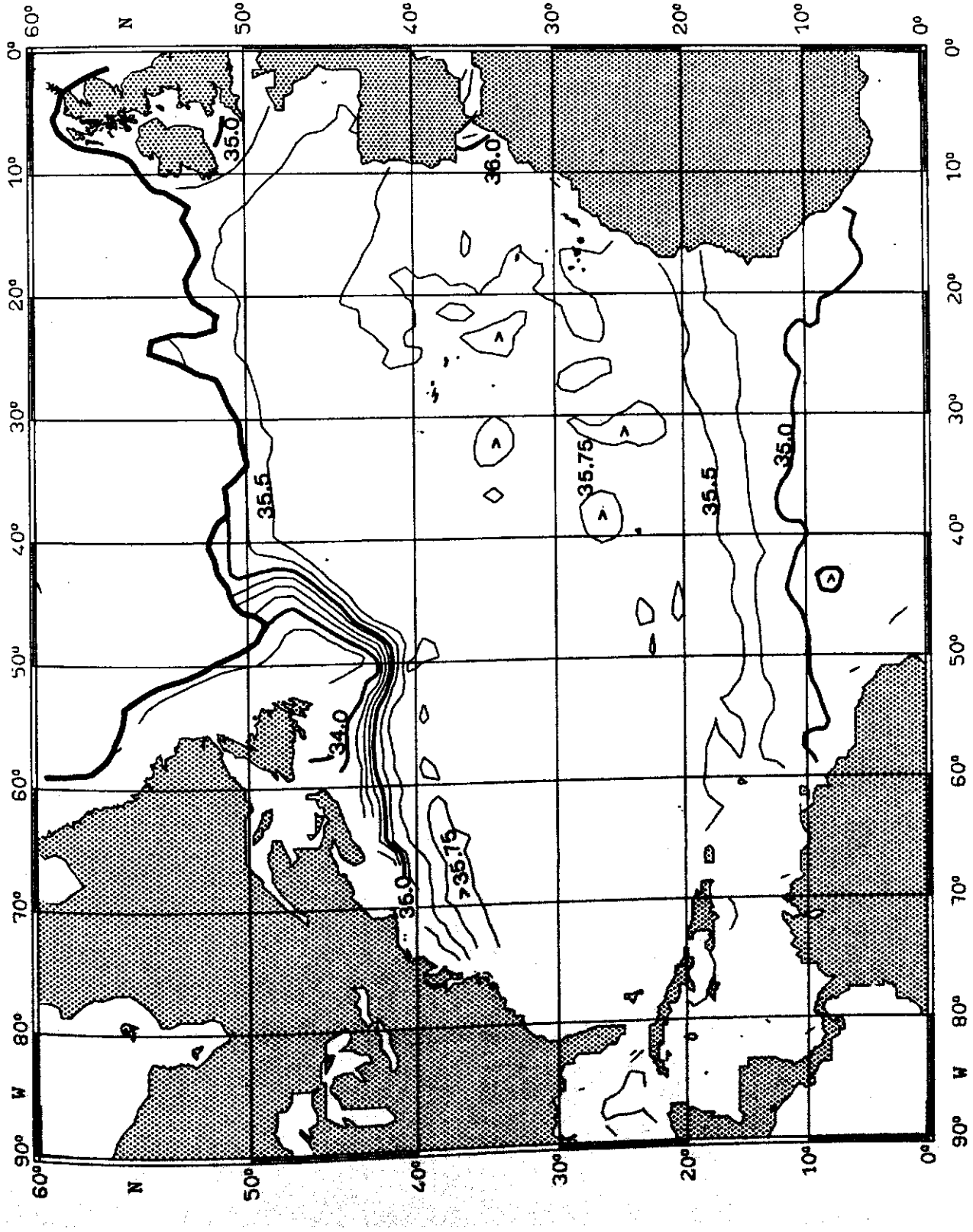

Fig. 55:

PRESSURE (10^4 Pa) on σ_θ = 25.0 kg m^{-3} JUNE

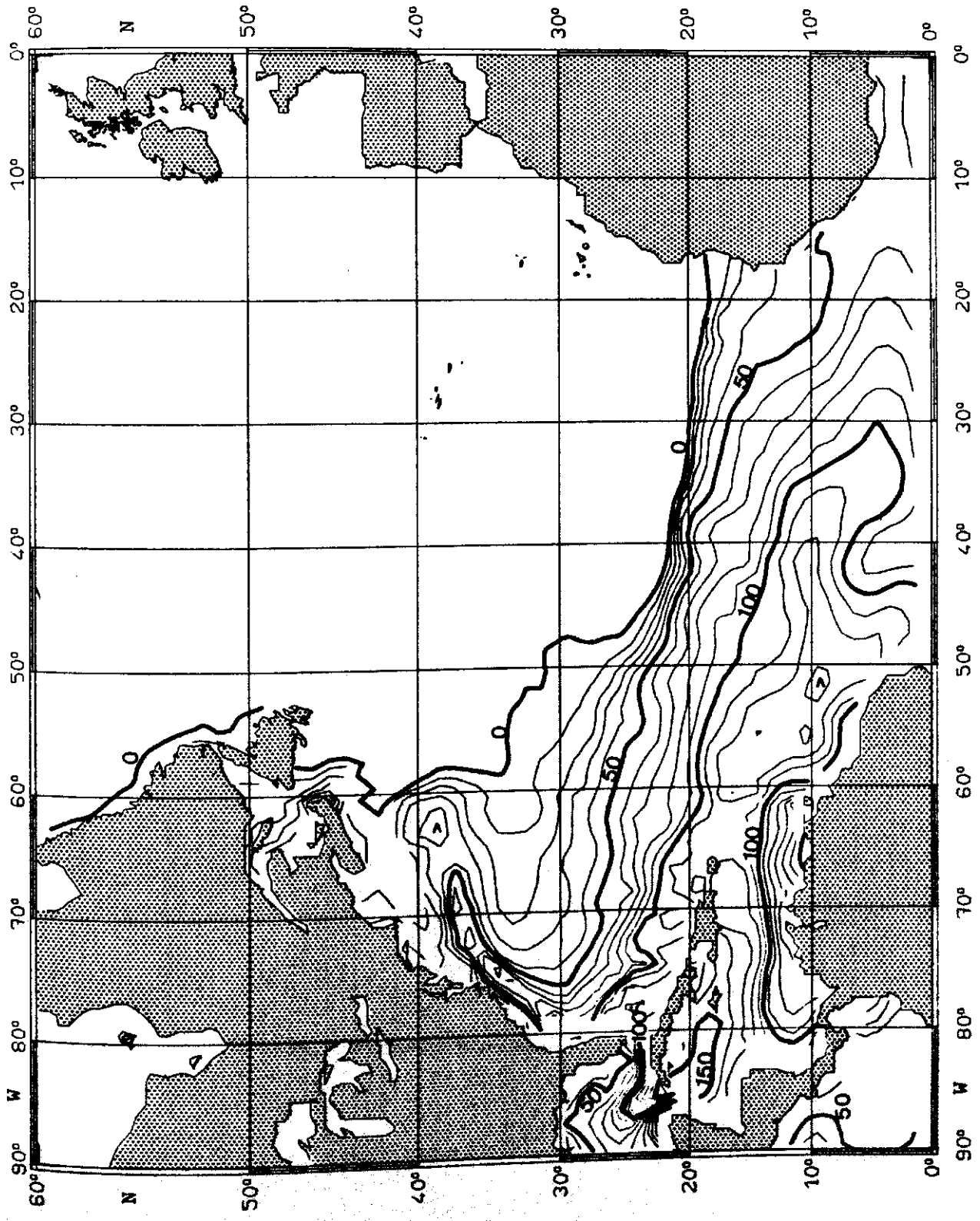

Fig. 57:

TEMPERATURE (°C) on σ_θ = 25.0 kg m^{-3} JUNE

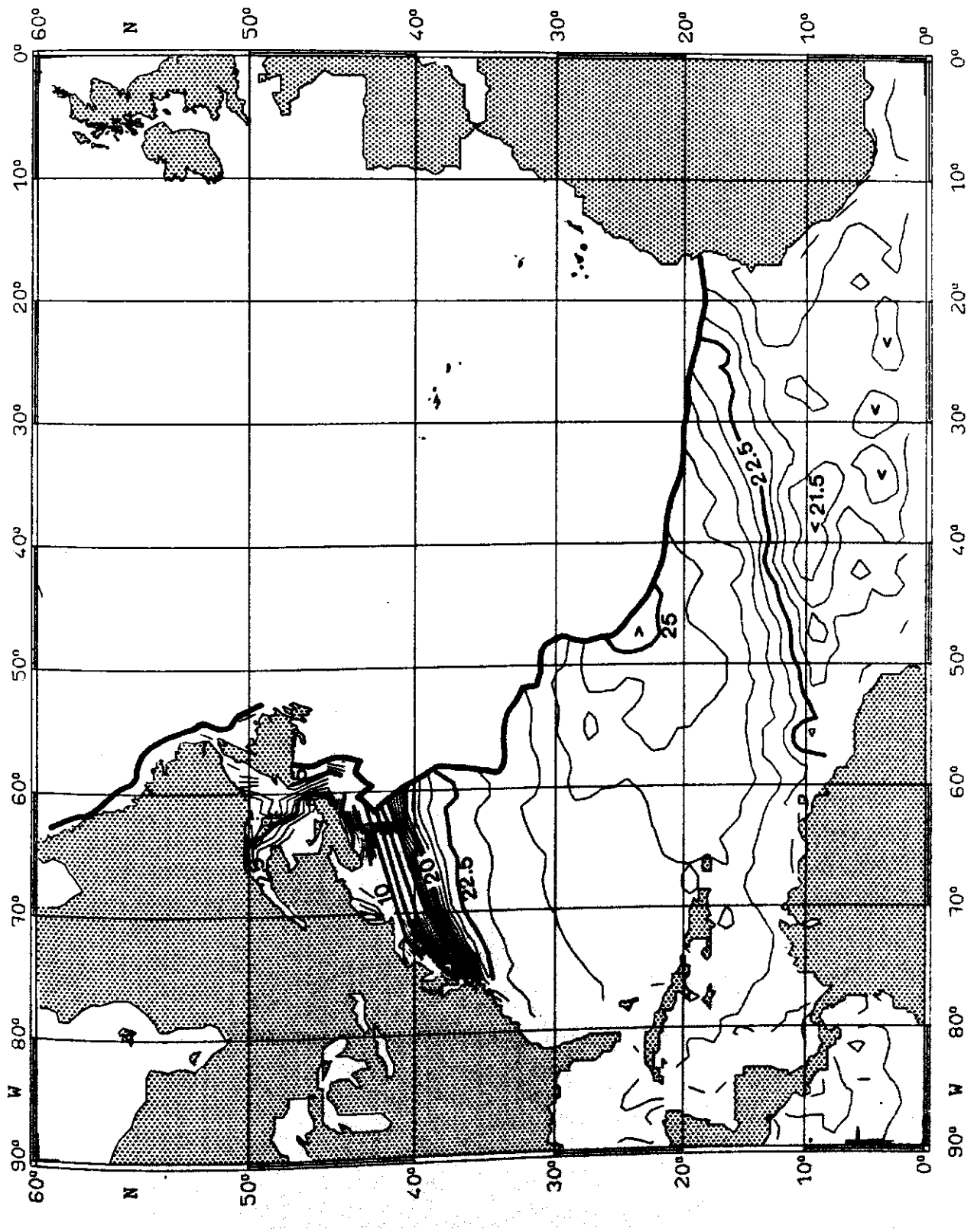

Fig. 58:

SALINITY (10^{-3}) on σ_θ = 25.0 kg m^{-3} JUNE

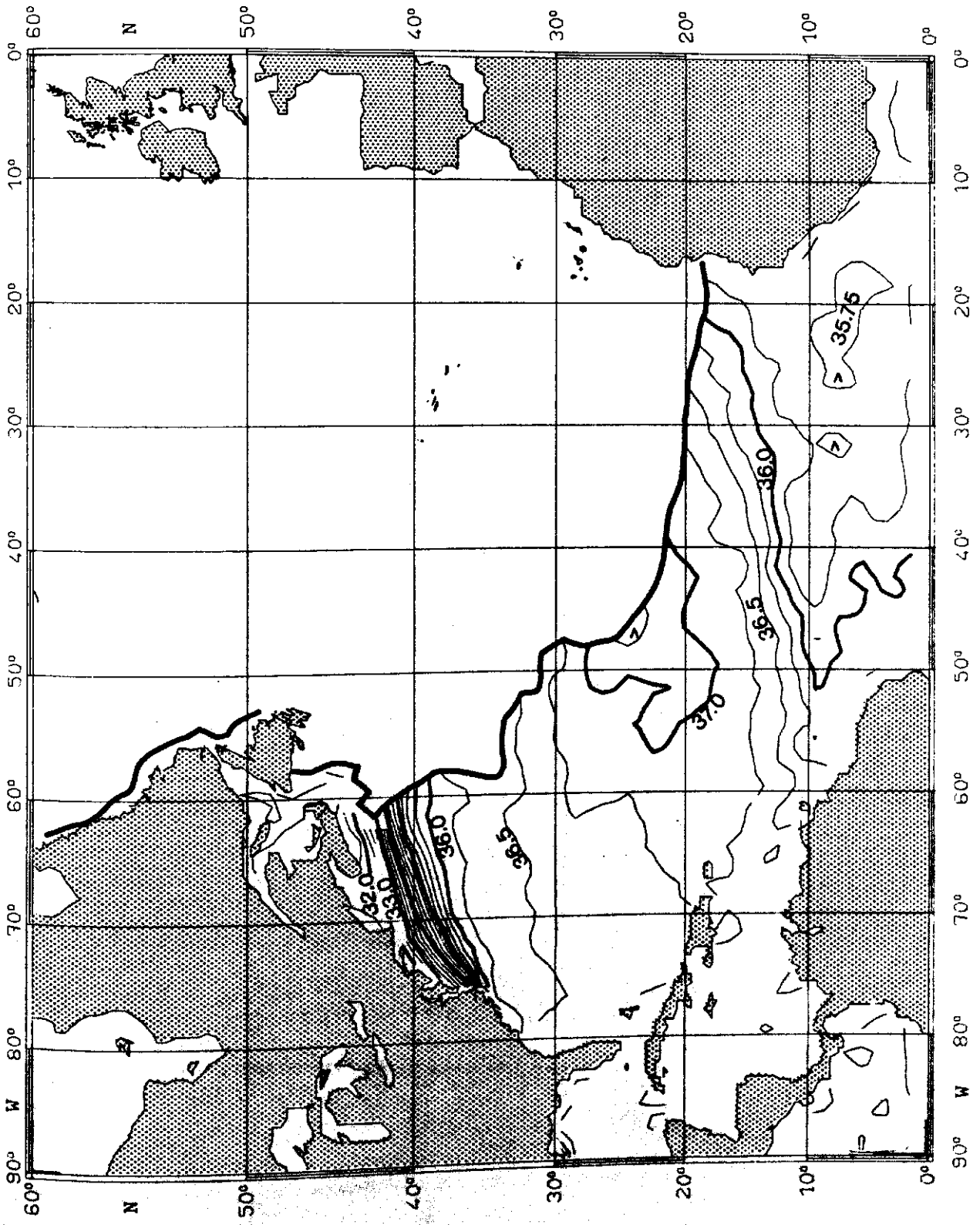

Fig. 58:

PRESSURE (10^4 Pa) on σ_θ = 25.5 kg m^{-3} JUNE

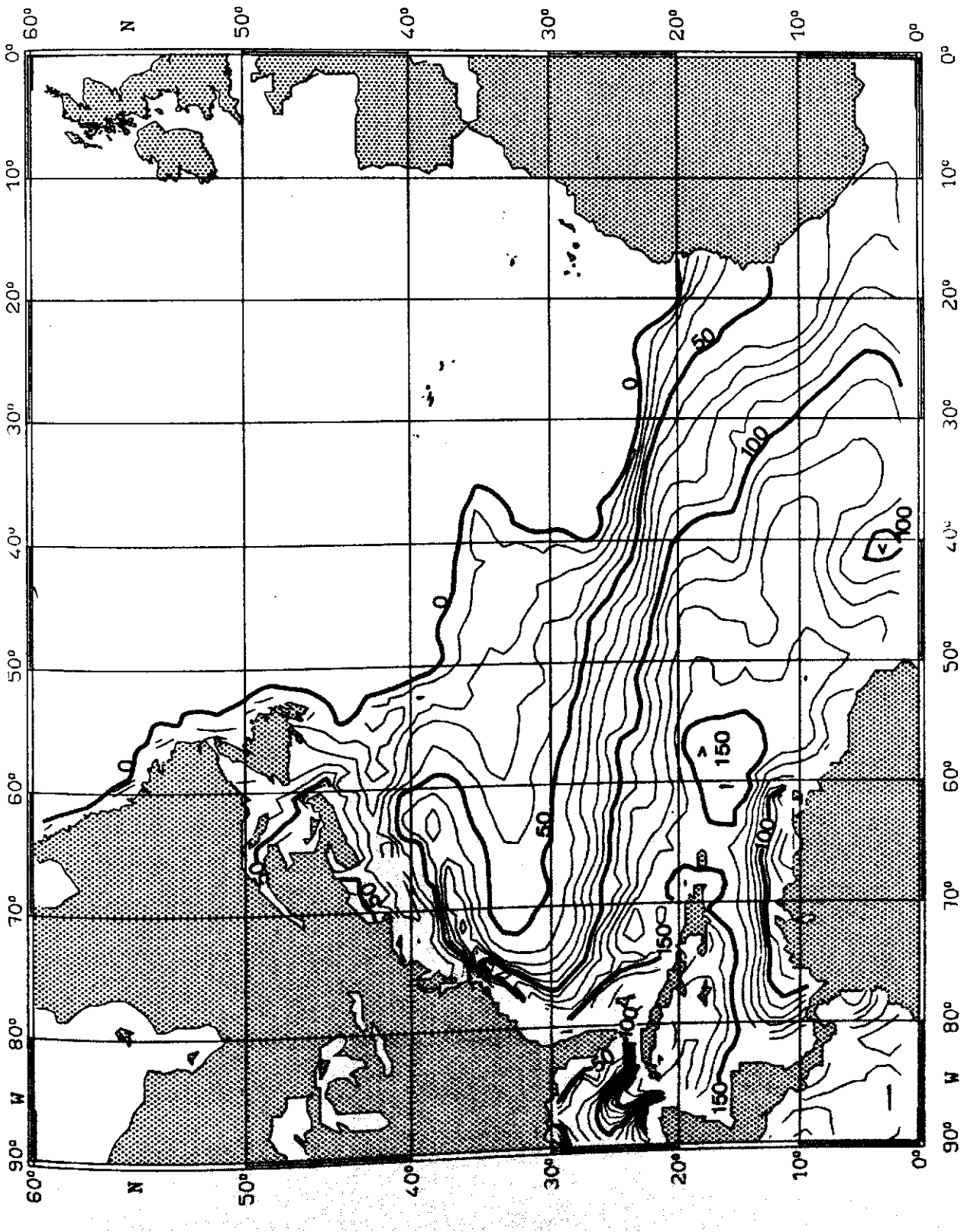

Fig. 59:

TEMPERATURE (°C) on σ_θ = 25.5 kg m^{-3} JUNE

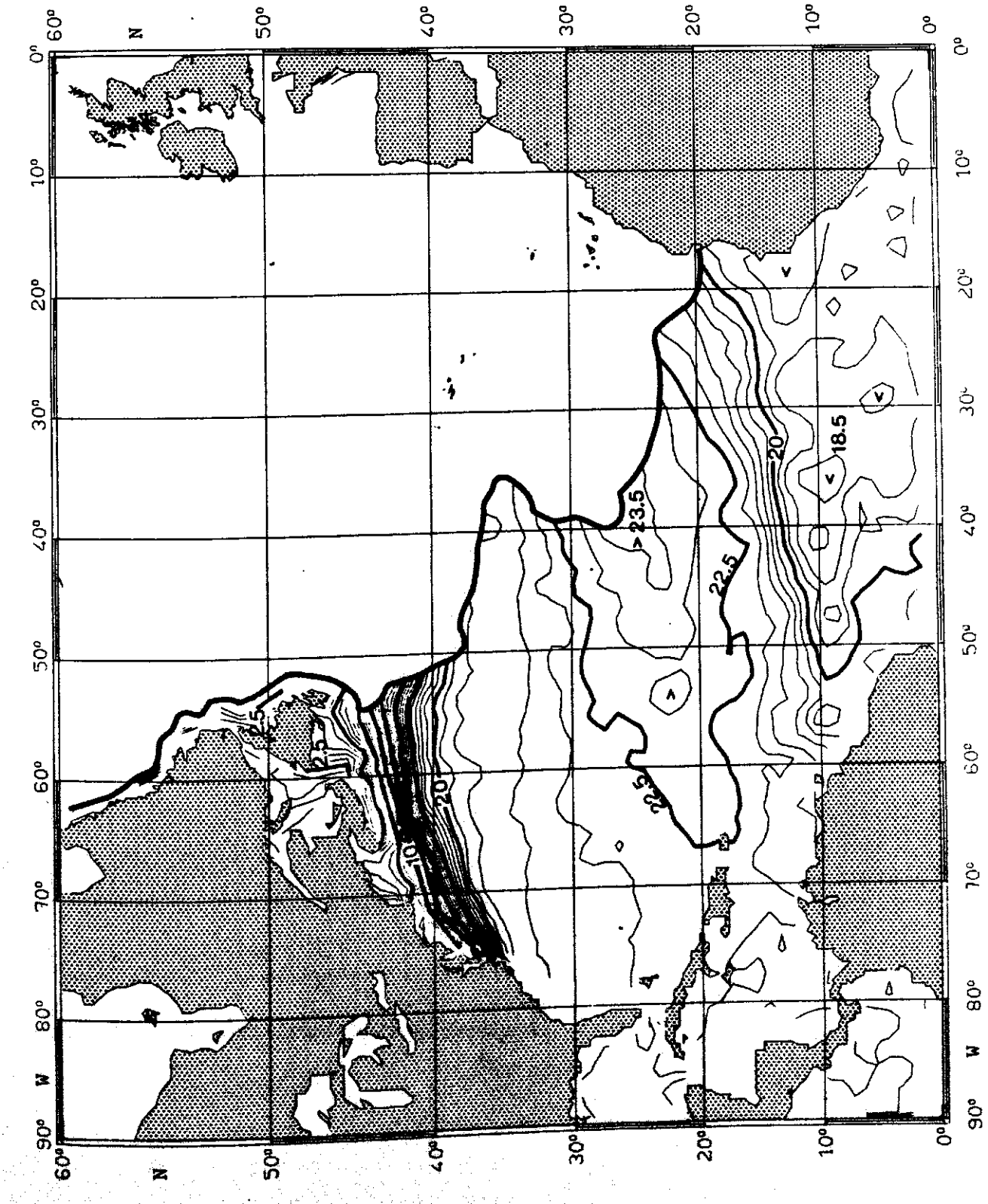

Fig. 60:

SALINITY (10^{-3}) on σ_θ = 25.5 kg m^{-3} JUNE

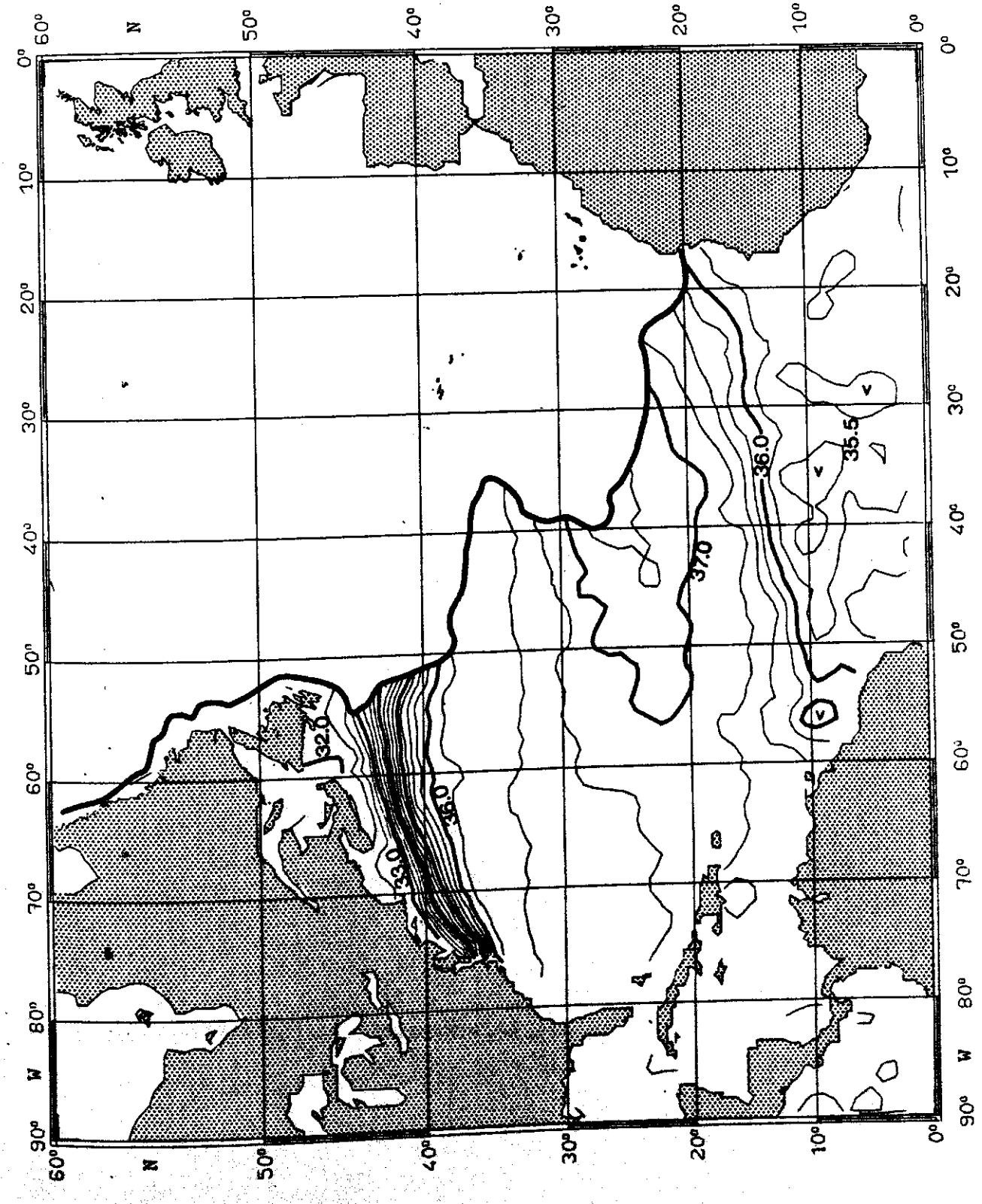

Fig. 61:

PRESSURE (10^4 Pa) on σ_θ = 26.0 kg m^{-3} JUNE

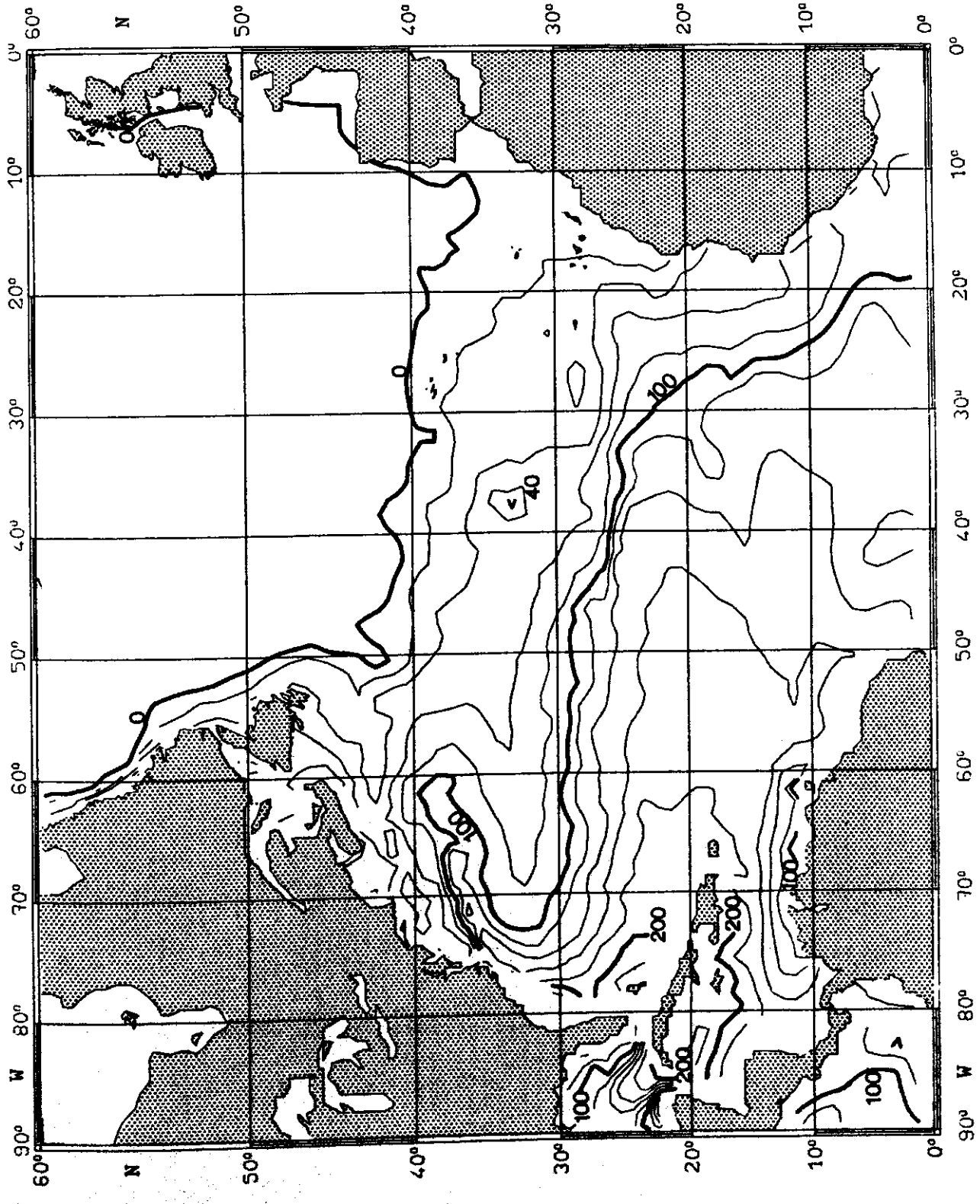

Fig. 62:

TEMPERATURE (°C) on σ_θ = 26.0 kg m^{-3} JUNE

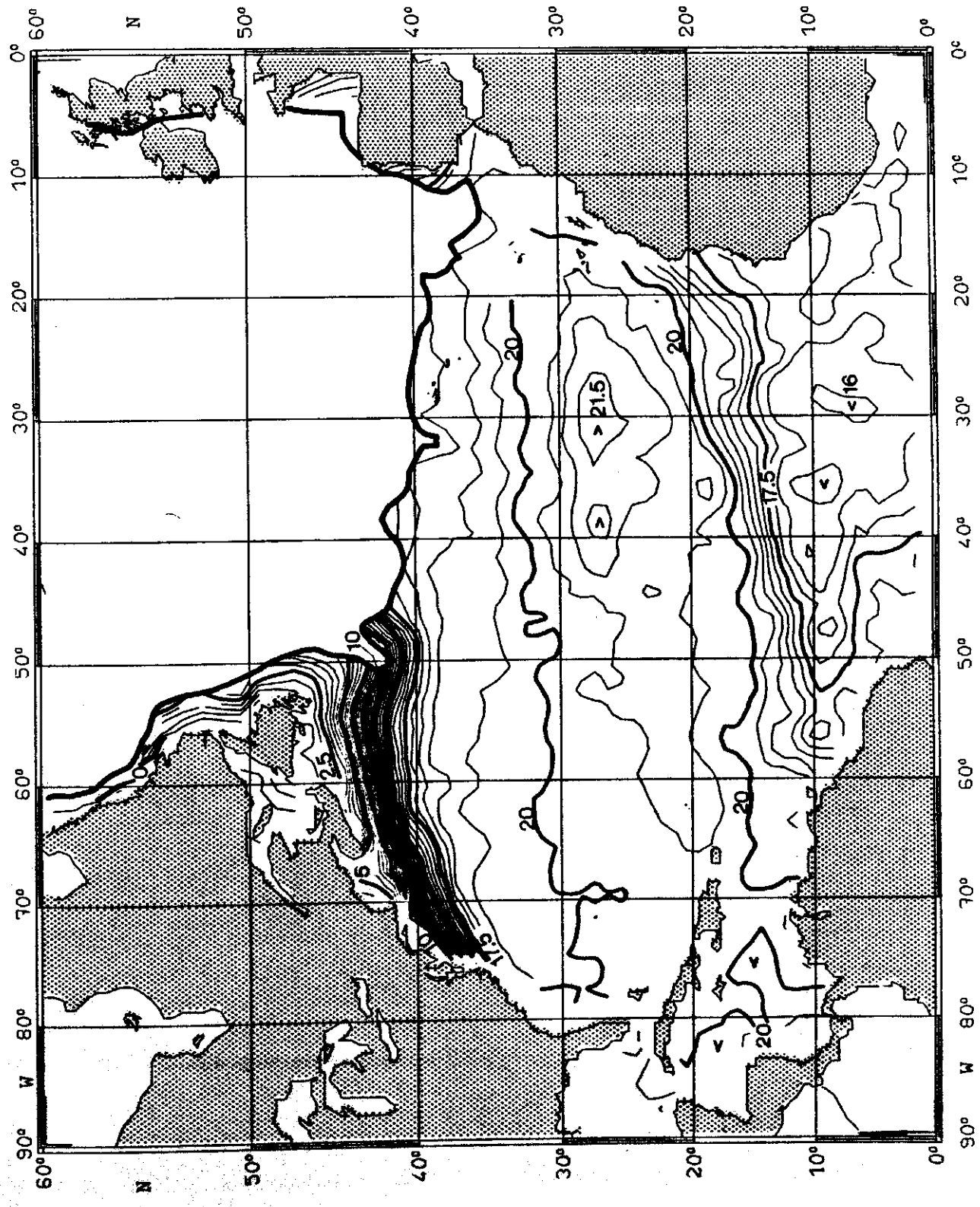

Fig. 63:

SALINITY (10^{-3}) on σ_θ = 26.0 kg m^{-3} JUNE

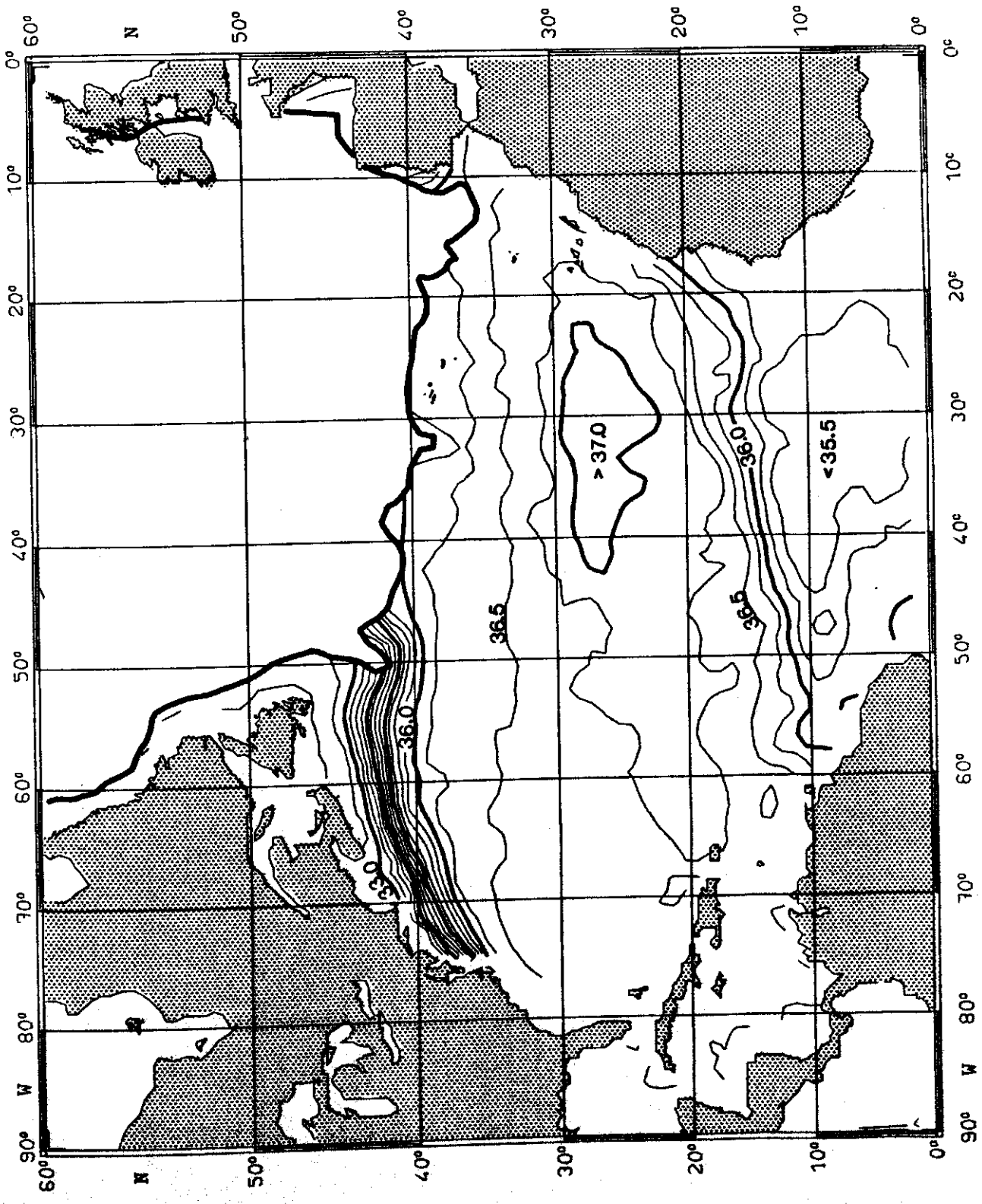

Fig. 64:

PRESSURE (10^4 Pa) on σ_θ = 26.5 kg m^{-3} JUNE

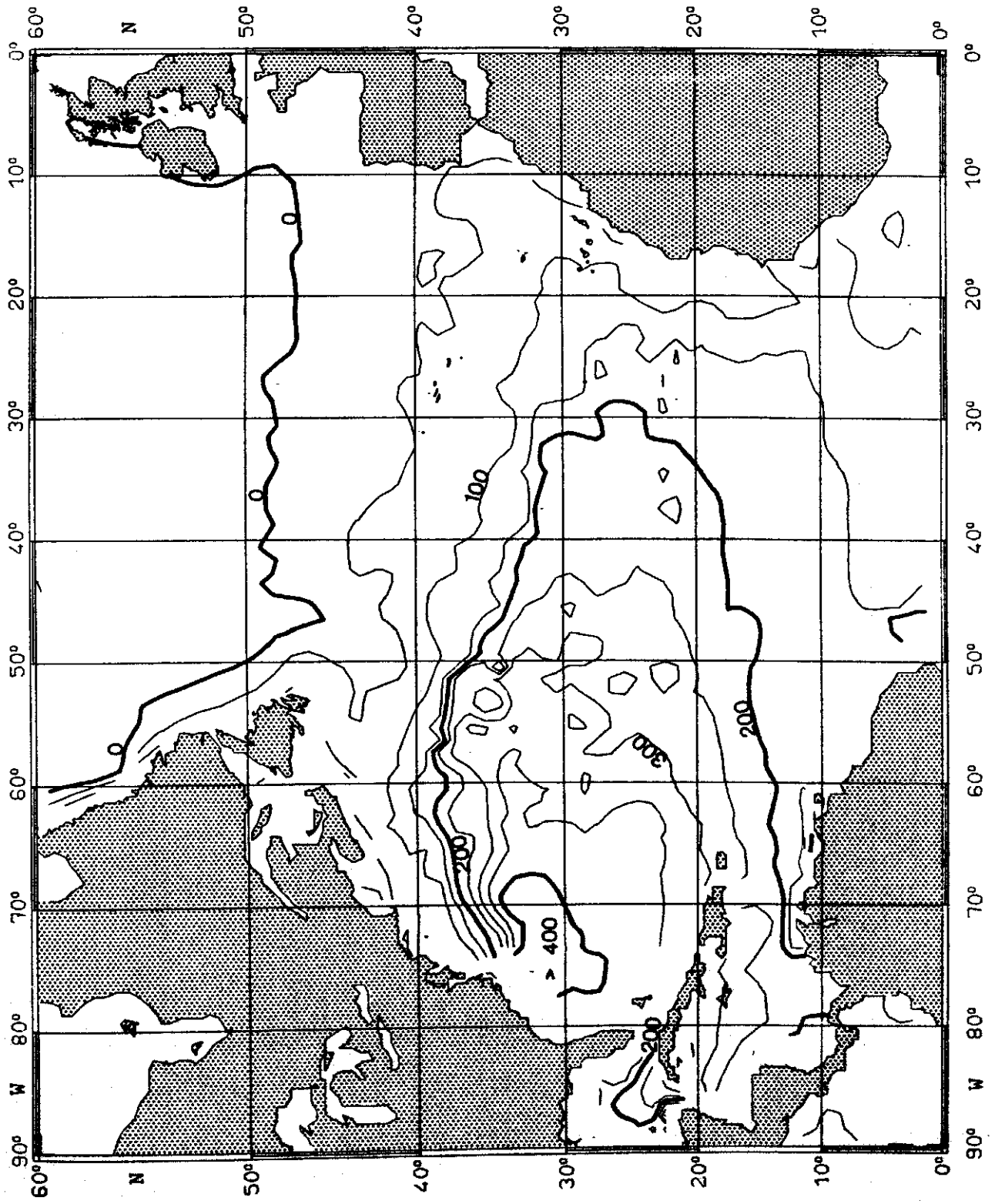

Fig. 65:

TEMPERATURE (°C) on σ_θ = 26.5 kg m^{-3} JUNE

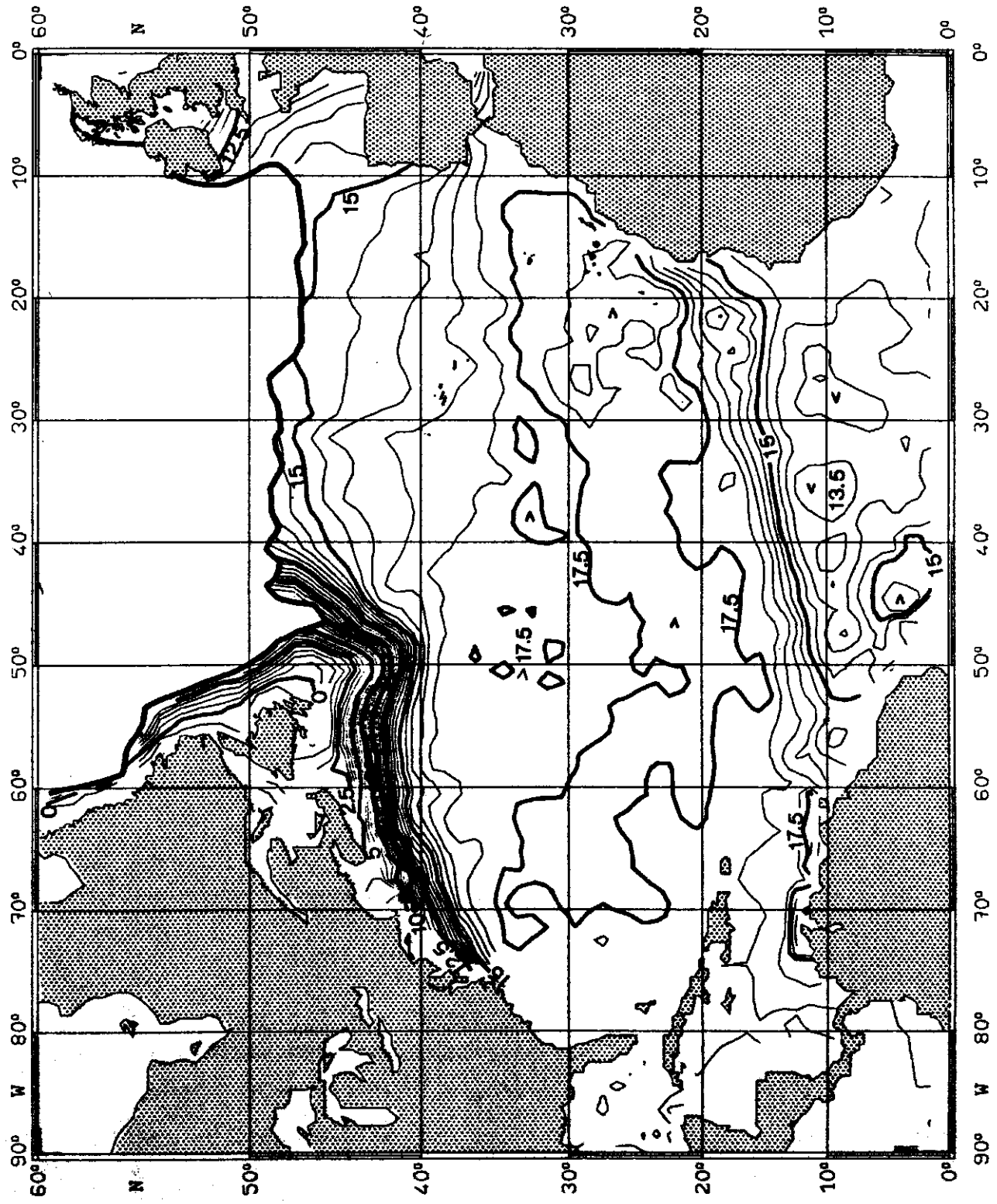

Fig. 66:

SALINITY (10^{-3}) on σ_θ = 26.5 kg m^{-3} JUNE

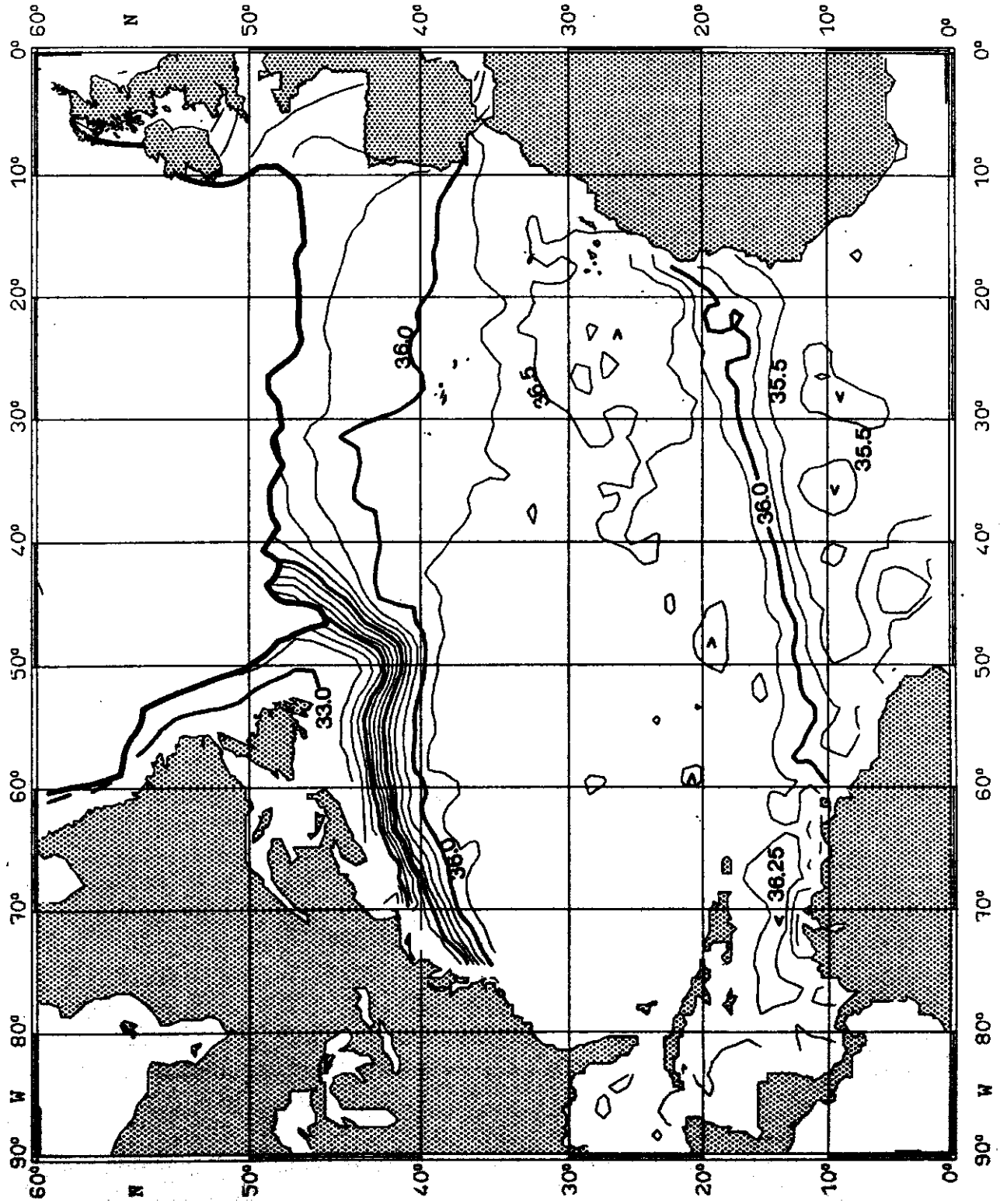

Fig. 67:

PRESSURE (10^4 Pa) on σ_θ = 27.0 kg m^{-3} JUNE

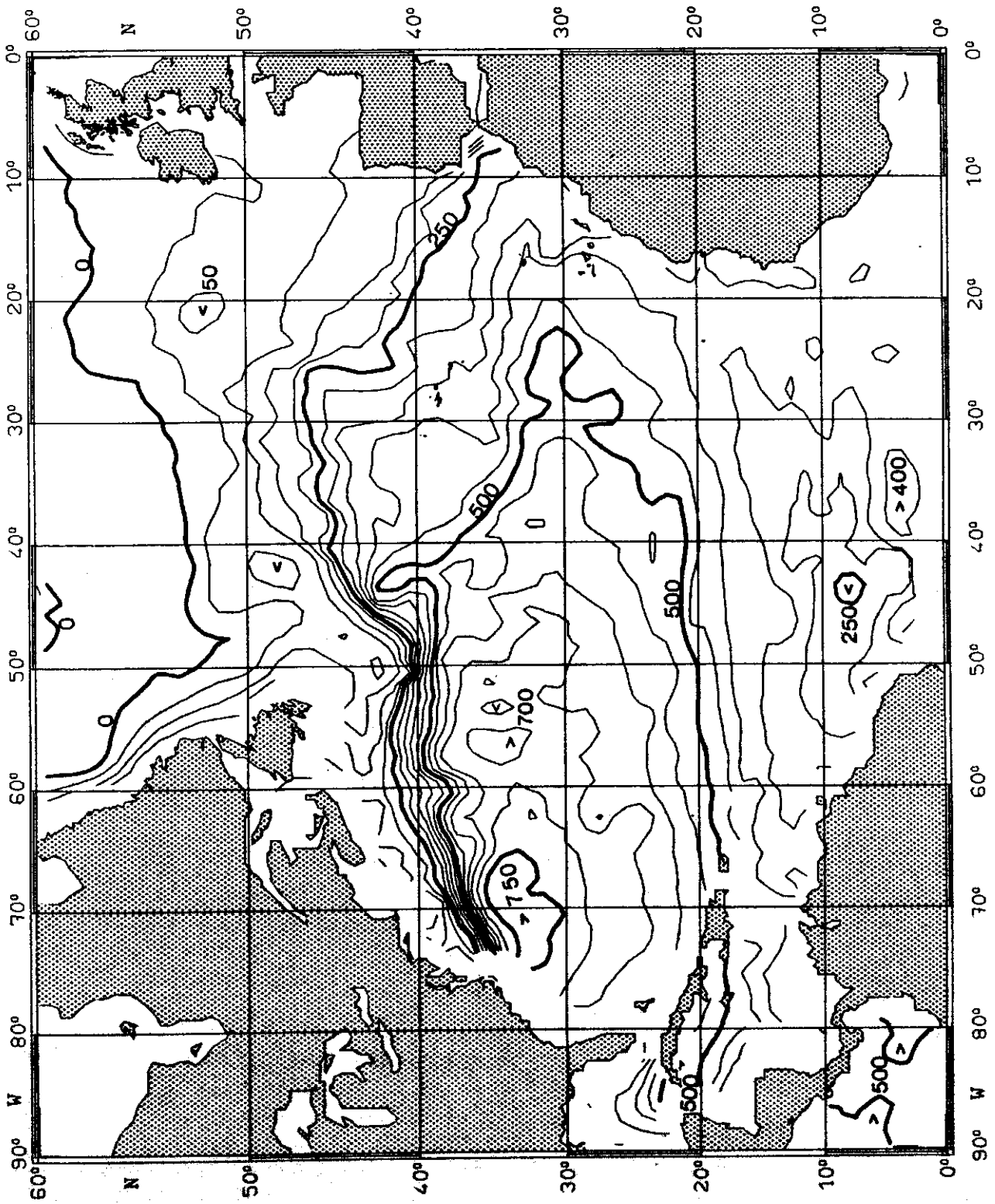

Fig. 68:

TEMPERATURE (°C) on σ_θ = 27.0 kg m^{-3} JUNE

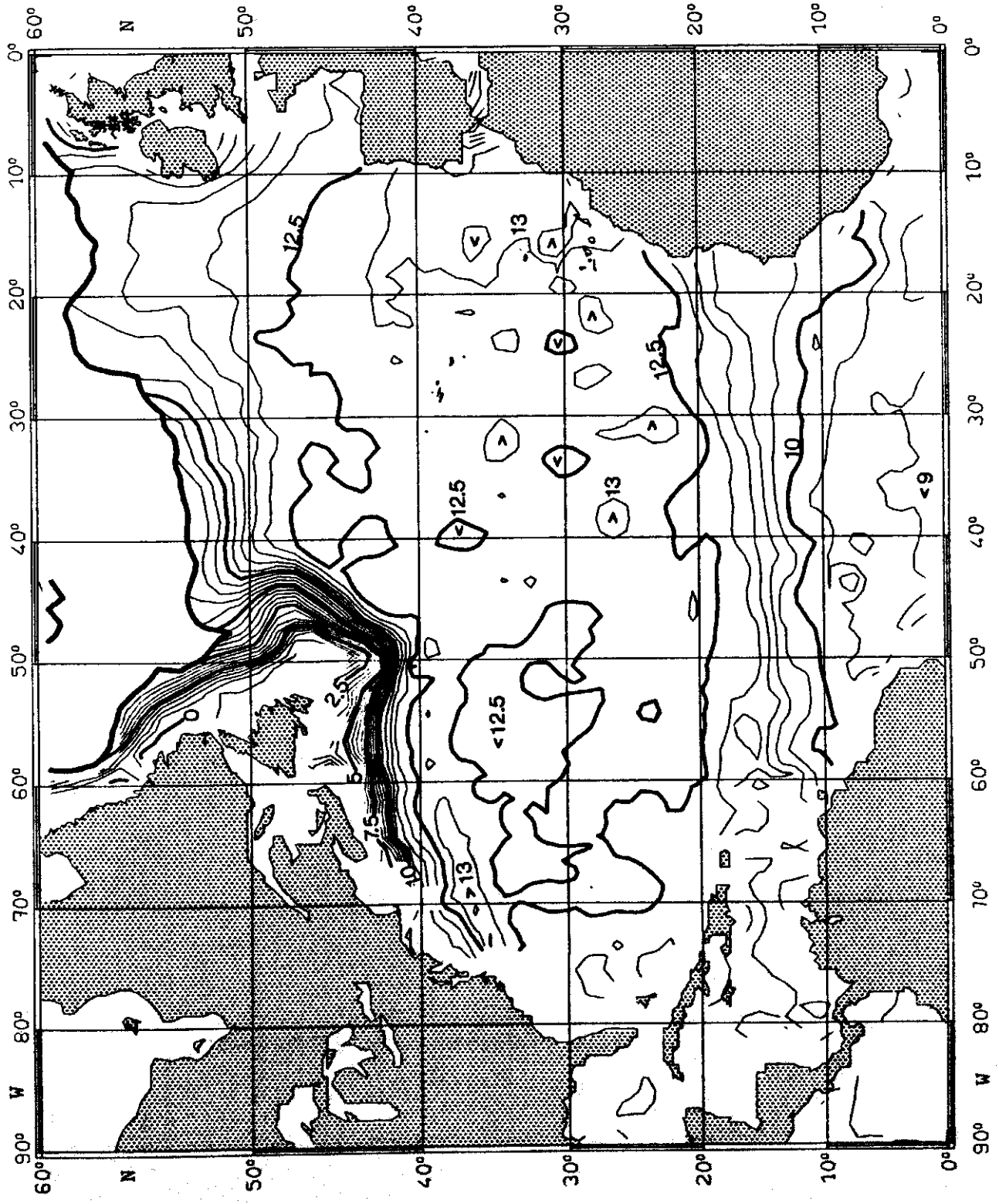

Fig. 69:

SALINITY (10^{-3}) on σ_θ = 27.0 kg m^{-3} JUNE

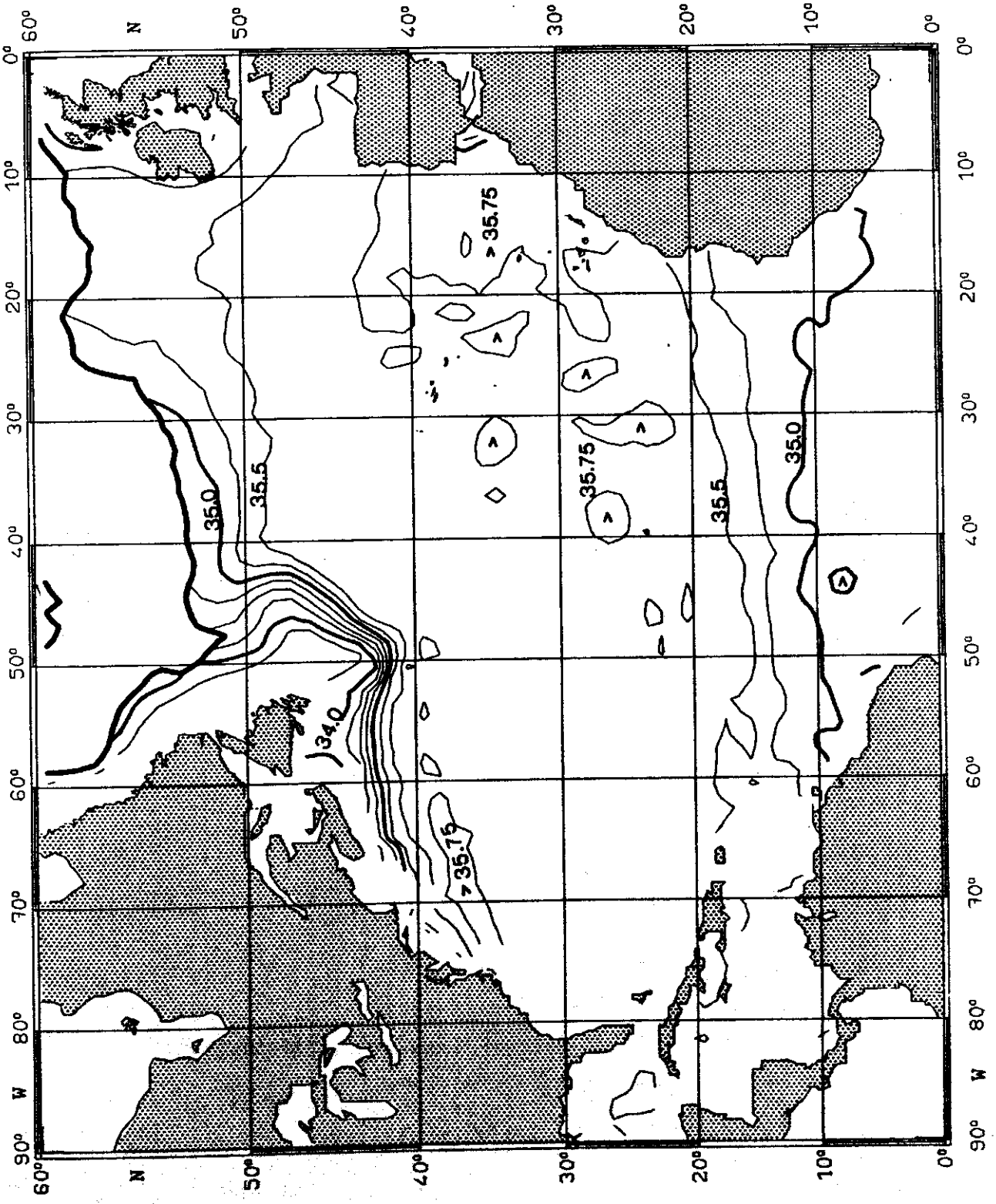

Fig. 70:

PRESSURE (10^4 Pa) on σ_θ = 25.0 kg m^{-3} JULY

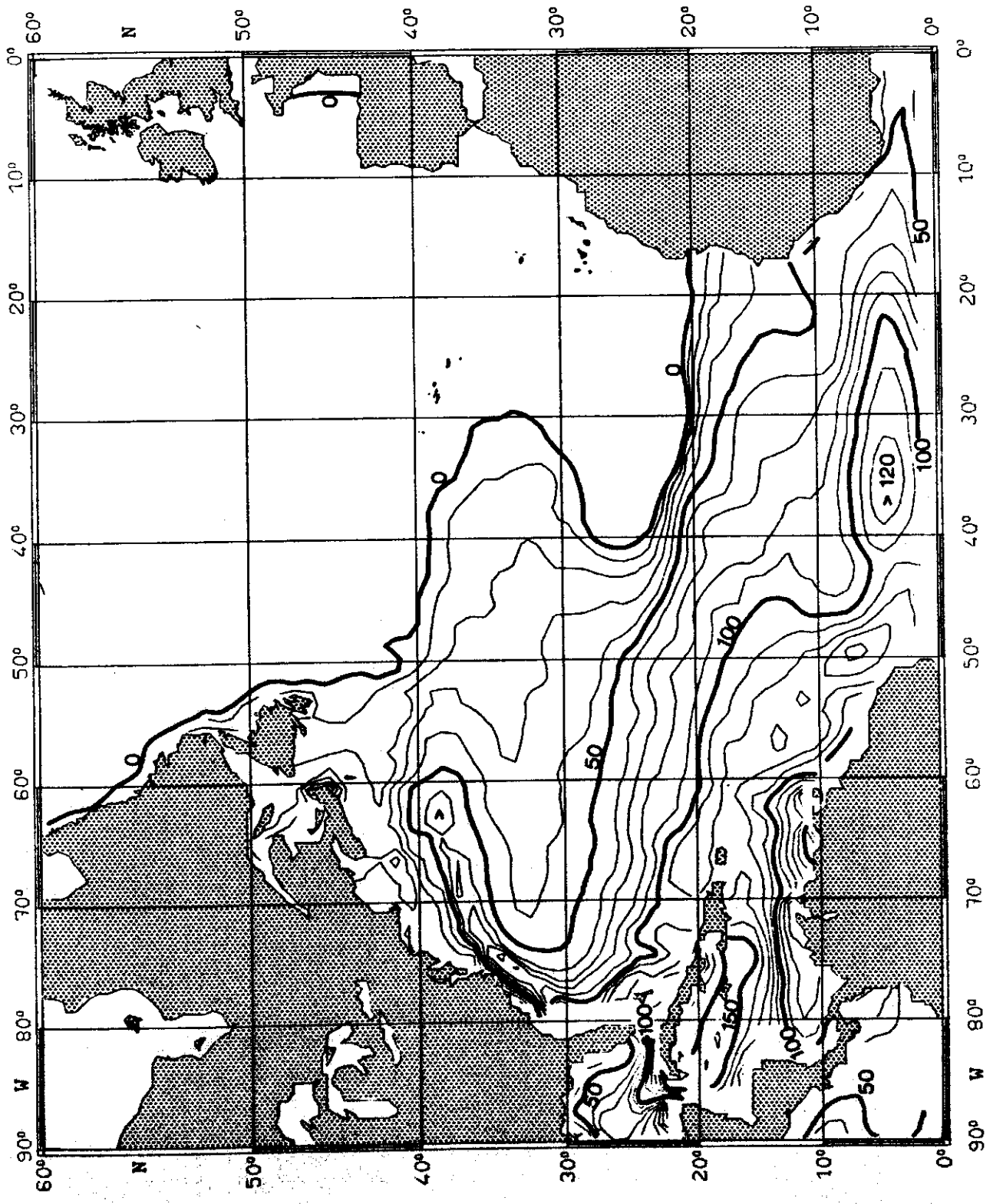

Fig. 71:

TEMPERATURE (°C) on σ_θ = 25.0 kg m^{-3} JULY

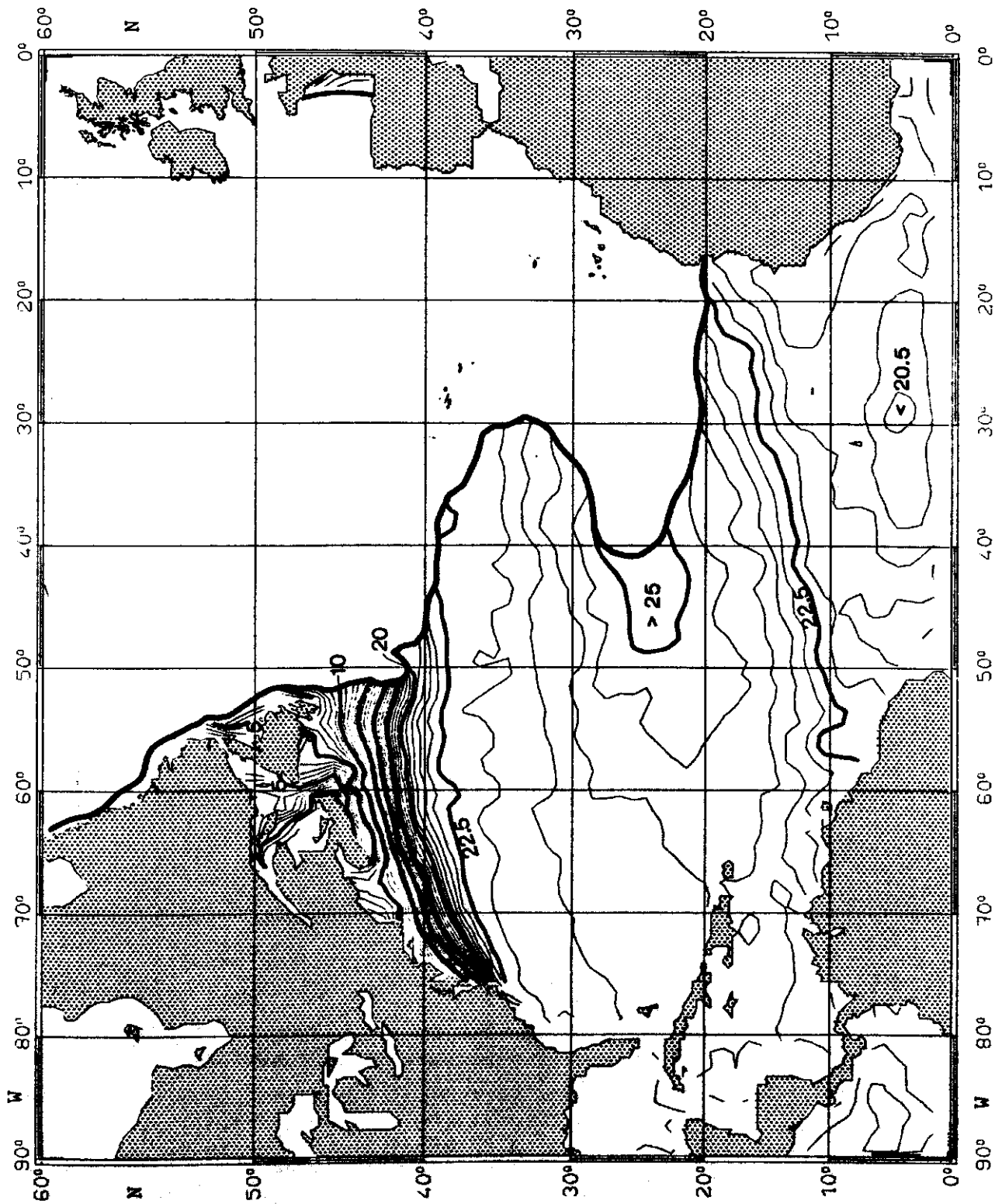

Fig. 72:

SALINITY (10^{-3}) on σ_θ = 25.0 kg m^{-3} JULY

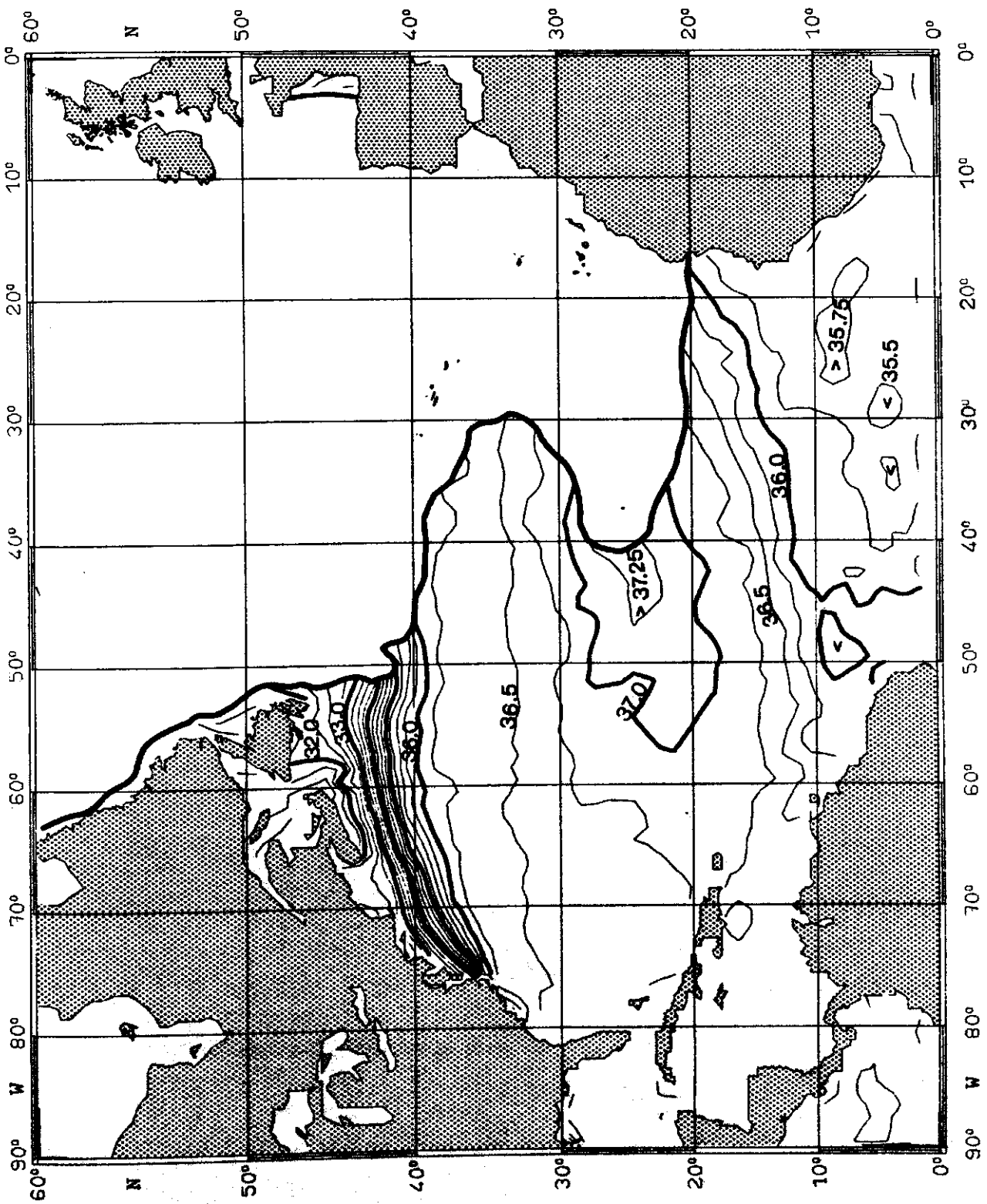

Fig. 73:

PRESSURE (10^4 Pa) on σ_θ = 25.5 kg m^{-3} JULY

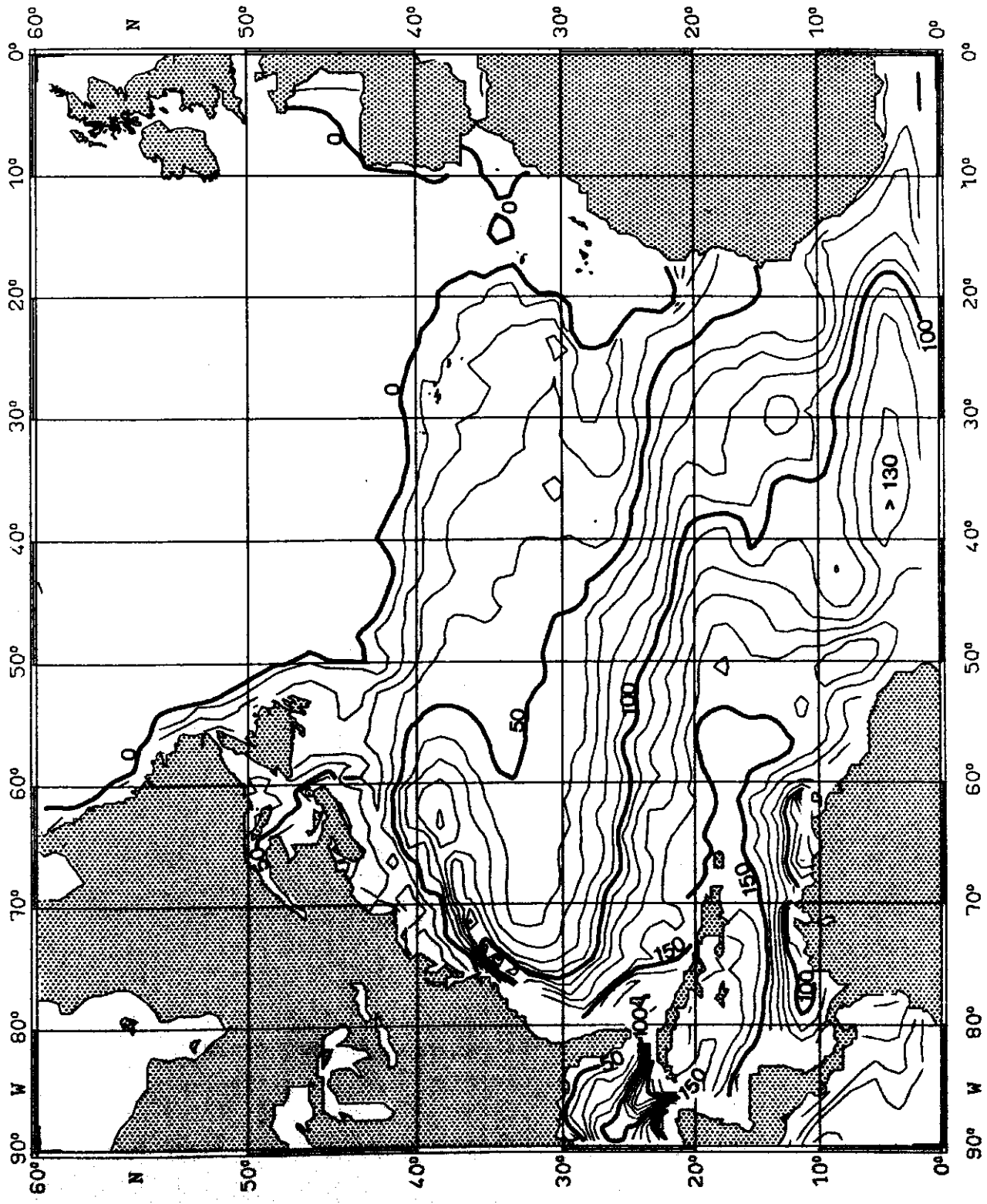

Fig. 74:

TEMPERATURE (°C) on σ_θ = 25.5 kg m^{-3} JULY

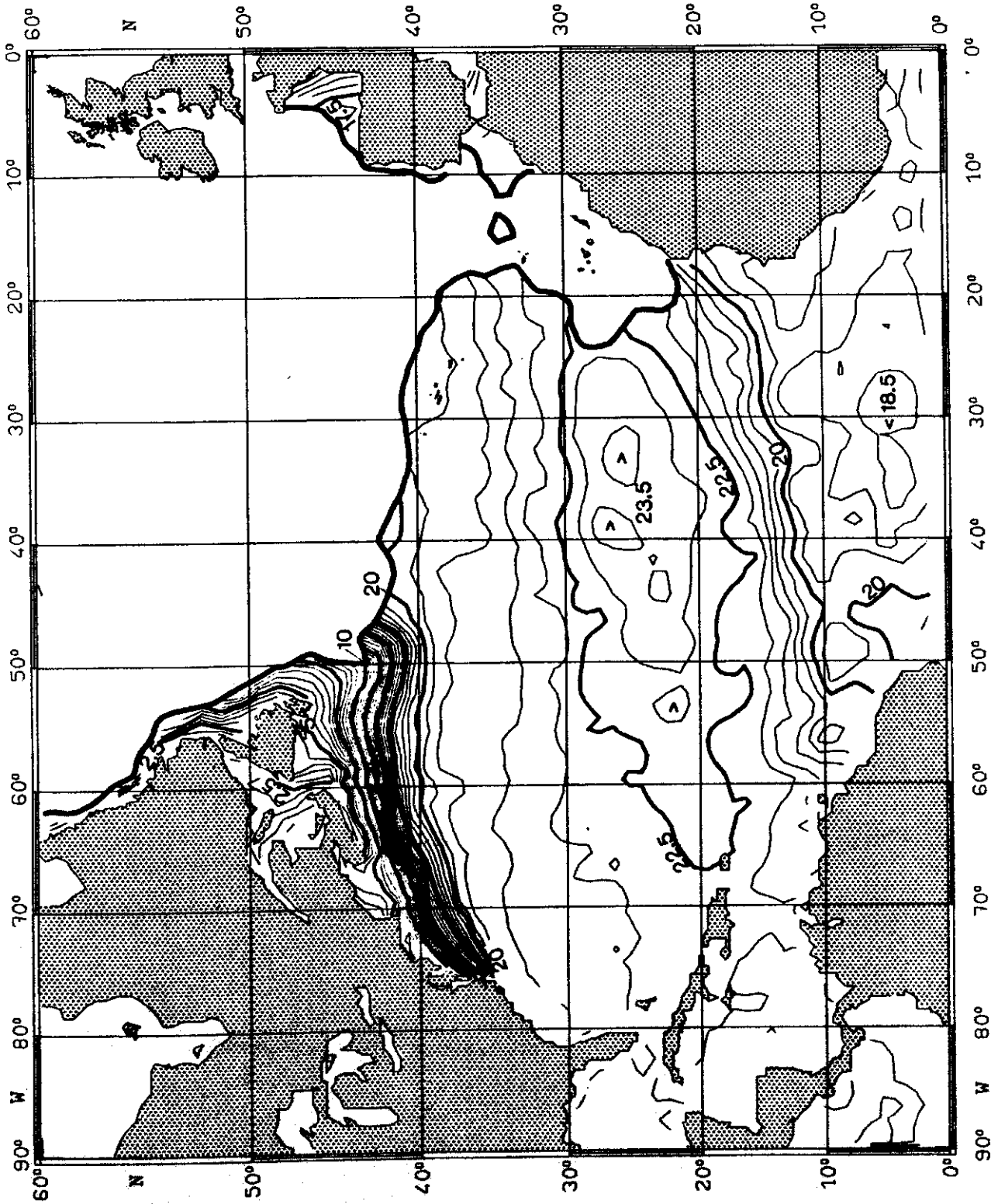

Fig. 75:

SALINITY (10^{-3}) on σ_θ = 25.5 kg m^{-3} JULY

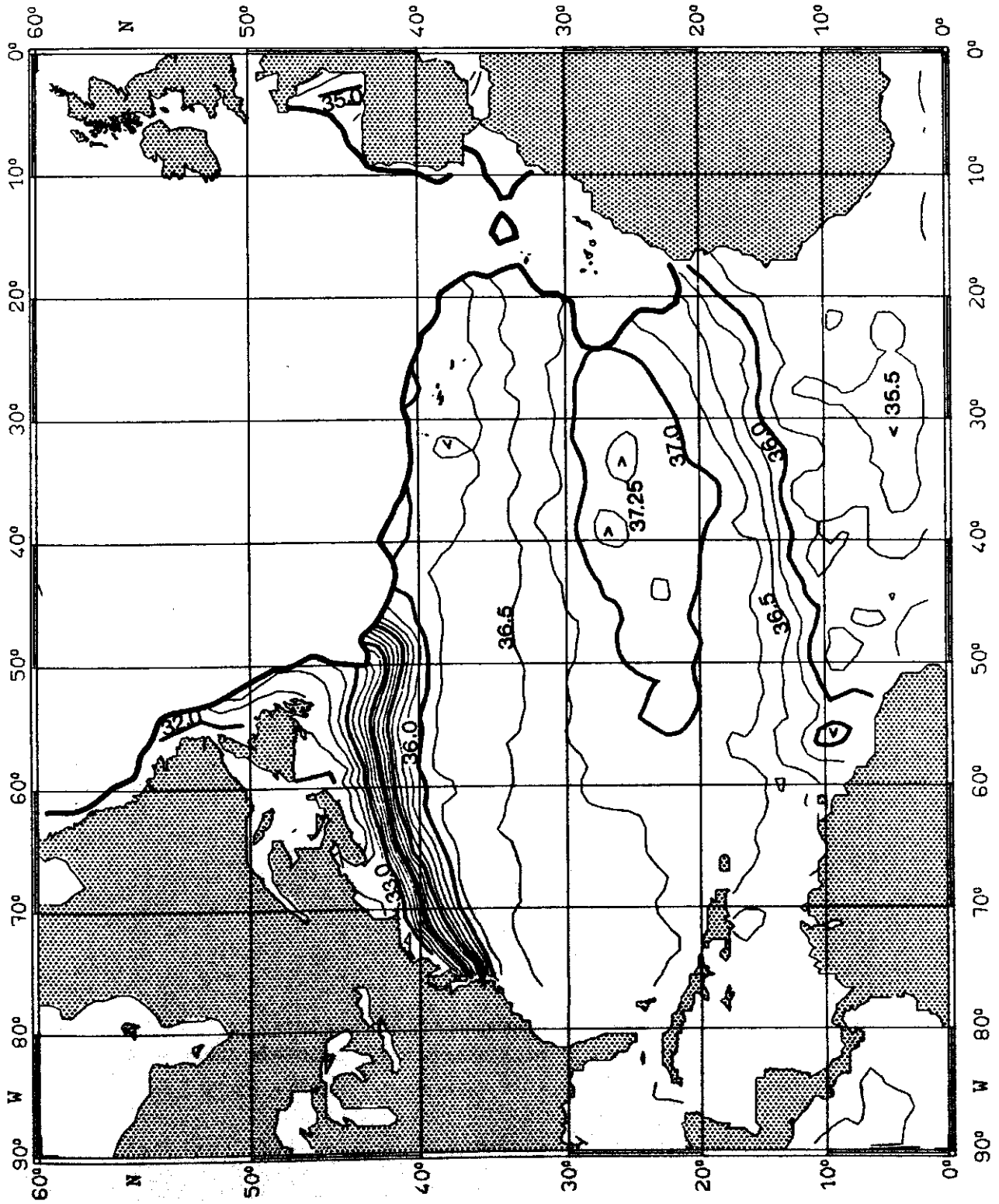

Fig. 76:

PRESSURE (10^4 Pa) on σ_θ = 26.0 kg m^{-3} JULY

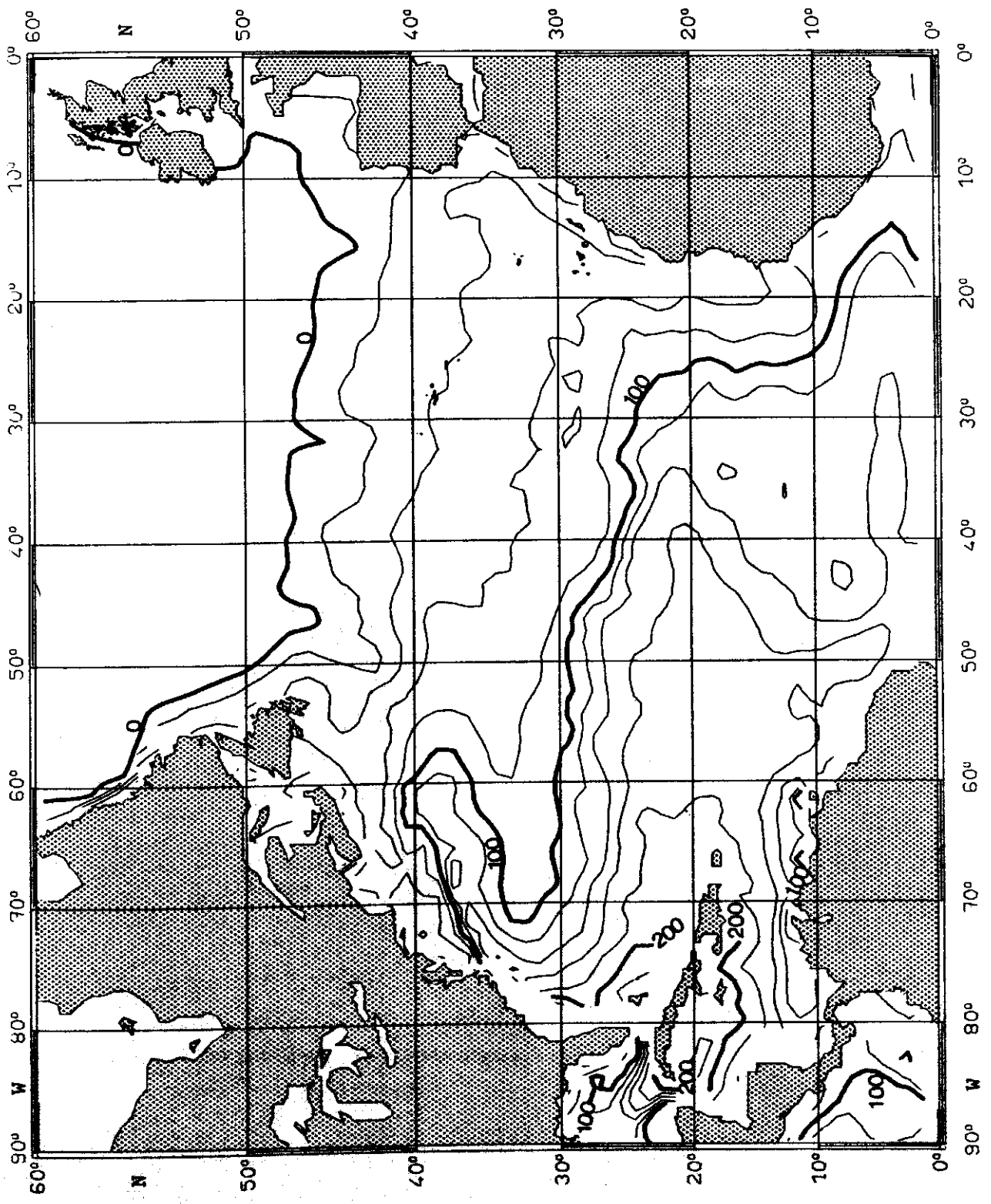

Fig. 77:

TEMPERATURE (°C) on σ_θ = 26.0 kg m^{-3} JULY

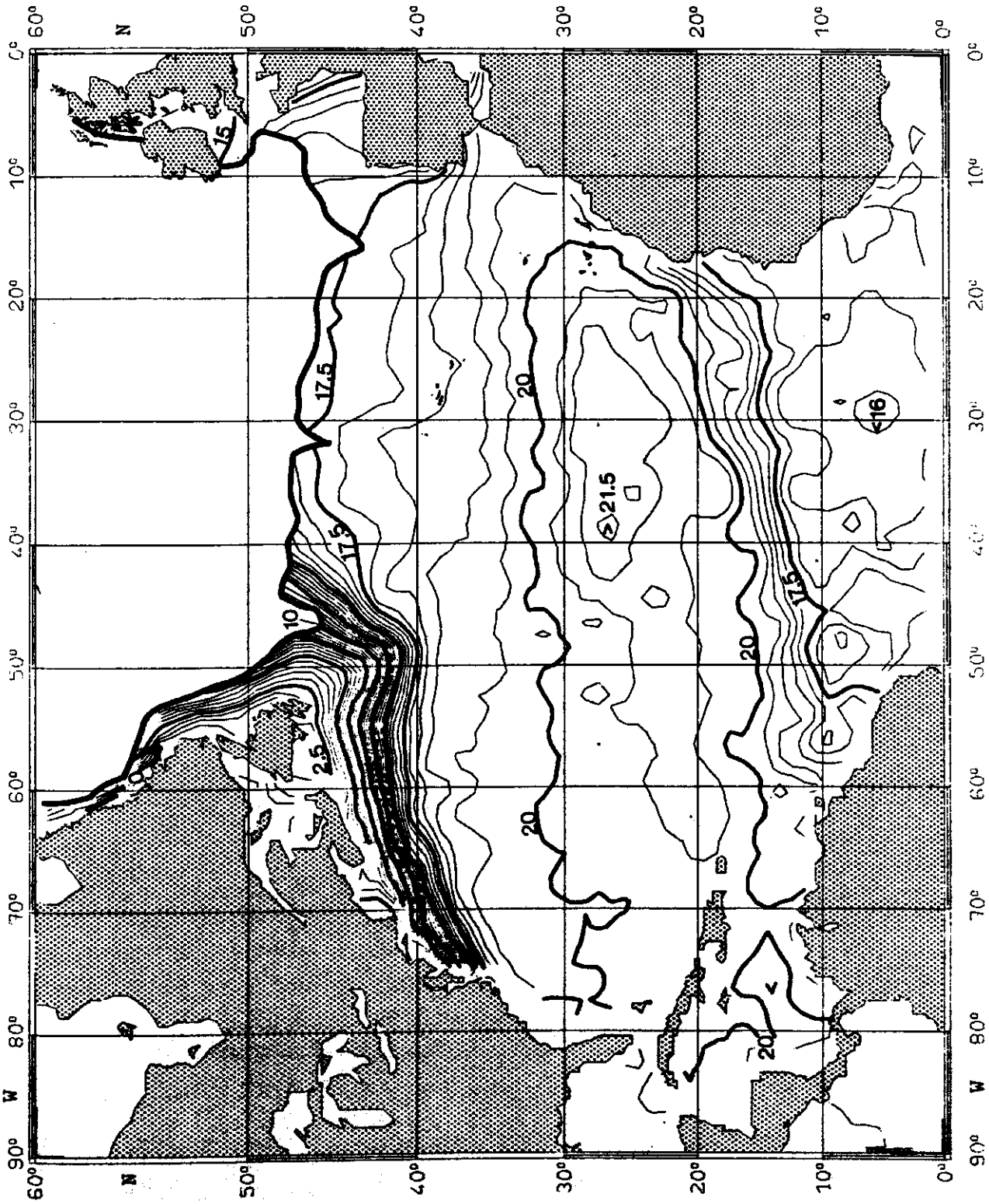

Fig. 78:

SALINITY (10^{-3}) on σ_θ = 26.0 kg m^{-3} JULY

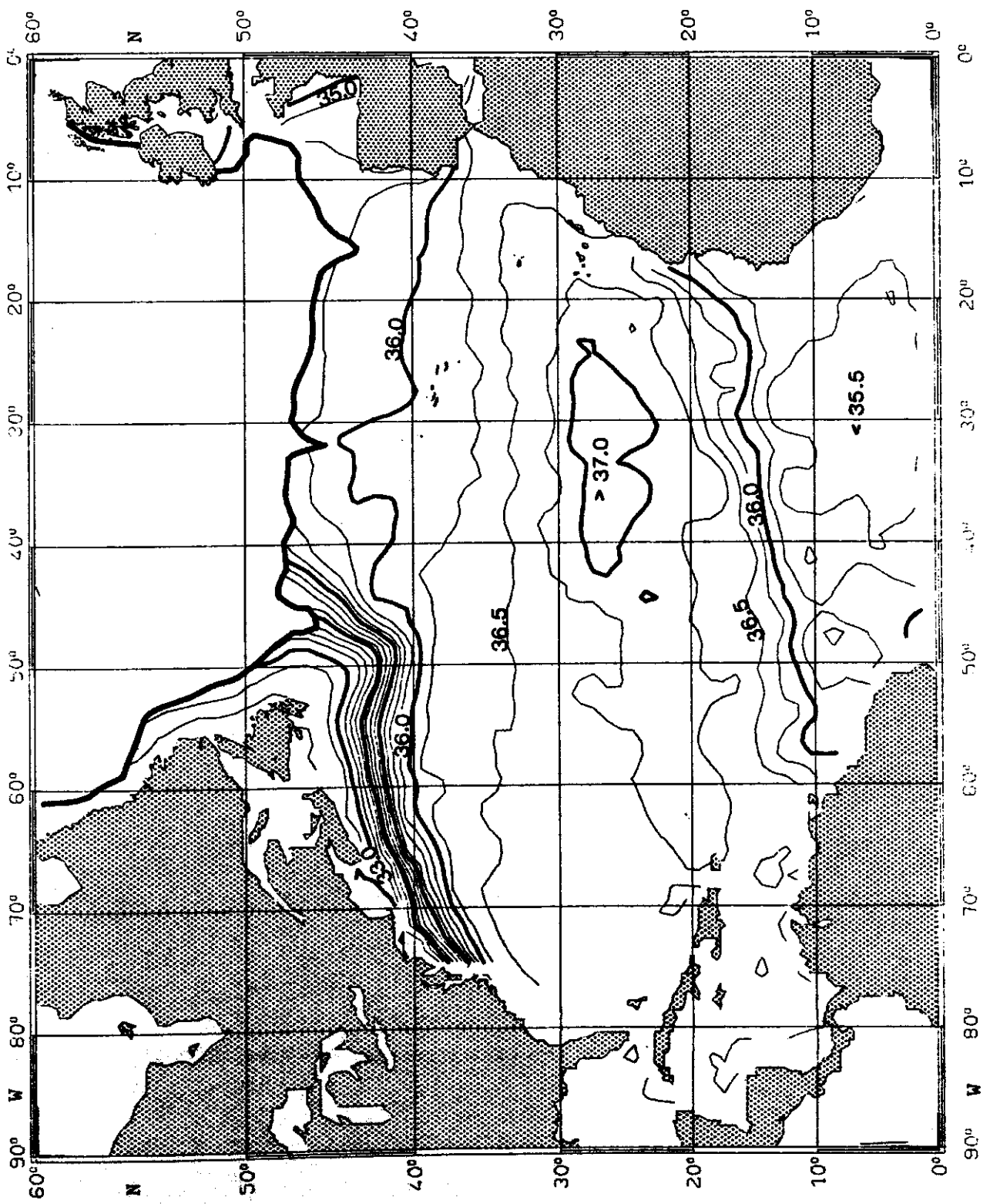

Fig. 79:

PRESSURE (10^4 Pa) on σ_θ = 26.5 kg m^{-3} JULY

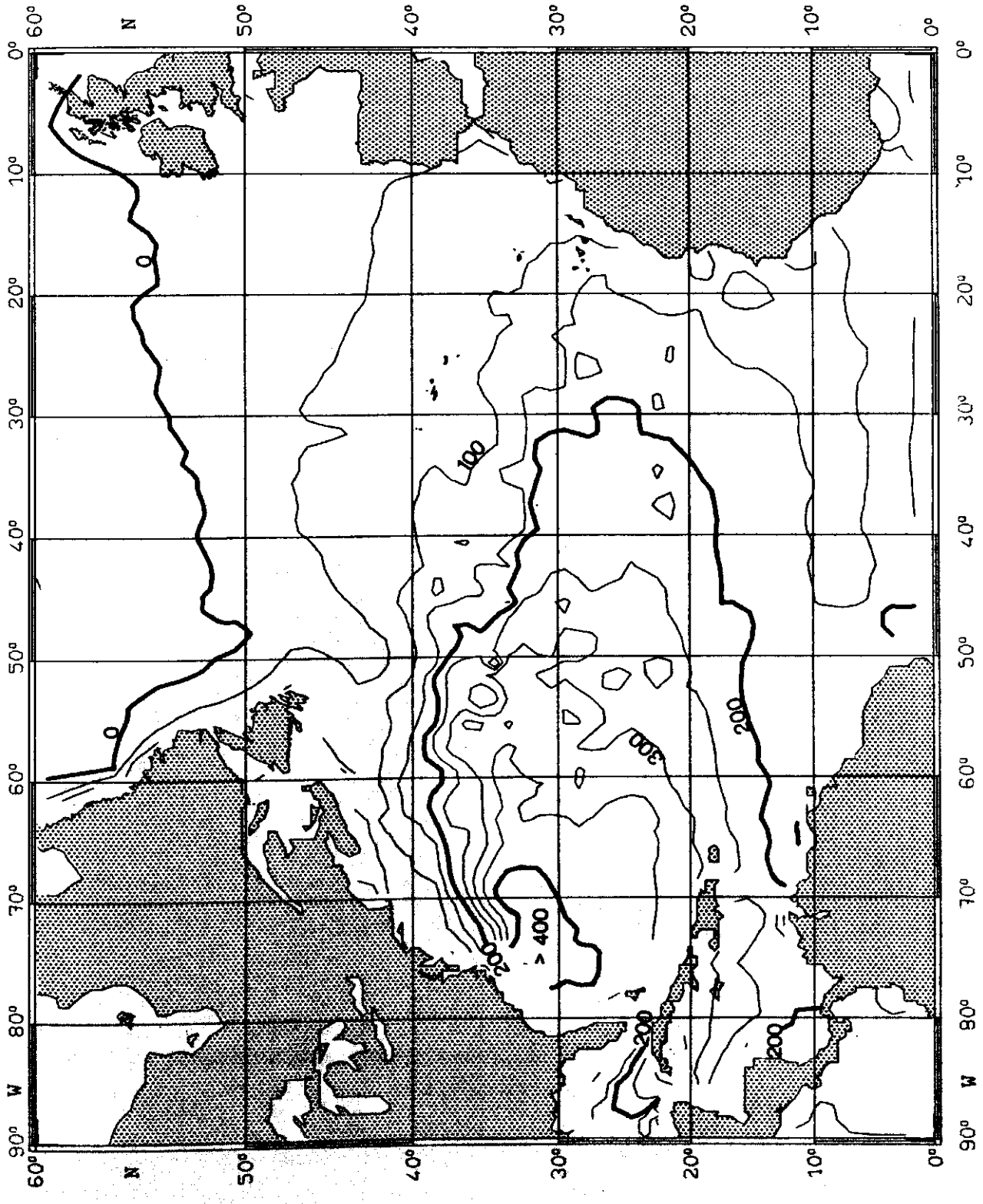

Fig. 80:

TEMPERATURE (°C) on σ_θ = 26.5 kg m^{-3} JULY

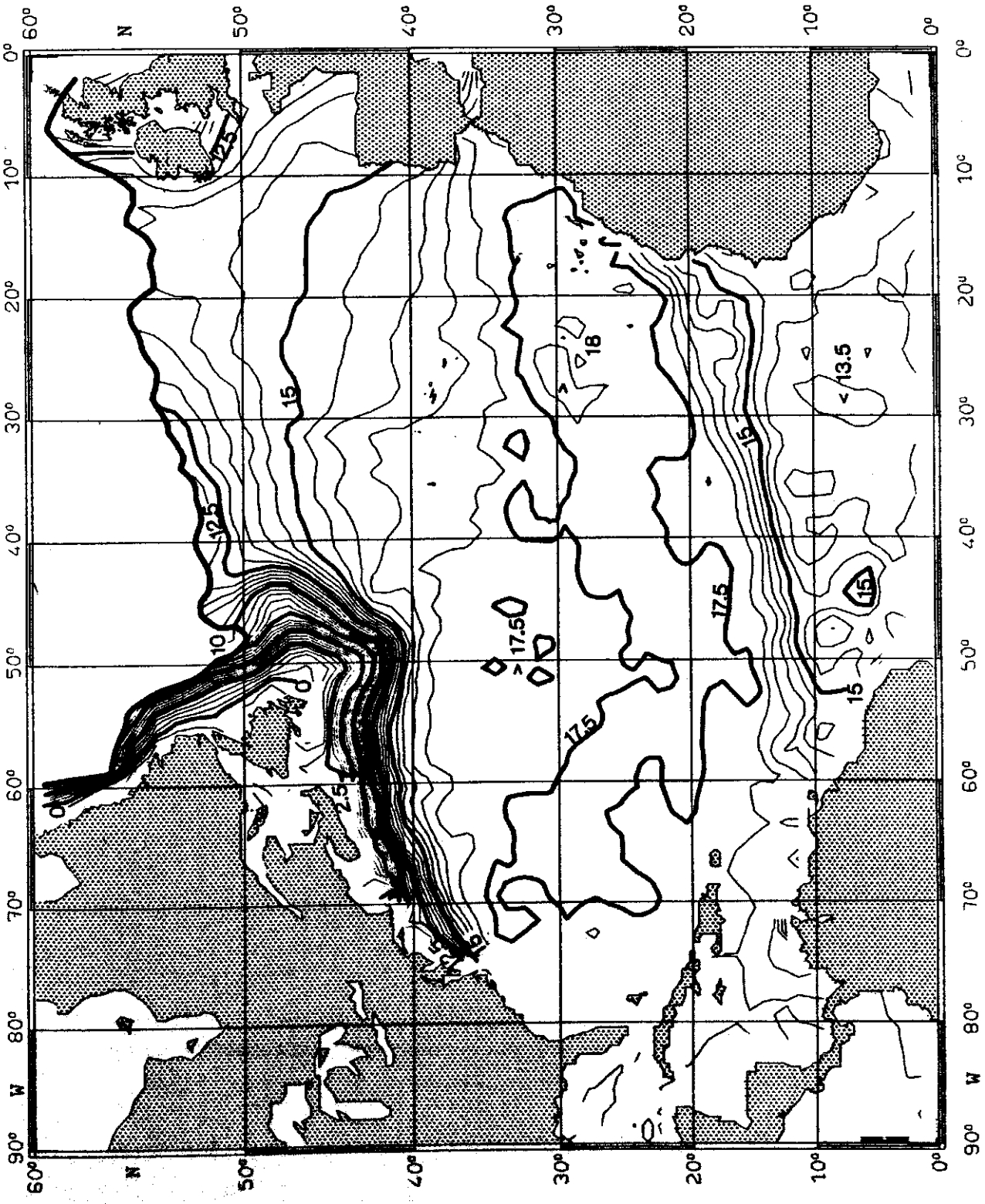

Fig. 81:

SALINITY (10^{-3}) on σ_θ = 26.5 kg m^{-3} JULY

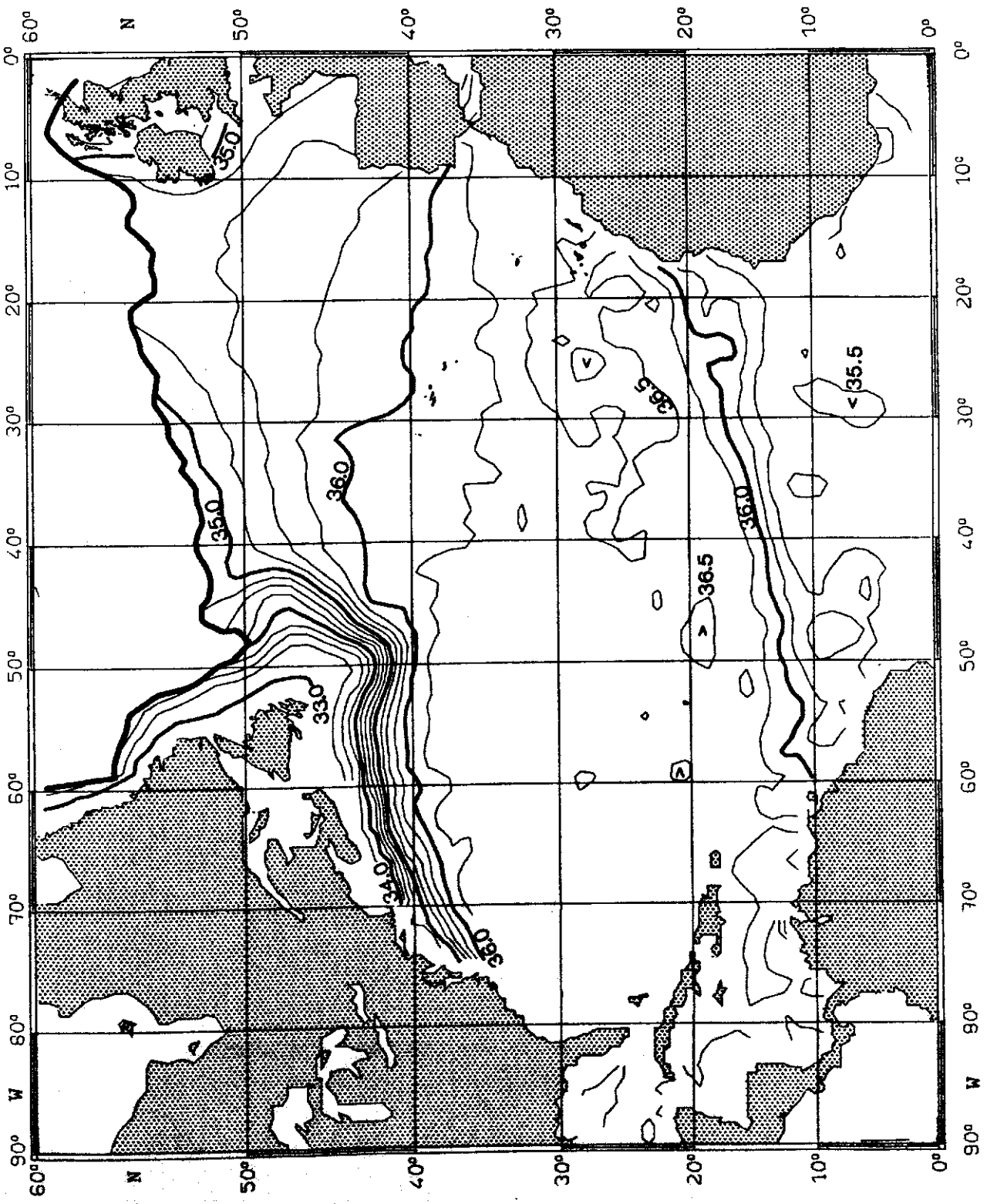

Fig. 82:

PRESSURE (10^4 Pa) on σ_θ = 27.0 kg m^{-3} JULY

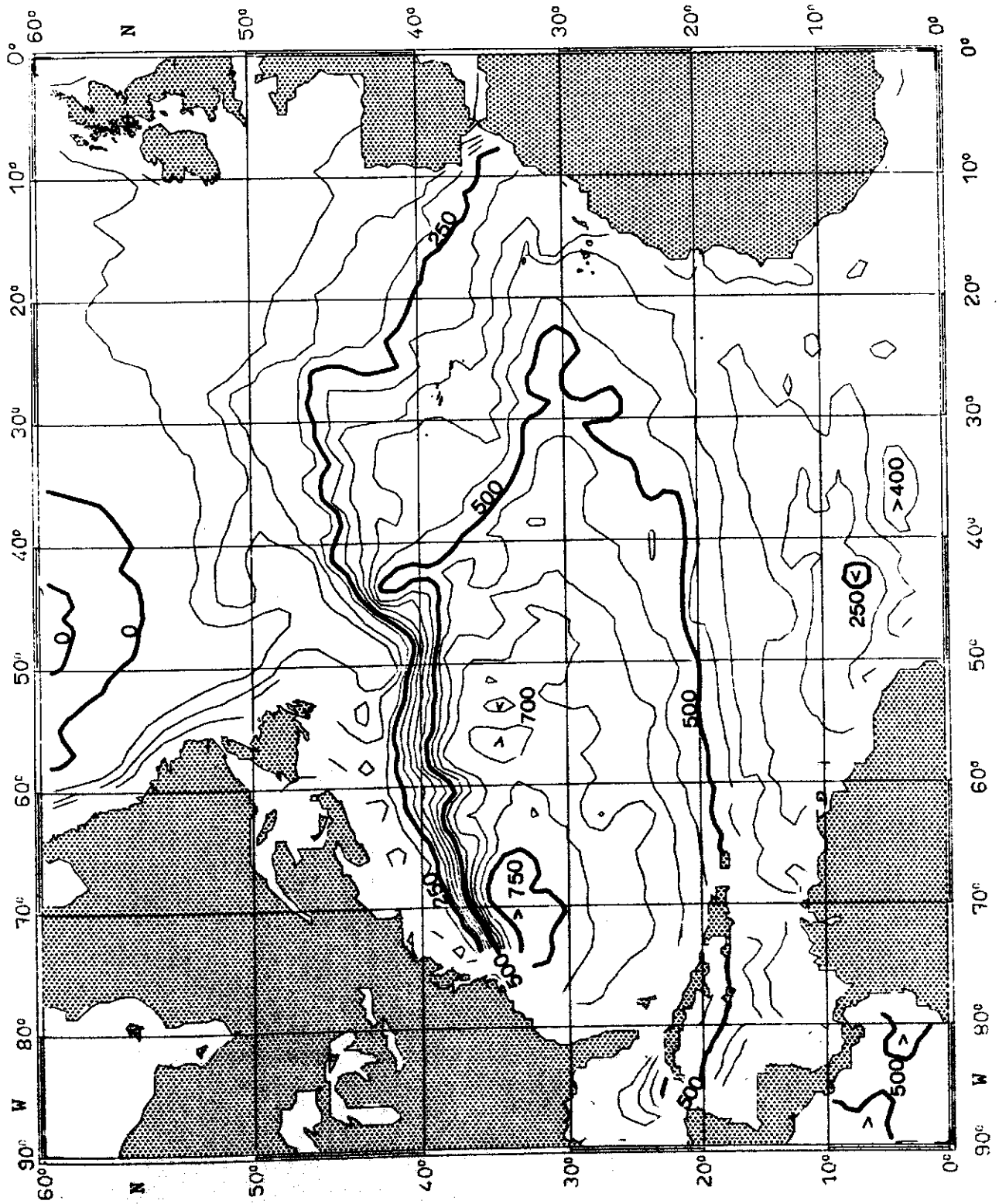

Fig. 83:

TEMPERATURE (°C) on σ_θ = 27.0 kg m^{-3} JULY

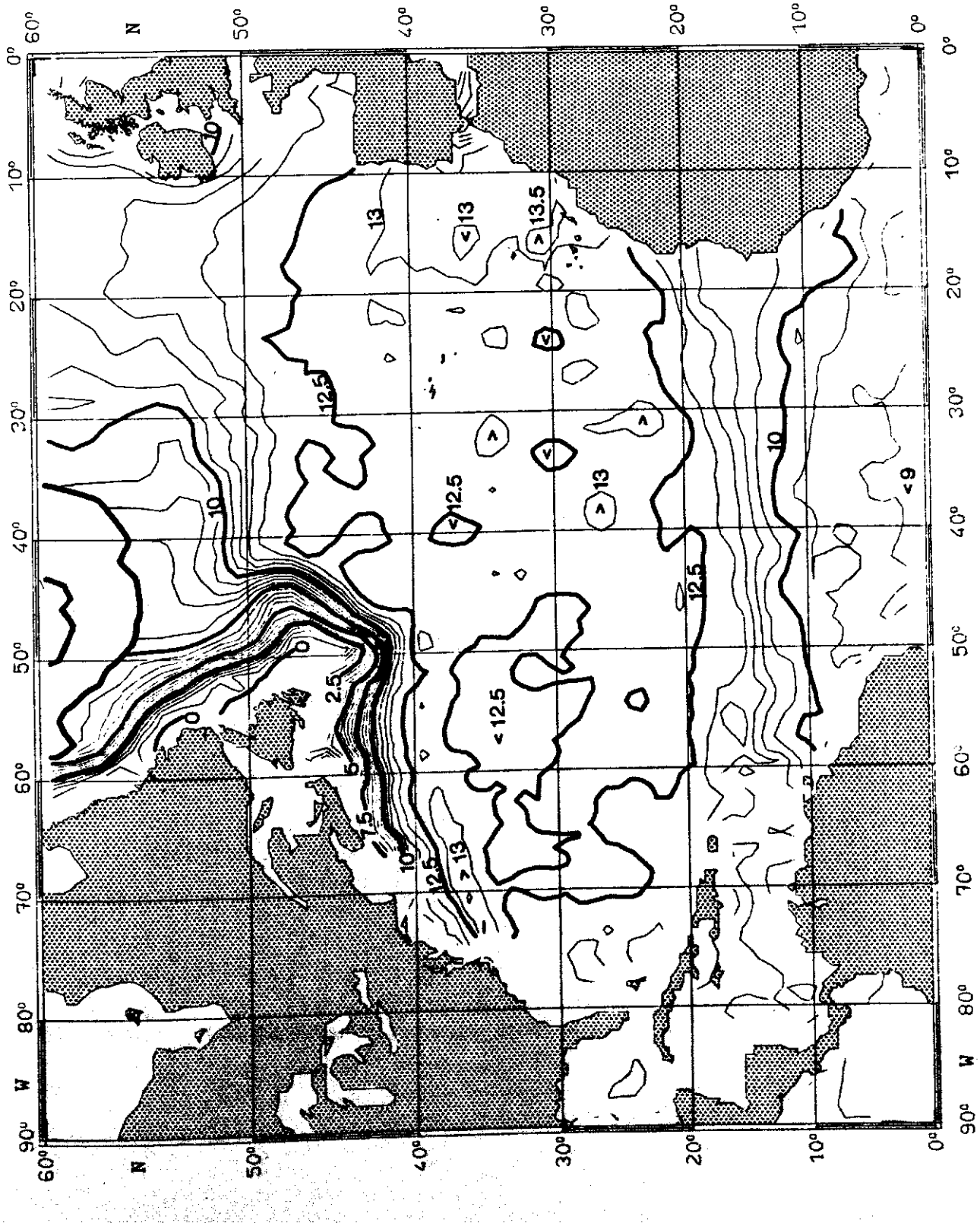

Fig. 84:

SALINITY (10^{-3}) on σ_θ = 27.0 kg m^{-3} JULY

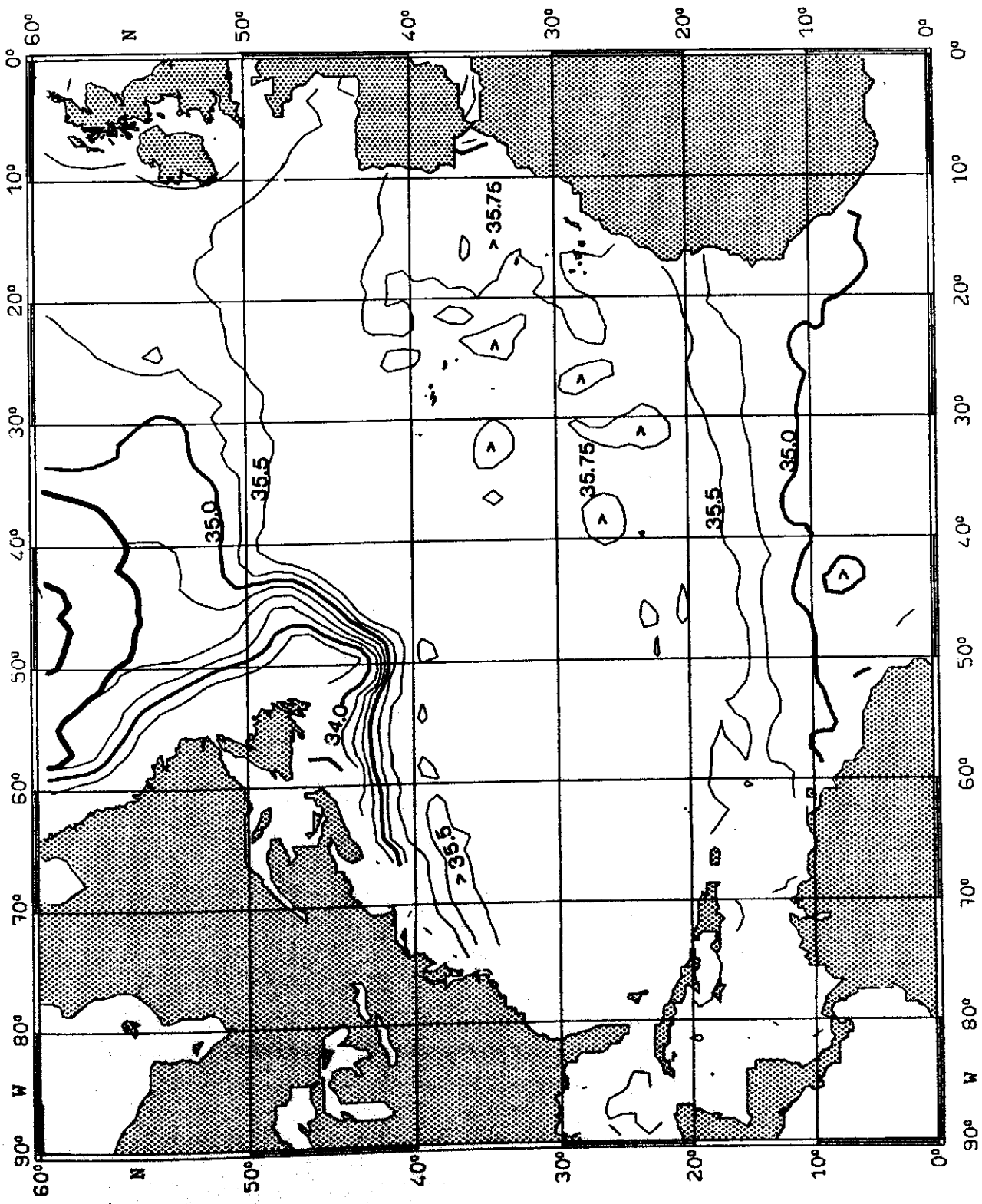

Fig. 85:

PRESSURE (10^4 Pa) on σ_θ = 25.0 kg m^{-3} AUGUST

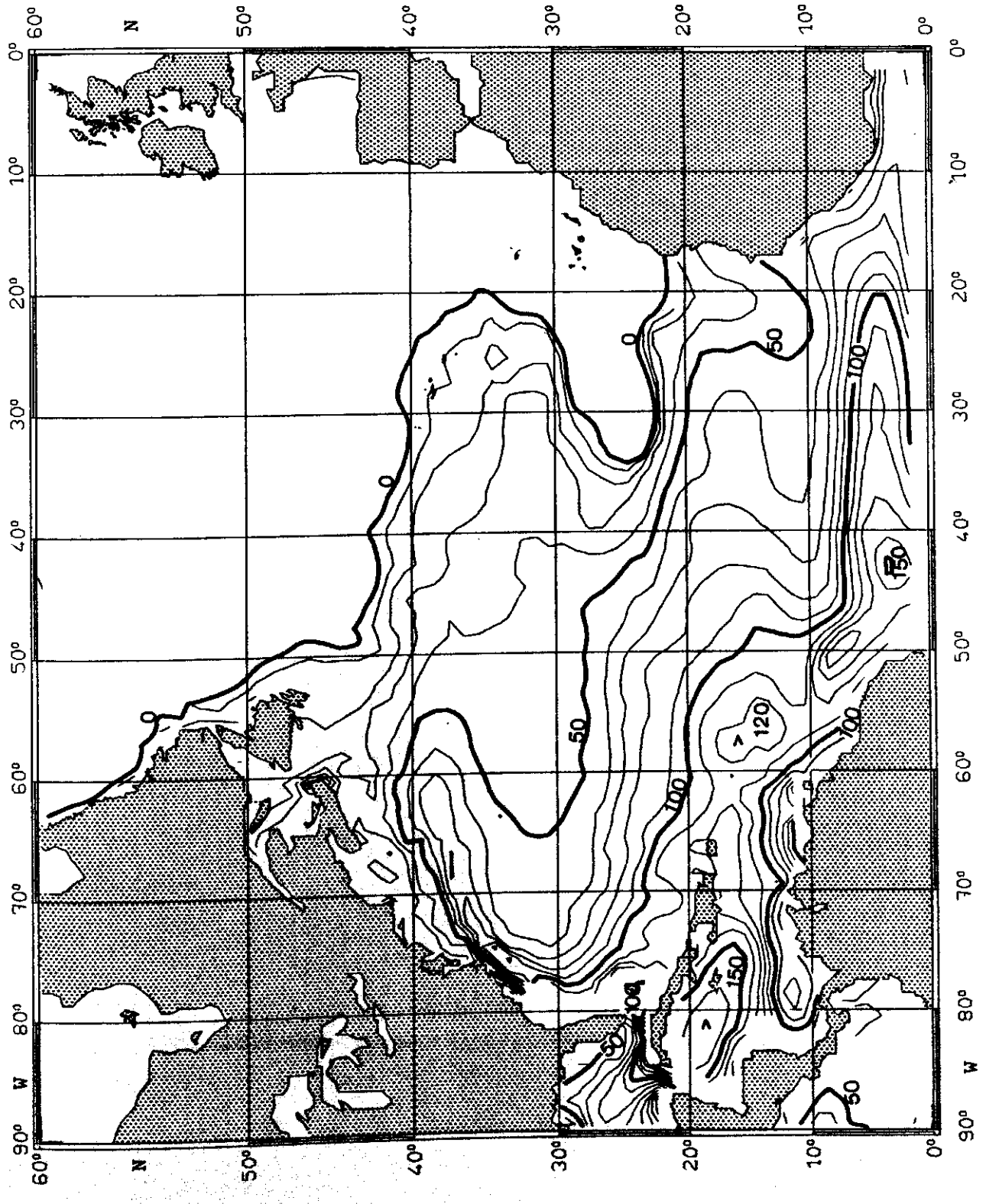

Fig. 86:

TEMPERATURE (°C) on σ_θ = 25.0 kg m^{-3} AUGUST

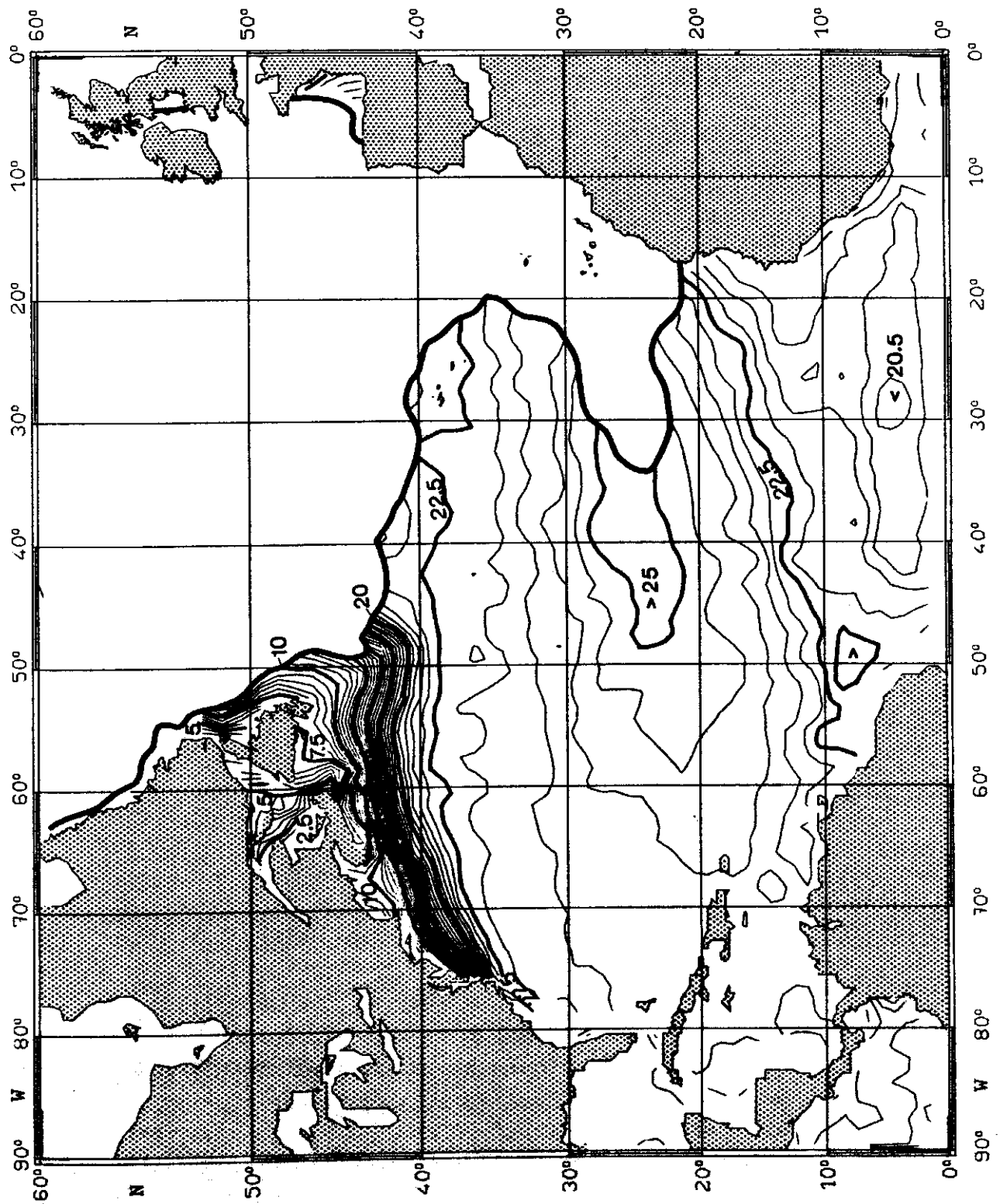

Fig. 87:

SALINITY (10^{-3}) on σ_θ = 25.0 kg m^{-3} AUGUST

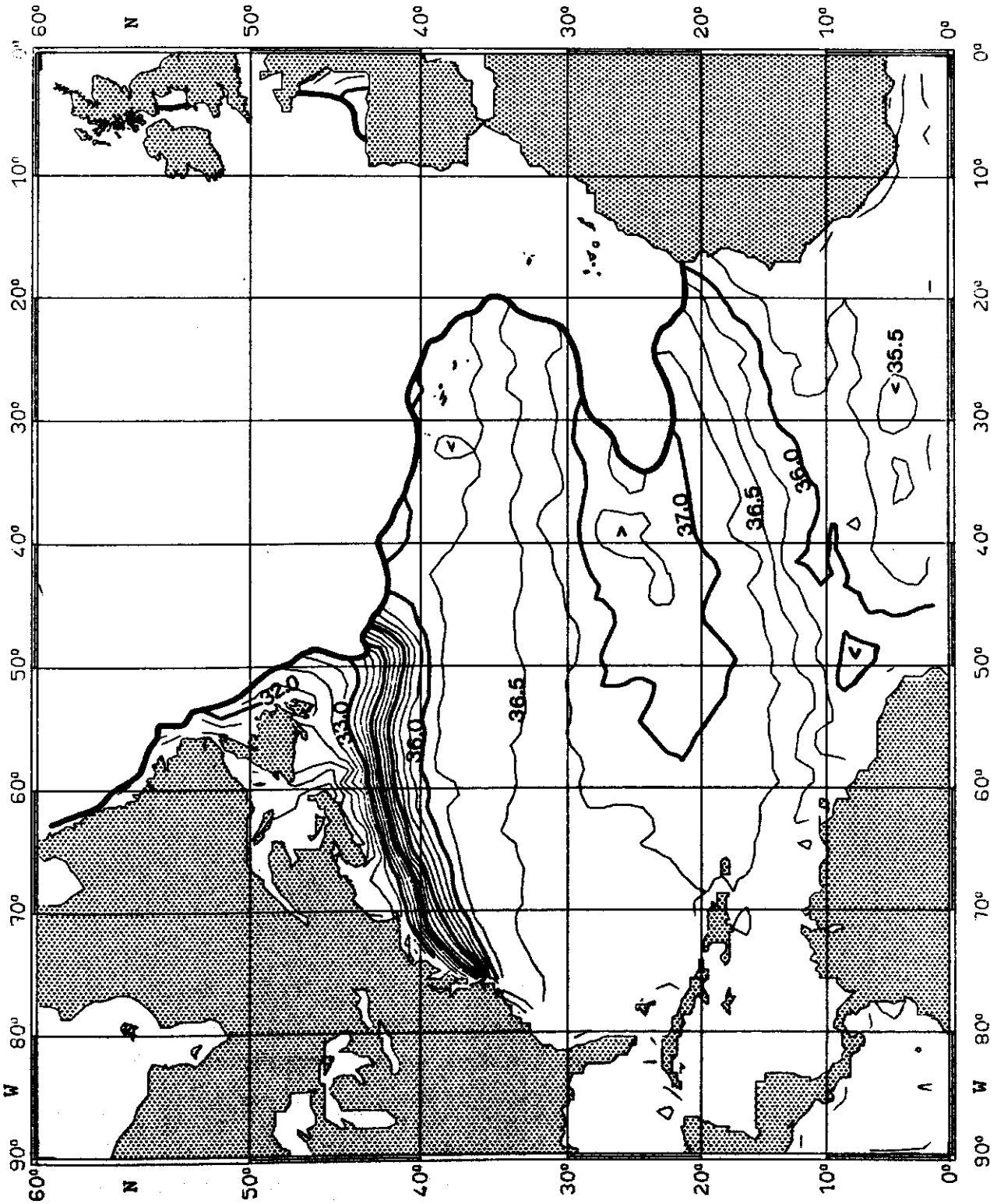

Fig. 88:

PRESSURE (10^4 Pa) on σ_θ = 25.5 kg m^{-3} AUGUST

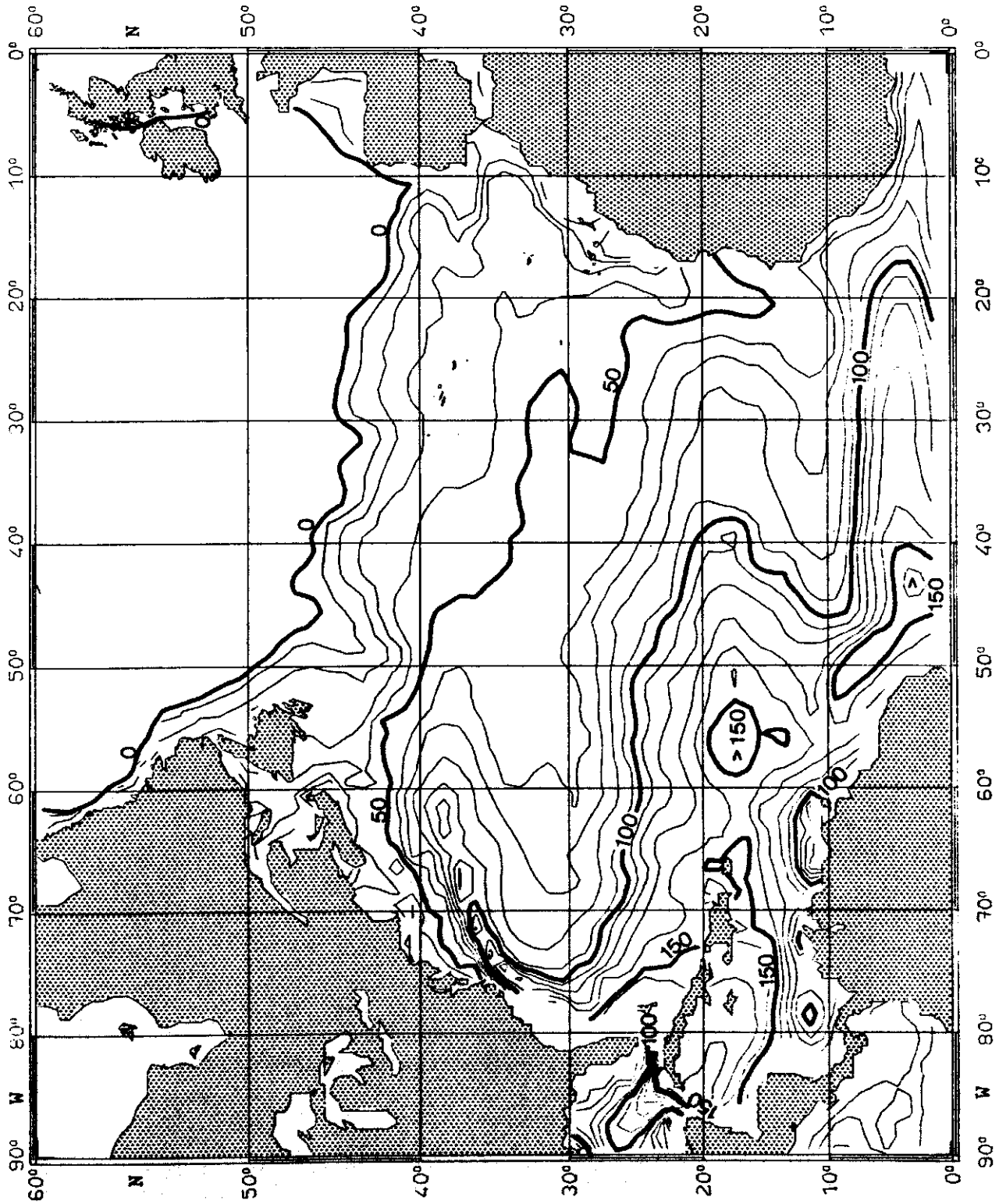

Fig. 89:

TEMPERATURE (°C) on σ_θ = 25.5 kg m^{-3} AUGUST

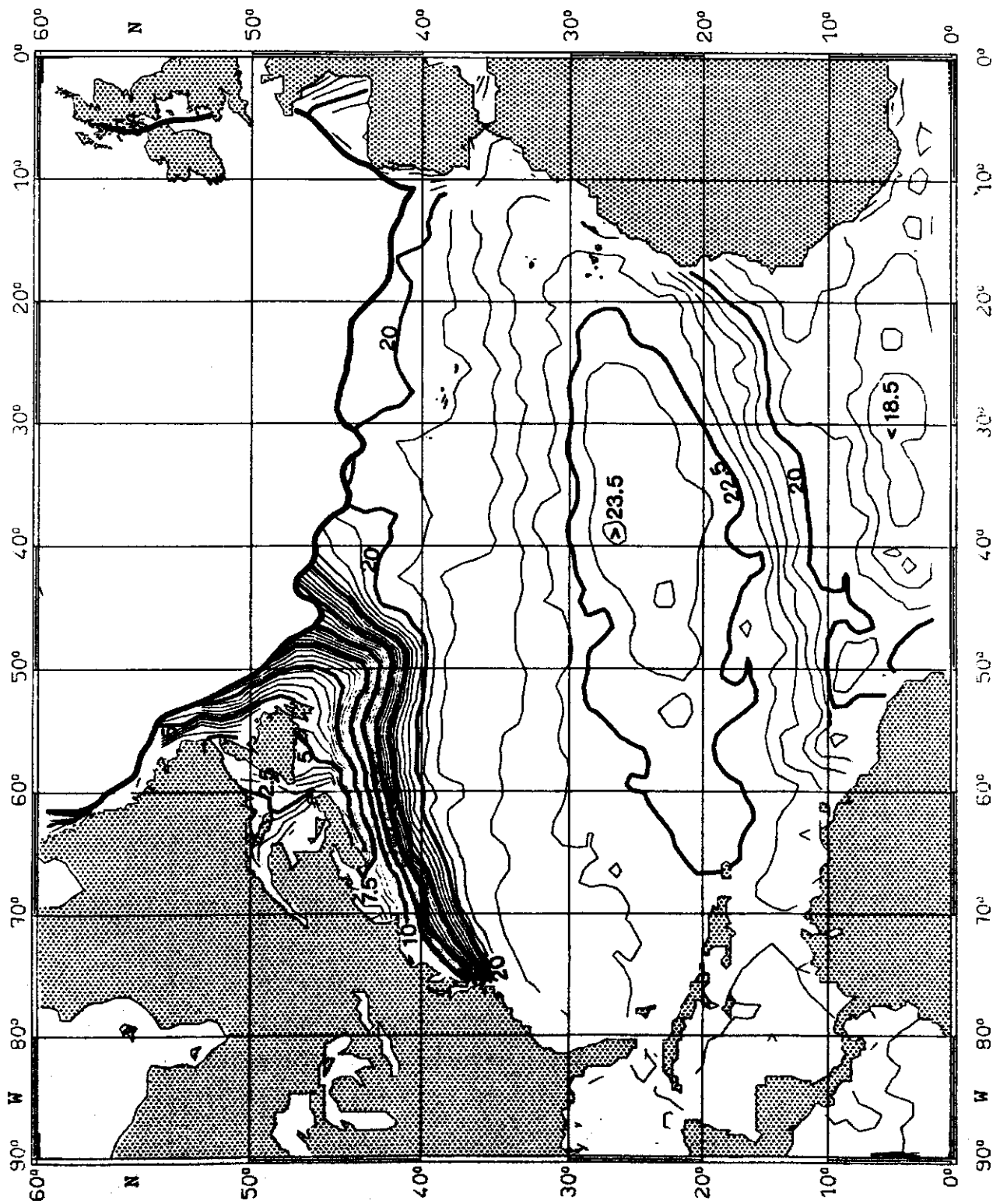

Fig. 90:

SALINITY (10^{-3}) on σ_θ = 25.5 kg m^{-3} AUGUST

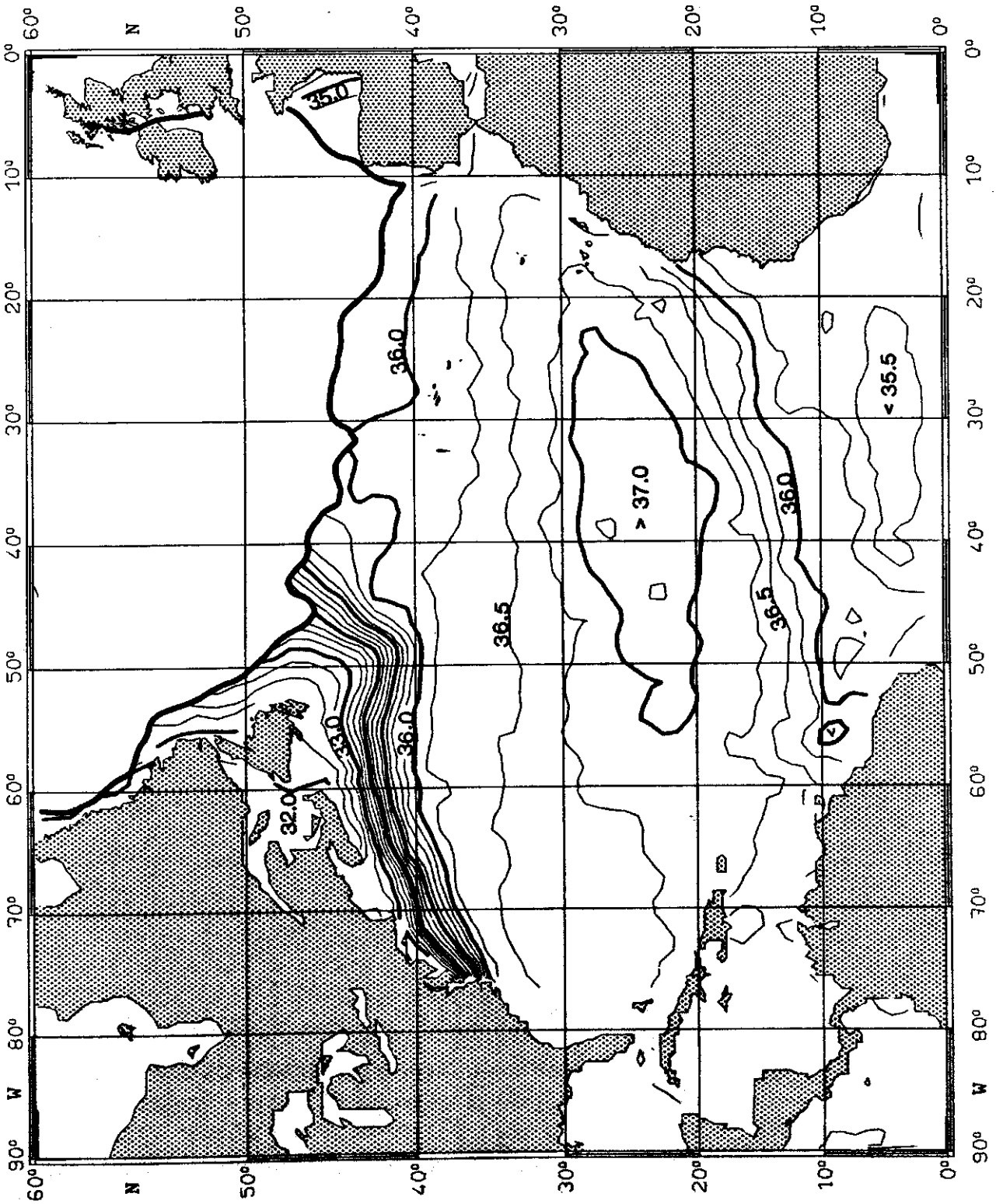

Fig. 91:

PRESSURE (10^4 Pa) on σ_θ = 26.0 kg m^{-3} AUGUST

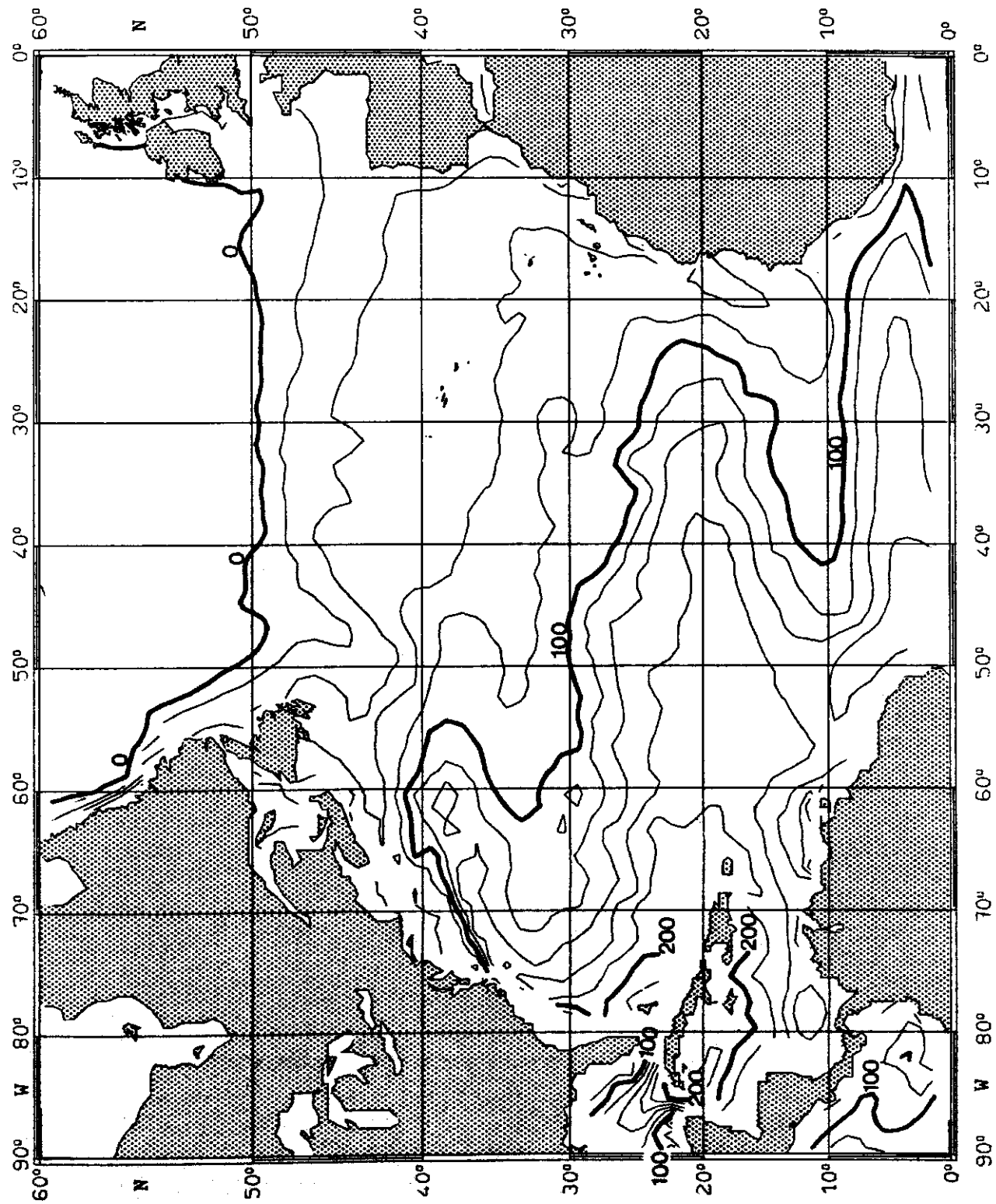

Fig. 92:

TEMPERATURE (°C) on σ_θ = 26.0 kg m^{-3} AUGUST

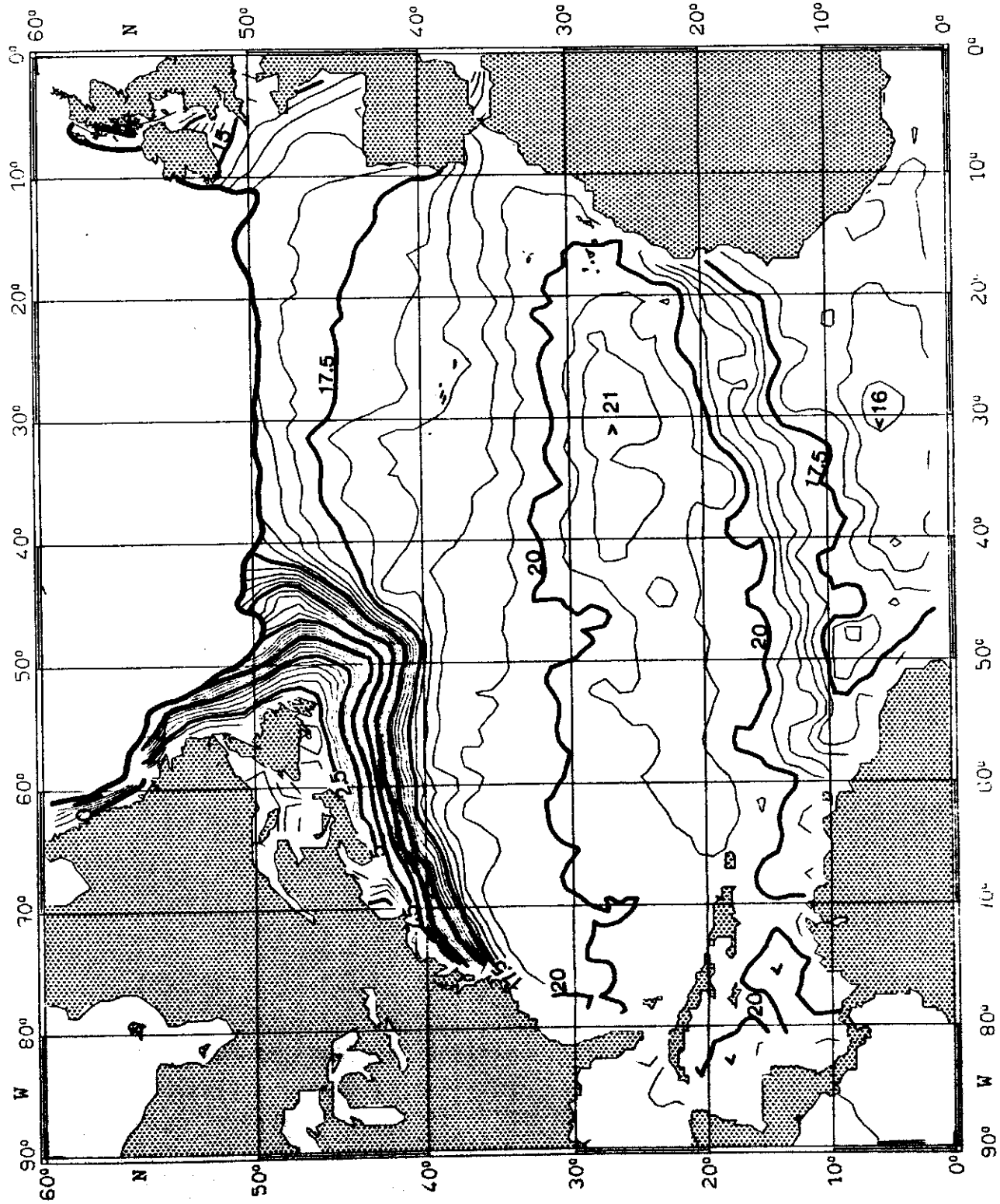

Fig. 93:

SALINITY (10^{-3}) on σ_θ = 26.0 kg m^{-3} AUGUST

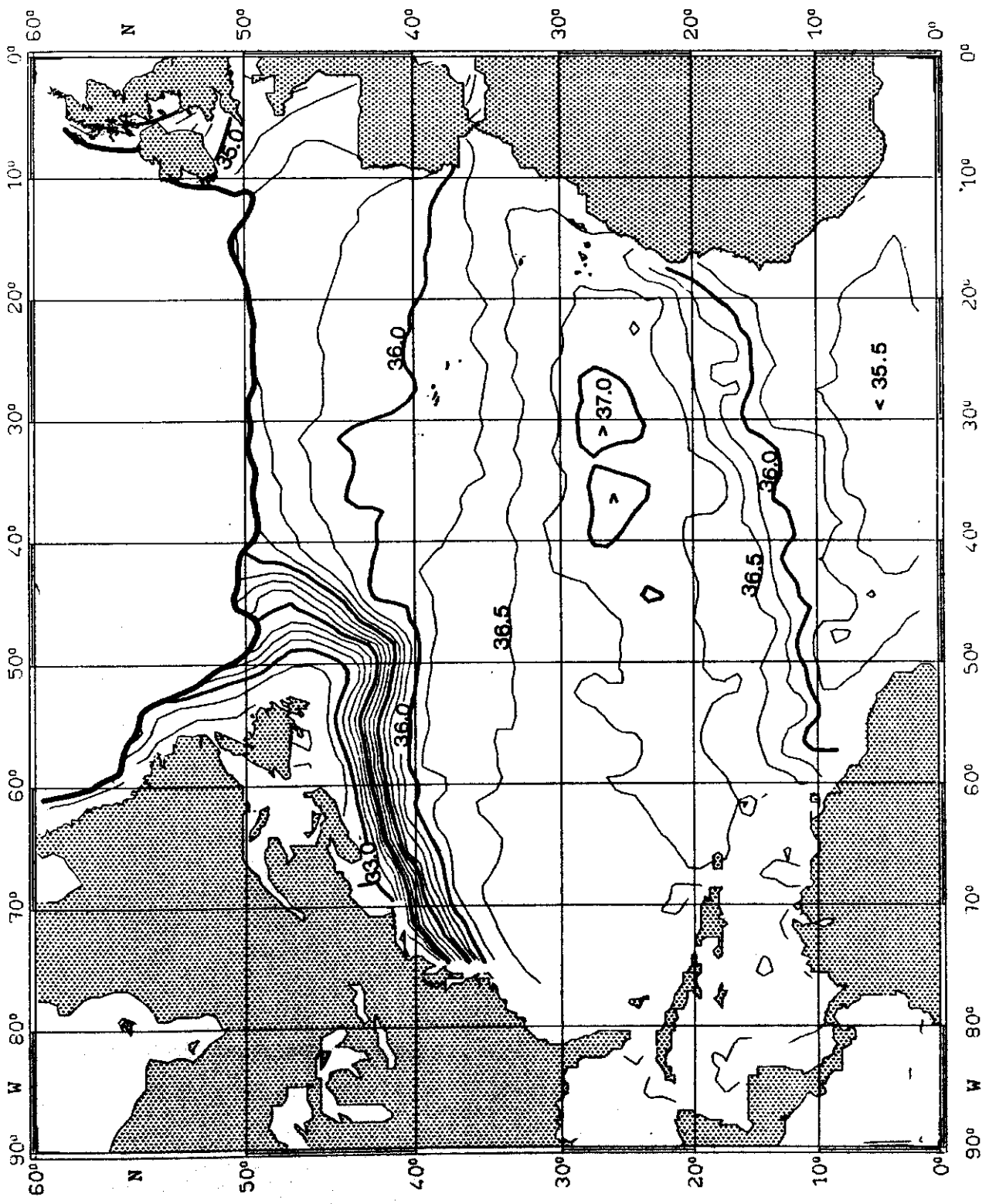

Fig. 94:

PRESSURE (10^4 Pa) on σ_θ = 26.5 kg m^{-3} AUGUST

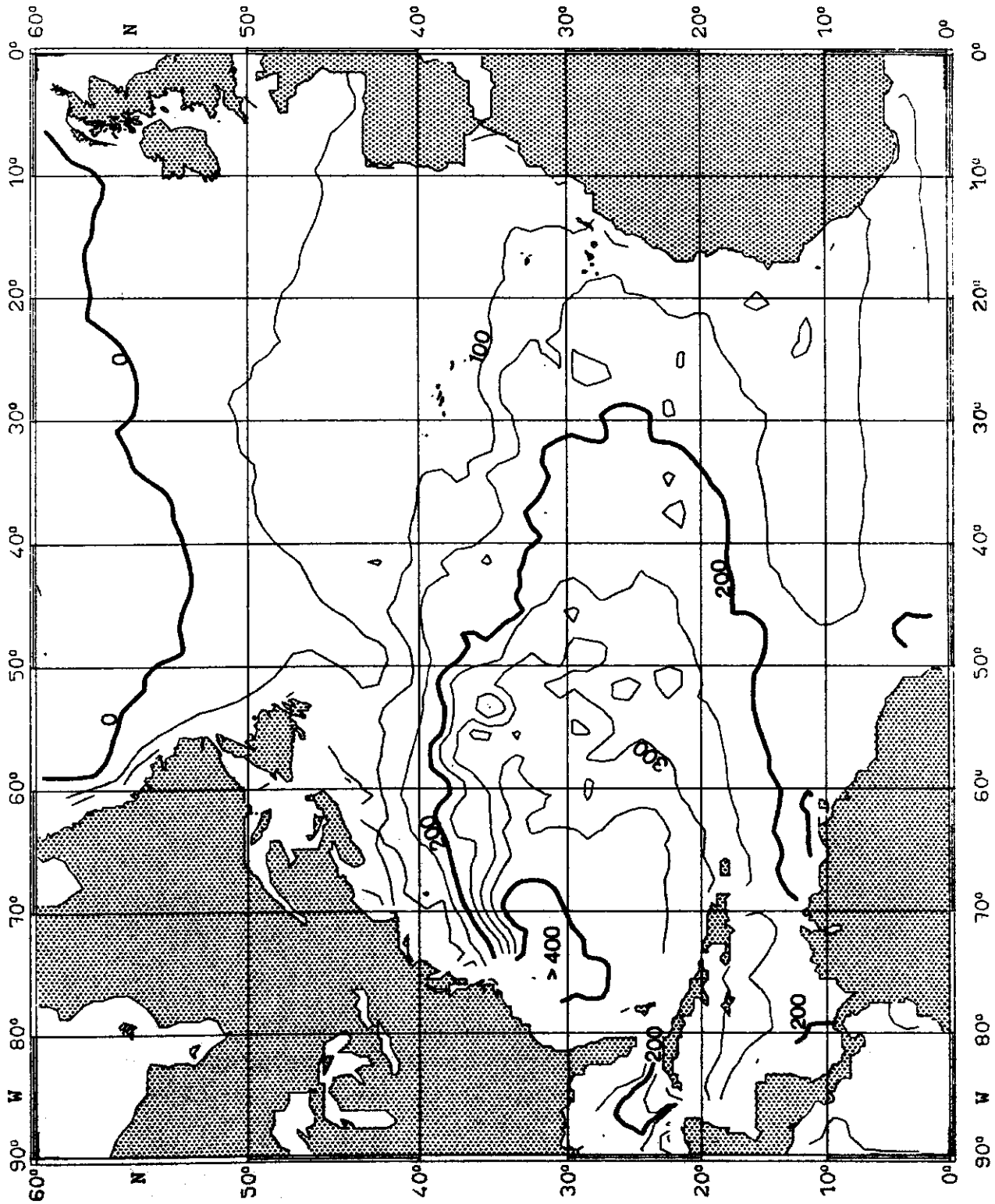

Fig. 95:

TEMPERATURE (°C) on σ_θ = 26.5 kg m^{-3} AUGUST

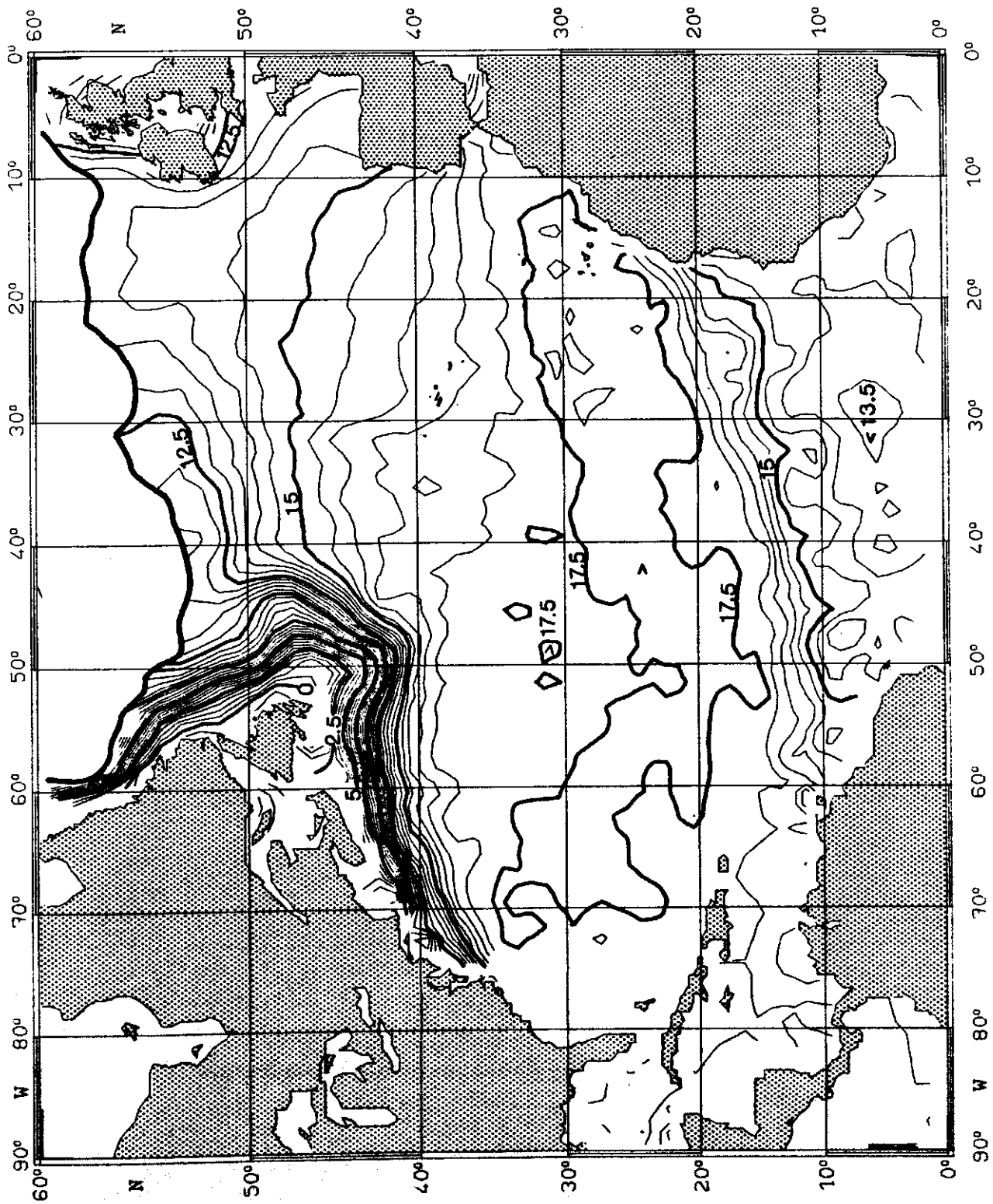

Fig. 96:

SALINITY (10^{-3}) on σ_θ = 26.5 kg m^{-3} AUGUST

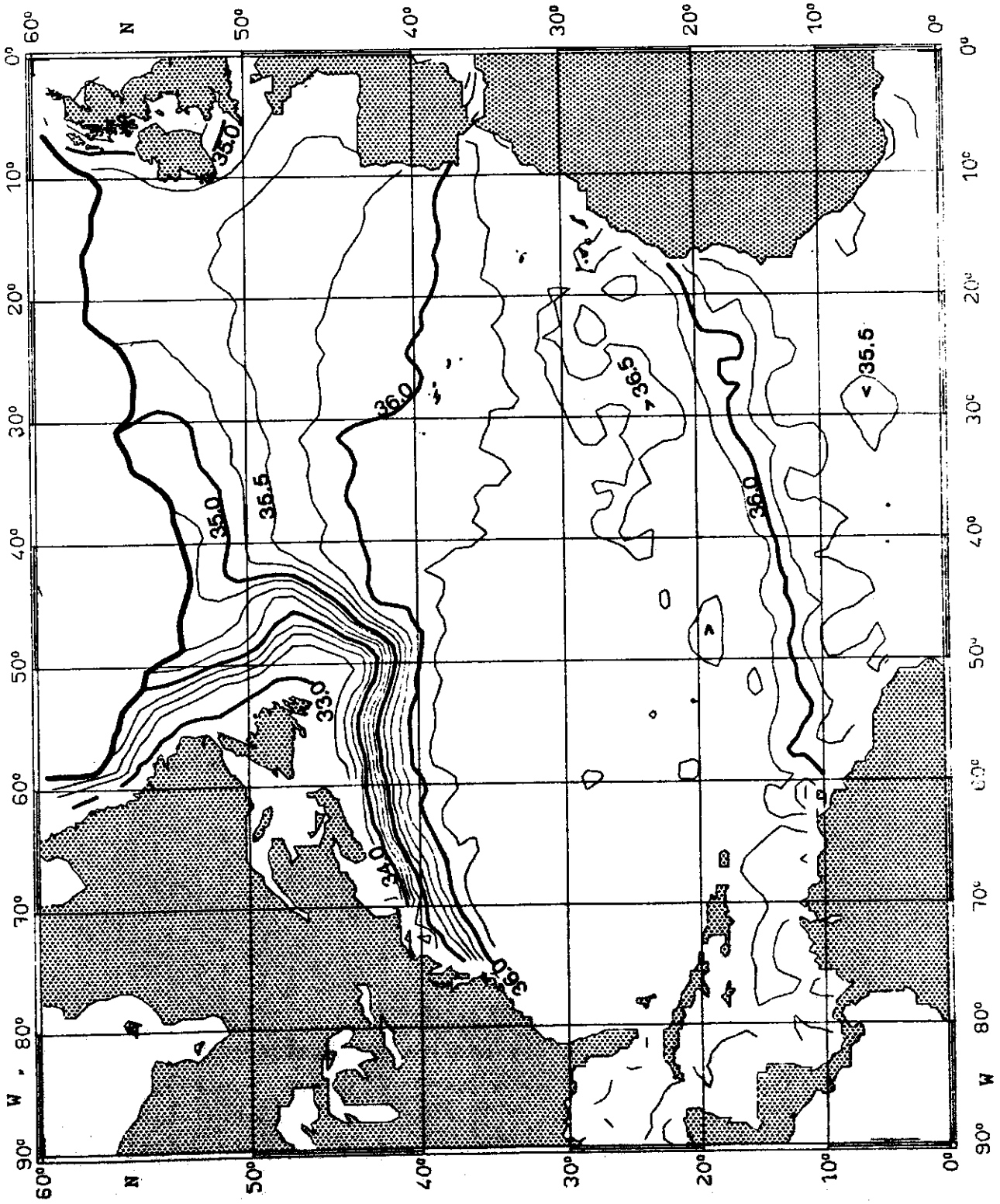

Fig. 97:

PRESSURE (10^4 Pa) on σ_θ = 27.0 kg m^{-3} AUGUST

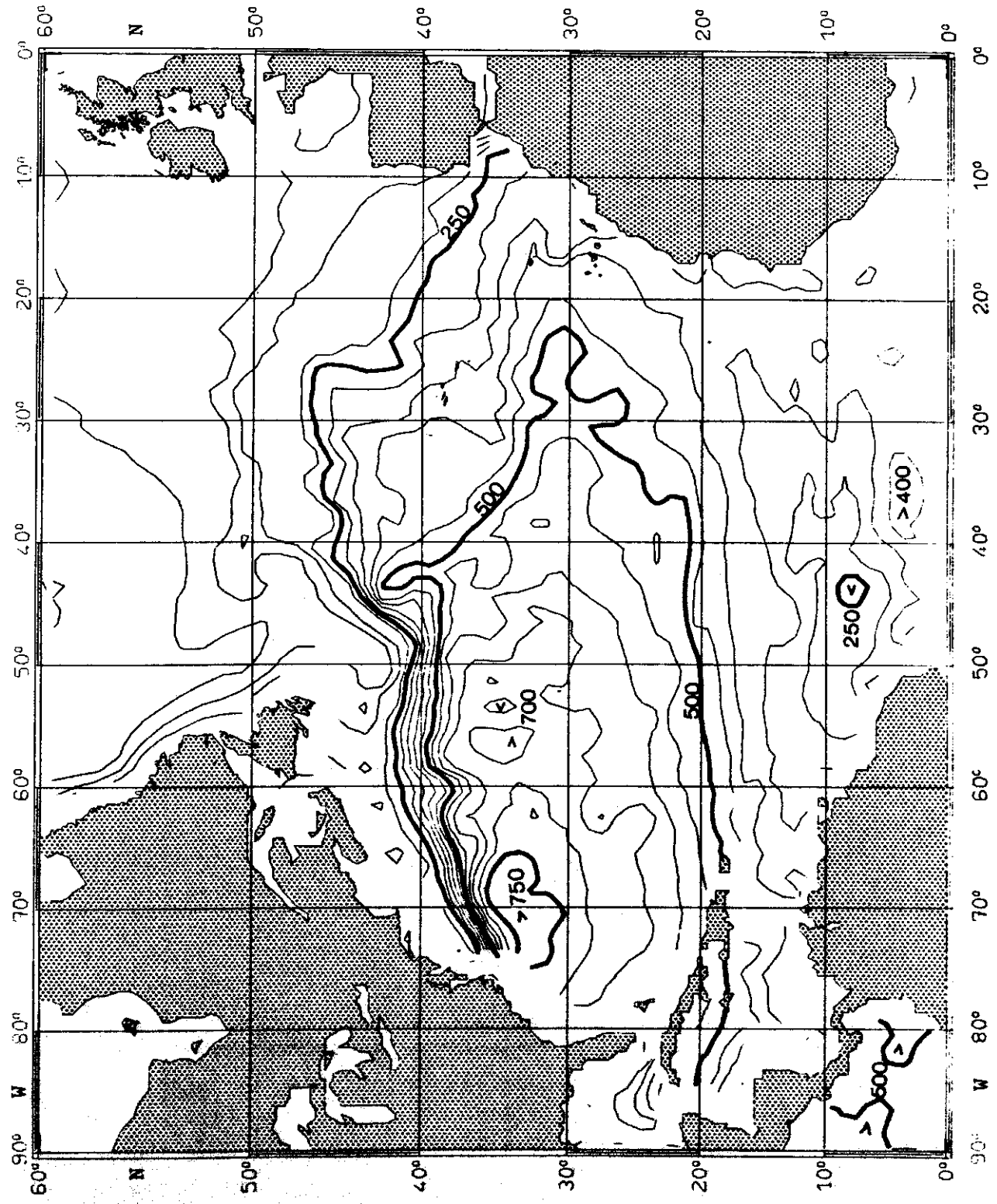

Fig. 98:

TEMPERATURE (°C) on σ_θ = 27.0 kg m^{-3} AUGUST

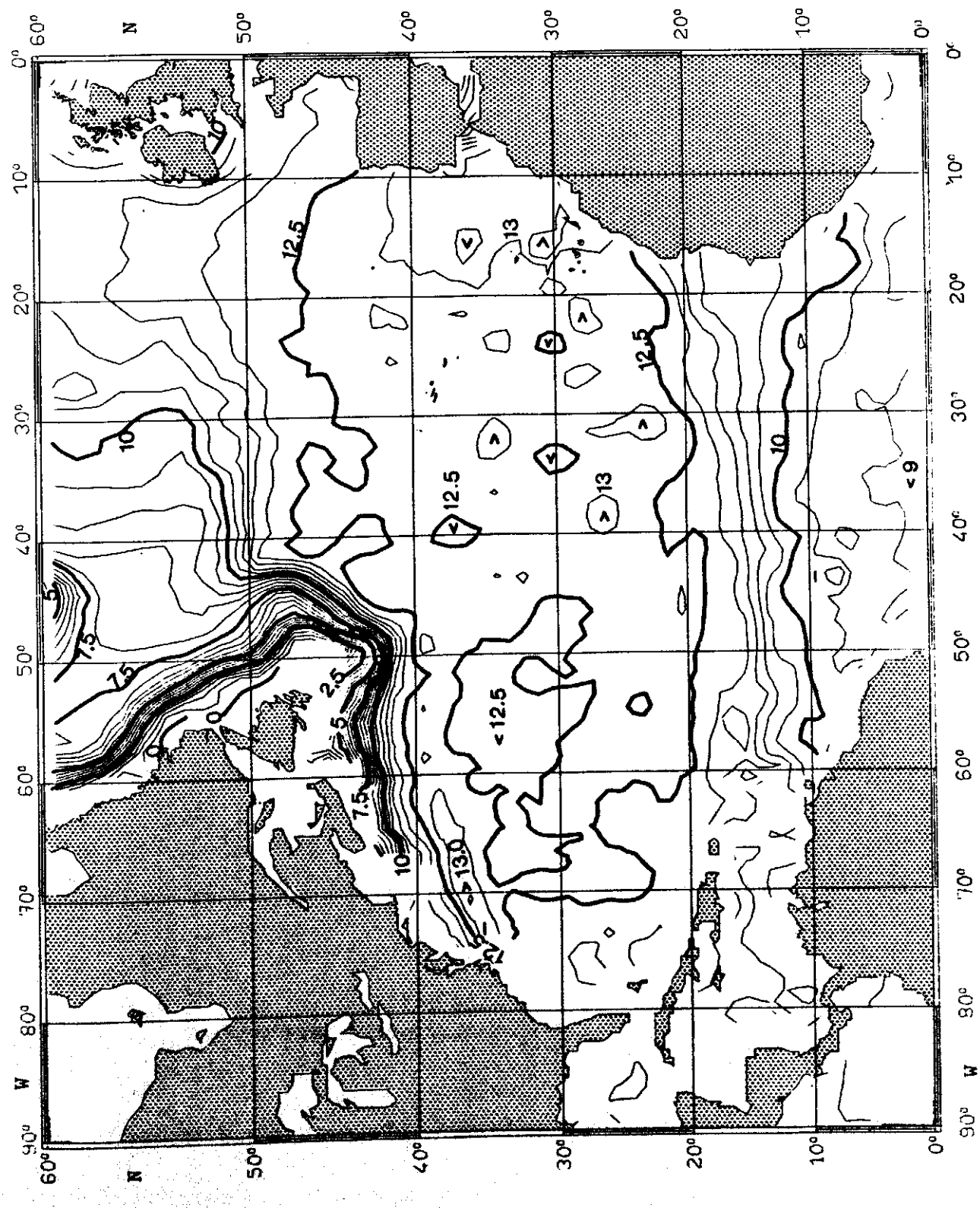

Fig. 99:

SALINITY (10^{-3}) on σ_θ = 27.0 kg m^{-3} AUGUST

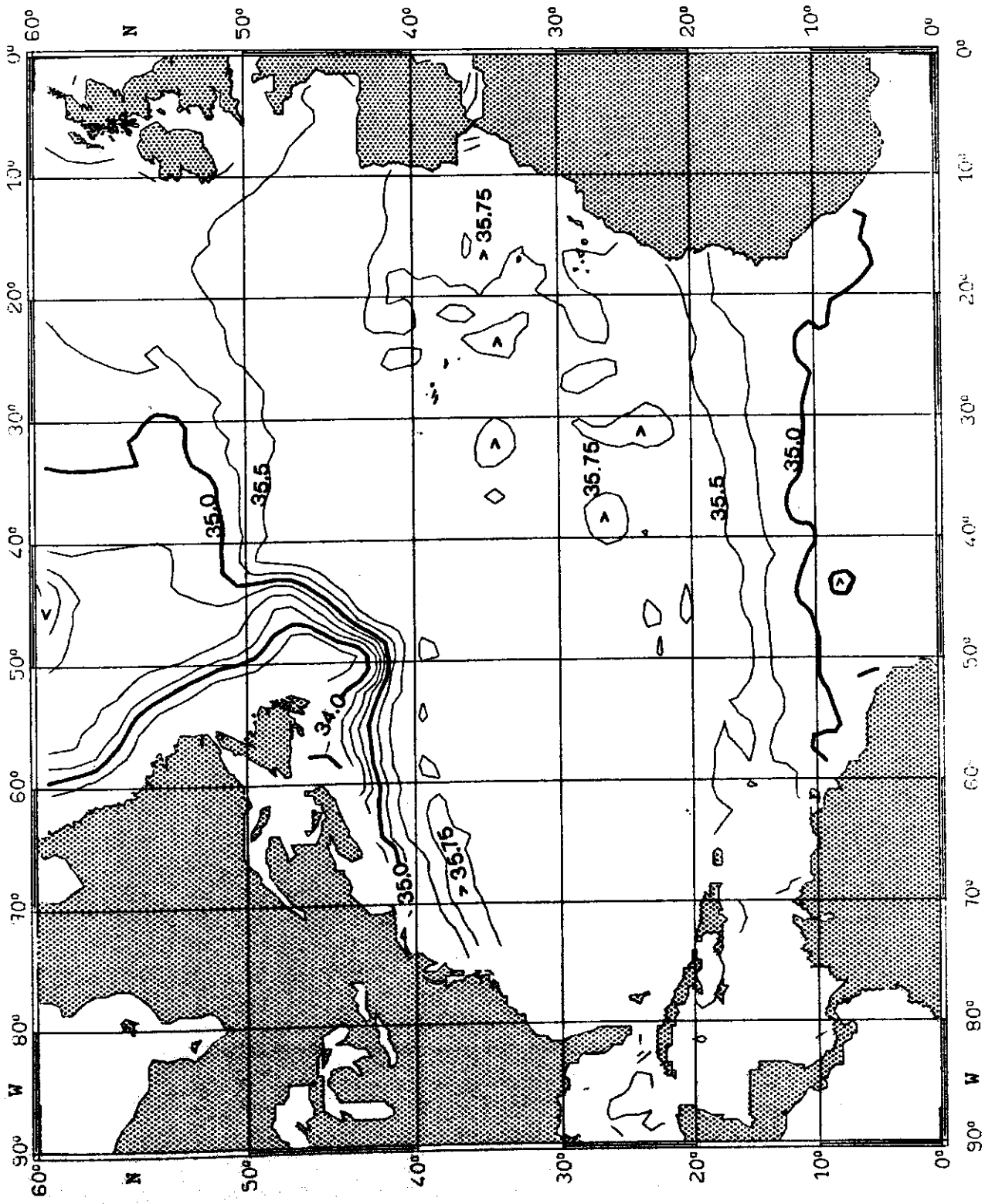

Fig. 100:

PRESSURE (10^4 Pa) on σ_θ = 25.0 kg m^{-3} SEPTEMBER

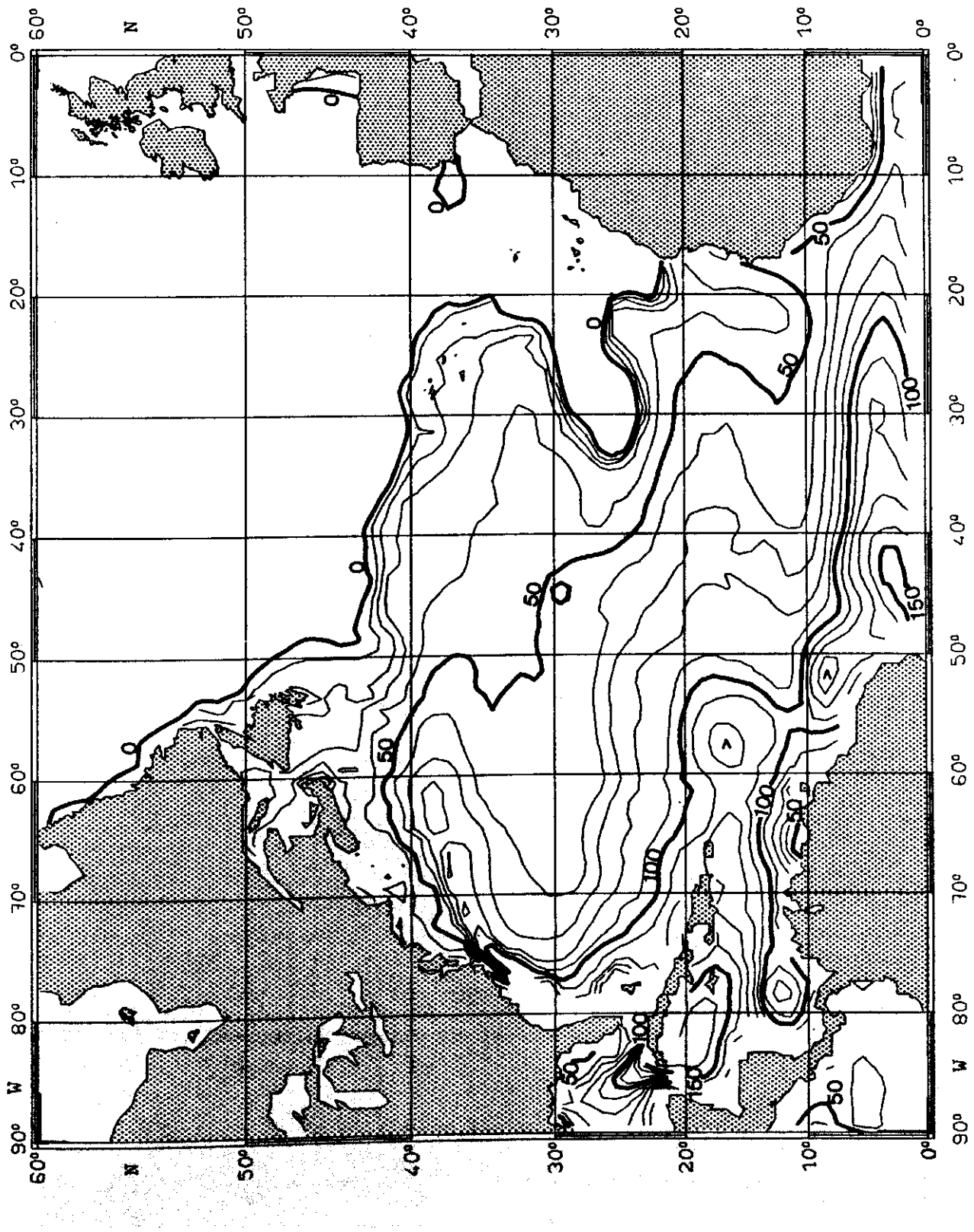

Fig. 101:

TEMPERATURE (°C) on σ_θ = 25.0 kg m^{-3} SEPTEMBER

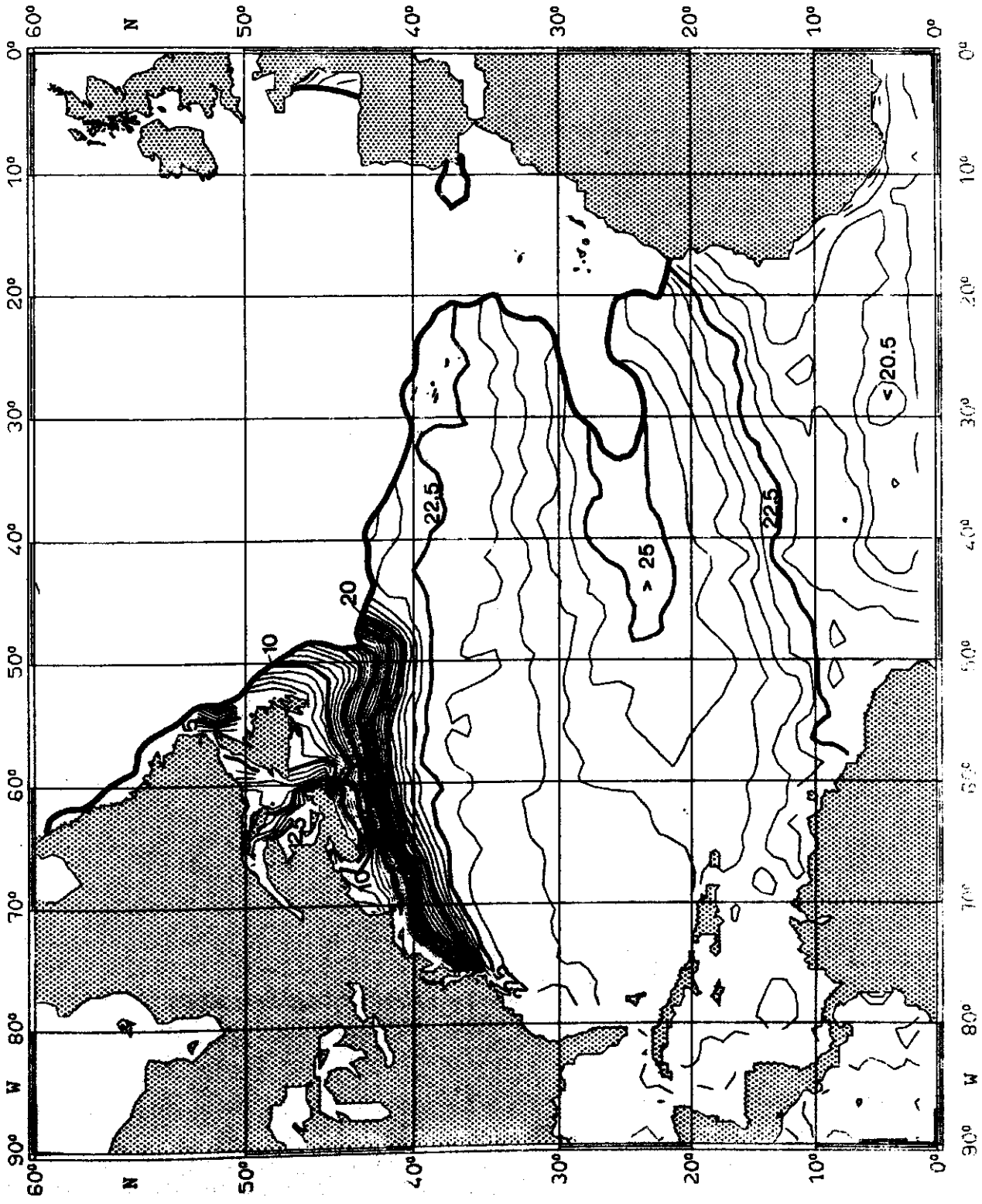

Fig. 102:

SALINITY (10^{-3}) on σ_θ = 25.0 kg m^{-3} SEPTEMBER

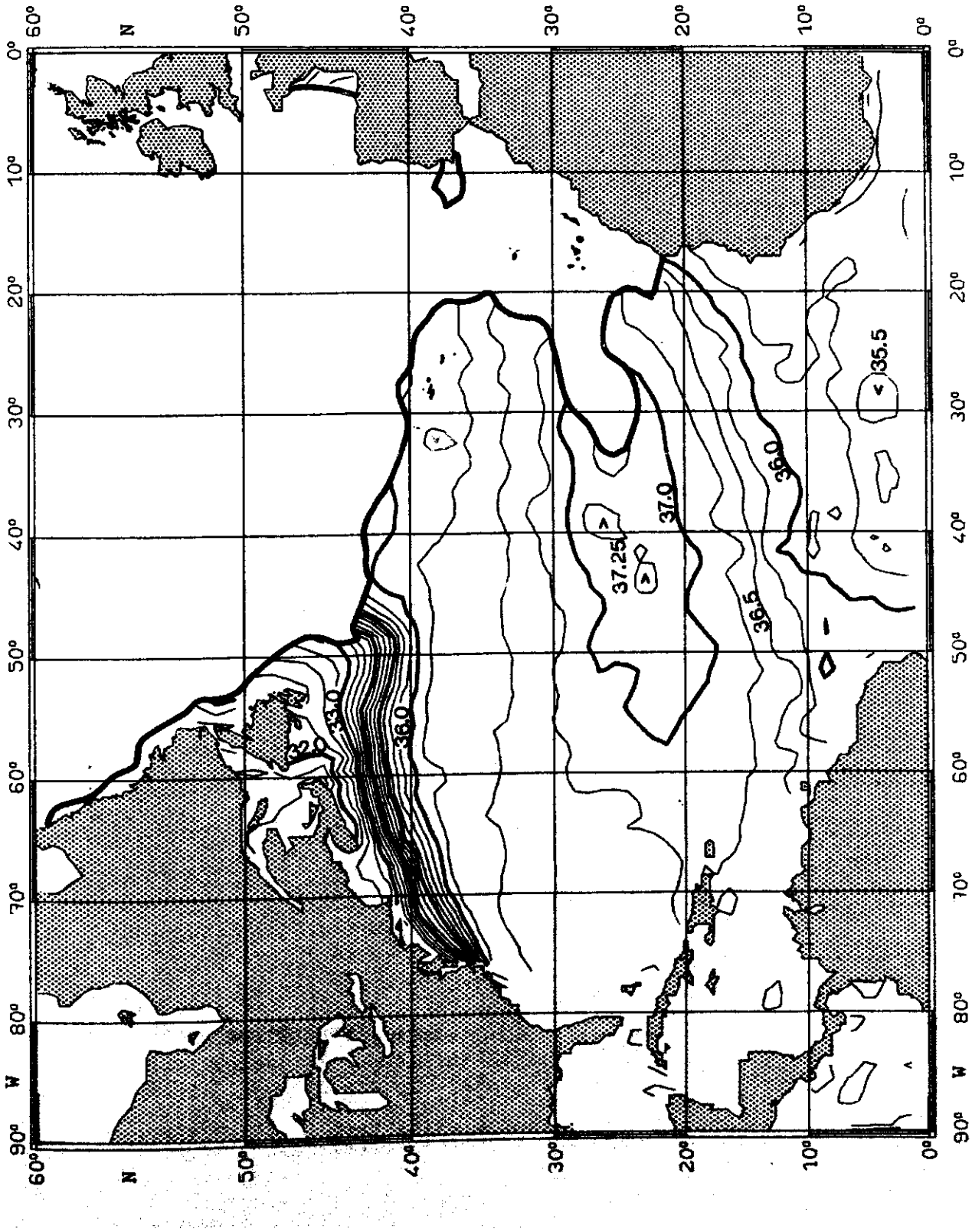

Fig. 103:

PRESSURE (10^4 Pa) on σ_θ = 26.0 kg m^{-3} SEPTEMBER

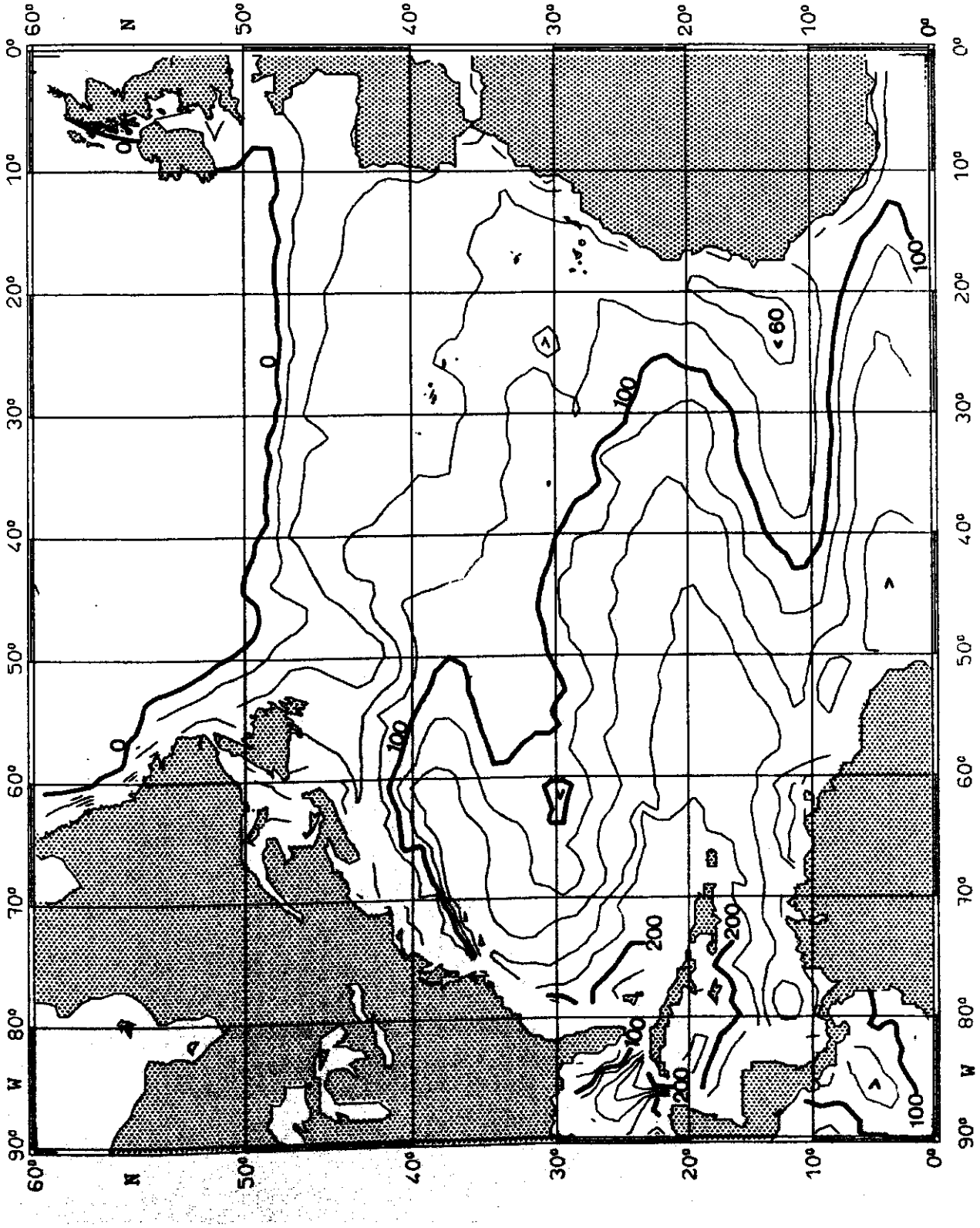

Fig. 104:

TEMPERATURE (°C) on σ_θ = 26.0 kg m^{-3} SEPTEMBER

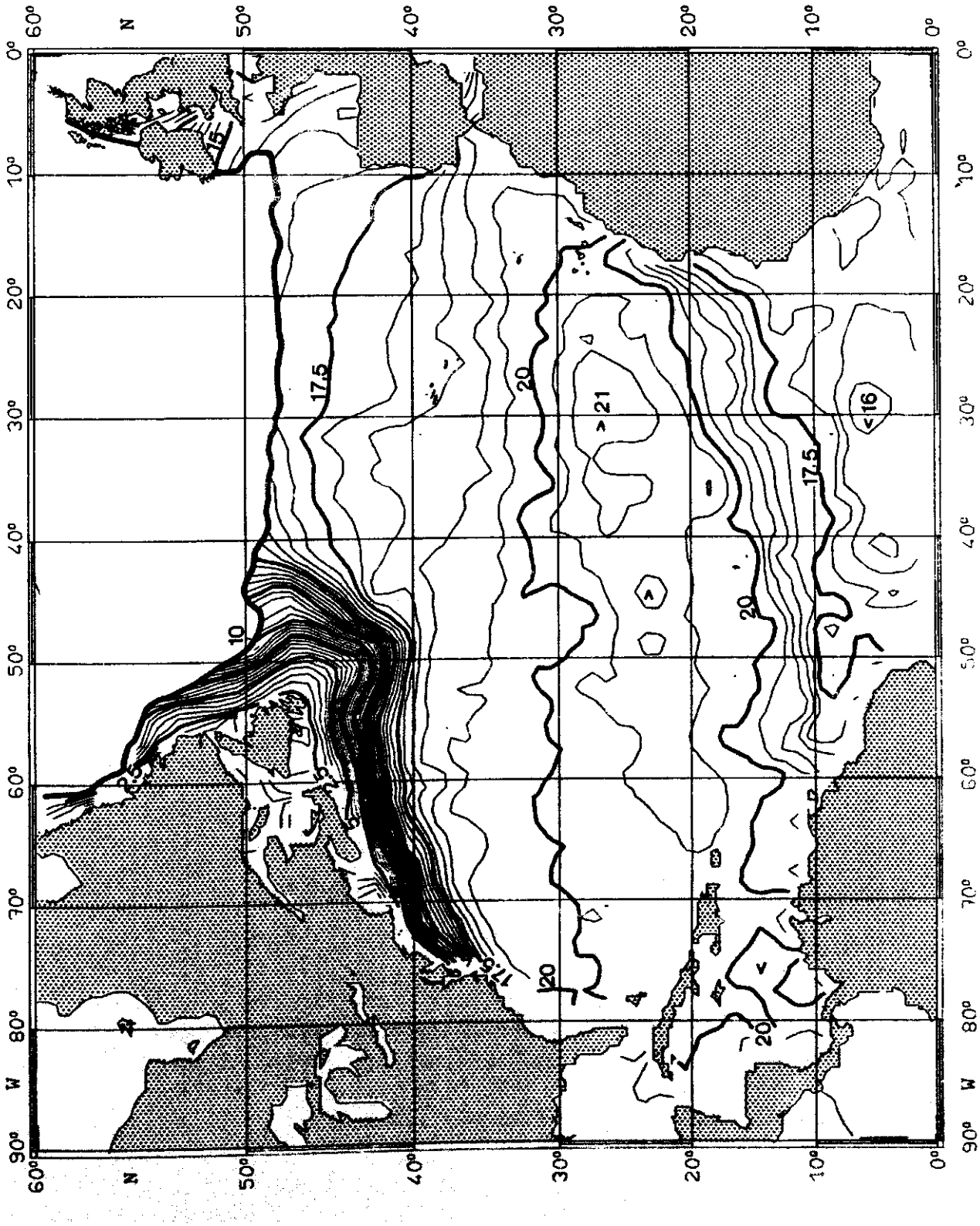

Fig. 105:

SALINITY (10^{-3}) on σ_θ = 26.0 kg m^{-3} SEPTEMBER

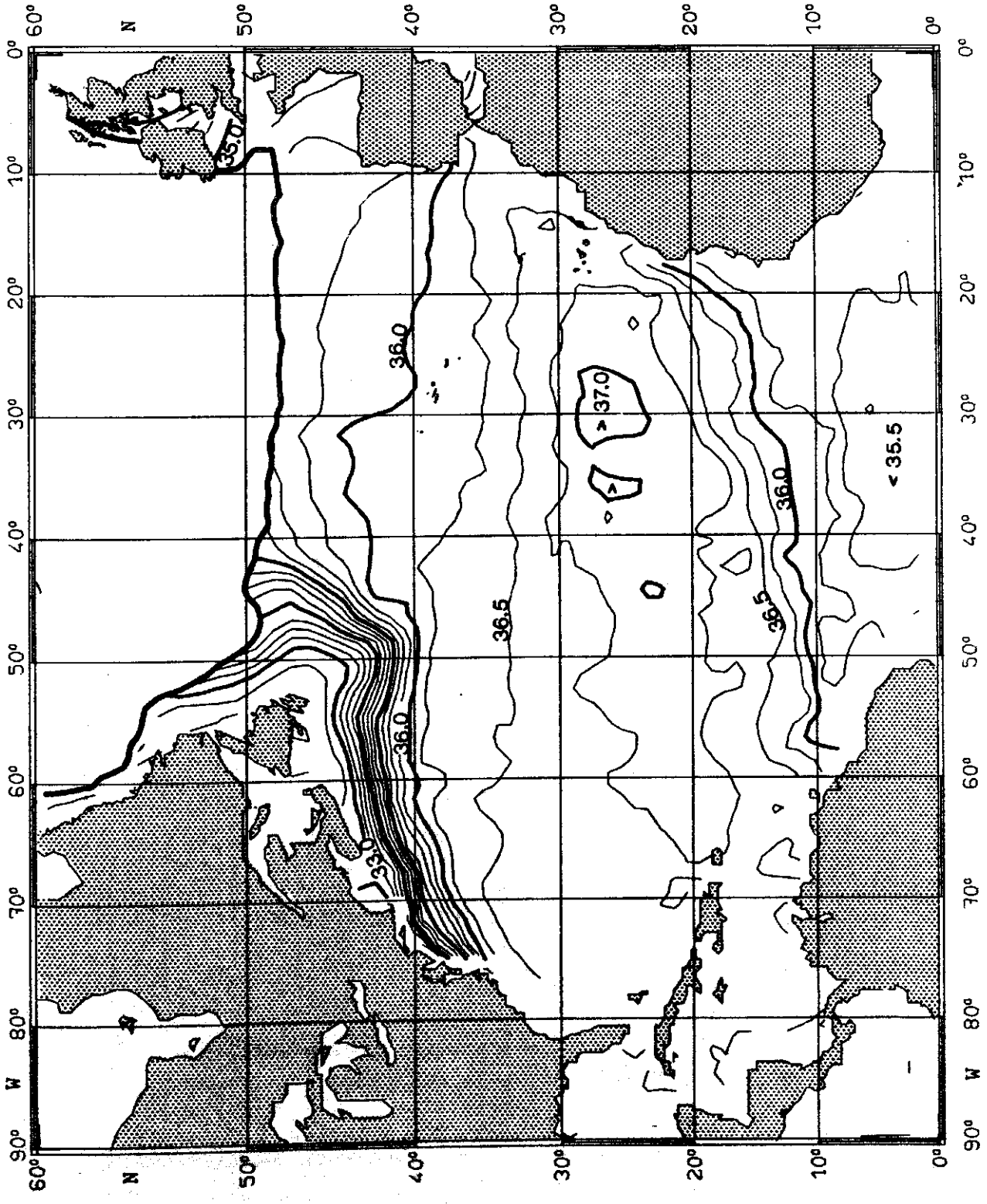

Fig. 106:

PRESSURE (10^4 Pa) on σ_θ = 27.0 kg m^{-3} SEPTEMBER

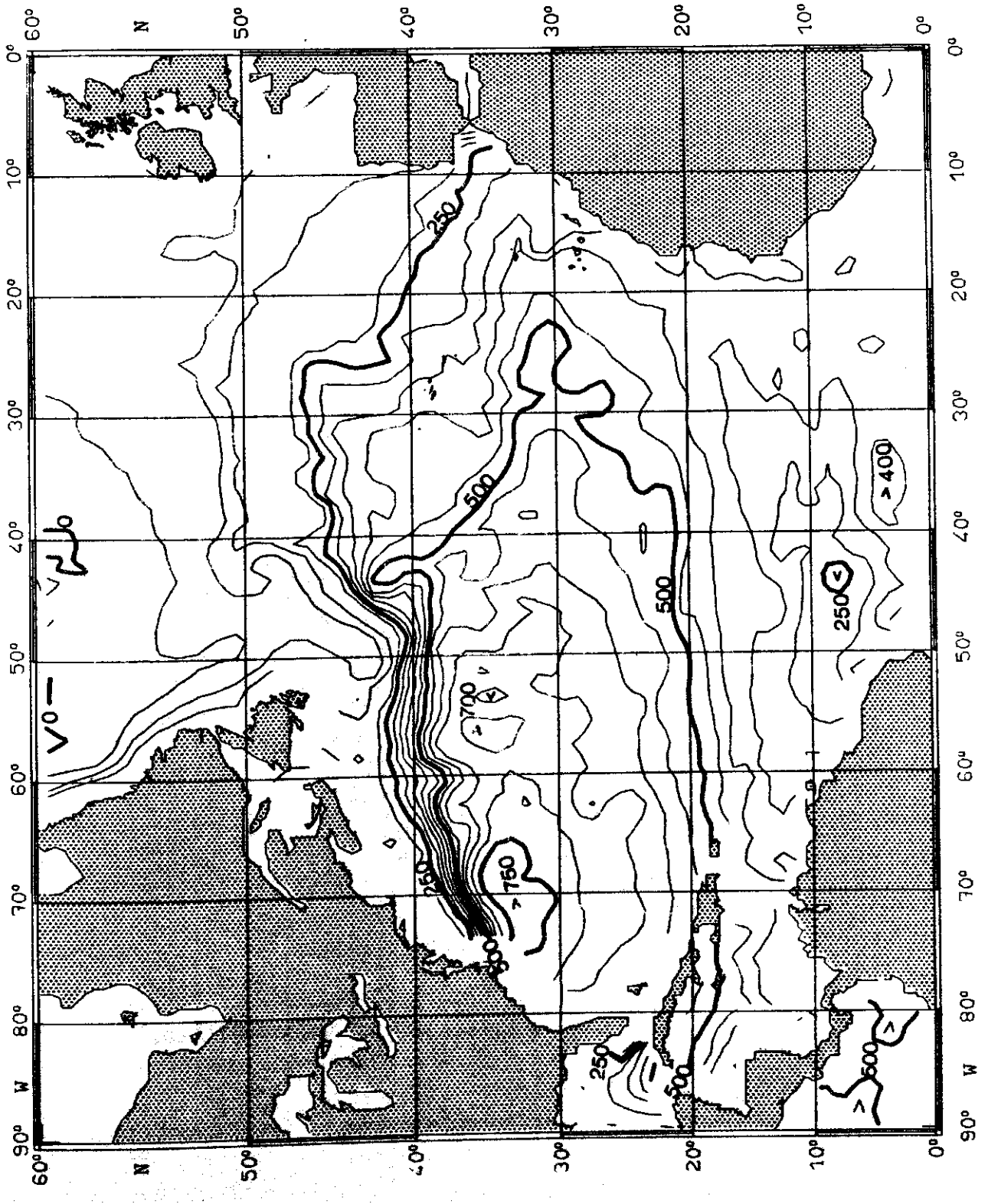

Fig. 107:
TEMPERATURE (°C) on σ_θ = 27.0 kg m^{-3} SEPTEMBER

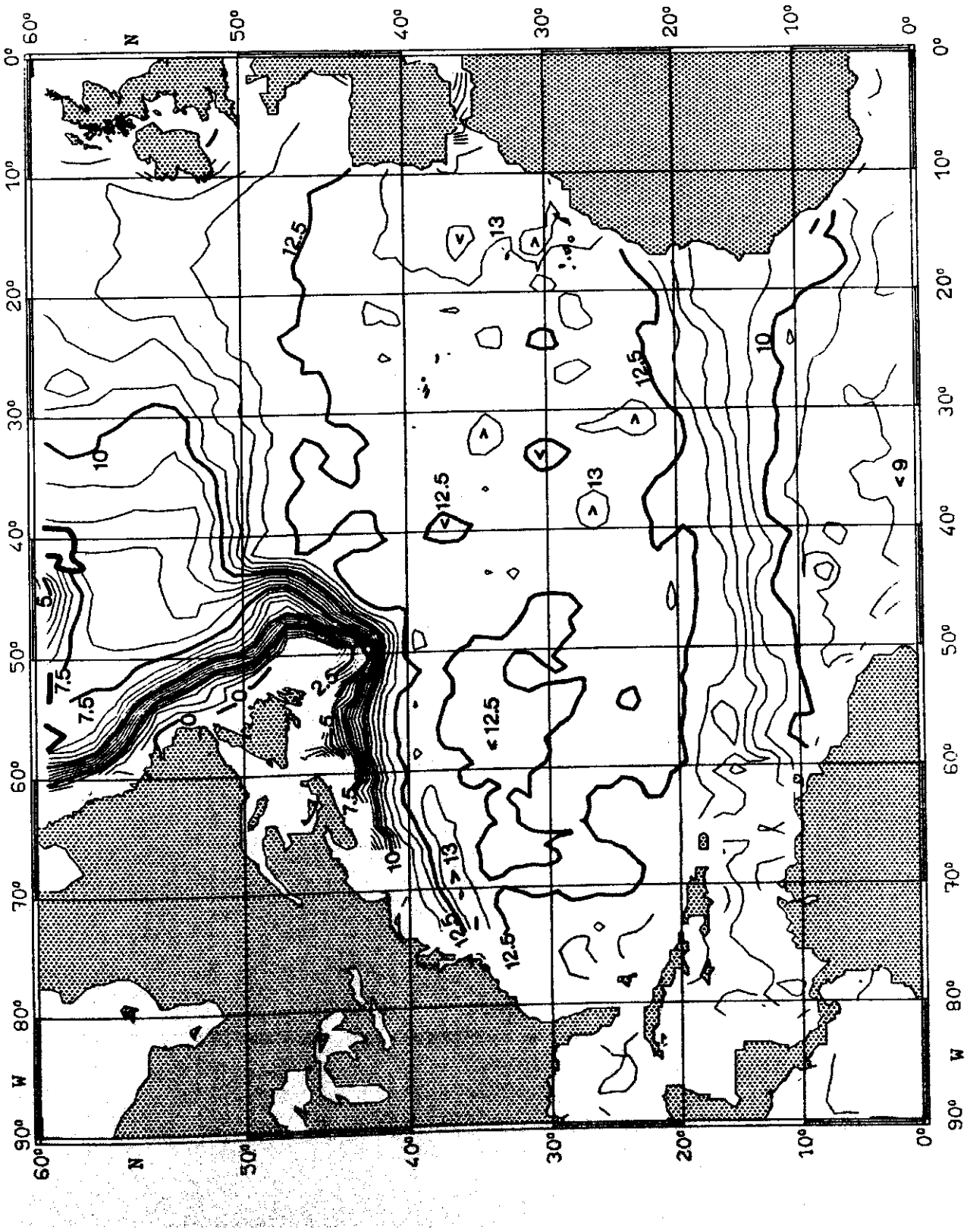

Fig. 108:

SALINITY (10^{-3}) on σ_θ = 27.0 kg m^{-3} SEPTEMBER

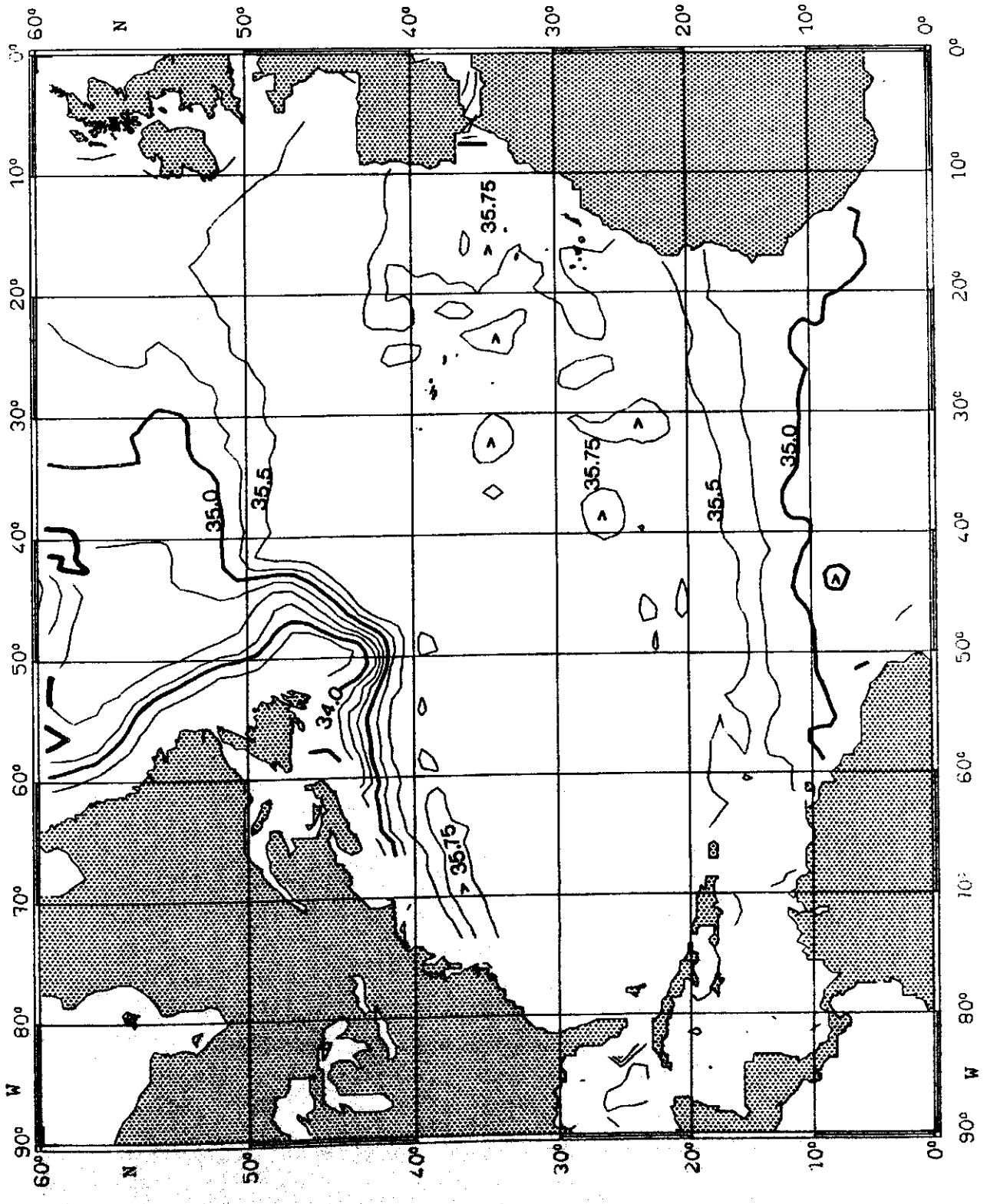

Fig. 109:

PRESSURE (10^4 Pa) on σ_θ = 25.0 kg m^{-3} OCTOBER

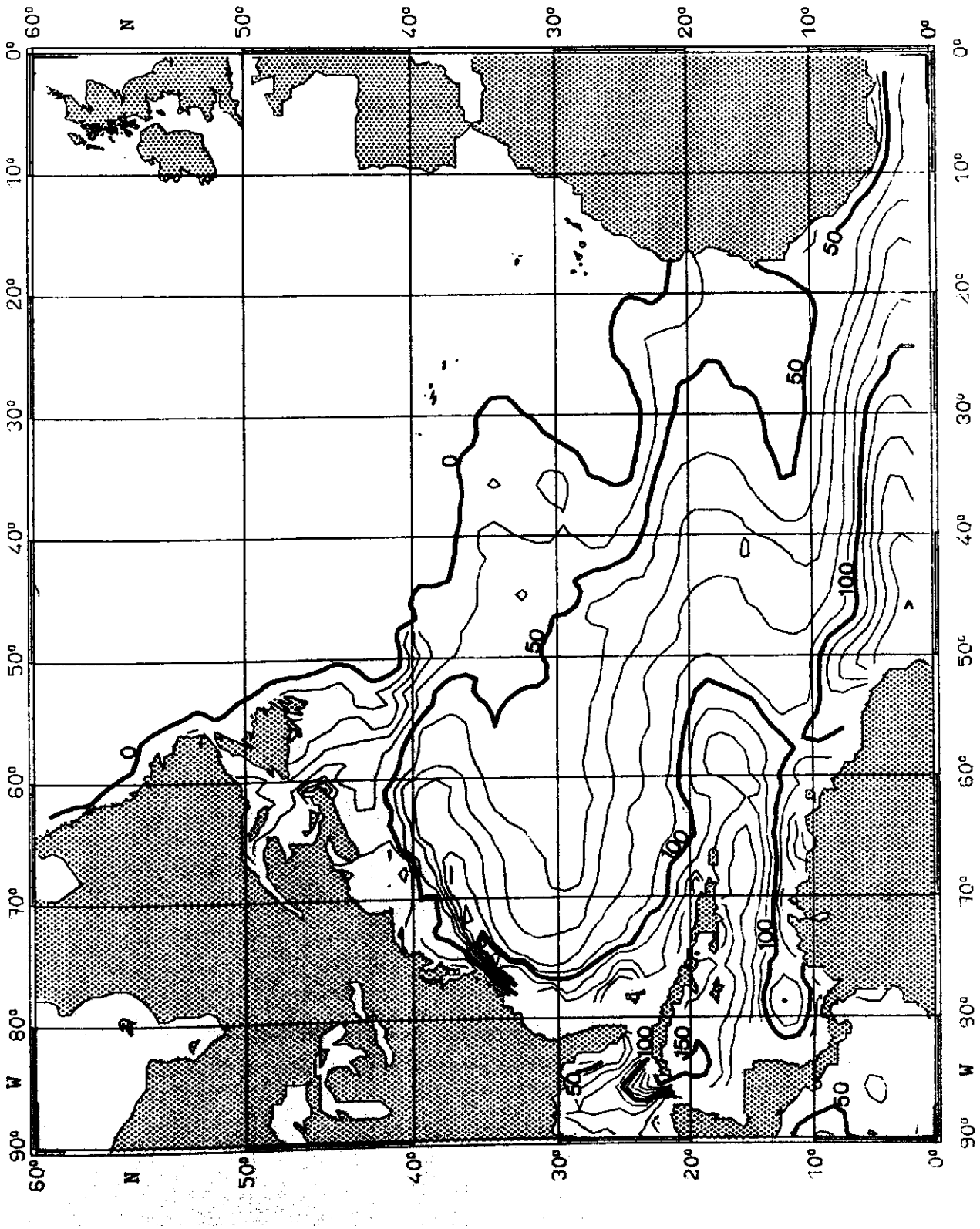

Fig. 110:

TEMPERATURE (°C) on σ_θ = 25.0 kg m^{-3} OCTOBER

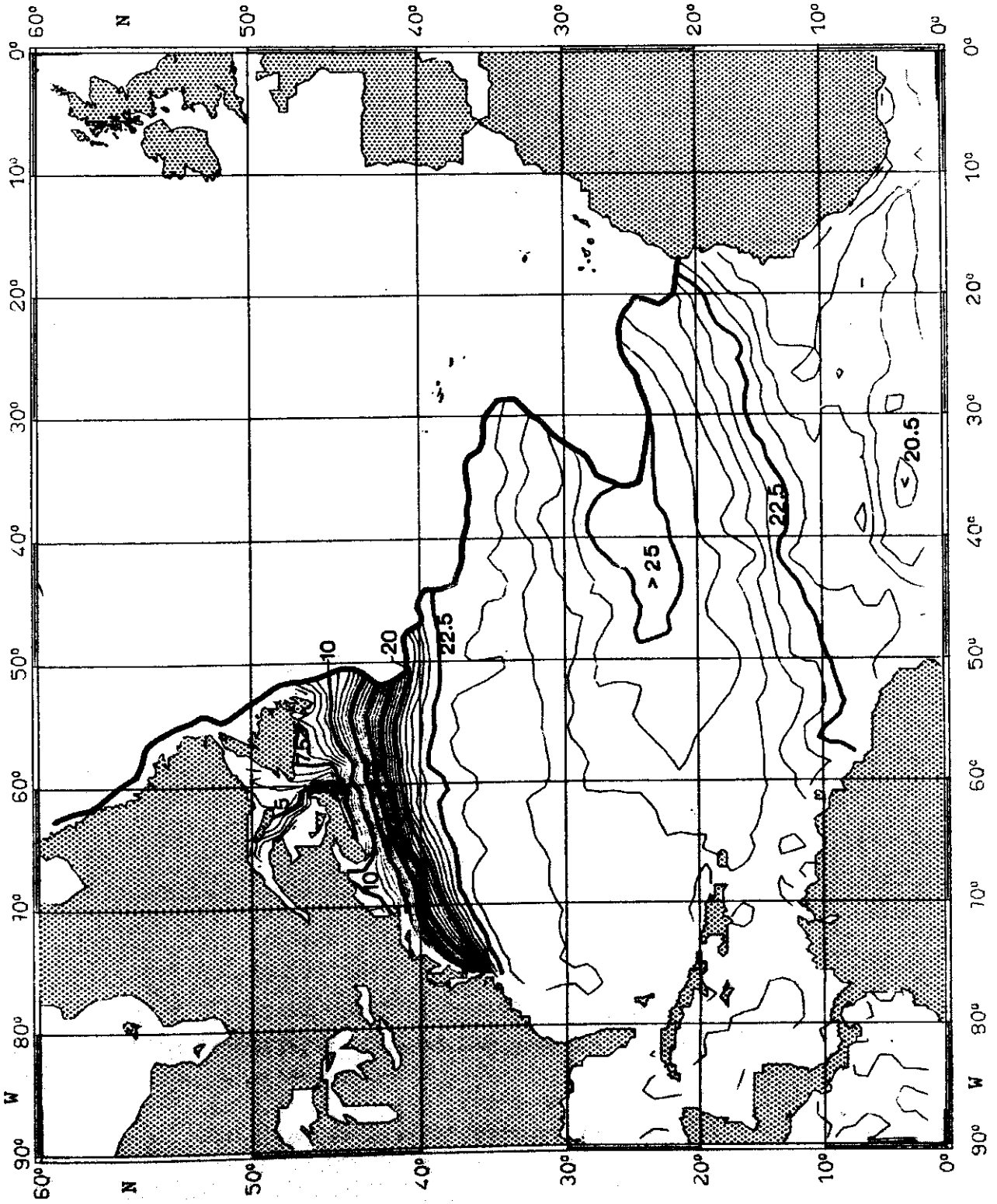

Fig. 111:

SALINITY (10^{-3}) on σ_θ = 25.0 kg m^{-3} OCTOBER

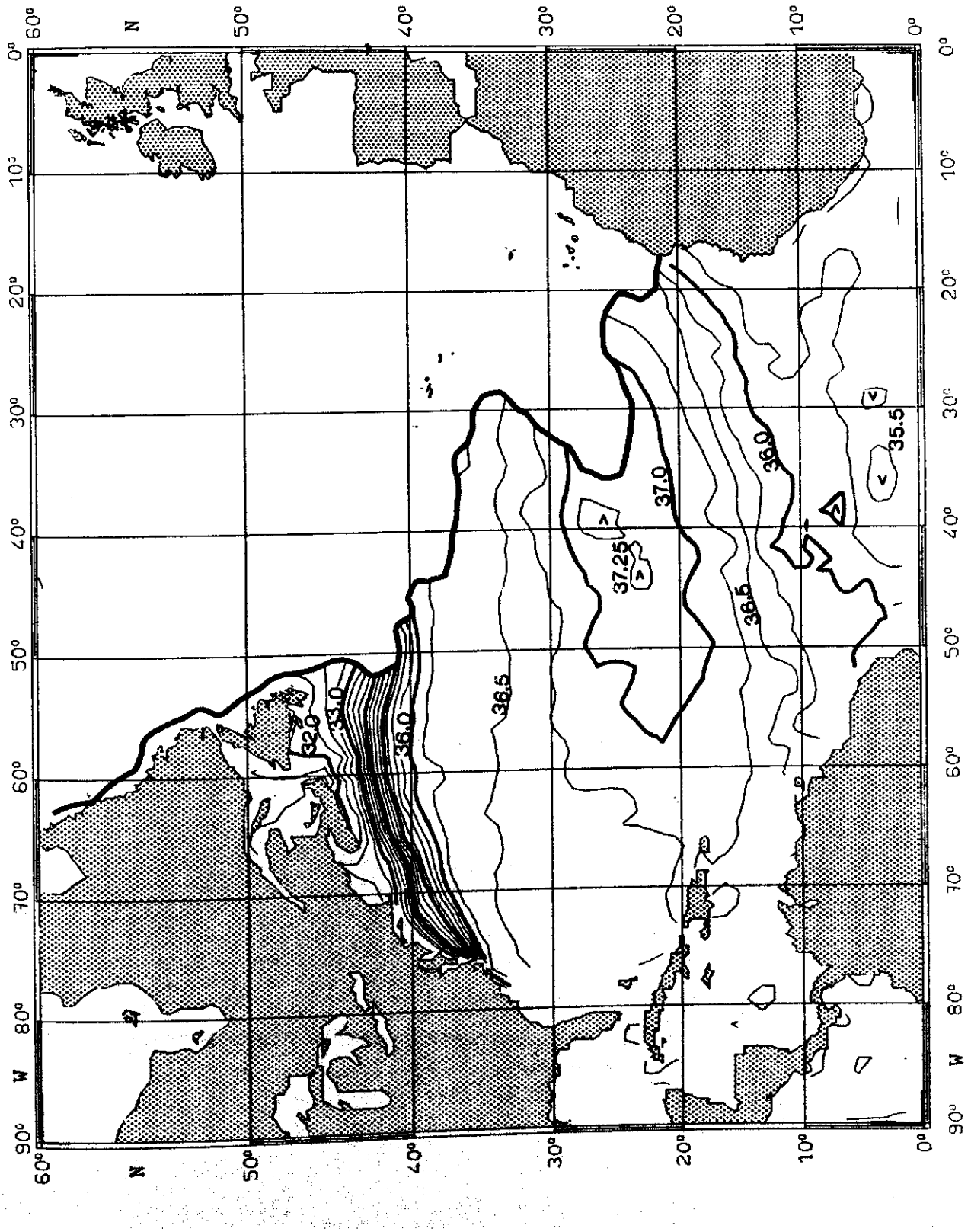

Fig. 112:

PRESSURE (10^4 Pa) on σ_θ = 26.0 kg m^{-3} OCTOBER

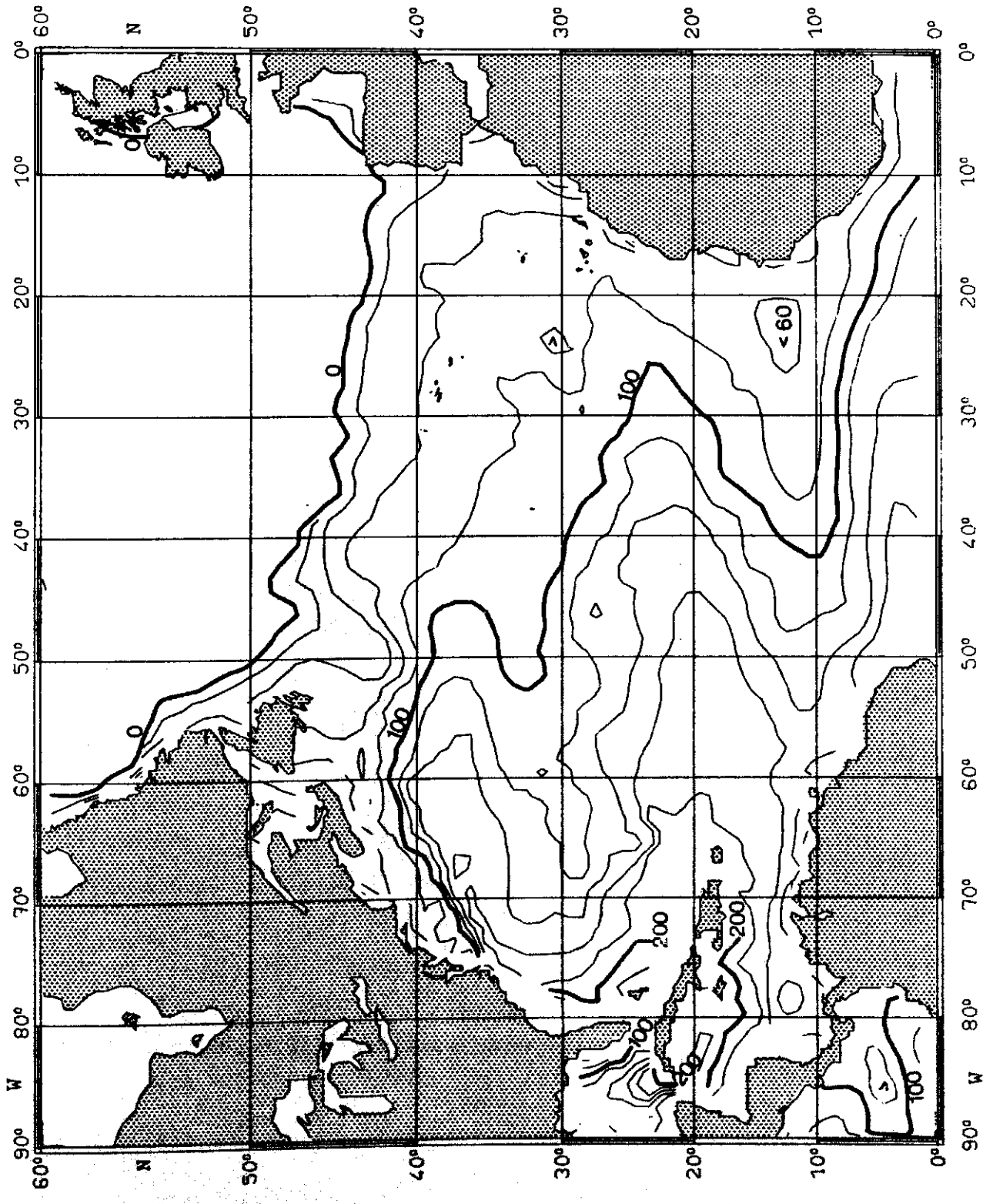

Fig. 113:

TEMPERATURE (°C) on σ_θ = 26.0 kg m^{-3} OCTOBER

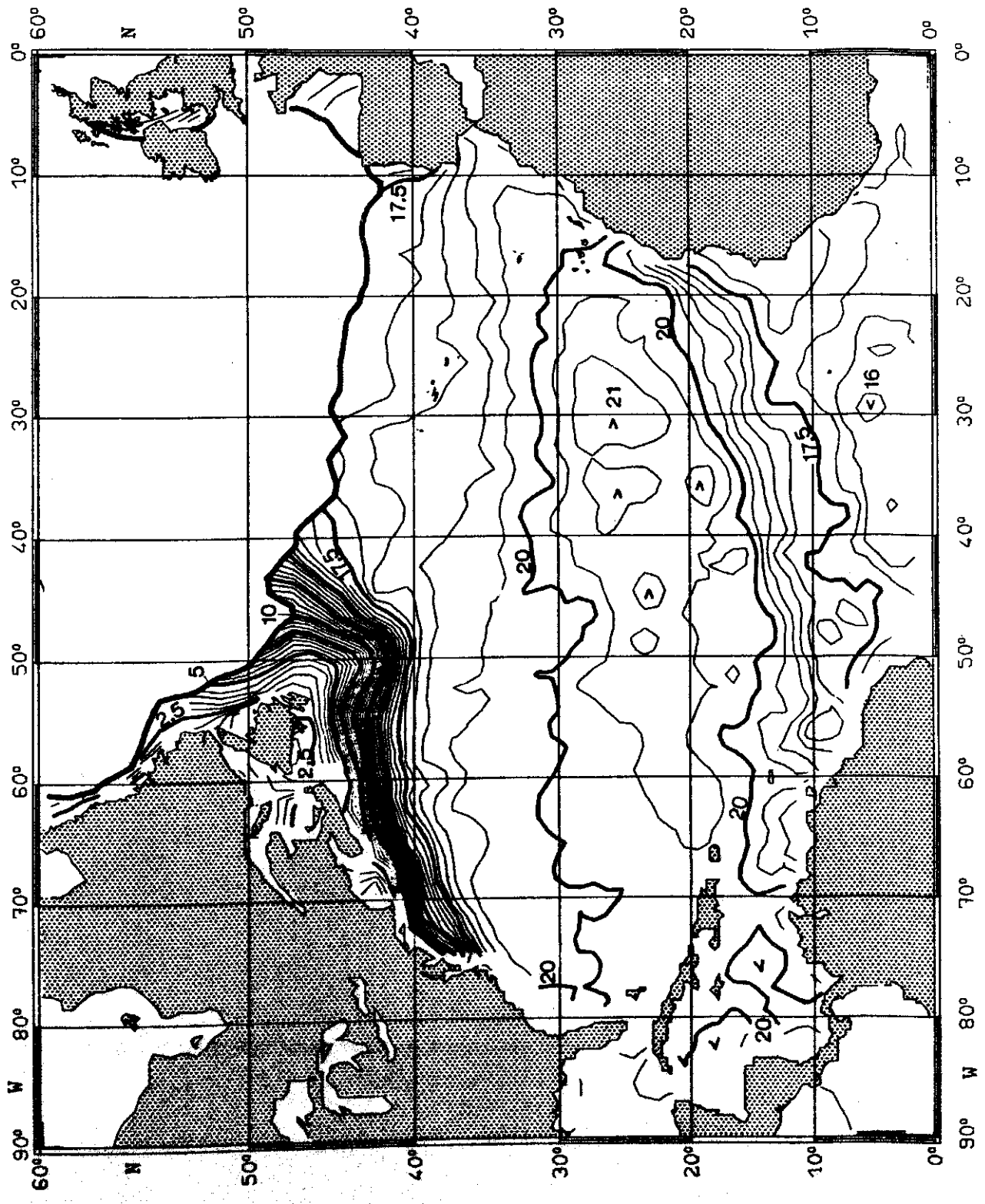

Fig. 114:

SALINITY (10^{-3}) on σ_θ = 26.0 kg m^{-3} OCTOBER

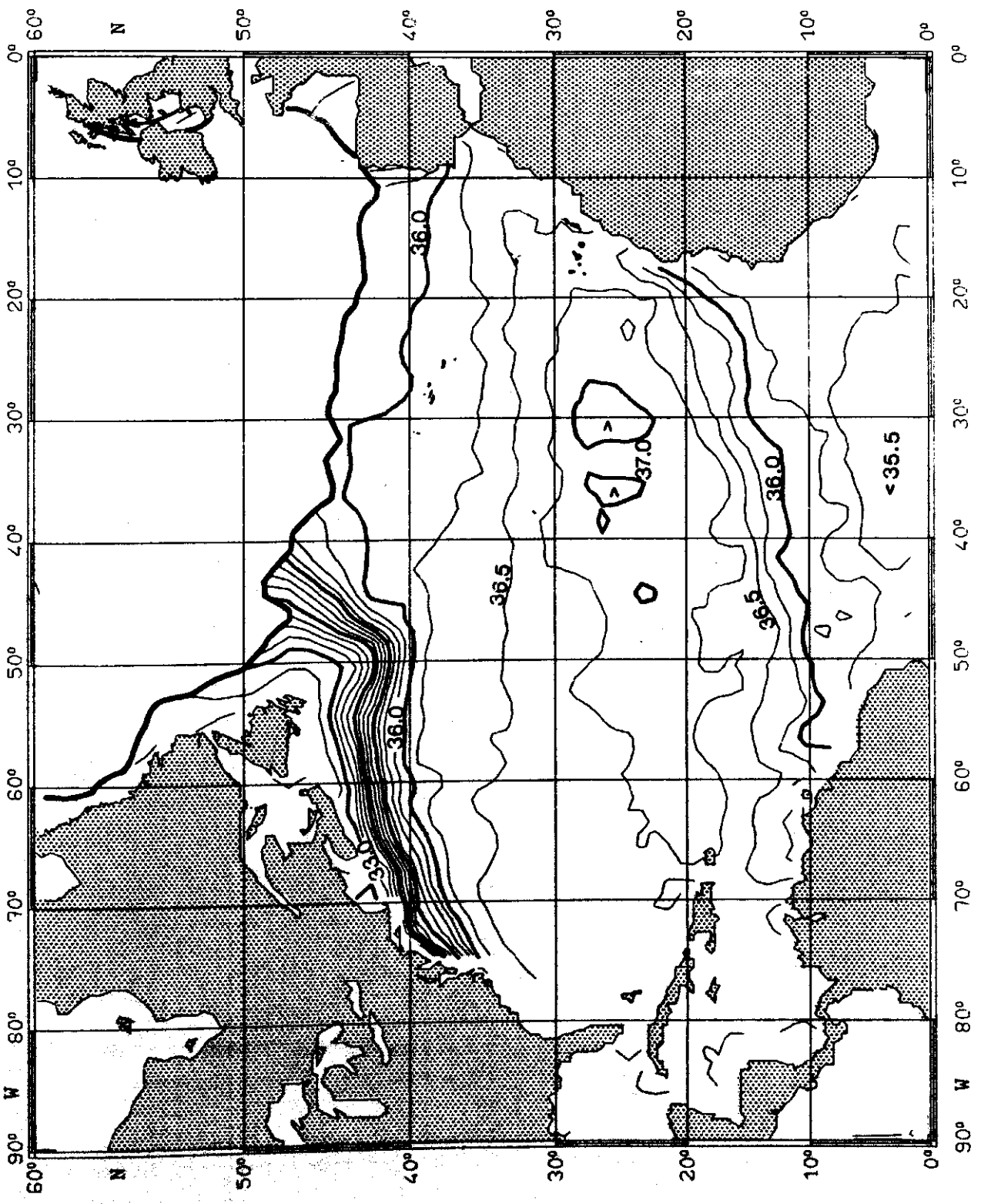

Fig. 115:

PRESSURE (10^4 Pa) on σ_θ = 27.0 kg m^{-3} OCTOBER

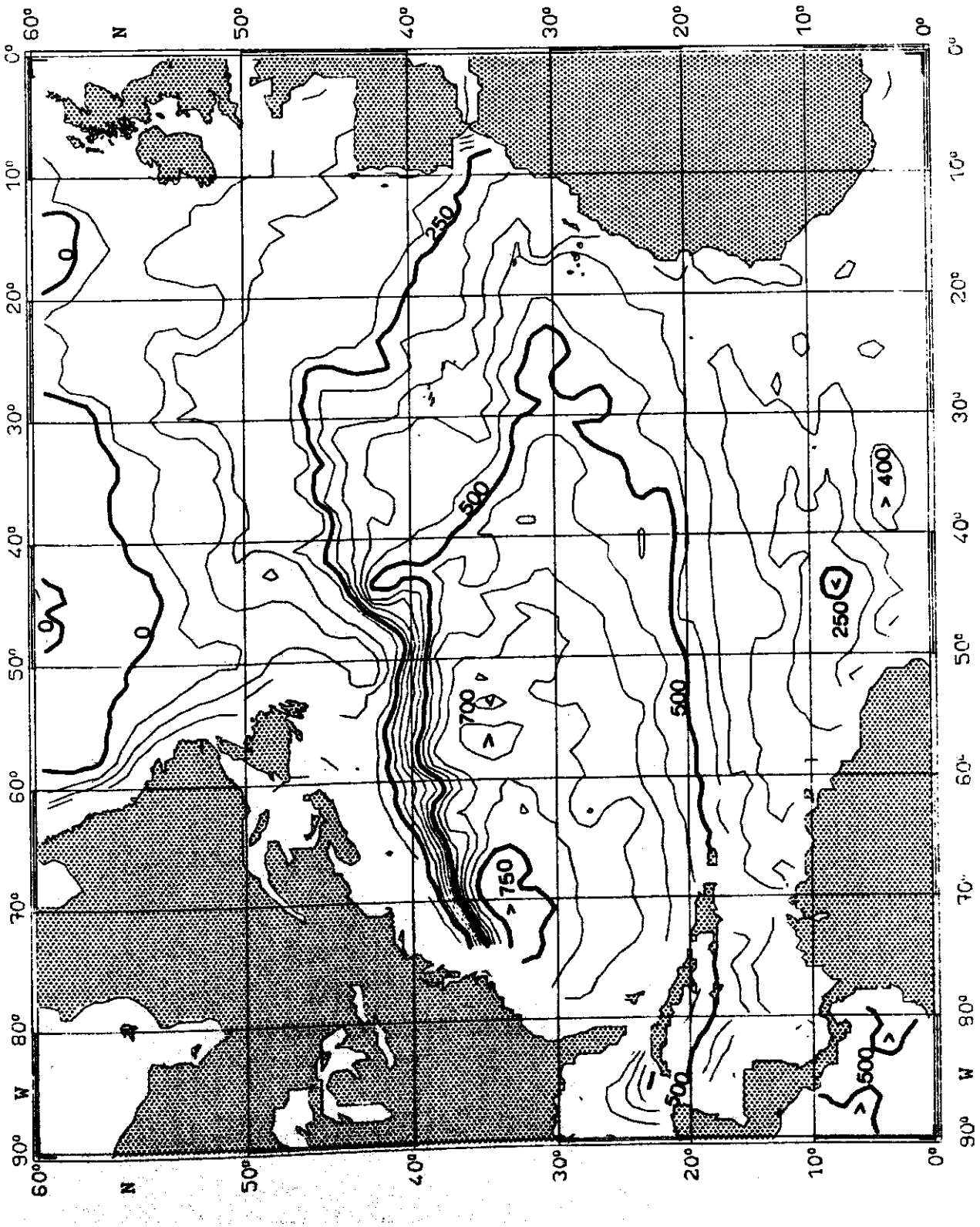

Fig. 116:

TEMPERATURE (°C) on σ_θ = 27.0 kg m^{-3} OCTOBER

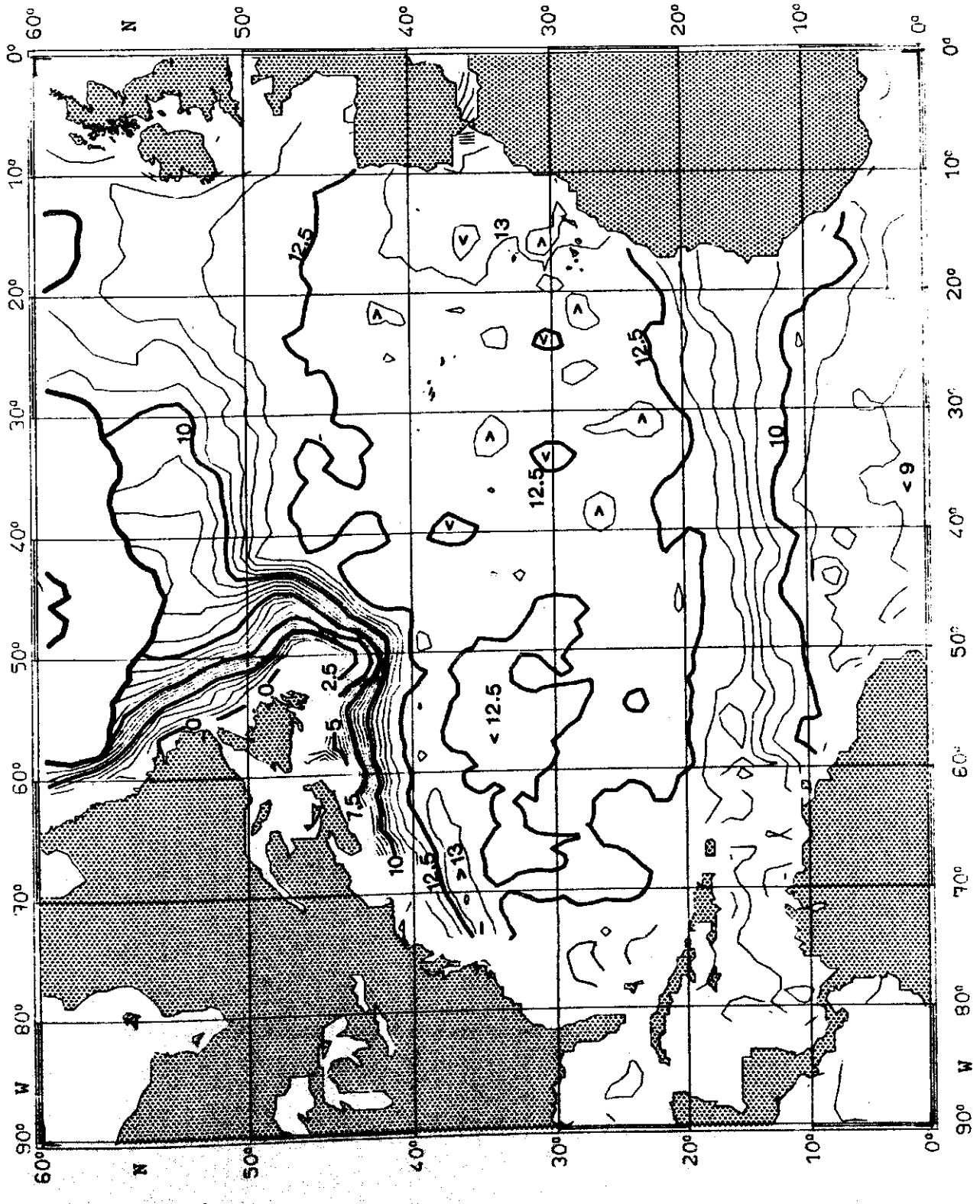

Fig. 117:

SALINITY (10^{-3}) on σ_θ = 27.0 kg m^{-3} OCTOBER

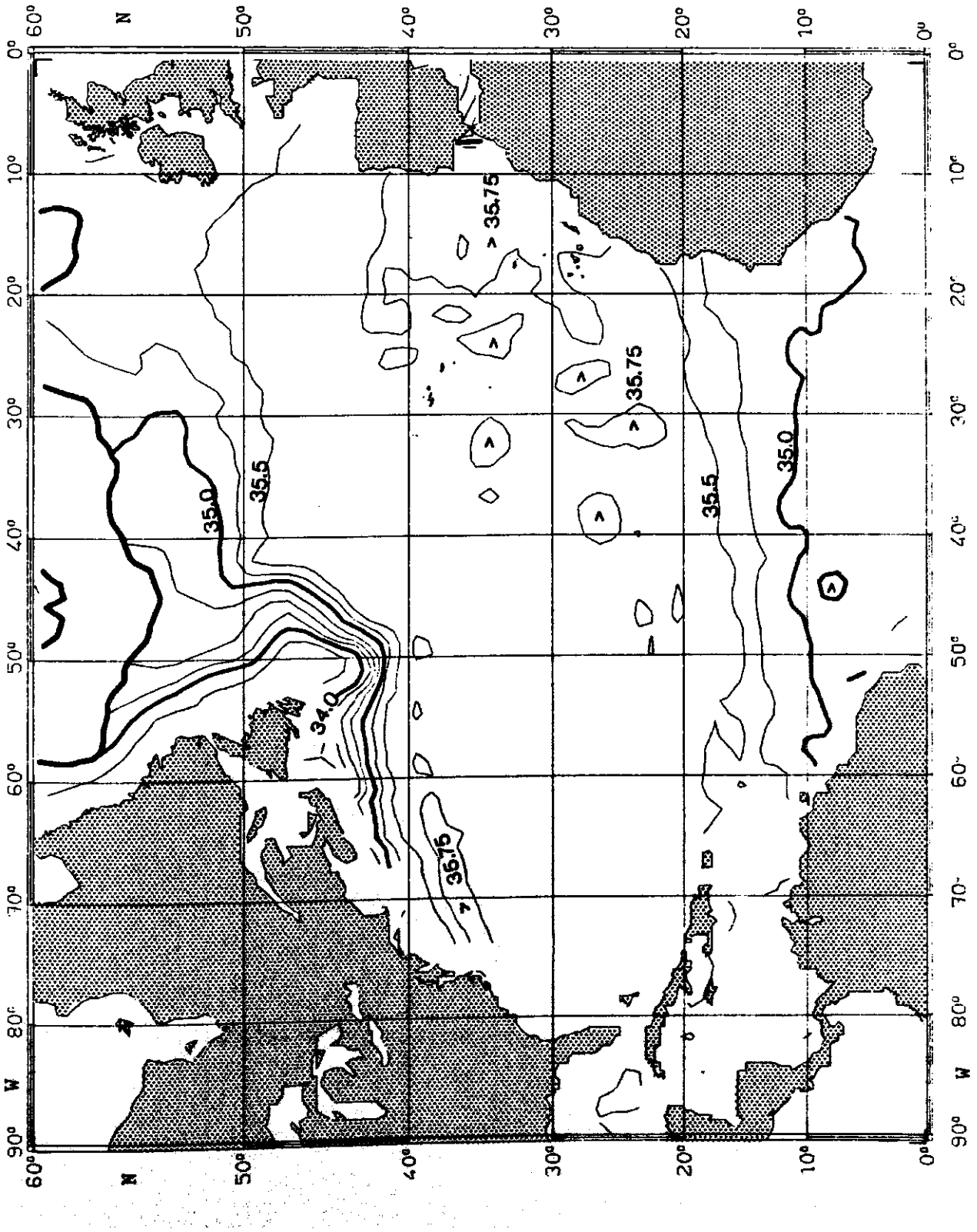

Fig. 118:

PRESSURE (10^4 Pa) on σ_θ = 25.0 kg m^{-3} NOVEMBER

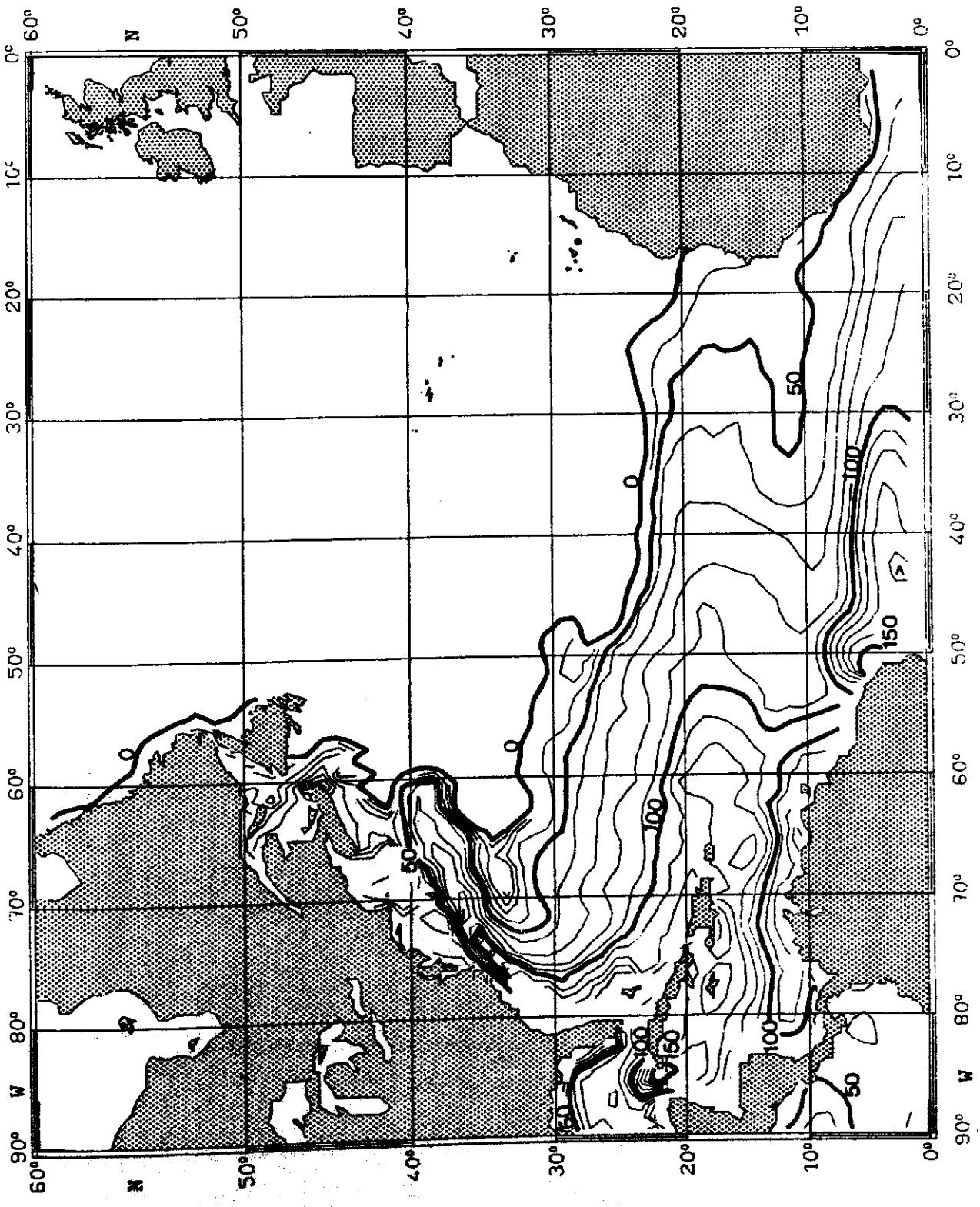

Fig. 119:

TEMPERATURE (°C) on σ_θ = 25.0 kg m^{-3} NOVEMBER

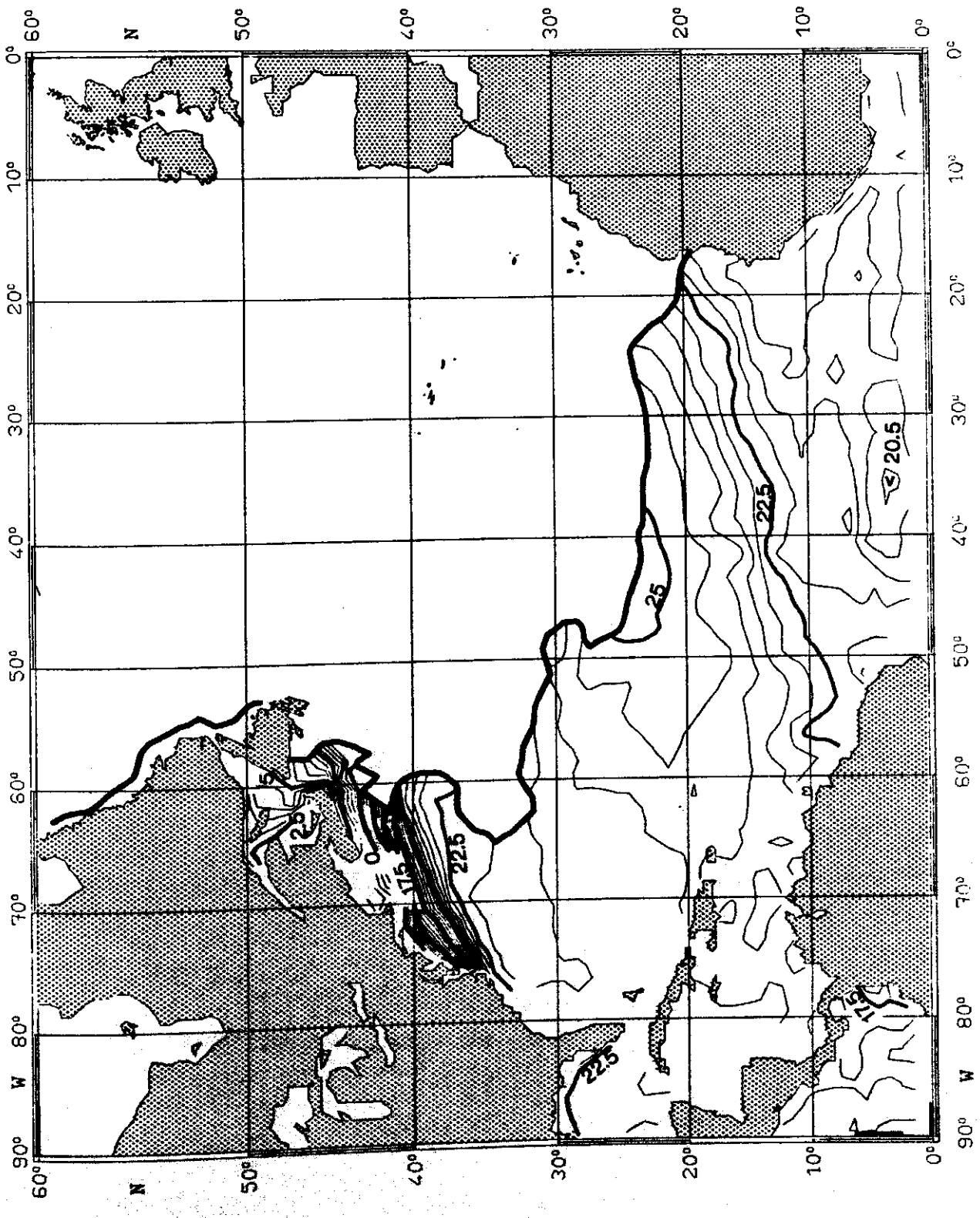

Fig. 120:

SALINITY (10^{-3}) on σ_θ = 25.0 kg m^{-3} NOVEMBER

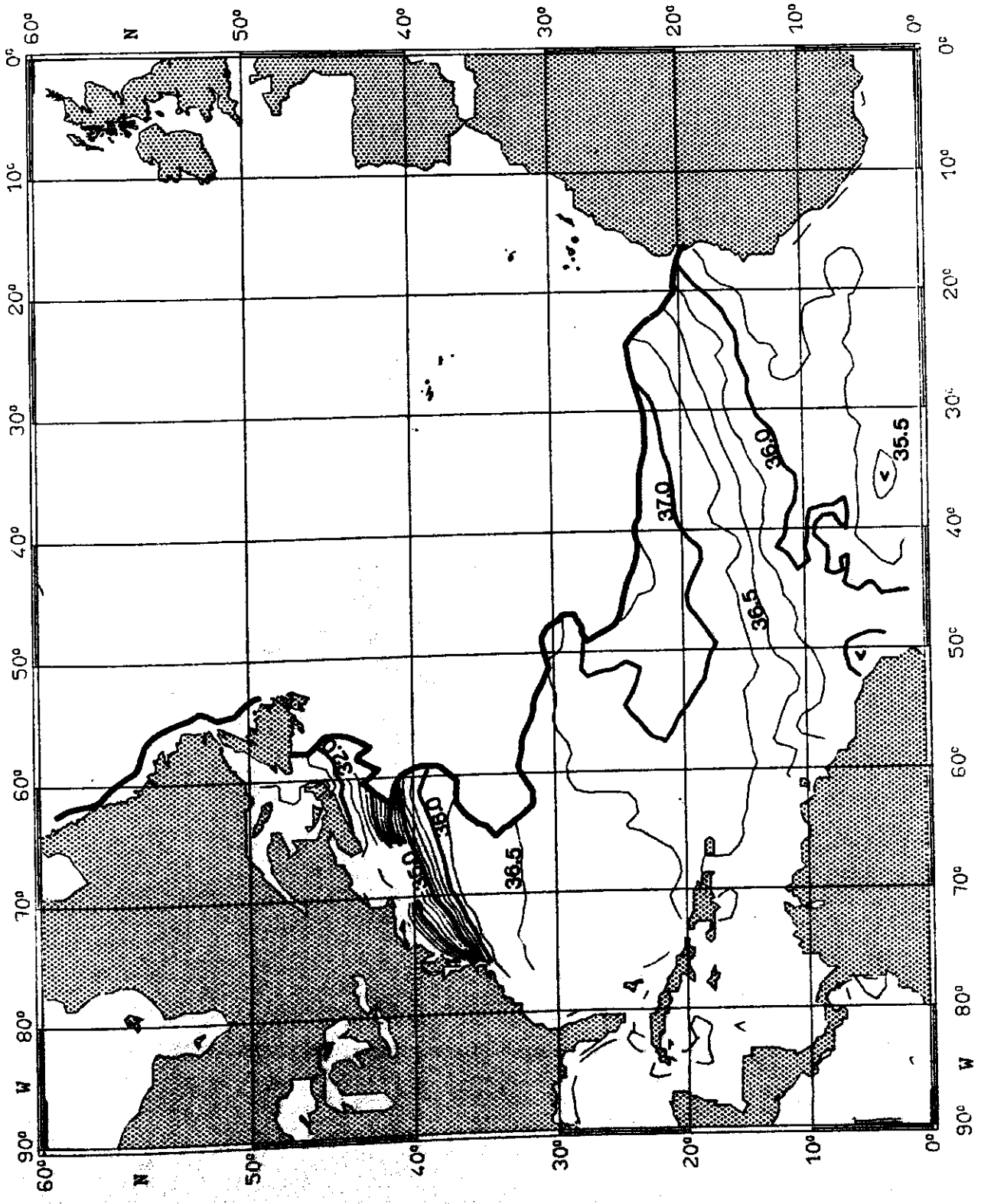

Fig. 121:

PRESSURE (10^4 Pa) on σ_θ = 26.0 kg m^{-3} NOVEMBER

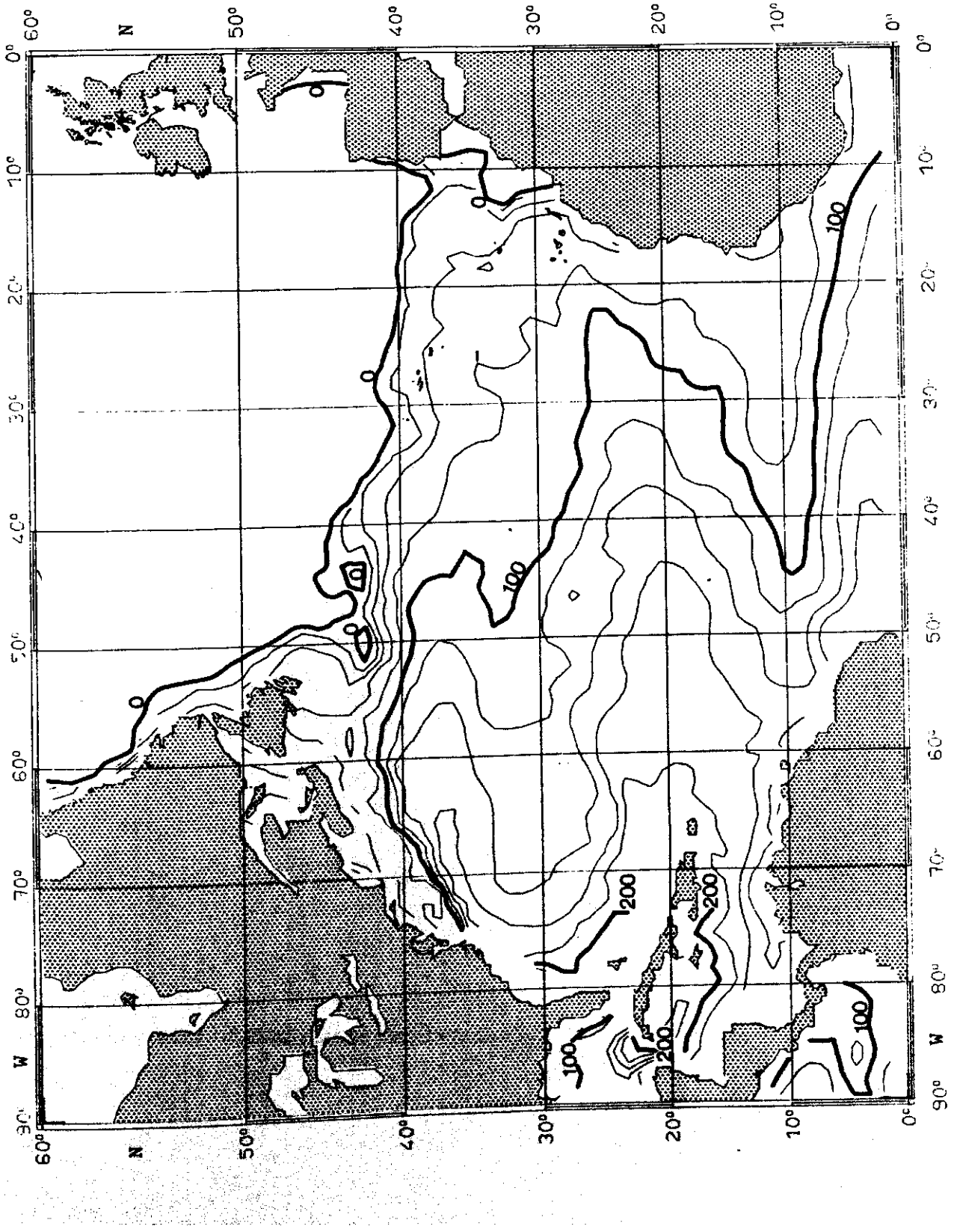

Fig. 122:

TEMPERATURE (°C) on σ_θ = 26.0 kg m^{-3} NOVEMBER

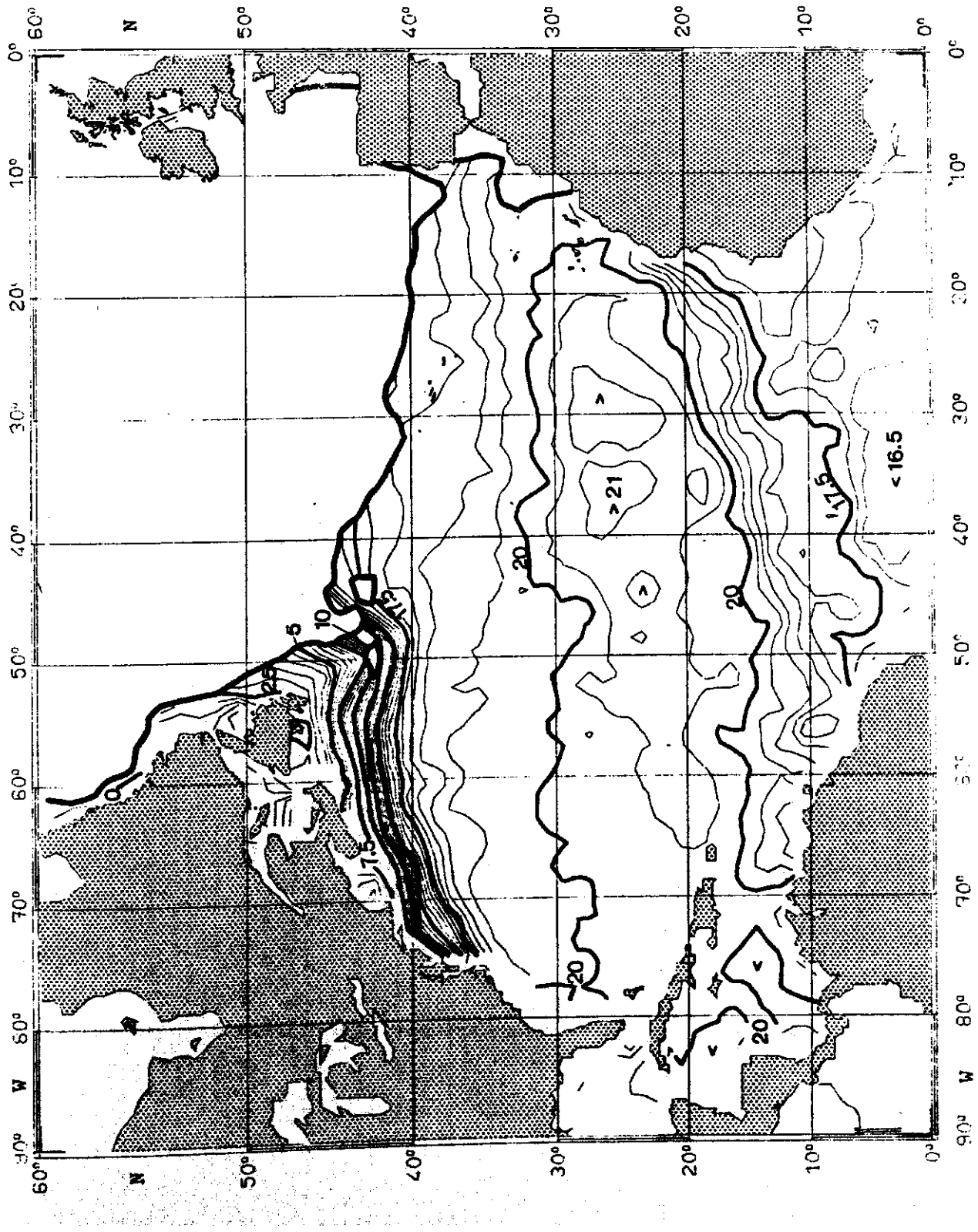

Fig. 123:

SALINITY (10^{-3}) on σ_θ = 26.0 kg m^{-3} NOVEMBER

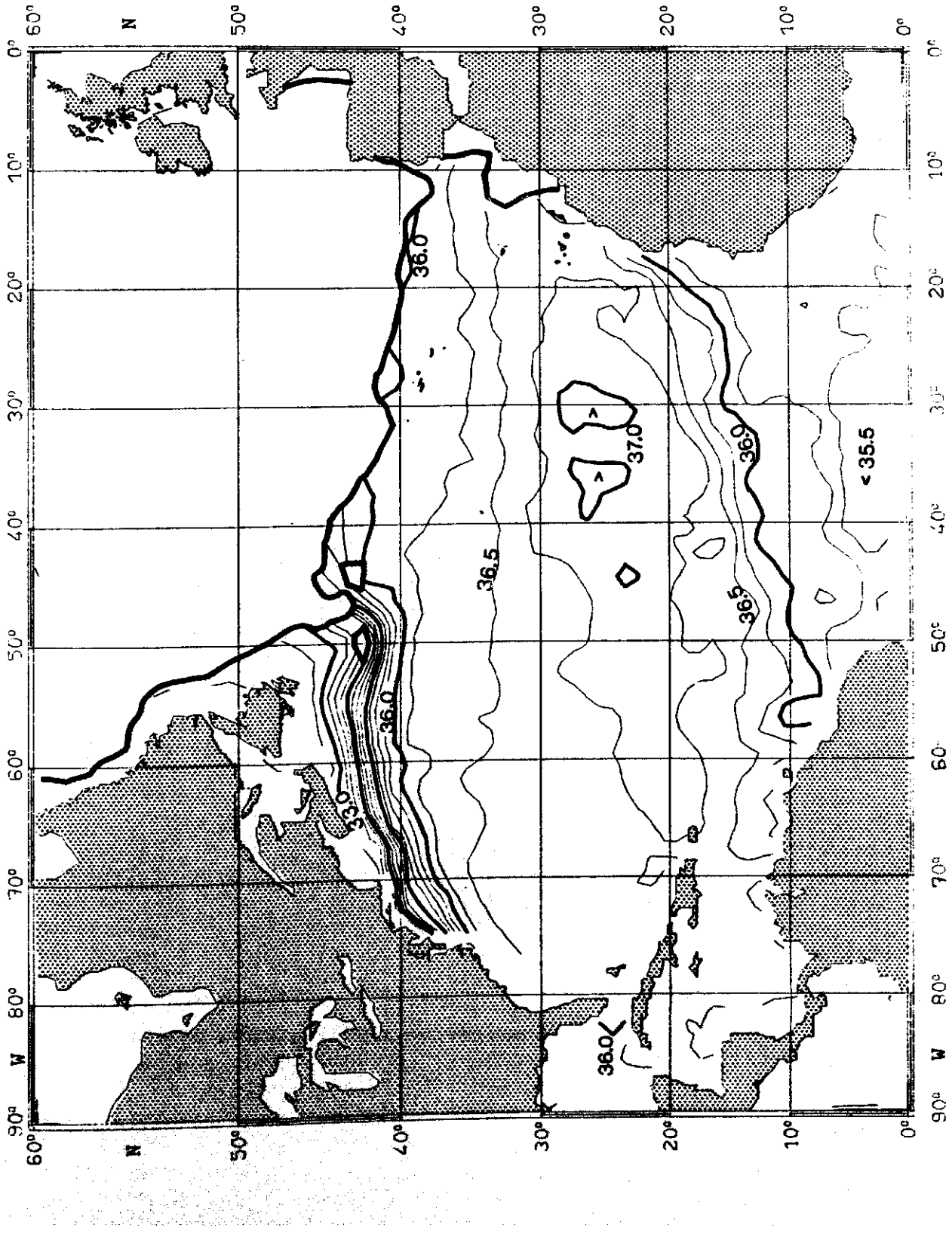

Fig. 124:

PRESSURE (10^4 Pa) on σ_θ = 27.0 kg m^{-3} NOVEMBER

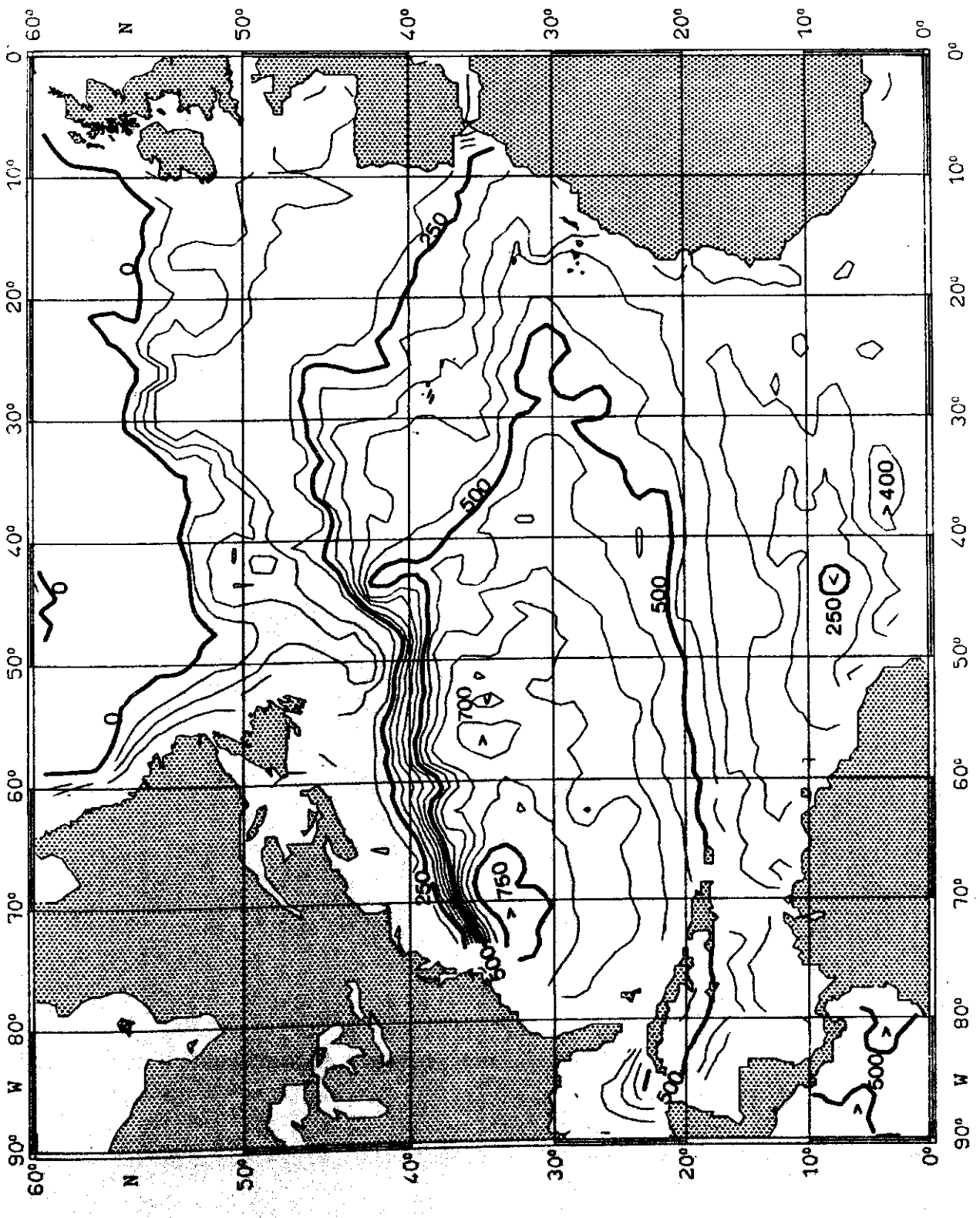

Fig. 125:

TEMPERATURE (°C) on σ_θ = 27.0 kg m^{-3} NOVEMBER

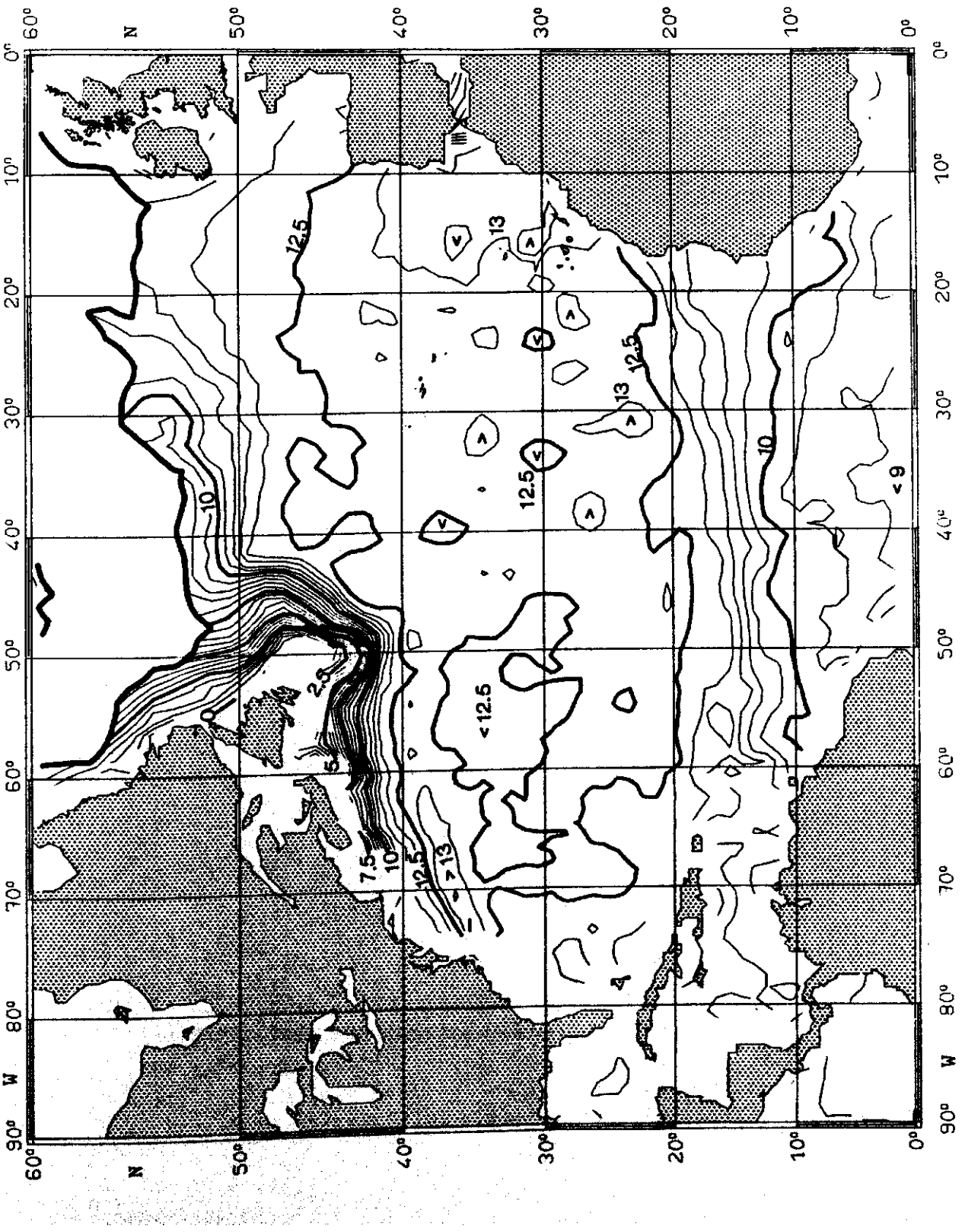

Fig. 126:

SALINITY (10^{-3}) on σ_θ = 27.0 kg m^{-3} NOVEMBER

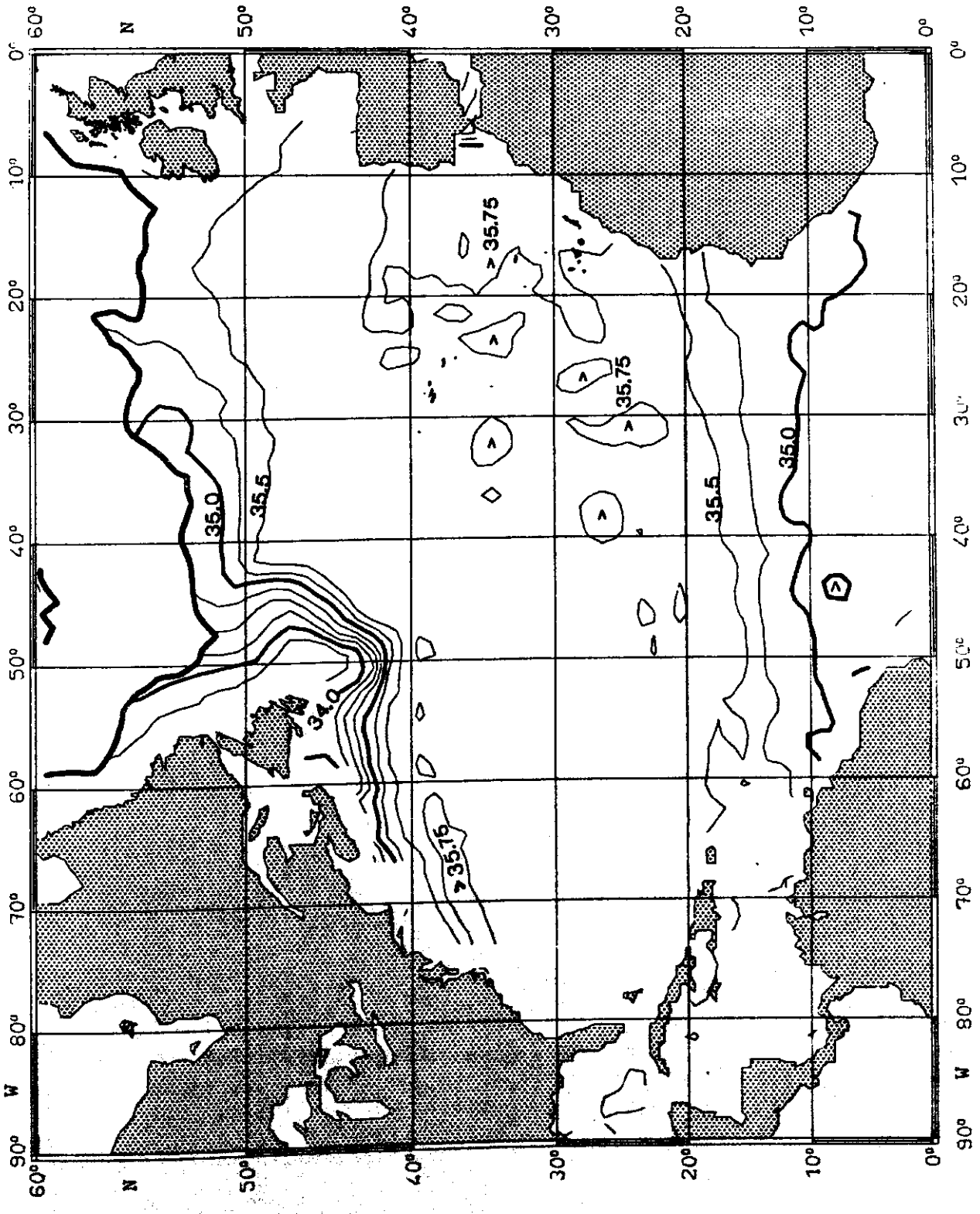

Fig. 127:

PRESSURE (10^4 Pa) on σ_θ = 25.0 kg m^{-3} DECEMBER

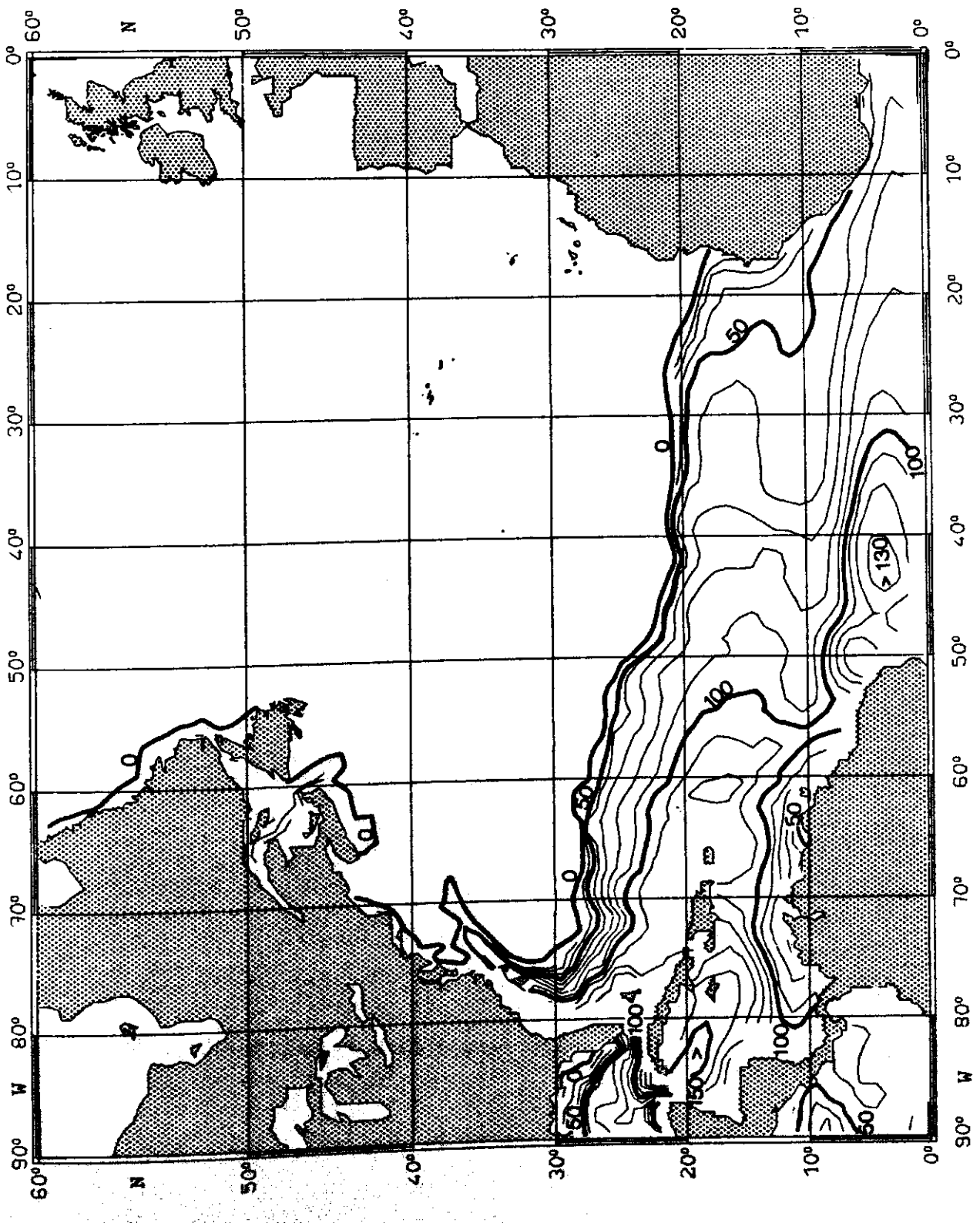

Fig. 128:

TEMPERATURE (°C) on σ_θ = 25.0 kg m^{-3} DECEMBER

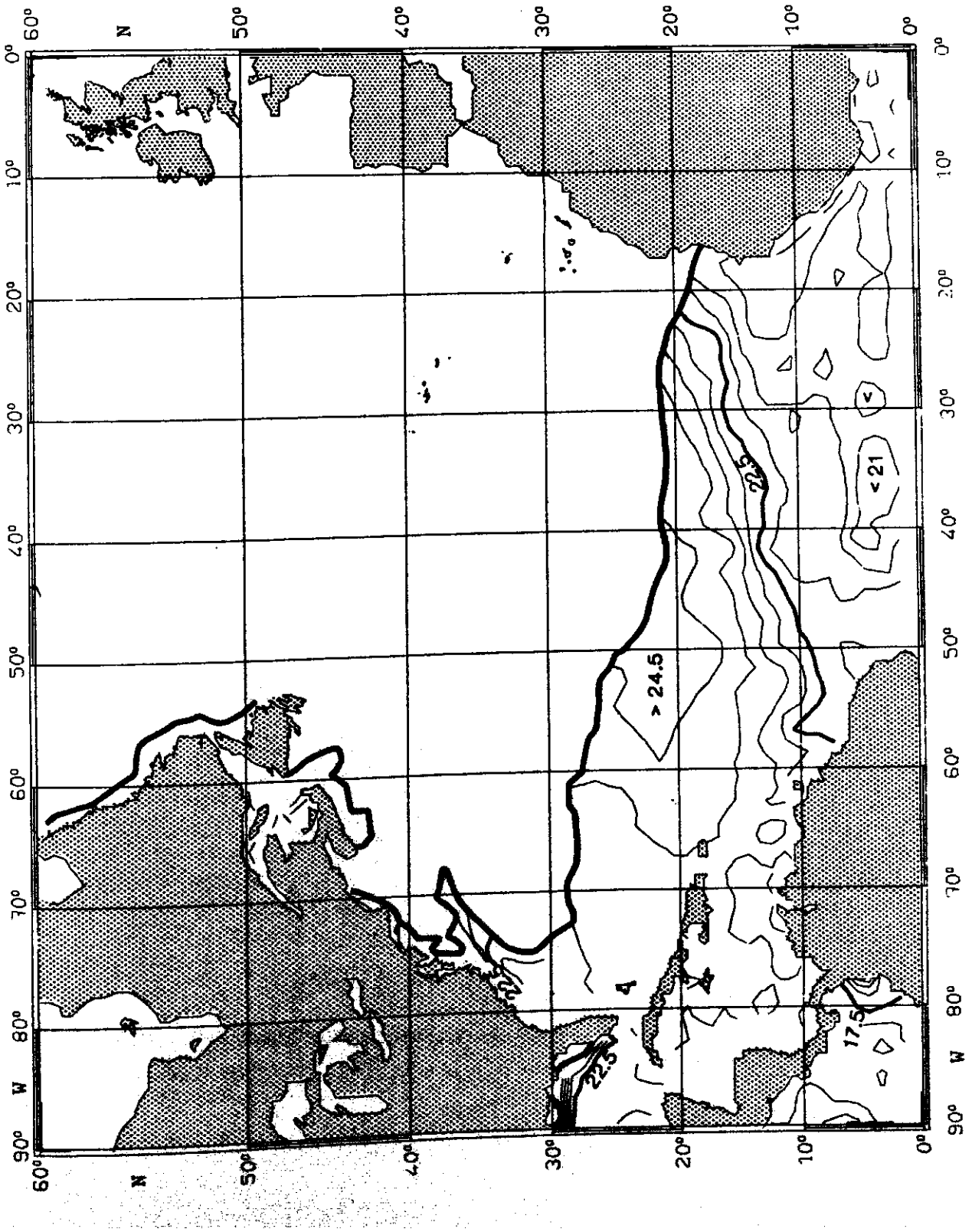

Fig. 129:

SALINITY (10^{-3}) on σ_θ = 25.0 kg m^{-3} DECEMBER

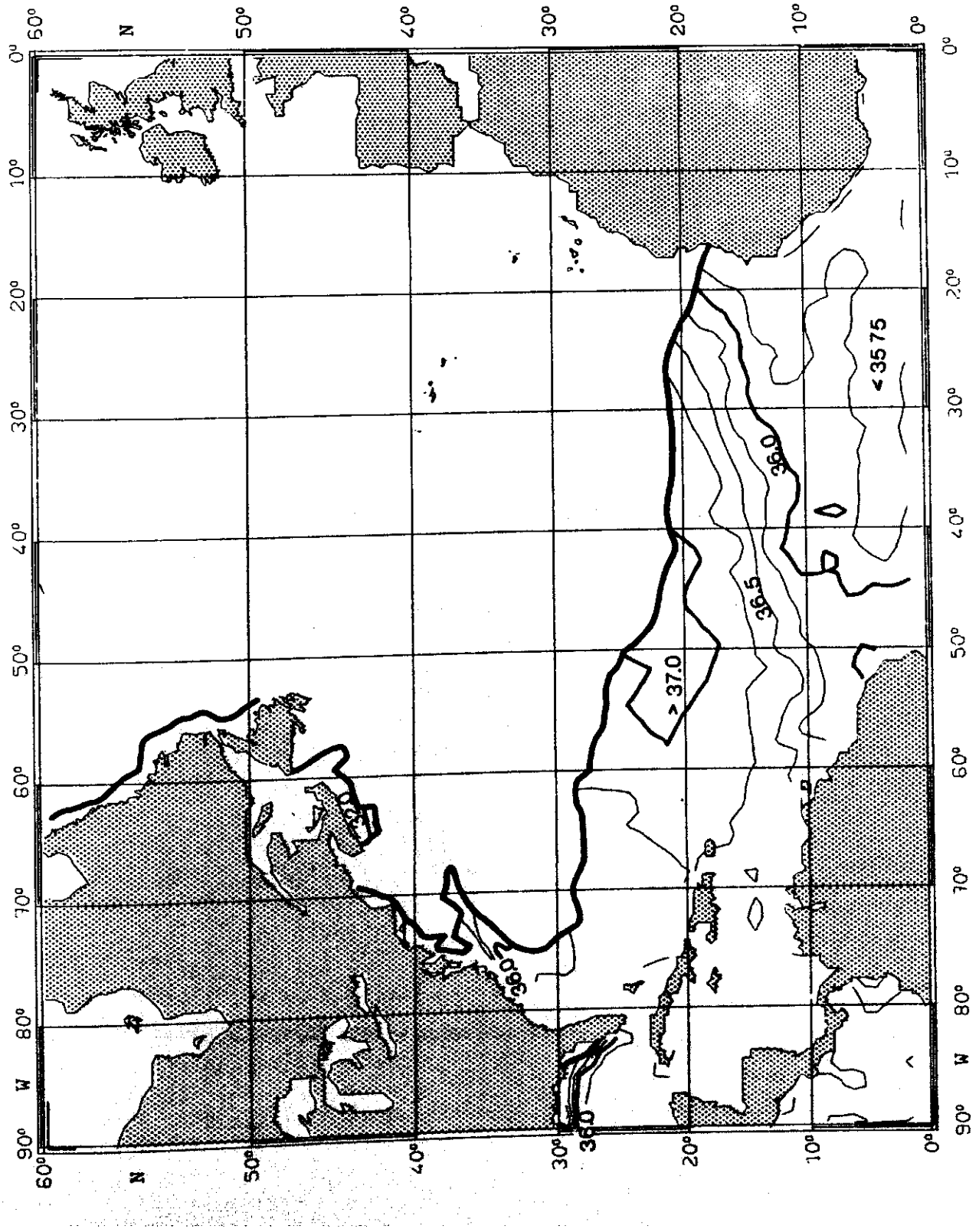

Fig. 130:

PRESSURE (10^4 Pa) on σ_θ =26.0 kg m^{-3} DECEMBER

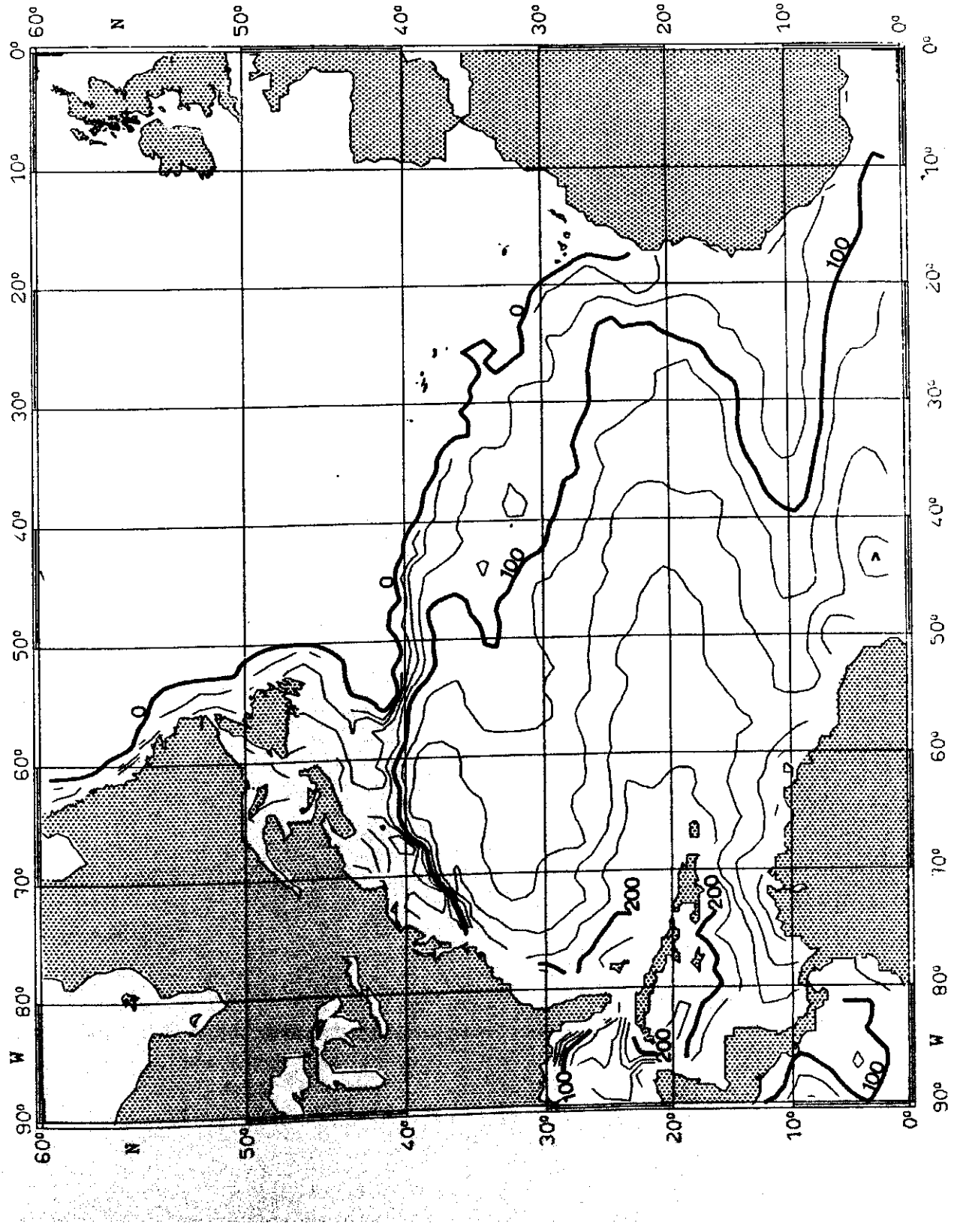

Fig. 131:

TEMPERATURE (°C) on σ_θ = 26.0 kg m^{-3} DECEMBER

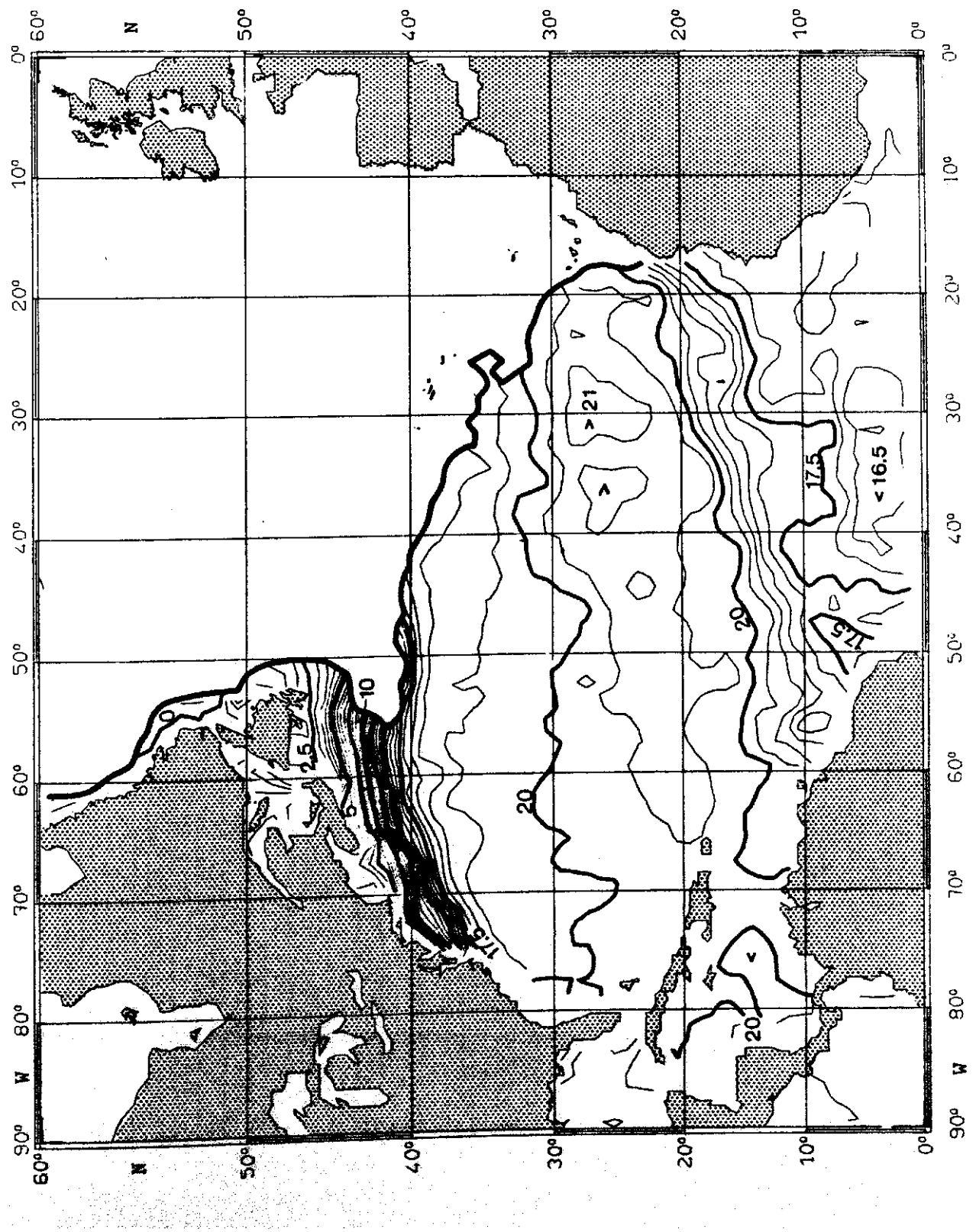

Fig. 132:

SALINITY (10^{-3}) on σ_θ = 26.0 kg m^{-3} DECEMBER

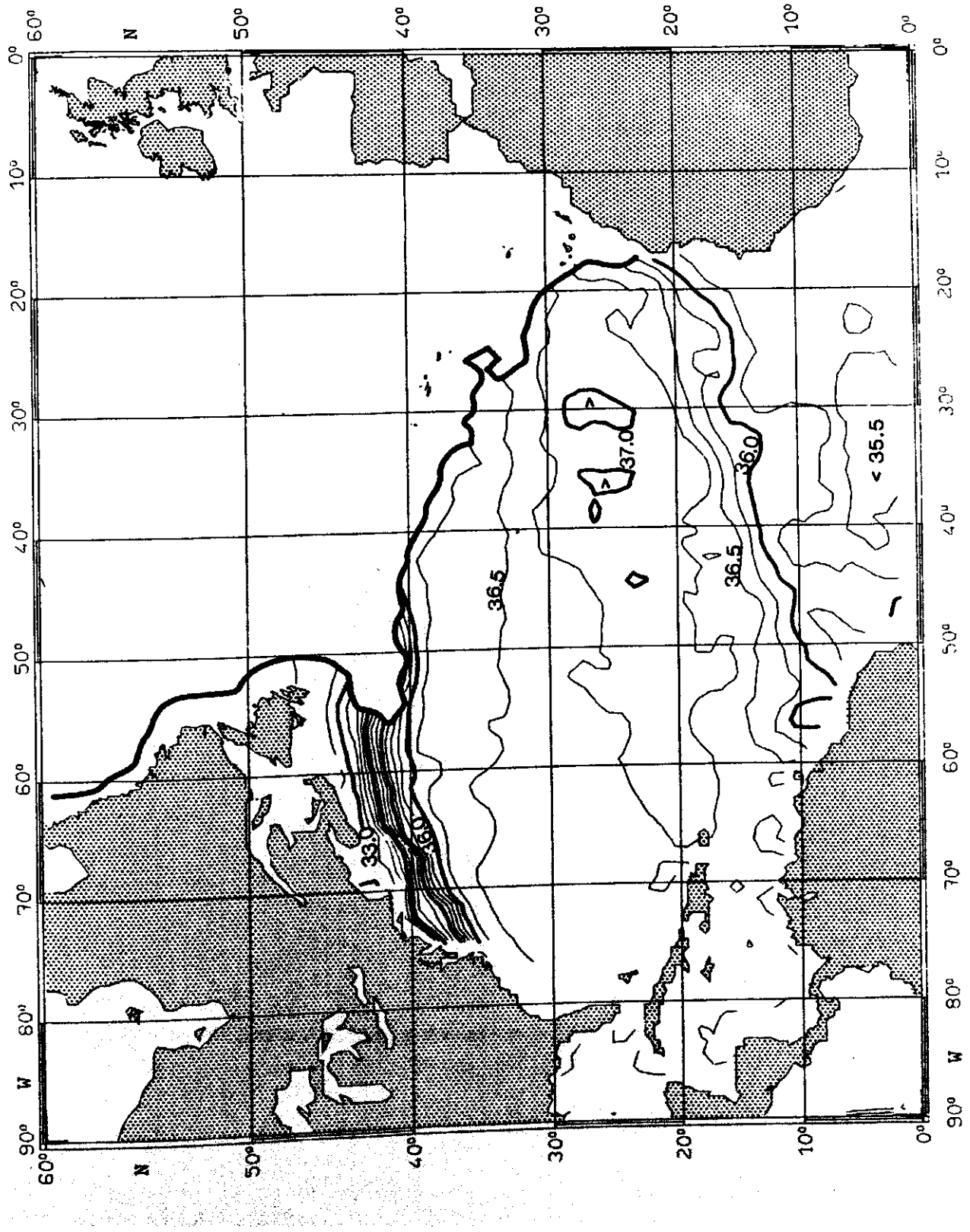

Fig. 133:

PRESSURE (10^4 Pa) on σ_θ = 27.0 kg m^{-3} DECEMBER

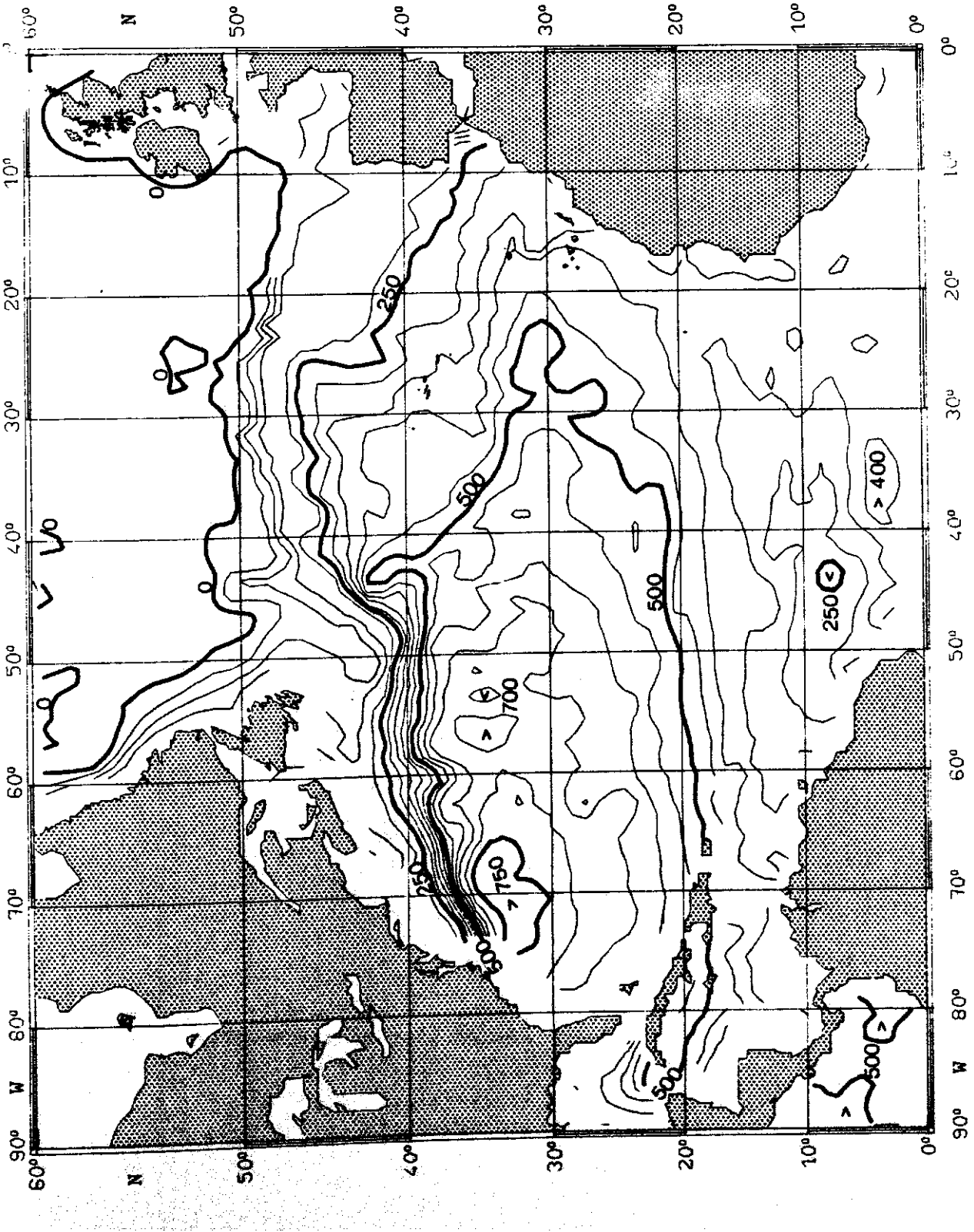

Fig. 134:

TEMPERATURE (°C) on σ_θ = 27.0 kg m^{-3} DECEMBER

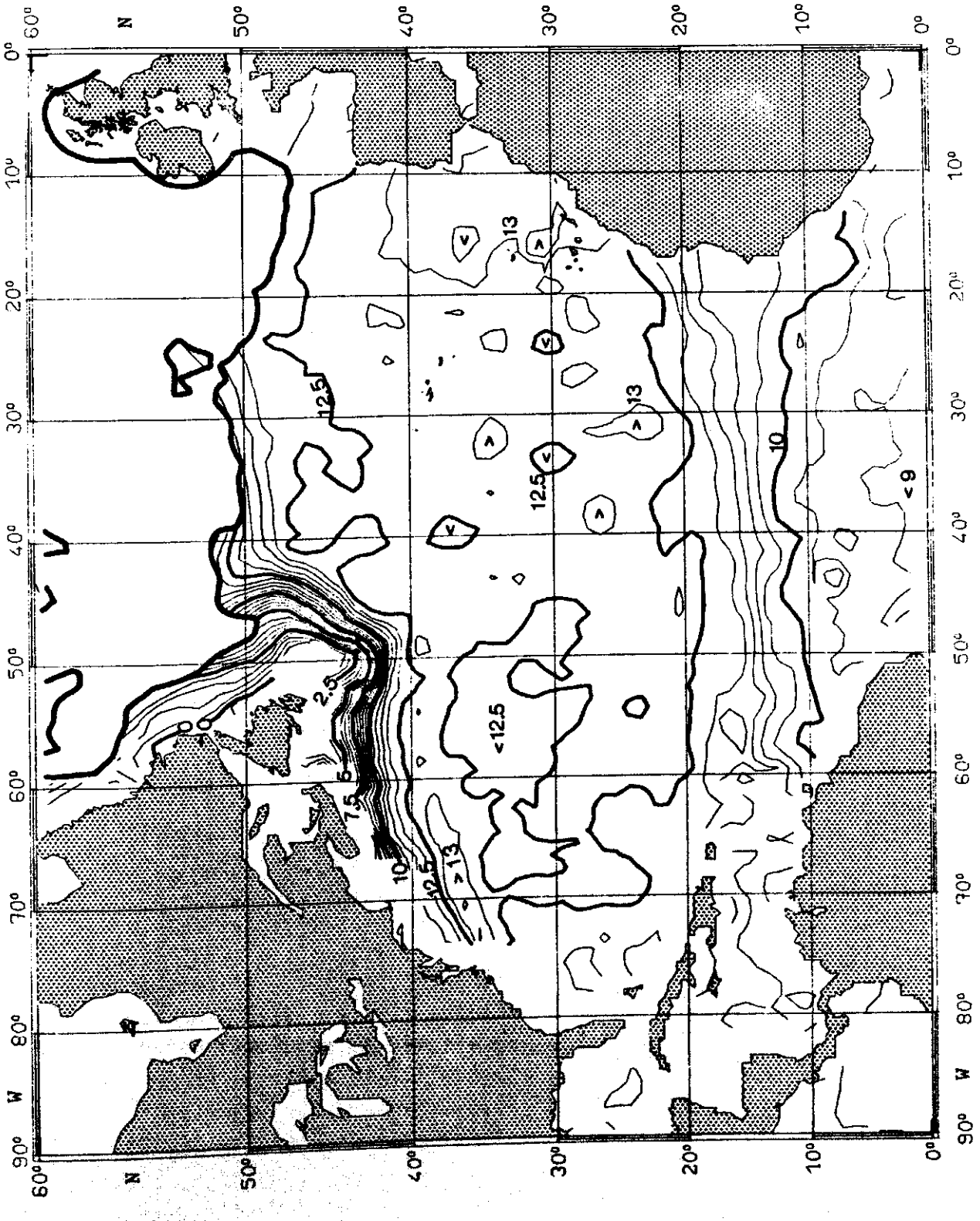

Fig. 135:

SALINITY (10^{-3}) on σ_θ = 27.0 kg m^{-3} DECEMBER

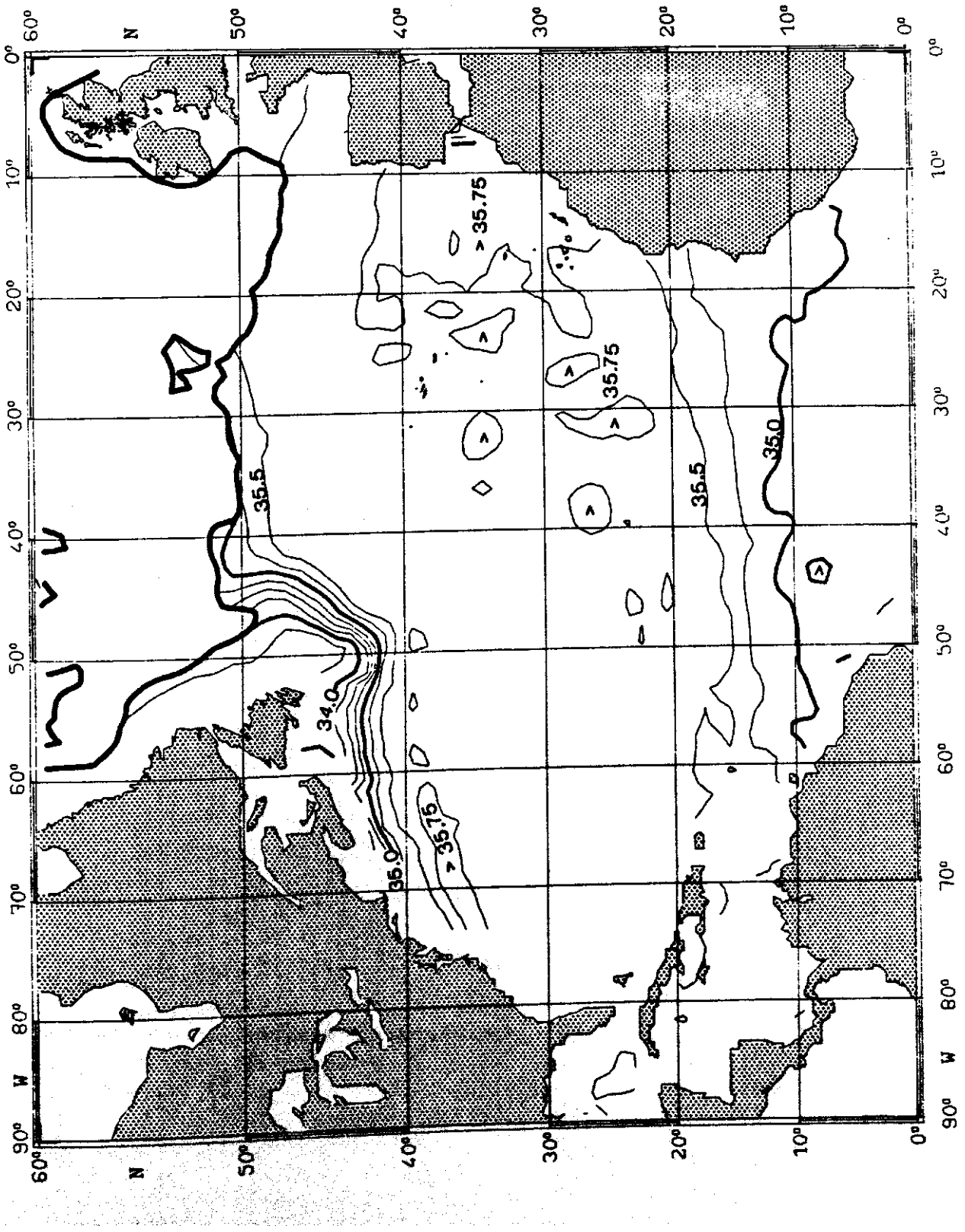

Fig. 136: Location of vertical sections
Azores - Greenland and Azores - English Channel

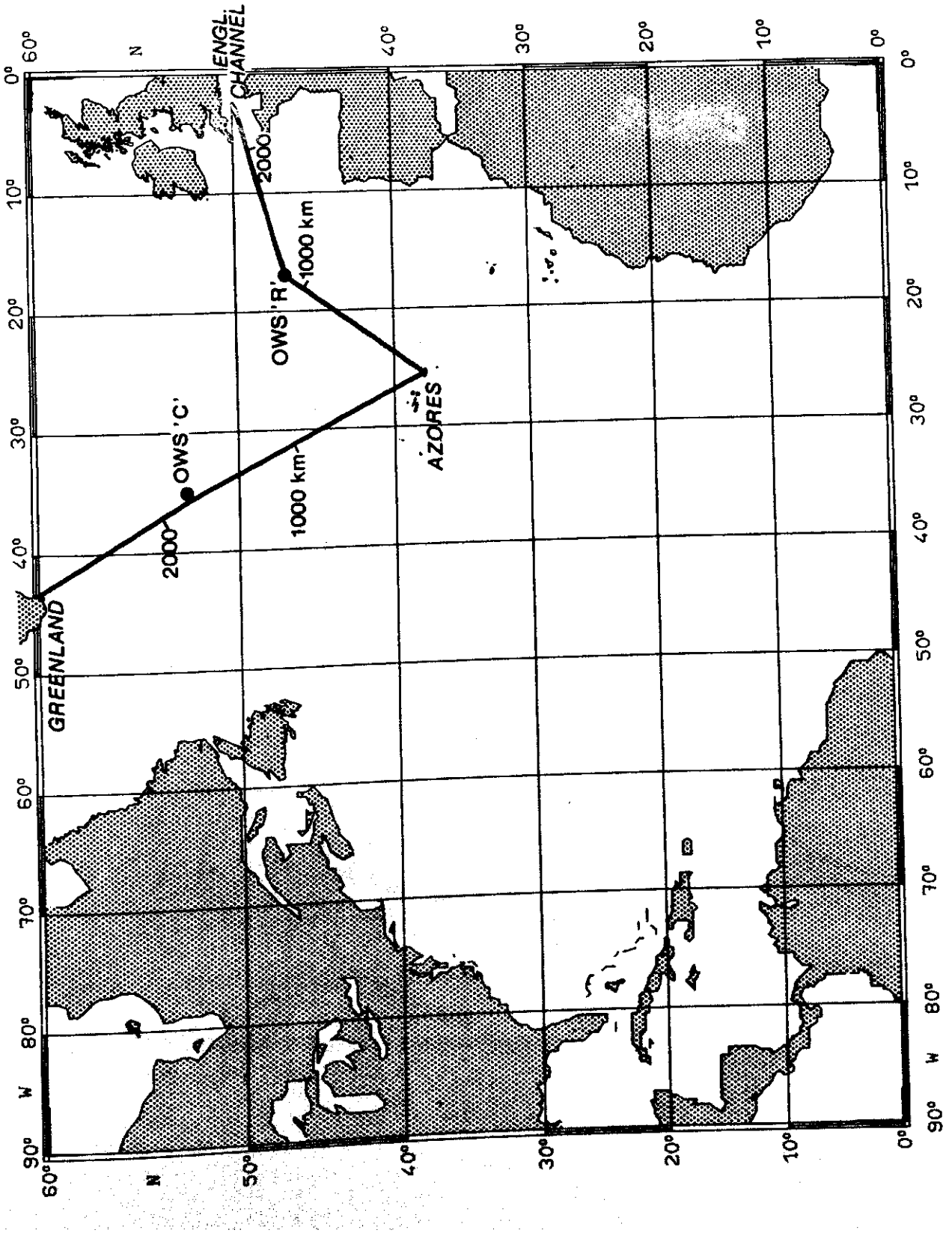

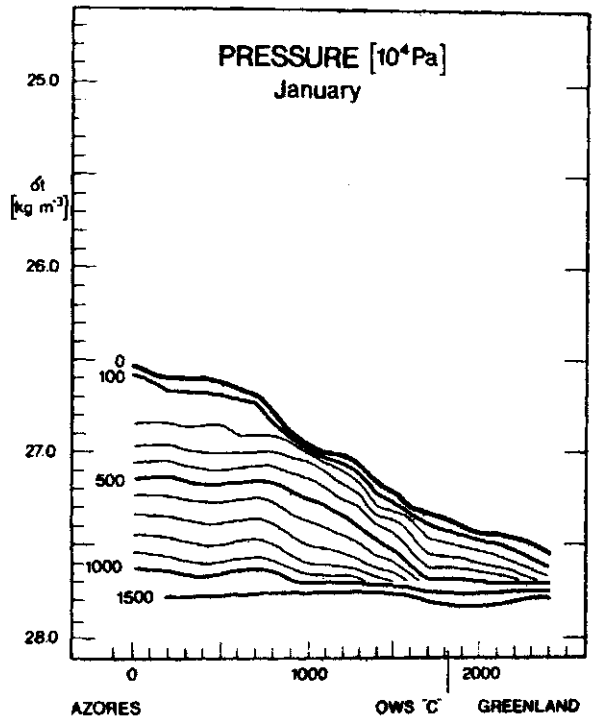

Fig. 137:

AZORES - GREENLAND

January

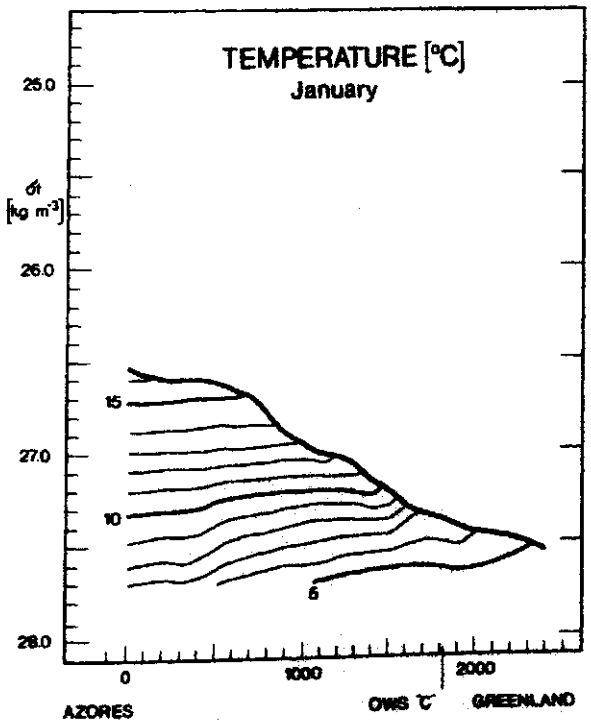

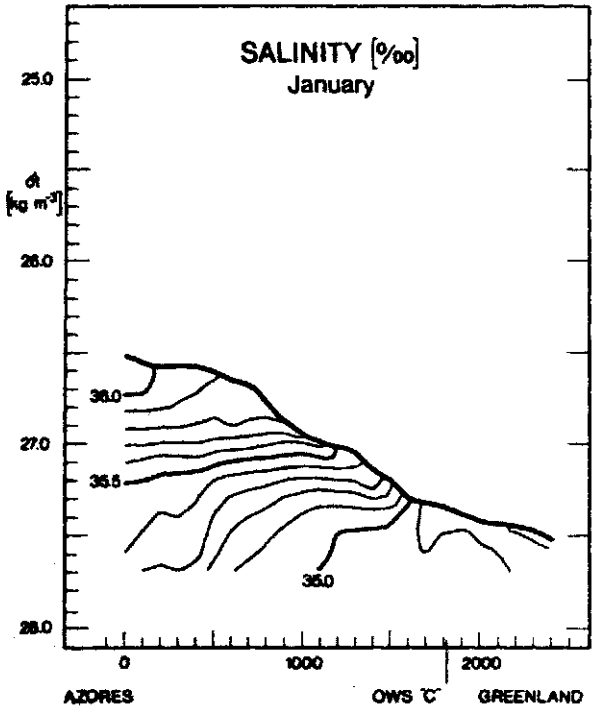

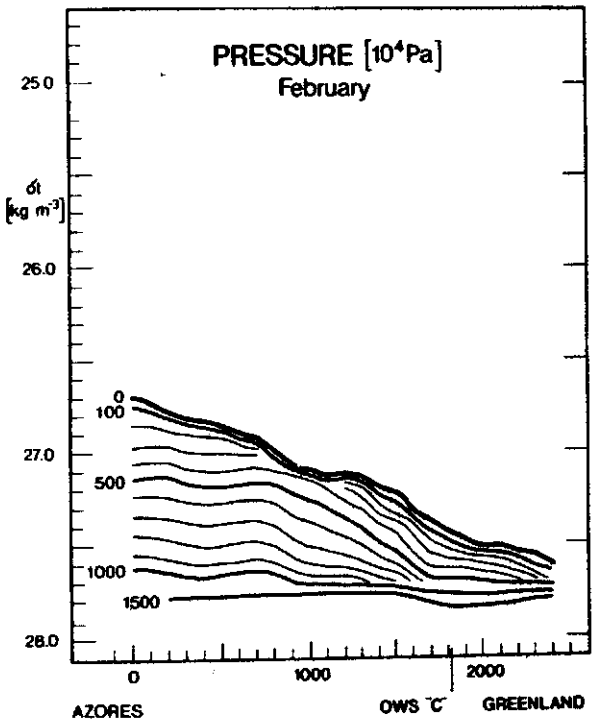

Fig. 138:

AZORES - GREENLAND

February

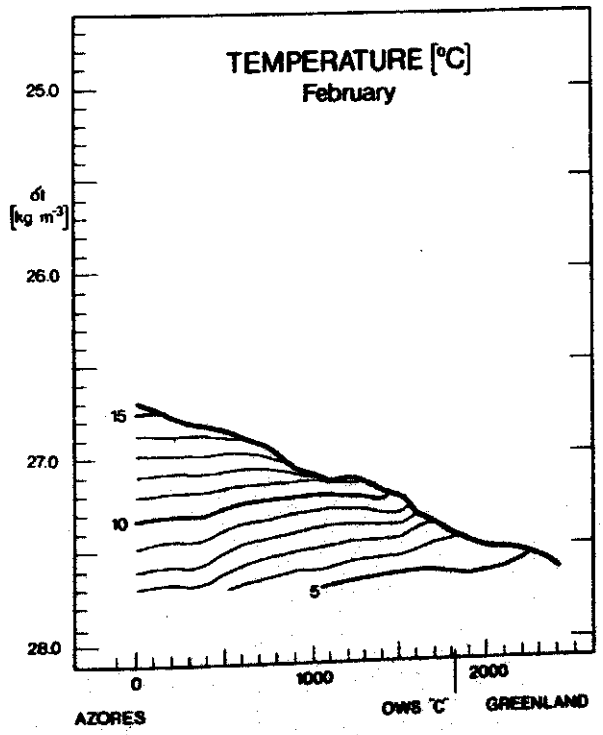

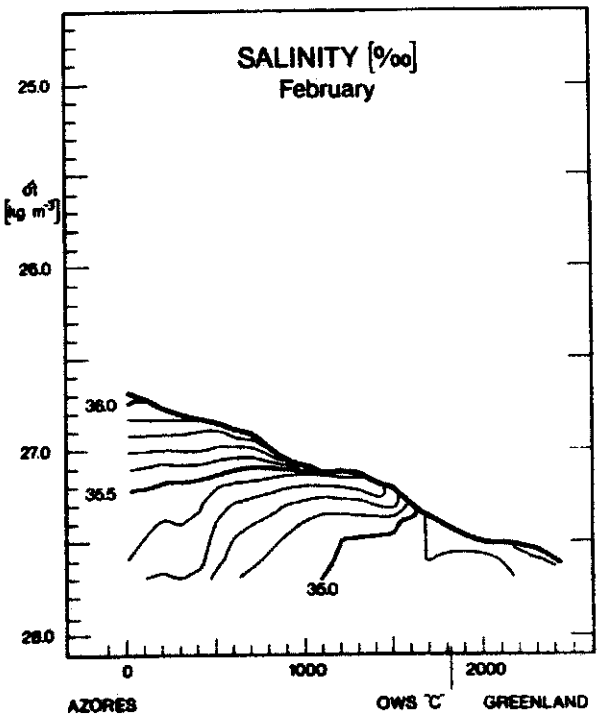

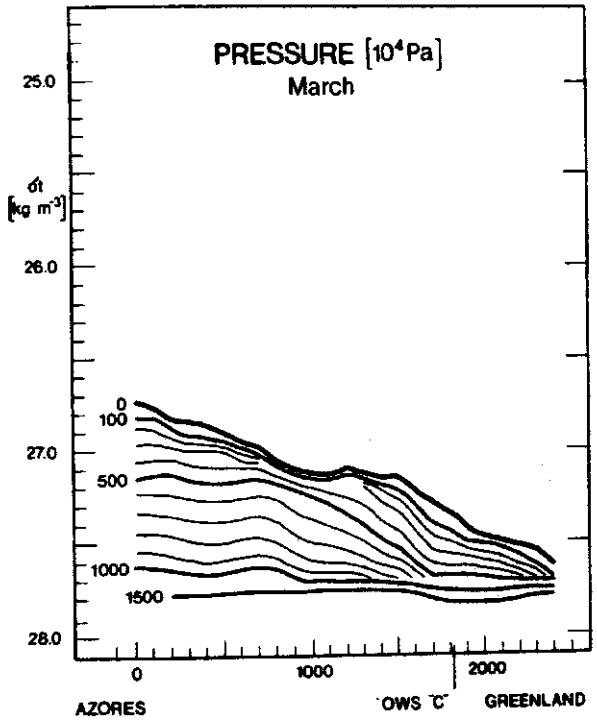

Fig. 139:

AZORES - GREENLAND
March

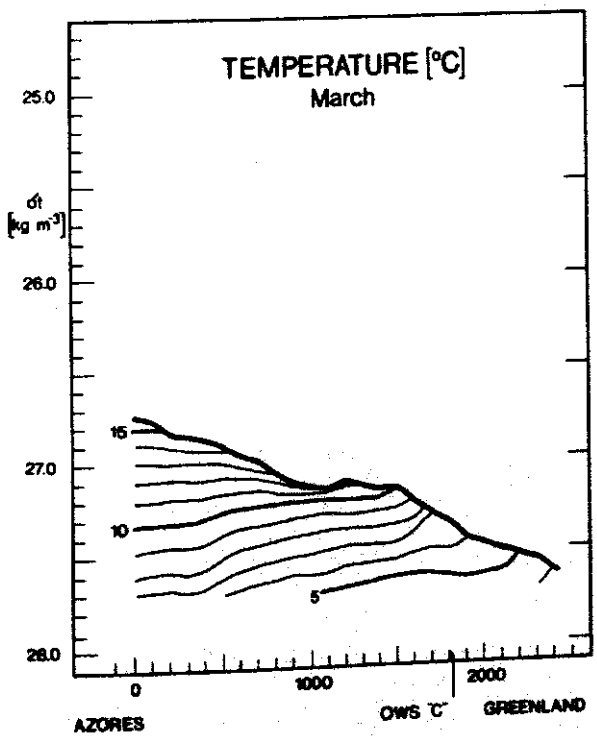

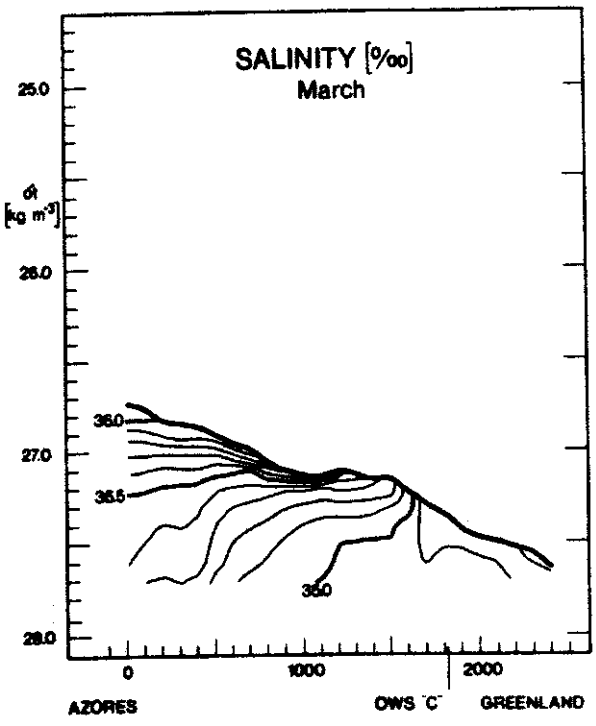

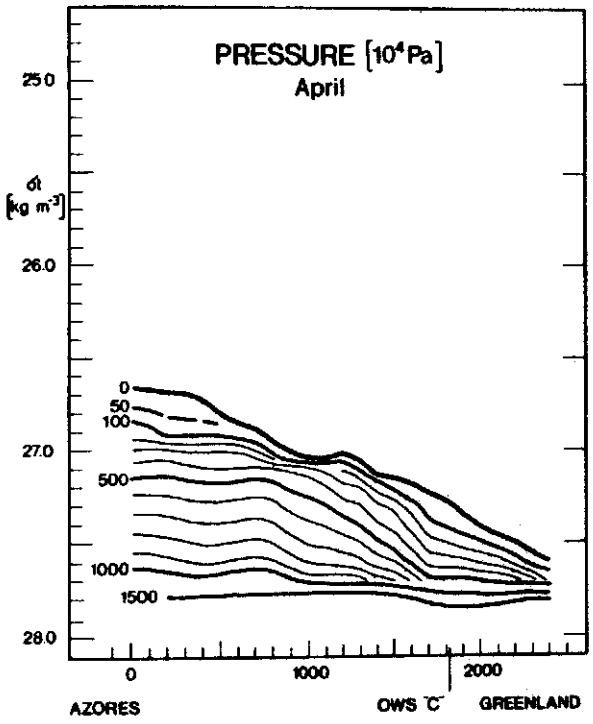

Fig. 140:

AZORES - GREENLAND
April

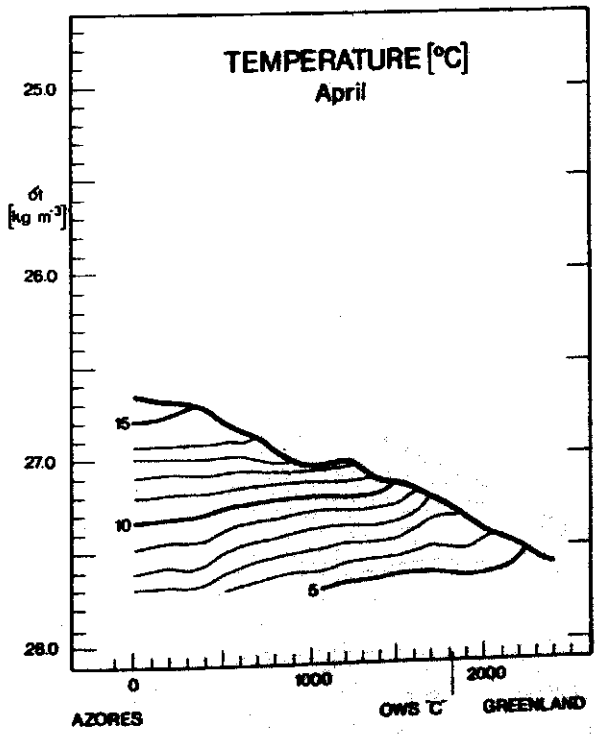

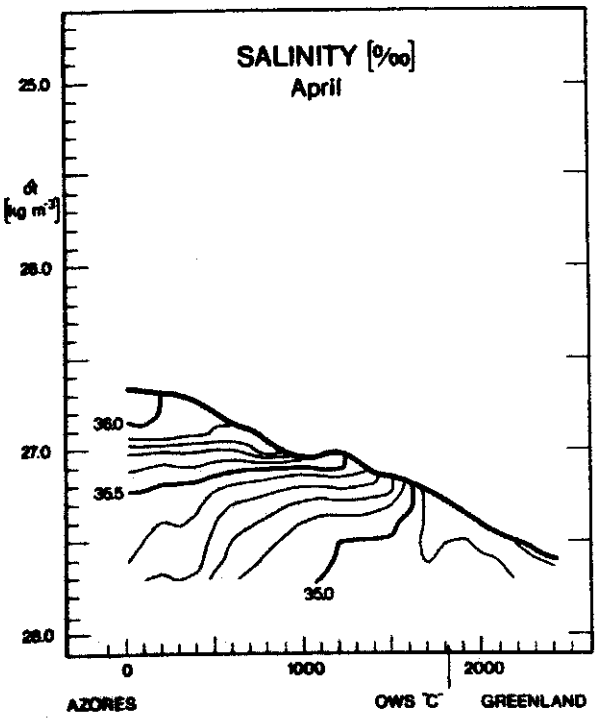

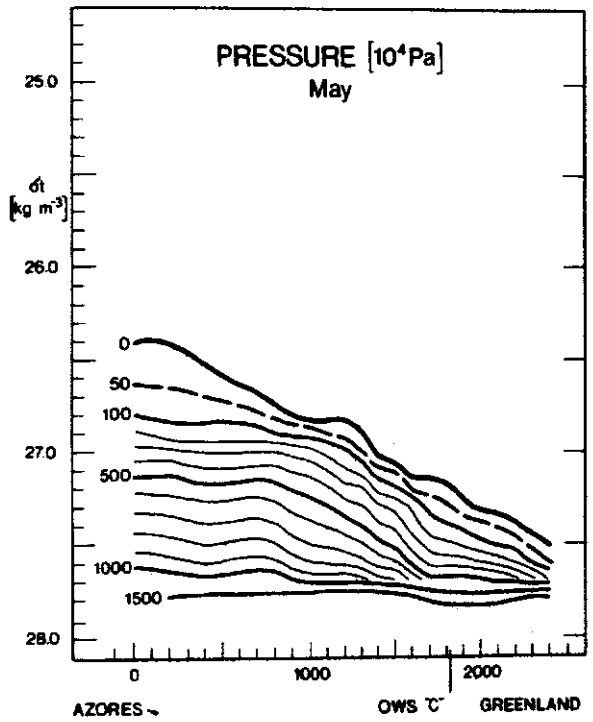

Fig. 141:

AZORES - GREENLAND

May

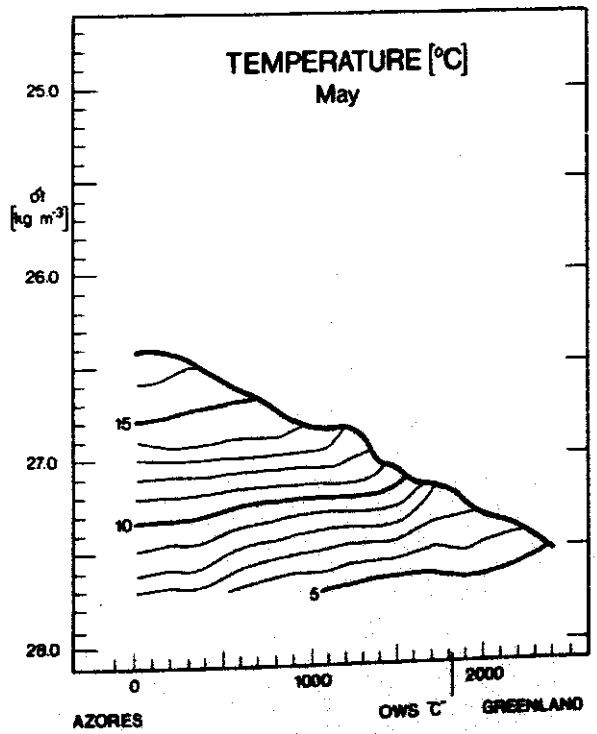

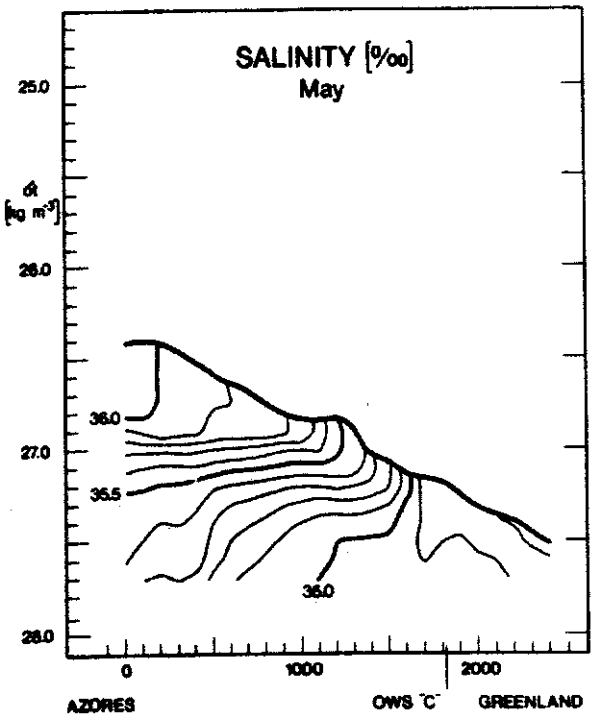

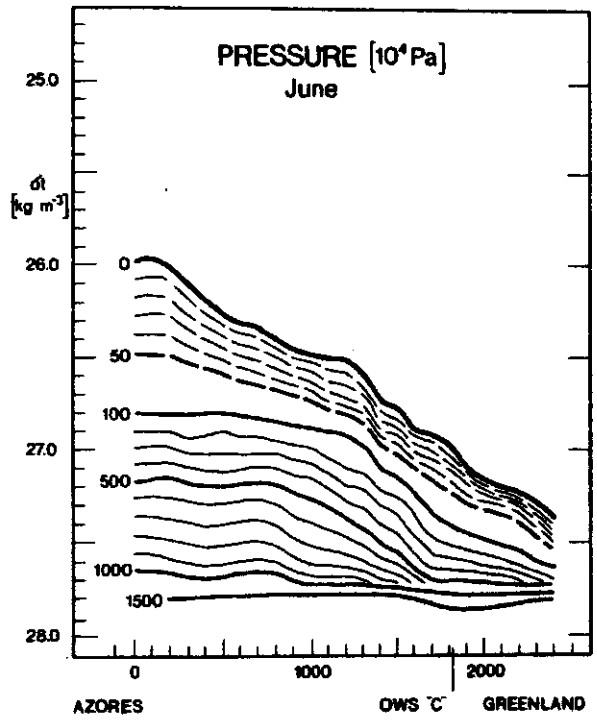

Fig. 142:

AZORES - GREENLAND
June

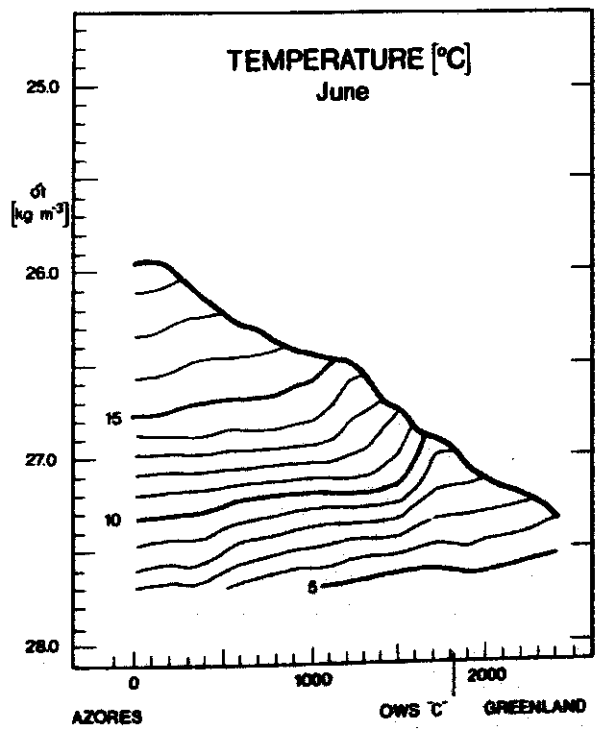

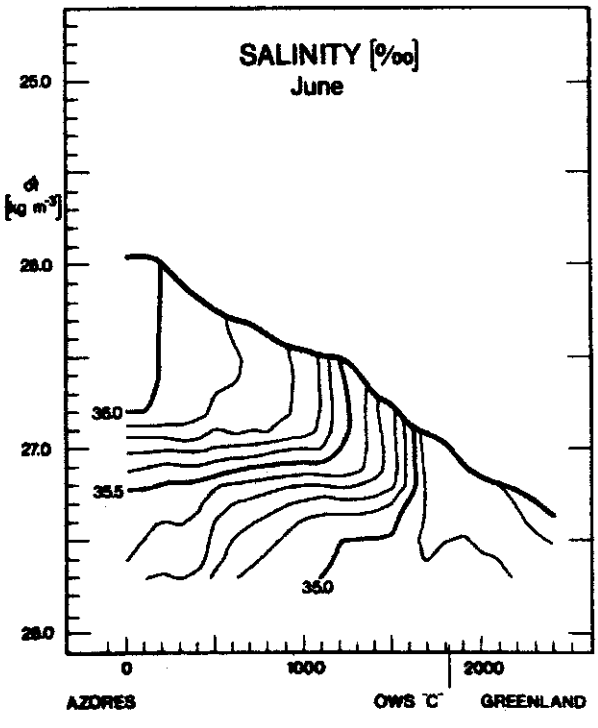

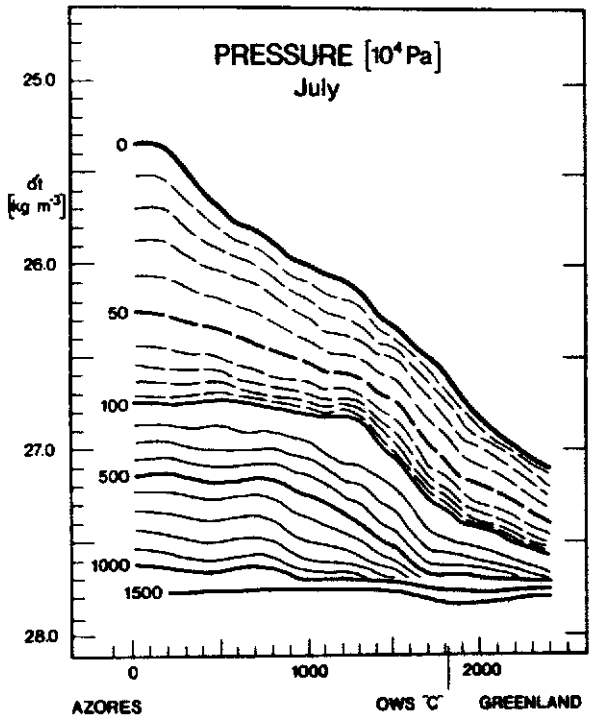

Fig. 143:

AZORES - GREENLAND

July

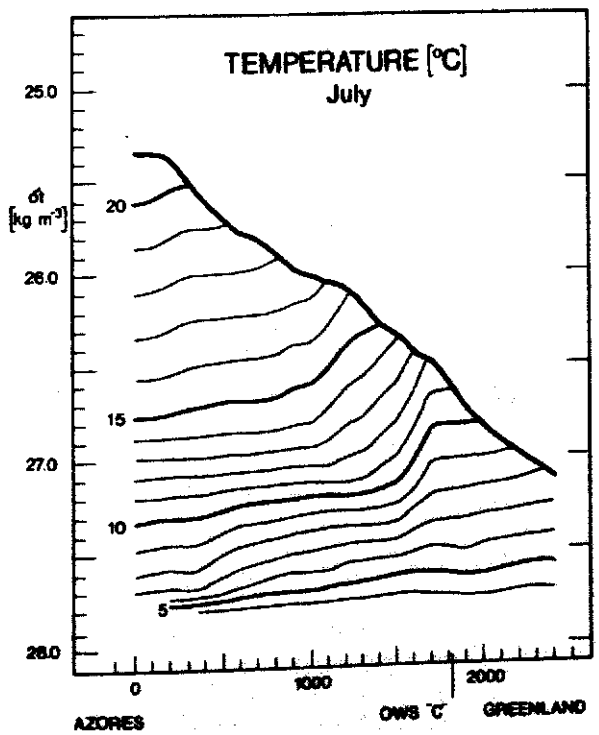

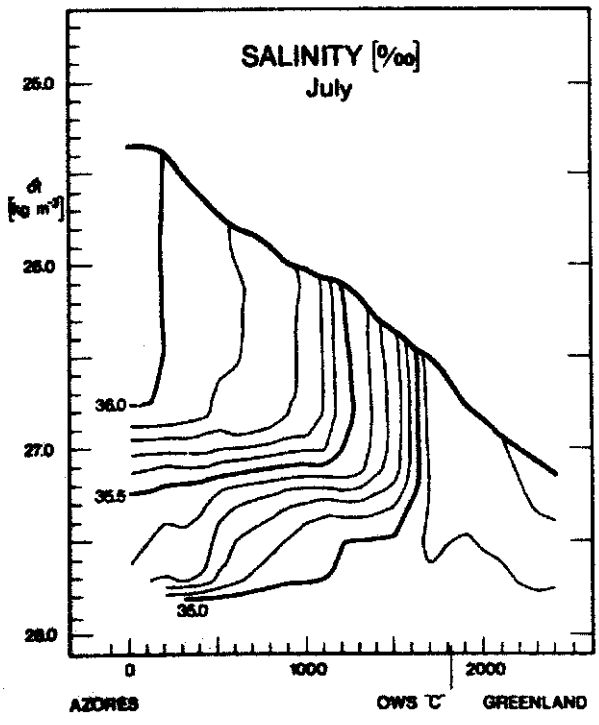

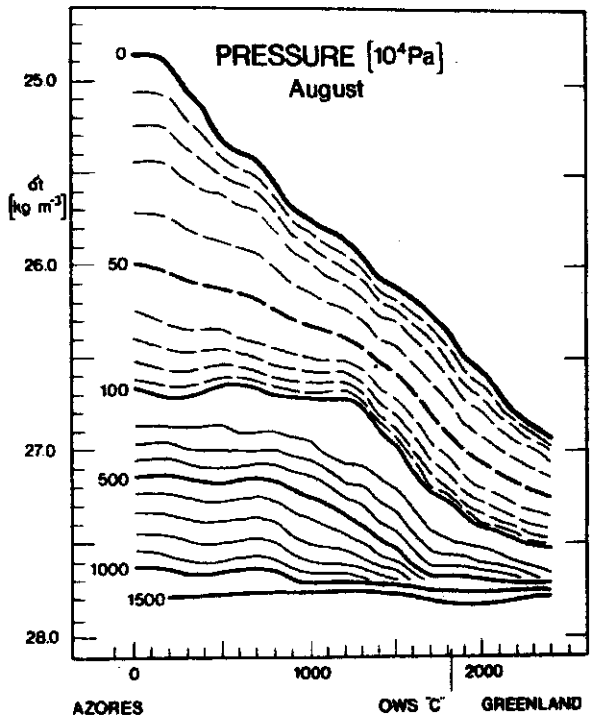

Fig. 144:

AZORES - GREENLAND
August

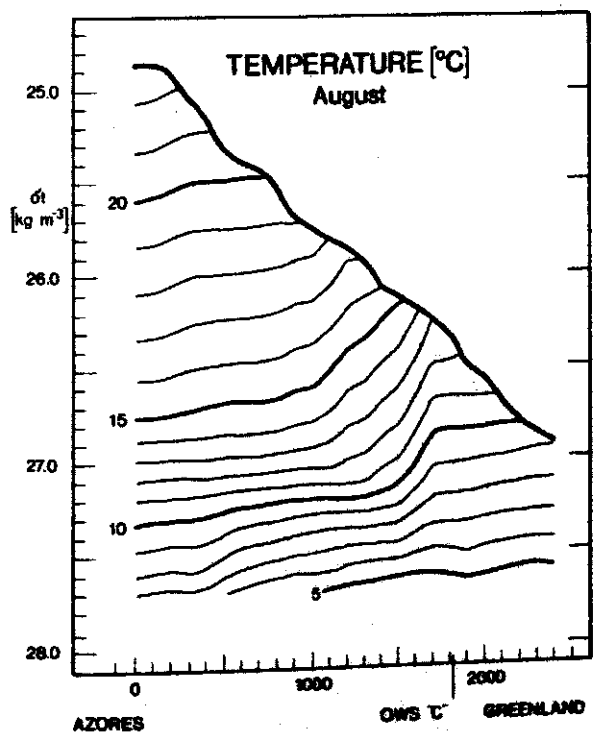

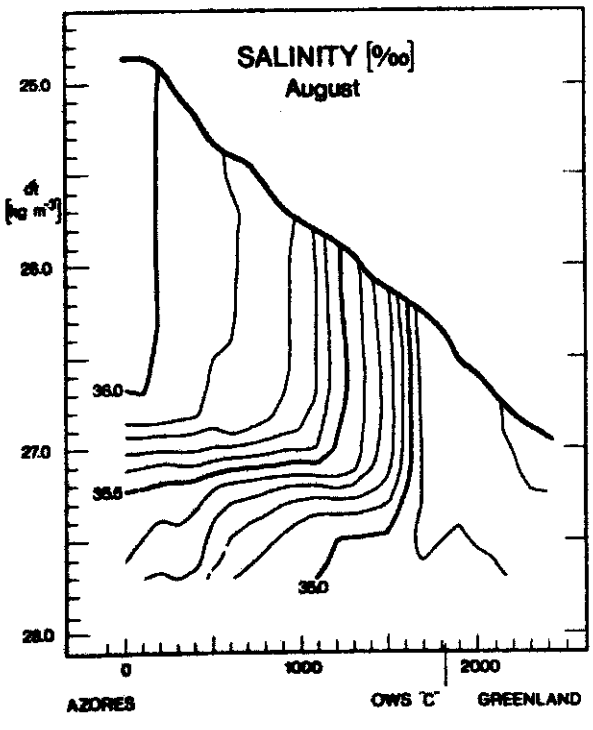

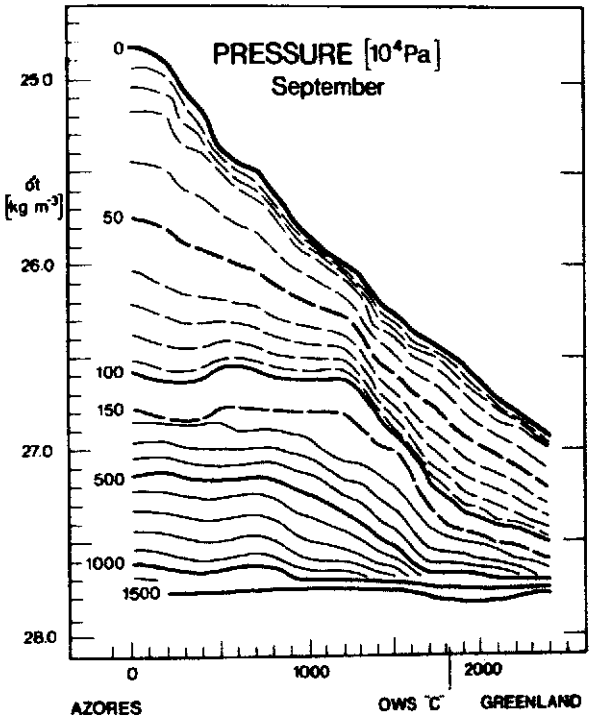

Fig. 145:

AZORES - GREENLAND
September

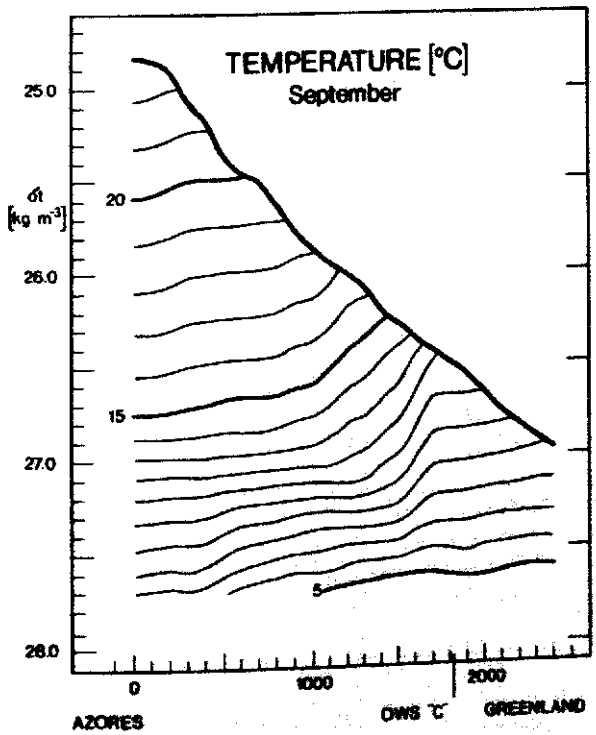

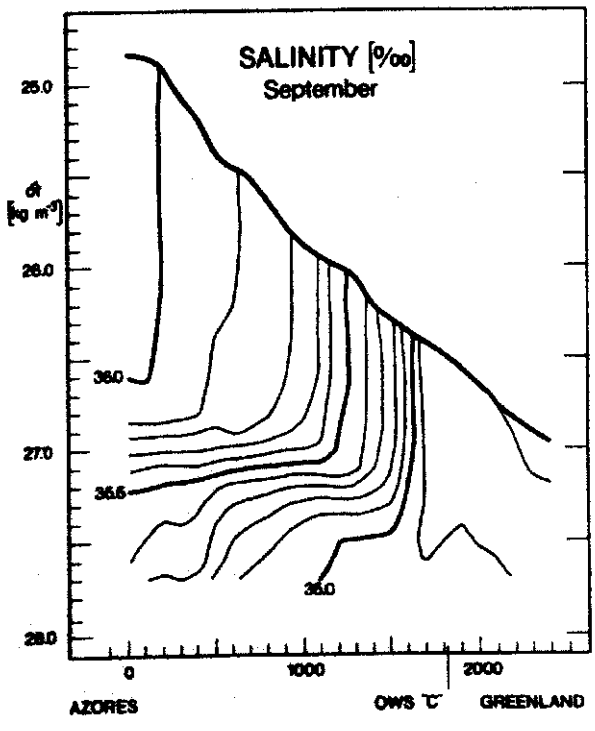

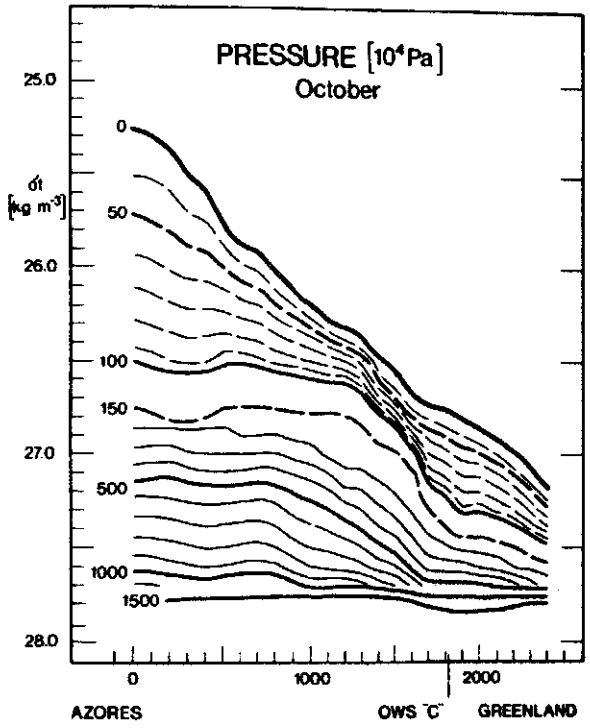

Fig. 146:

AZORES - GREENLAND
October

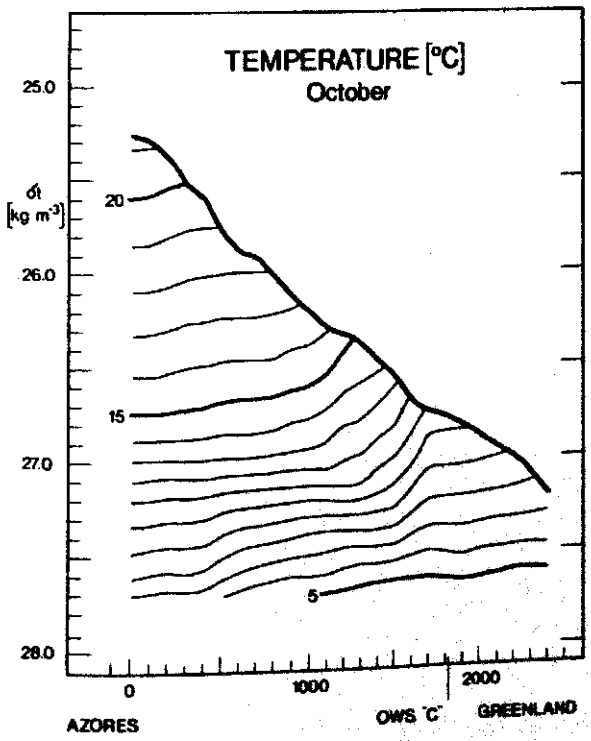

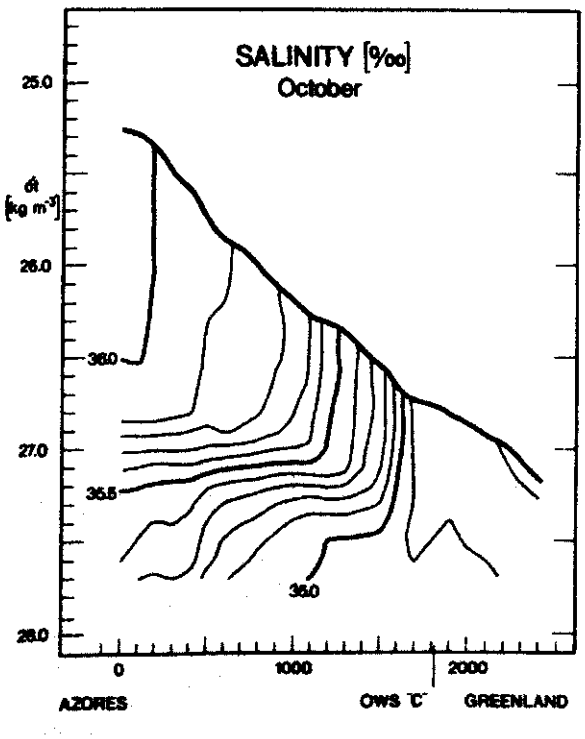

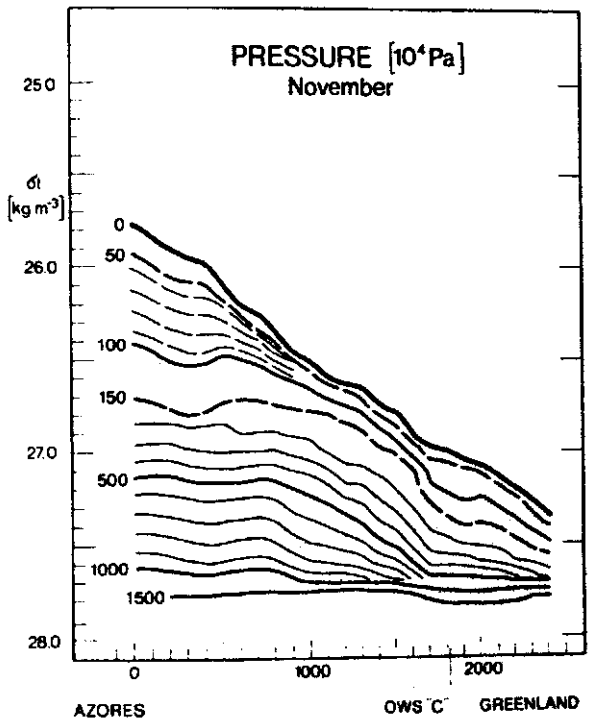

Fig. 147:

AZORES - GREENLAND
November

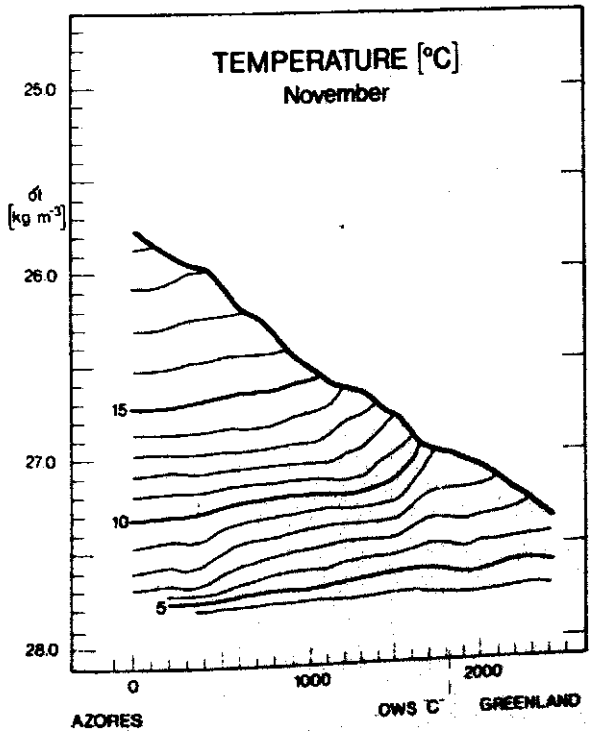

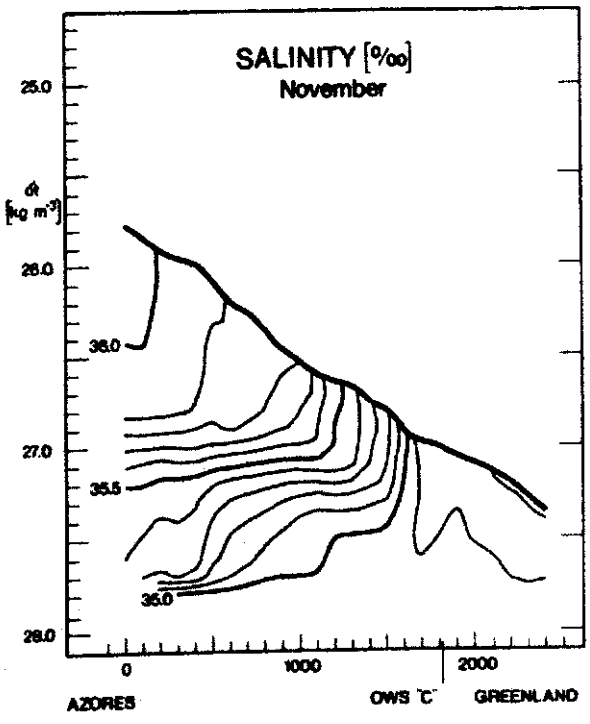

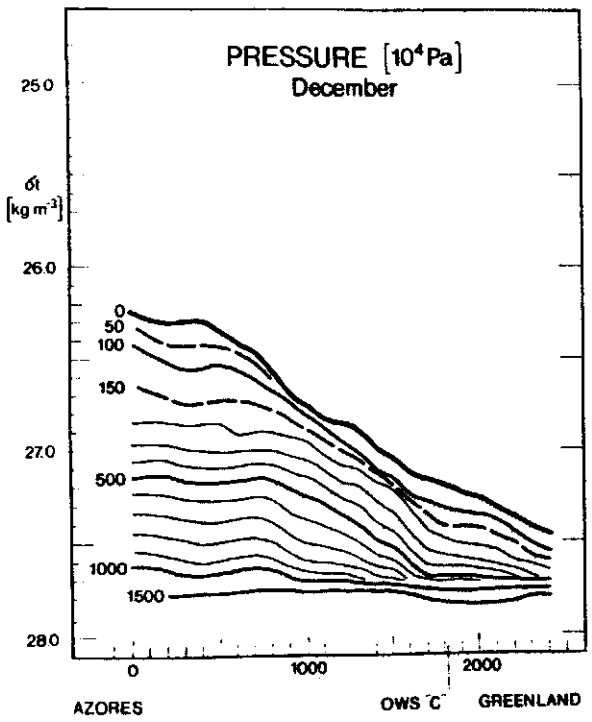

Fig. 148:

AZORES - GREENLAND
December

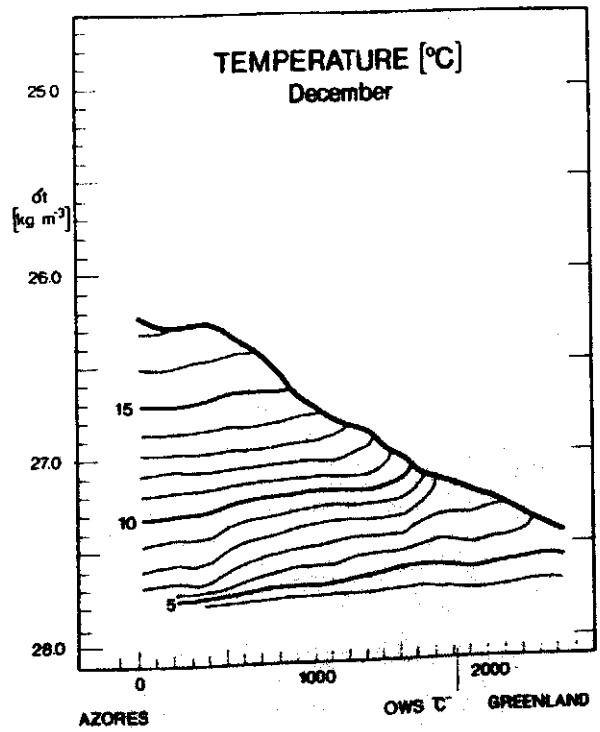

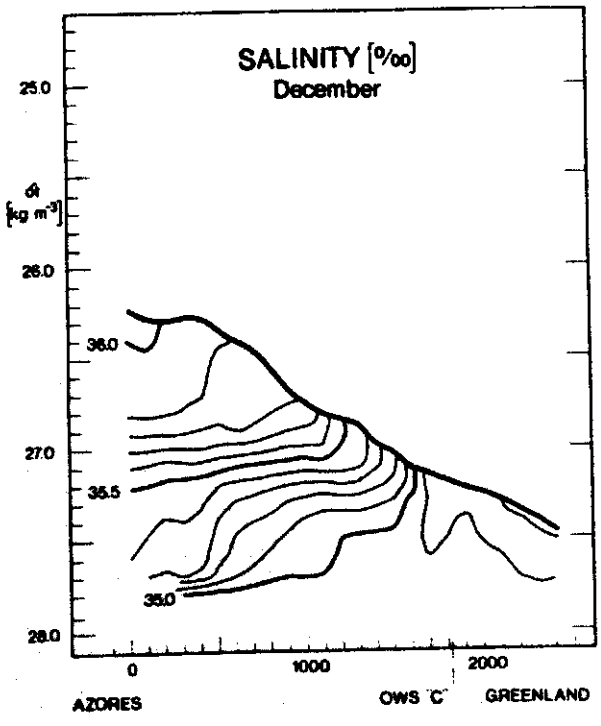

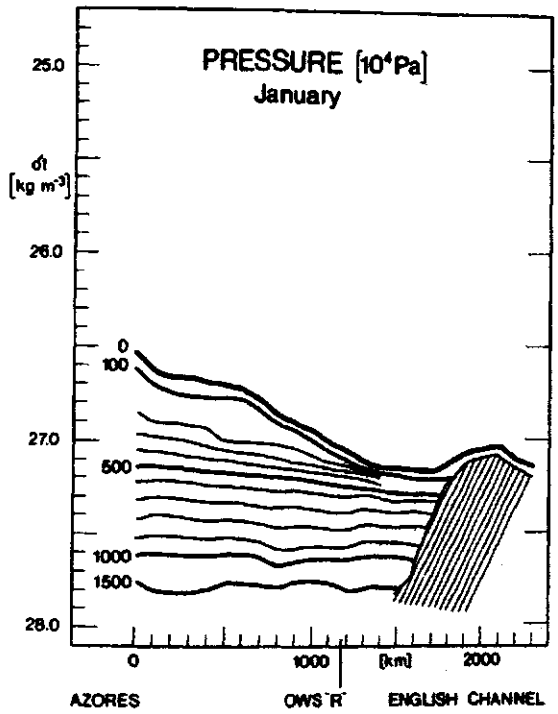

Fig. 149:

AZORES - ENGLISH CHANNEL
January

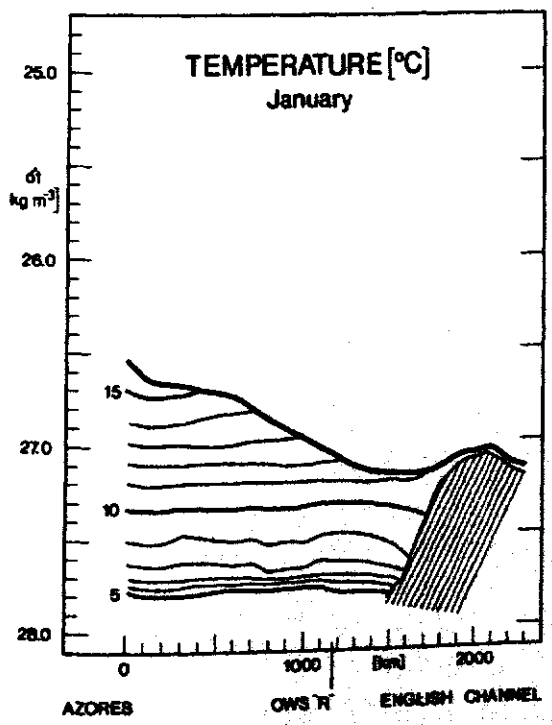

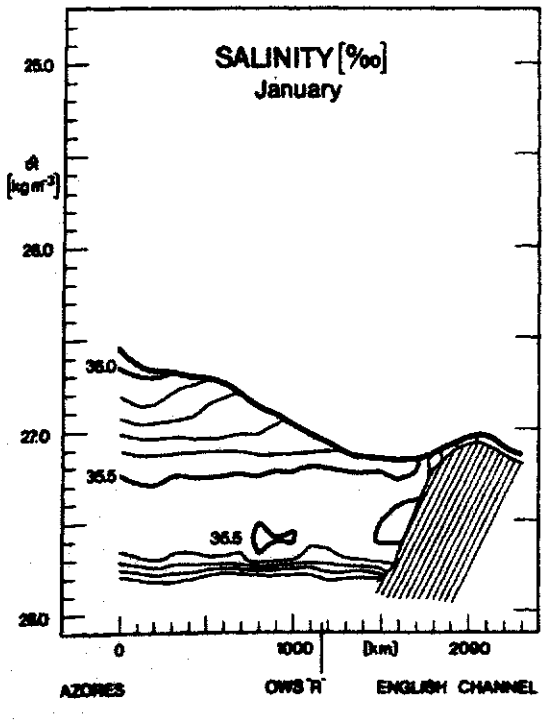

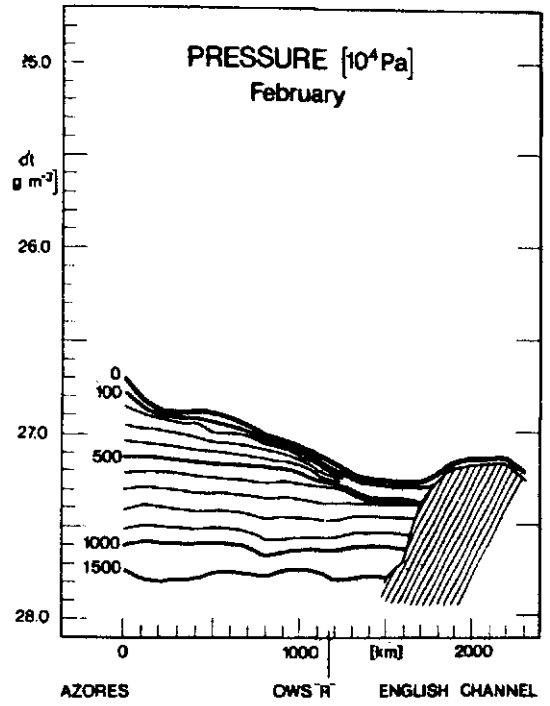

Fig. 150:

AZORES - ENGLISH CHANNEL
February

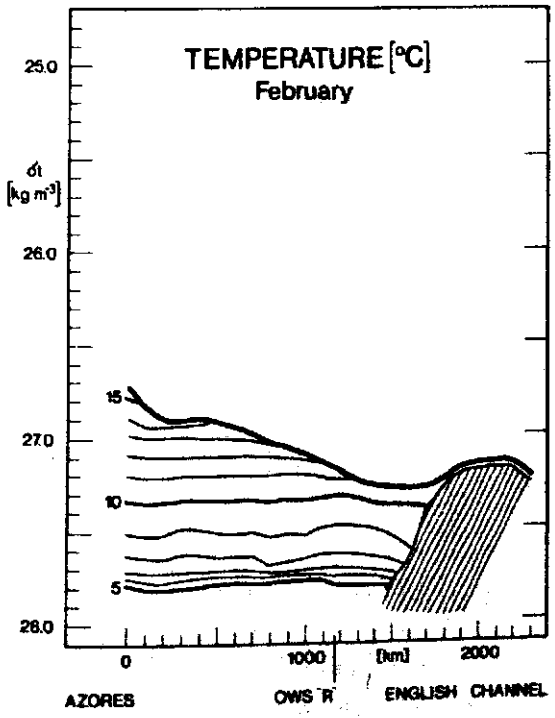

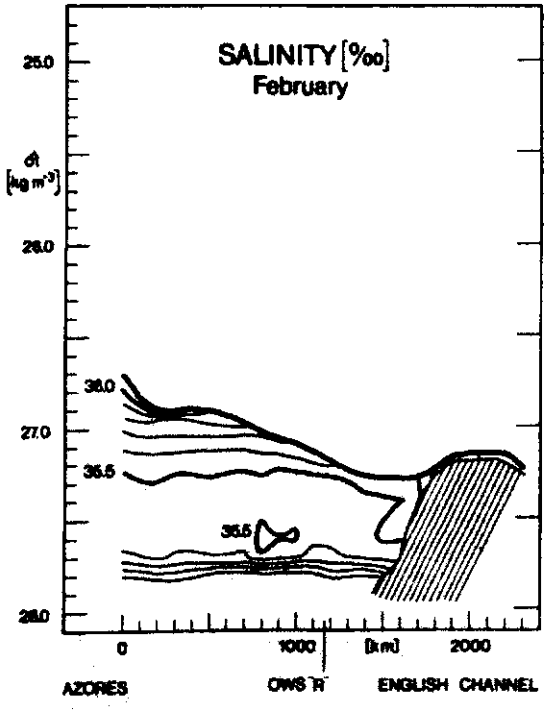

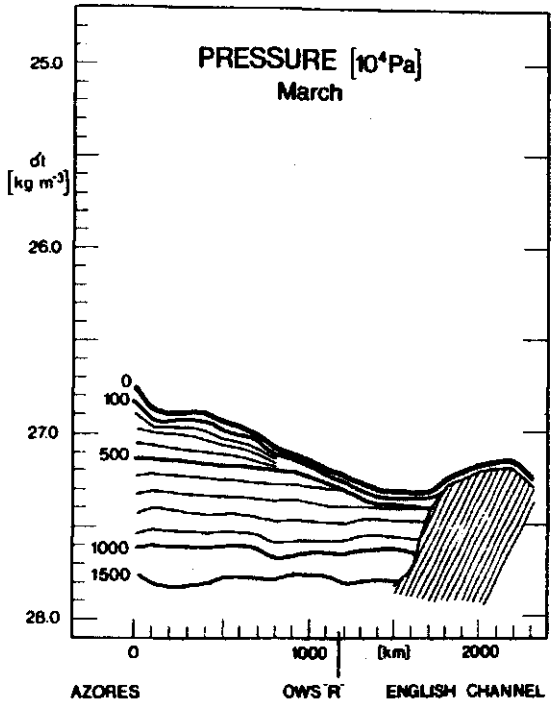

Fig. 151:

AZORES - ENGLISH CHANNEL
March

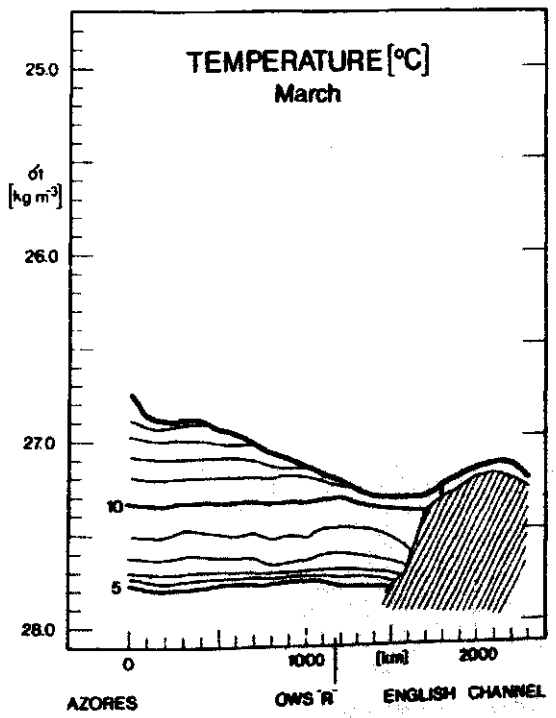

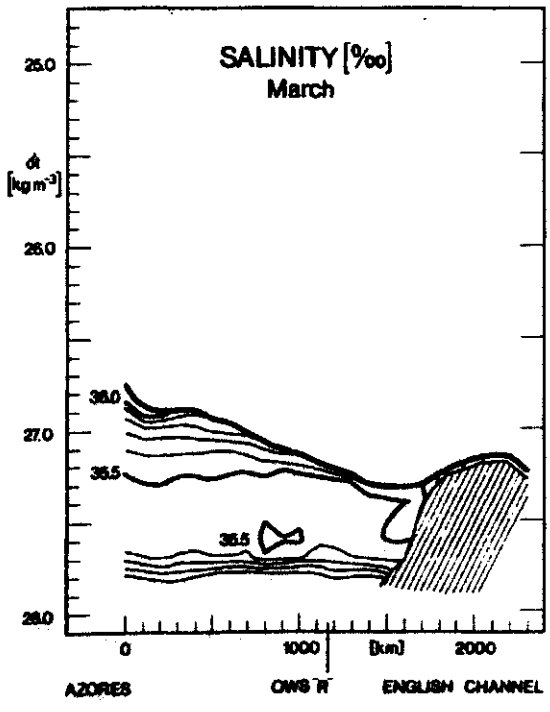

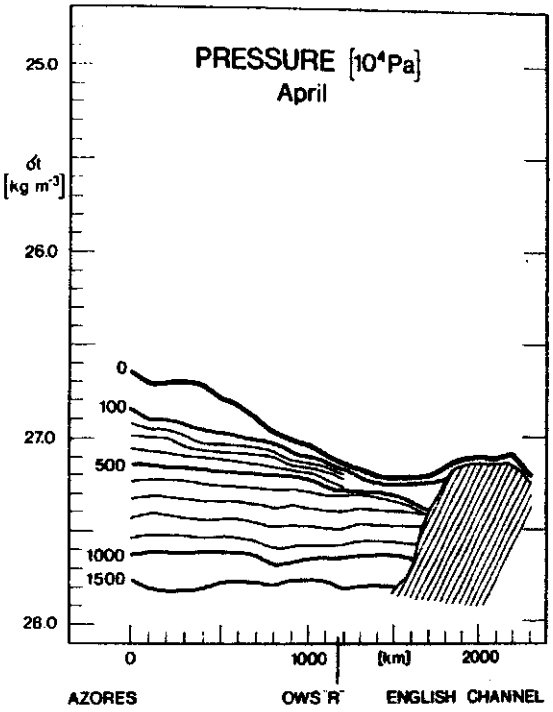

Fig. 152:

AZORES - ENGLISH CHANNEL
April

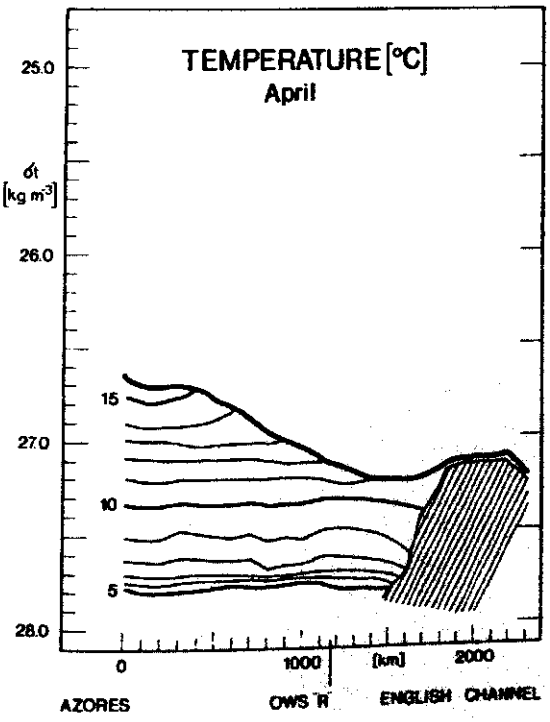

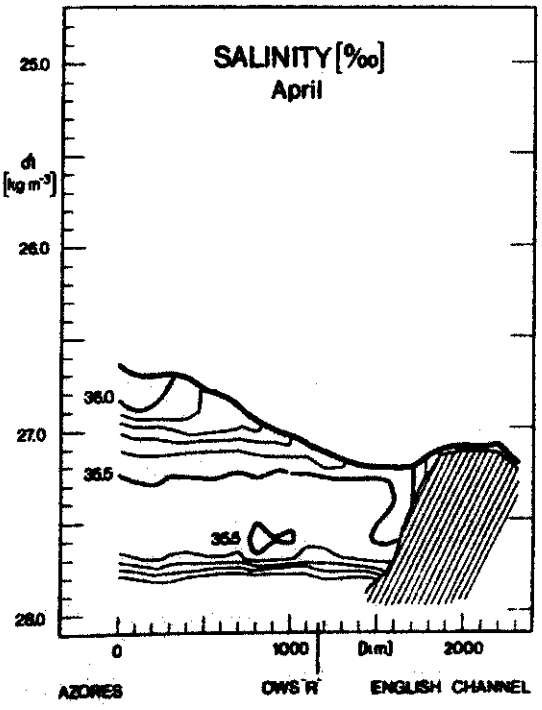

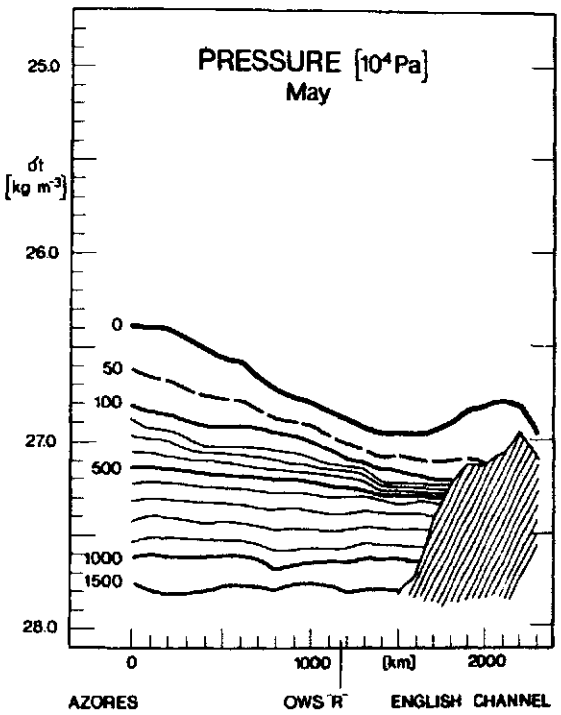

Fig. 153:

AZORES - ENGLISH CHANNEL
May

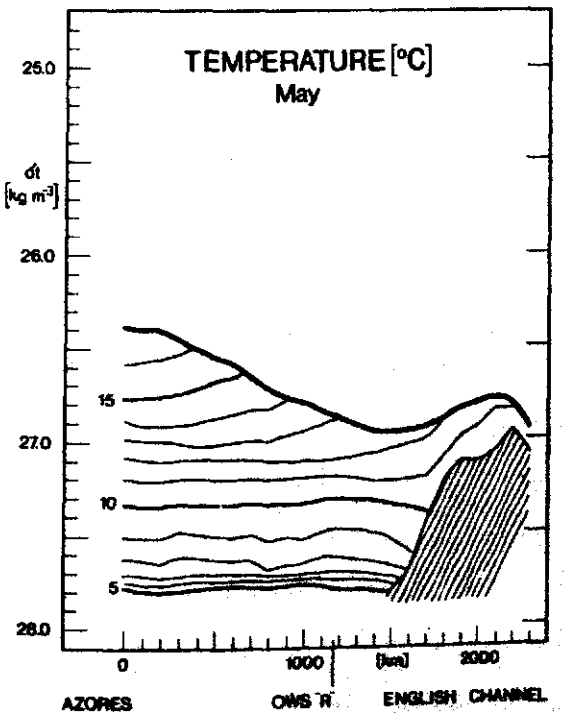

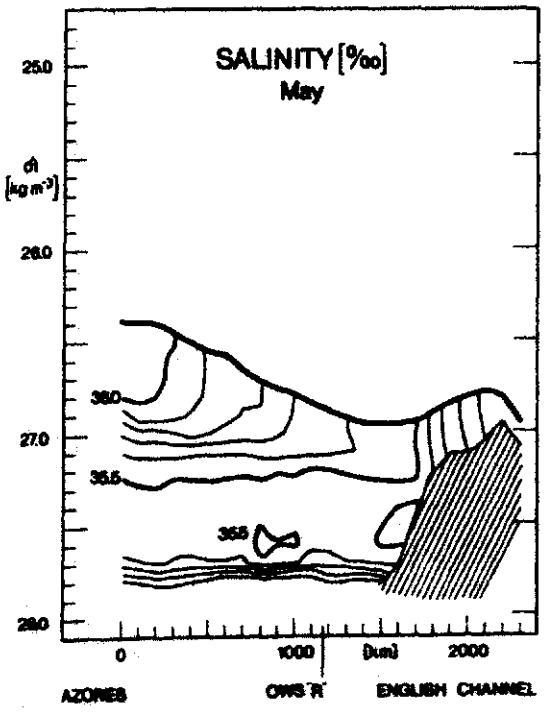

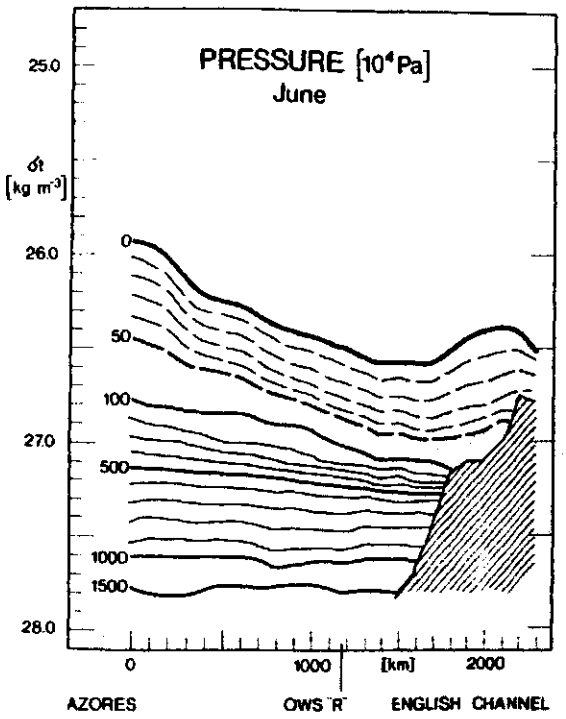

Fig. 154:

AZORES - ENGLISH CHANNEL
June

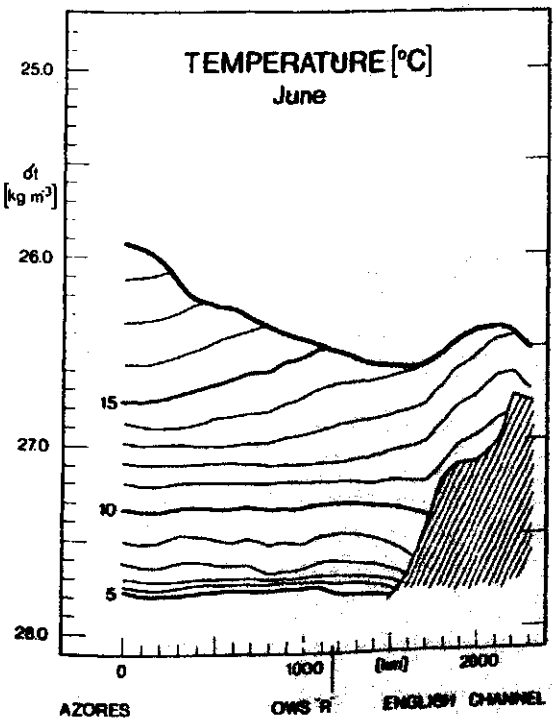

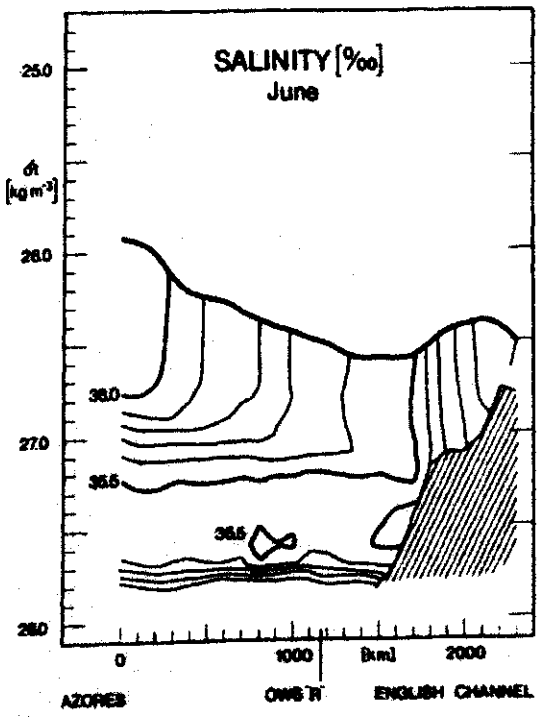

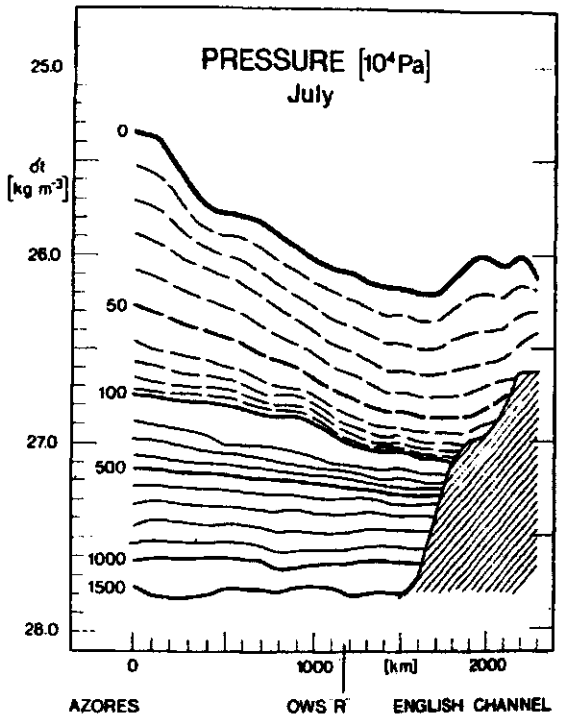

Fig. 155:

AZORES - ENGLISH CHANNEL
July

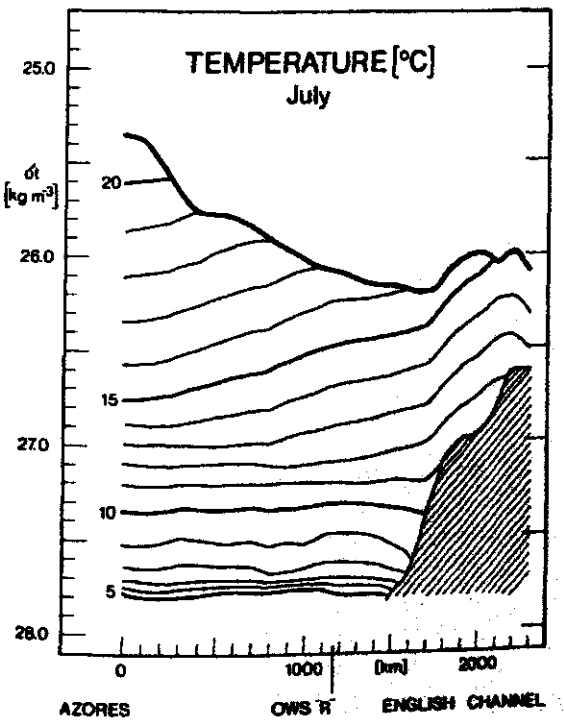

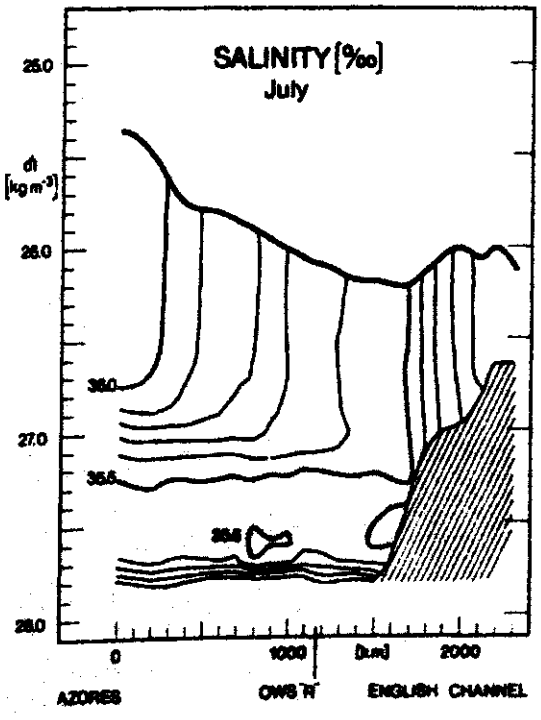

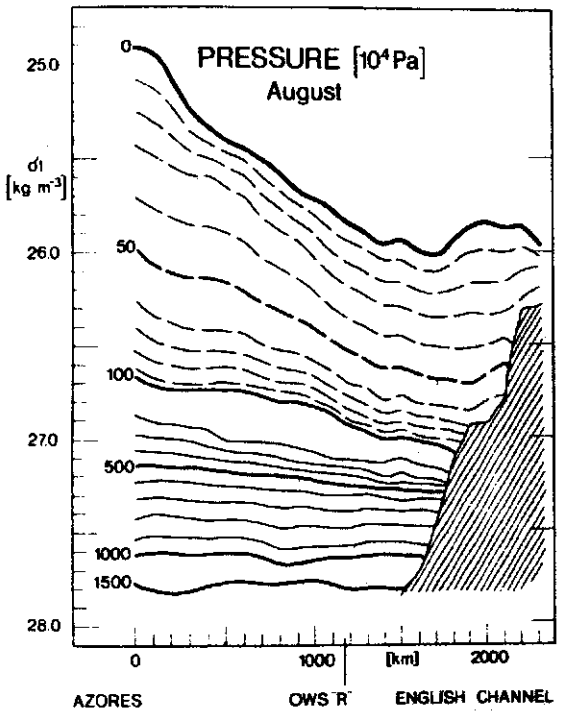

Fig. 156:

AZORES - ENGLISH CHANNEL
August

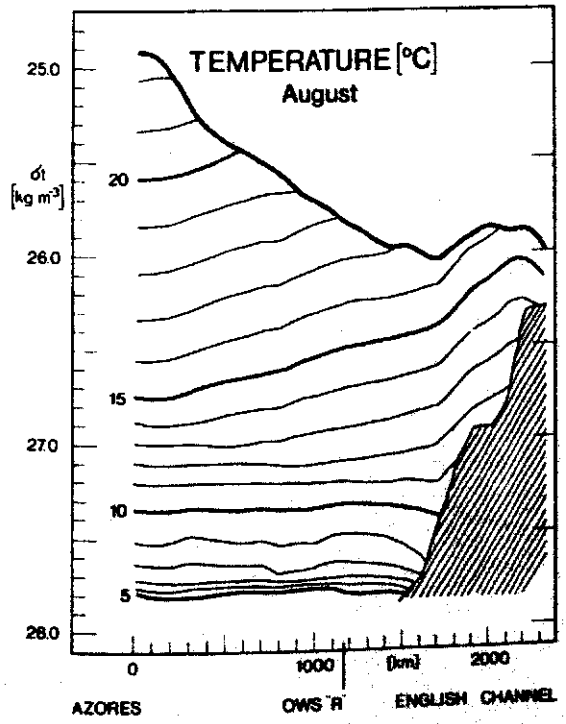

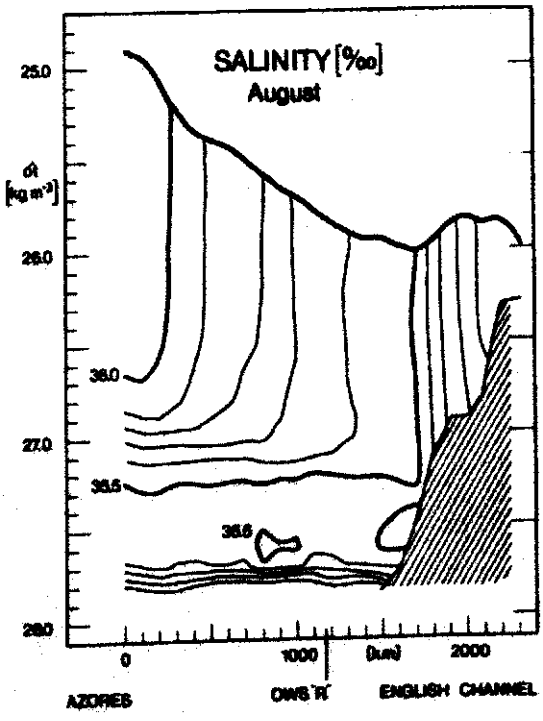

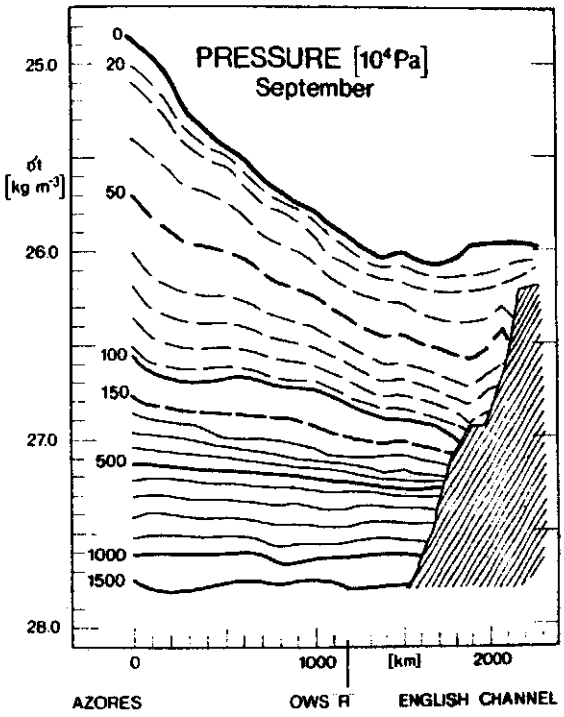

Fig. 157:

AZORES - ENGLISH CHANNEL
September

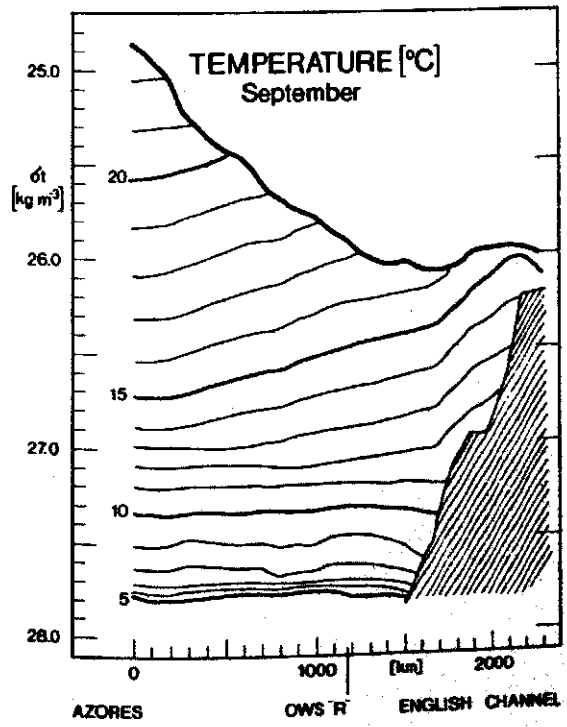

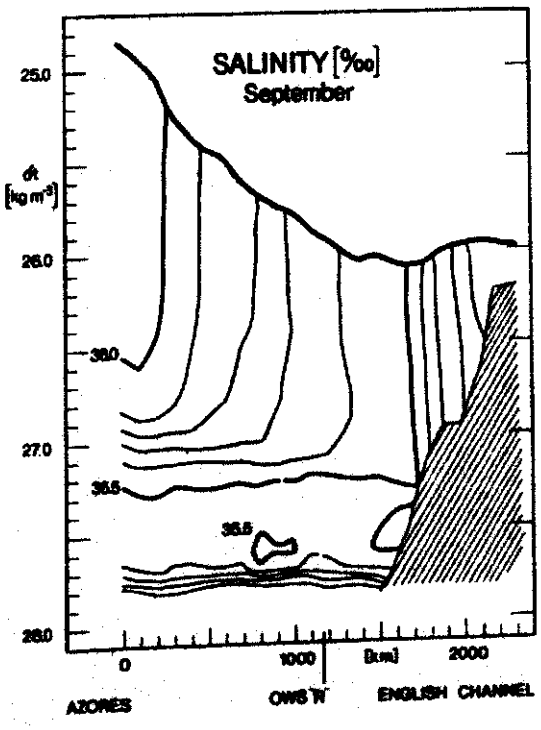

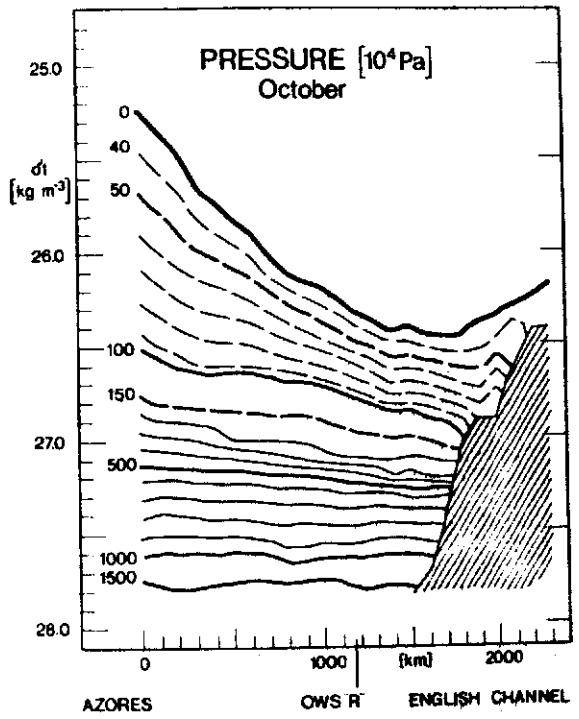

Fig. 158:

AZORES - ENGLISH CHANNEL
October

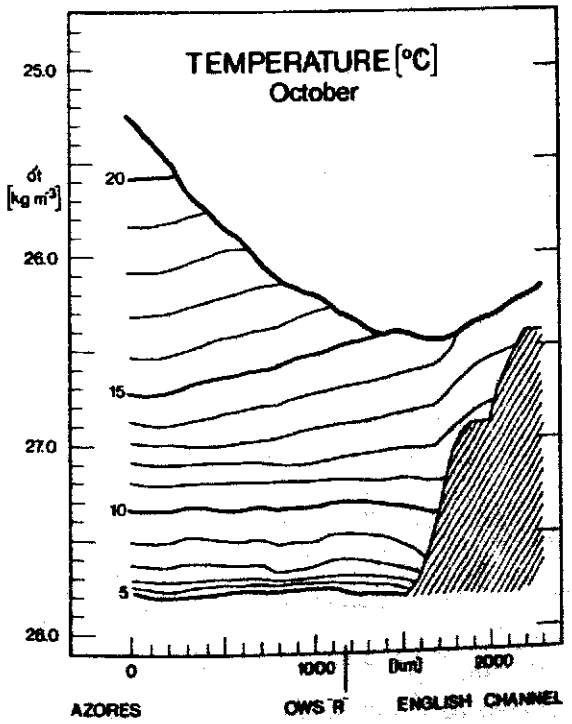

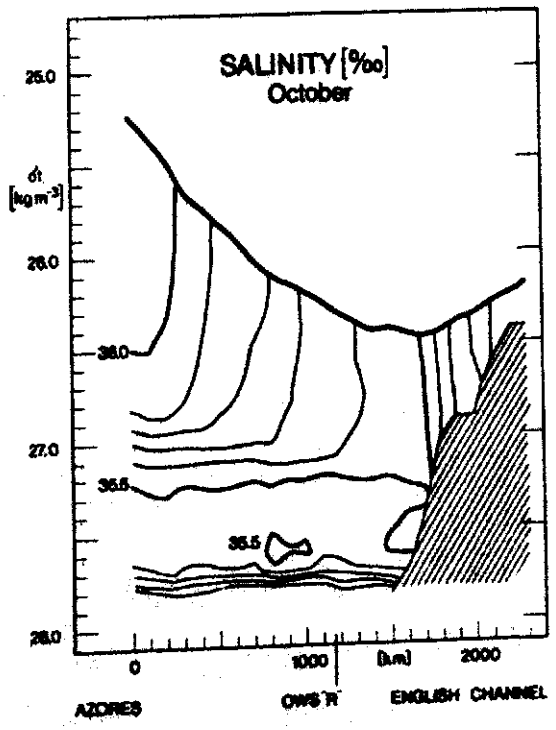

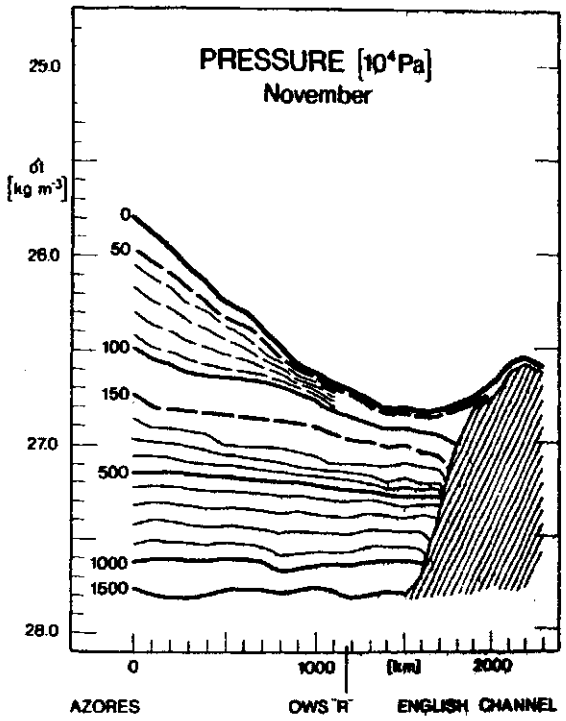

Fig. 159:

AZORES - ENGLISH CHANNEL
November

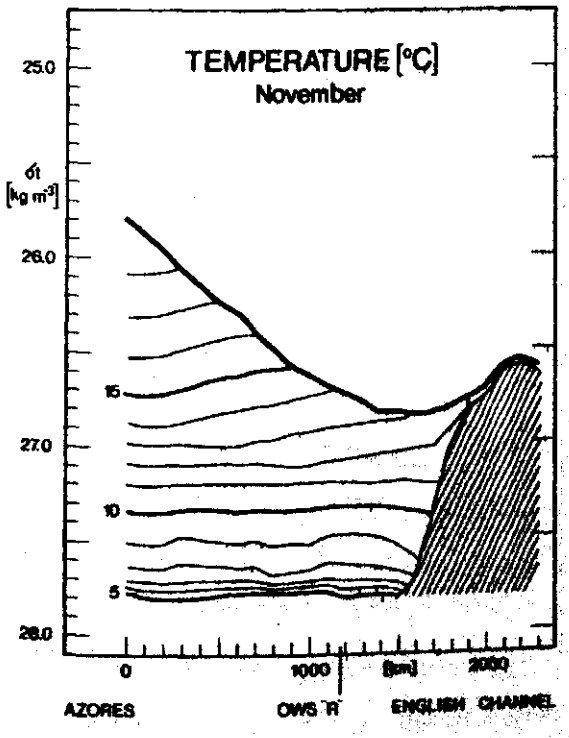

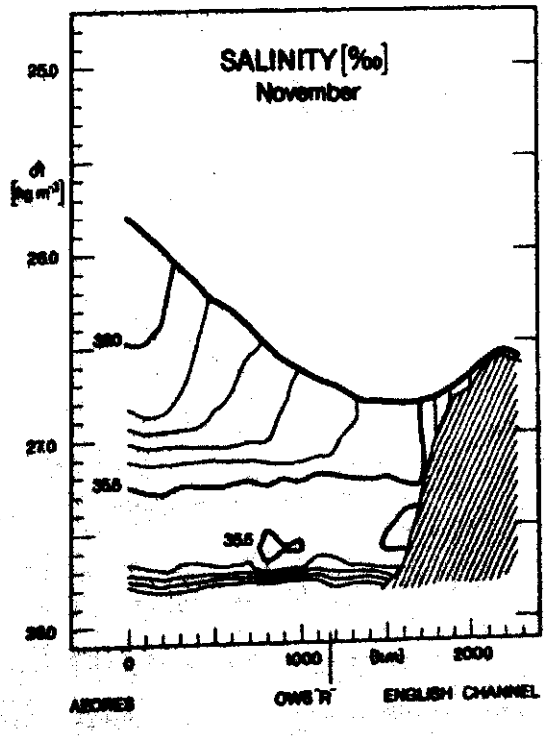

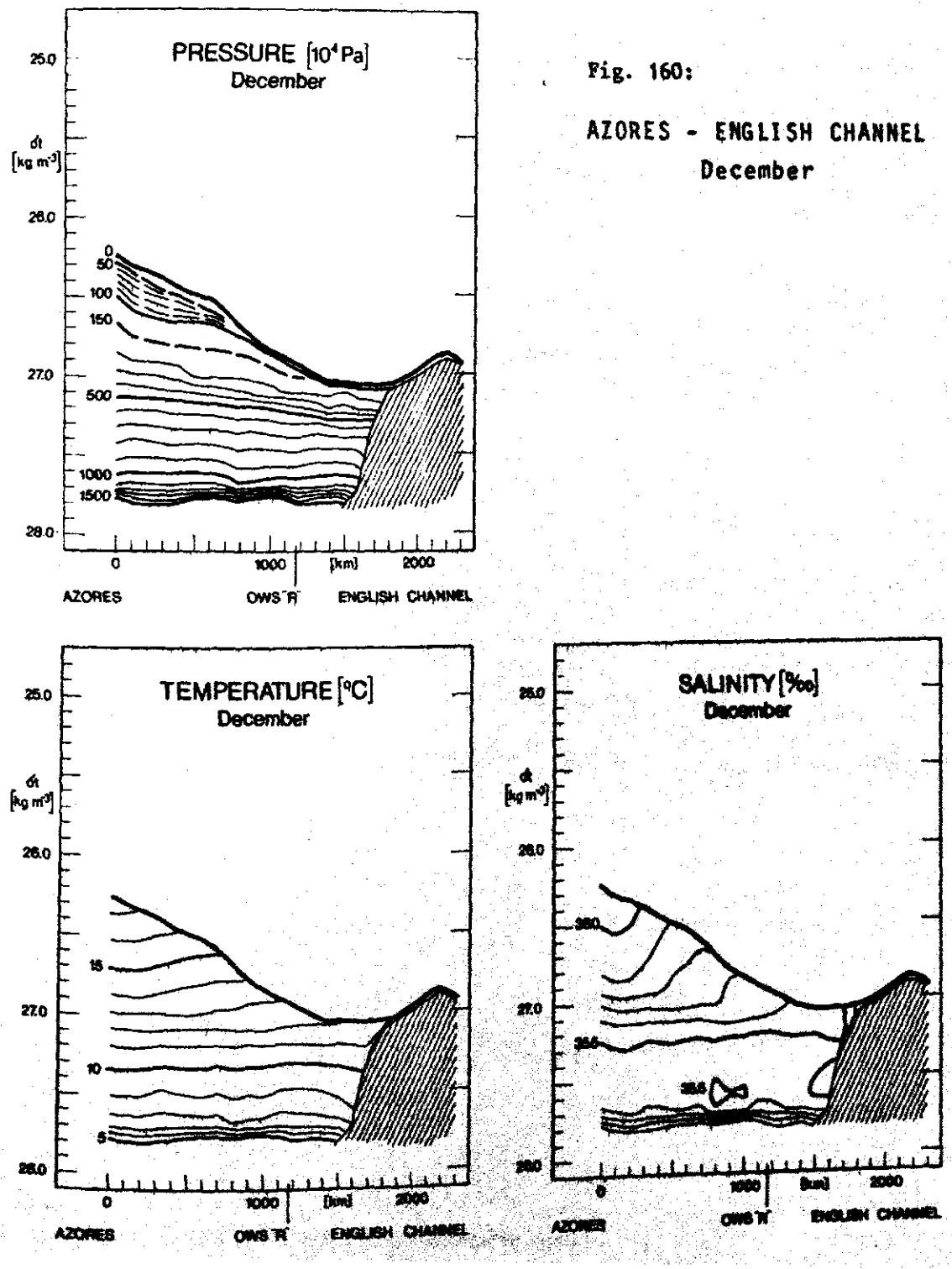

Fig. 160:

AZORES - ENGLISH CHANNEL
December